Barts and The London
Queen Mary's School of Medicine and Dentistry

Immortalization of Human Oral Keratinocytes with Defined Genetic Elements in the Development of Organotypic Oral Culture

Thesis submitted with regulations

for the degree of doctor of philosophy

by

Saira Athar

Supervisors:

Dr. Alan Cruchley

Prof. Eric Kenneth Parkinson

October 2013

Department of Clinical and Diagnostic Oral Sciences

Barts and the London, Queen Mary School of Medicine and Dentistry

Abstract

Primary cell culture is limited by the increase in cellular levels of $p16^{INK4a}$ in response to an *in vitro* culture environment and, in conjunction with telomere shortening following cell division, presents a barrier to cellular proliferation. The use of transformed cell lines is limited for studies wherein the aim is to generate data akin to an *in vivo* environment as commonly such cell lines achieve their immortal benefits by down regulating important tumour suppressive mechanisms and inhibiting cell cycle checkpoints.

Normal Human Oral Keratinocyte (NHOK) cells expressing shp16+hTERT were generated and compared to NHOK cells expressing Bmi1 +hTERT using an optimized retroviral transduction protocol and compared simultaneously to an epidermal control. Population doubling assessment of cell lines revealed that shp16+hTERT was not sufficient to extend replicative lifespan in the absence of p53 whilst cell lifespan extension was observed not only in cells expressing Bmi1+hTERT, but also in cells transduced with Bmi1 alone. Upon characterization, cells showed expression of p53 and responsiveness to UVB-induced apoptosis as demonstrated by an increase in p53 expression. $NHOK^{Bmi1+hTERT}$ displayed adaptability to serum free culture when weaned into keratinocyte serum free media (KSFM) and retained the ability to stratify into multiple layers when supported by feeders on polycarbonate membrane inserts.

The cell line $NHOK^{Bmi1+hTERT}$ will be beneficial for *in vitro* studies looking to utilise an alternative to transformed or spontaneously derived cell lines and holds potential for further development and optimization into a well characterized SSE in a user friendly, and reproducible system for the testing for oral products.

Author's declaration

I declare that I am the sole author of this thesis and that all the work presented herein was performed by myself, unless otherwise stated.

This thesis has not been submitted for consideration for any other degree in this or any other university.

Saira Athar.

Acknowledgements

I would like to thank my supervisors Dr. Alan Cruchley and Prof. Ken Parkinson for their constant help, guidance and support throughout my project. Their kindness, encouragement and optimism helped me get through the hard times in this study and especially to ken for always having an explanation for everything!

I would also like to thank all the people who helped in this study including Dr.Gary Warnes for help with the FACS analysis, Tony Price and the staff at the BSU for irradiating countless cells, Chris Evagora for membrane sectionning and Dr. Ann Wheeler for help with the fluorescence microscopy.

I am also grateful to the former and present members of the 'KP group' Alice, Hara, Bianca and Ann-Marie for all their help and for always being very friendly and supportive. Thank you to all my CDOS friends and my bay neighbours for making my PhD journey a very enjoyable one in particular the KP gang , Louise, Mandy, Ceceilia, Yori, Ahmad, Mojgan, Kaveh and ofcourse my twilight buddy Miguel and my good friend from bharat, Amrita ! I would also like to thank the staff of CDOS including Simon, Hong, Ryan, Eleni, Waseem and Steve for their kindness and support whenever I needed it and for providing a good working atmosphere.

I would like to thank my family worldwide in particular to my grandmother for her constant love, support and prayers and her strong positive attitude which inspires me to keep going even in tough times. I am grateful to my second set of parents, my in-laws, for all their love, care and support right from the beginning, especially to my brother Abbas whose positive words kept me going in tough times. A special thank you to my brother Sulman and an apology aswell for always bearing the brunt of my thesis-writing frustrations (always in the wrong place at the wrong time!). I would like to thank my sweet little sister Laila for actually looking interested by what I had to say and feeding me amazingly scrumptious desserts and my Ana 'babes' for being my little star and always being there for me, ready to help me in anything, listening to my many complaints and whining, for supporting me, encouraging me and telling me off aswell if need be!

This acknowledgement would be incomplete without thanking my parents, to whom this thesis is dedicated, for their unconditional love, support and encouragement not only for this study but in everything that I do and this thesis would not have been possible without them.

I had the opportunity to share every moment of this PhD, every up and every down with the most important person in my life, my husband Mehdi, without whom I would not have been able to complete this keeping my sanity intact (topic not open to discussion) ! I would like to thank you for all the positivity, encouragement, love, support and patience during this study, I would not have been able to sail through it in one piece without my lieutenant.

Last but not least I would like to thank God, for this opportunity, for the experiences of the past, the joys of the present and for hope of the future.

In remembrance of my loving grandparents Aboo, Amma and Pappa.

Table of Contents

List of Figures

Chapter 1

Chapter 2

Chapter 3

Chapter 4

Chapter 5

Chapter 6

List of Tables

Chapter 1

Chapter 2

Chapter 4

Chapter 5

Table of abbreviations

10C	3T3 Cell culture medium
53BP1	p53 Binding-Protein 1
8-oxo-dG	8-Oxo-2'-deoxyguanosine
A	Adenine
ALT	Alternate Lengthening of Telomeres
ARF	Alternate Reading Frame
ATM	Ataxia Telangiectasia Mutated gene
ATM	Ataxia Telangiectasia Mutated (serine/threonine protein kinase) ; activated by DNA double strand breaks and involved in DNA damage response
ATR	ATM and Rad-3 related ; activated by DNA double strand breaks and involved in DNA damage response
BCA	Bicinchoninic Acid Assay
BER	BASE Excision Repair
BICMS	Blizzard Institute of Cell and Molecular Sciences
Bmi1	B-lymphoma Mo-MLV insertion region 1 homolog
Bp	Base pair
cDNA	Complementary DNA
BRCA1	Breast cancer type 1 protein
BSA	Bovine serum albumin
C	Cytosine
CA2+	Calcium
Cdk	Cyclin-Dependent Kinase
CDOS	Centre for Diagnostic Oral Sciences
CHAPS	3-[(3-Cholamidopropyl)dimethylammonio]-1-Propanesulfonate
Chk1	kinase encoded by CHEK1 gene; involved in DNA damage response
Chk2	kinase encoded by CHEK2 gene; involved in DNA

	damage response
CKI	Cyclin-dependent kinase Inhibitor
CO_2	Carbon dioxide
CPD	Cumulative Population Doubling
Cy5	Cyanine 5
DAPI	4',6-diamidino-2-phenylindole
DDR	DNA Damage Response
d H_2O	Distilled water
DMEM	Dulbecco's Modified Eagle's Medium
DMSO	Dimethyl Sulfoxide
DNA	Deoxyribonucleic Acid
dNTP	Deoxyribonucleotide triphosphate
DSB	Double Strand Break
E	Ecotropic
E6, E7	Human papillomavirus proteins
EBV	Epstein-Barr Virus
ECM	Extra Cellular Matrix
EDTA	Ethylenediaminetetraacetic Acid
EGF	Epidermal Growth Factor
EGTA	Ethylene Glycol Tetraacetic Acid
ETOH	Ethanol
FACS	Fluorescence-Activated Cell Sorting
FAD	Keratinocyte medium; 10% FCII +DMEM+Hams F12 (3:1 ratio)
FAS	Apoptosis-Inducing Receptor
FBS	Fetal Bovine Serum
FCII	Fetal Clone II
FSC	Forward side scatter
G	Guanine
G_0	Gap 0 phase of the cell cycle

G_1	Gap 1 phase of the cell cycle
G_2	Gap 2 phase of the cell cycle
G418	Geneticin
GM	Growth medium
GM847	Telomerase negative cells
GSH	Glutathione
H2AX	Histone H2A ; contributes to nuclesome formation
H2O2	Hydrogen peroxide
HCL	Hydrochloric acid
HDM2	Human homologue of MDM2
Hela	Immortal cervical cancer cell line; named after patient taken from - Henrietta Lacks
HPV	Human Papilloma Virus
HR	Homologous Repair
HR	Homologous Recombination
Hr/min /sec	Hour/minute/second
hTERT	Catalytic subunit of telomerase; human TERT
HUC	Uroepithelial cells
IC	Internal Control
IF	Intermediate Filament
IgG	Immunoglobulin G
IRIF	Ionizing Radiation-Induced Foci
K1, K4, K5, K10	Types of keratins
KBM	Keratinocyte Basal Medium
KCL	Potassium Chloride
KGM	Keratinocyte Growth Medium
KSFM	Keratinocyte Serum Free Medium
M	Mitosis phase of the cell cycle
M0, M1, M2	Stages of Mortality
MDC1	Mediator of DNA-damage checkpoint protein 1

MDM2	Murine Double Minute 2
MeOH	Methanol
MGCL2	Magnesium chloride
mm Hg	millimeters of mercury; unit of pressure measurement
Mmlv	Moloney murine leukemia virus
MMR	Mismatch repair
mRNA	Messenger RNA
MTH1	MutT homologue 1
MTT	3-(4,5-Dimethylthiazol-2-yl)-2,5-diphenyltetrazolium bromide
MYH	Muty enzyme homologue
N	Normality
Nacl	Sodium chloride
NaOH	Sodium hydroxide
Neo	Neomycin
NFR	Nuclear Fast Red
NHEJ	Non-homologous end-joining
NHEK	Normal Human Epidermal Keratinocytes
NHOK	Normal Human Oral Keratinocytes
Nm	Nanometer
NP-40	nonyl phenoxypolyethoxylethanol 40
O2	Oxygen
O2--	Superoxide anion radical
OD	Optical Density
OGG1	8-Oxoguanine glycosylase; involved in base excision repair
-OH	Hydroxyl radical
OKF4	Immortalized Oral keratinocyte cell line
OKF6	Immortalized Oral keratinocyte cell line
$p14^{ARF}$	INK4A alternative reading frame protein

$p15^{INK4b}$	Cyclin-dependent kinase inhibitor 2B
$p16^{INK4a}$	Cyclin-dependent kinase inhibitor 2A
$p21^{WAF}$	Cyclin dependent kinase inhibitor 1A
p53	Tumour suppressor protein
PAGE	Polyacrylamide Gel Electrophoresis
PBS	Phosphate-Buffered Saline
PCR	Polymerase Chain Reaction
PD	Population Doubling
PE	PBS/EDTA
Ph E	Phoenix E
PI	Propidium Iodide
POT1	Protection Of Telomeres protein 1; part of shelterin complex proteins ; binds the telomeric double stranded TTAGGG repeat and negatively regulates telomere length and protects from chromosome instability
pRb	Retinoblastoma protein
PS	phosphatidylserine
PT67	Packaging cell line
Puro	Puromycin
PVDF Membrane	Polyvinylidene fluoride membrane
Q1234	Quadrant 1/2/3/4
Rad3	protein kinase; ; activated by DNA double strand breaks and involved in DNA damage response
RAP1	Ras related protein 1
Ras and HRAS	Harvey rat sarcoma virus oncogene
RIPA	Radioimmunoprecipitation assay
RNA	Ribonucleic acid
RNase	Ribonuclease
ROS	Reactive oxygen species
RS	Replicative senescence

RT	Room temperature
S	Synthesis phase of the cell cycle
SB	Stratum Basale
SC	Stratum Corneum
SCC	Squamous Cell Carcinomas
SD	Seeding Density
SDS	Sodium Dodecyl Sulfate
SEM	Standard Error of the Mean
Ser	Serine
SG	Stratum Granulosum
sh RNA	Small hairpin RNA
SMC-1	Structural Maintenance of Chromosome protein 1
SOD	Superoxide Dismutase
SS	Stratum Spinosum
SSB	Single strand break
SSE	Stratified Squamous Epithelium
SV40	Simian Virus-40
SVFHK	Immortalized cell line
Sw3T3	Swiss 3T3 cell line
T/EDTA	Trypsin/EDTA
TBS/TBS-T	Tris Buffered Saline (TBS-Tween 20)
TERT	Telomerase Reverse Transcriptase
TGF	Transforming Growth Factor
TEWL	Transepidermal waterloss
TIF	Telomere-dysfunction Induced Foci
TIN2	TRF1-interacting protein 2
TPP1	Tripeptidyl peptidase 1
TRAP	Telomere Repeat Amplification Protocol
TRF1	Telomere repeat binding factor 1 ; part of shelterin complex proteins ; binds the telomeric double stranded TTAGGG repeat and negatively regulates telomere

	length and protects from chromosome instability
TRF2	Telomere repeat binding factor 2 ; part of shelterin complex proteins ; binds the telomeric double stranded TTAGGG repeat and negatively regulates telomere length and protects from chromosome instability
TRIS	Tris(hydroxymethyl)aminomethane
TTAGGG	Tandem repeats of telomerase base sequence
UVB	Ultraviolet B
UVC	Ultraviolet C
WB	Western Blot
γ IR	Gamma irradiation
β-Gal	Beta-galactosidase
γH2AX	Phosphorylated form of H2AX

Chapter 1:

Introduction

Chapter 1

Introduction

1.1 Cell culture

Cell culture is a complex, multi step process by which cells are cultivated externally under controlled conditions outside their natural environment. The term cell culture has now come to refer to the culturing of animal cells derived from multicellular eukaryotes, in particular the culture of animal cells, but other cultures include plants, fungi and microbes including viruses, bacteria and protists (Abbott 2003). Animal cell culture became a common lab practice in the mid 1900's when techniques were advanced significantly to support research in virology for the manufacture of vaccines, with the polio vaccine being one of the first mass-produced product using cell culture techniques (Kevles and Geison 1995). Other research areas for which cell culture is used include drug discovery, cancer biology, regenerative medicine and basic life sciences. Cells can be isolated from tissues for *ex vivo* culture by either purification from blood (blood cells), released from soft tissue by enzymatic digestion (mononuclear cells) or explant culture (Abbott 2003). Cells cultured directly from an individual are known as 'primary' cells and these generally have limited lifespan in culture, known as the Hayflick limit, after which they stop dividing yet remain metabolically active, a phenomenon known as senescence (Campisi and d'Adda di Fagagna 2007). To overcome this barrier to cell lifespan and allow for the long term use of cell lines in research with little or no variation between samples, immortalized cell lines are used as they have the ability to proliferate indefinitely either through random mutation or deliberate modification of gene expression (Lee, Choi et al. 2004). In order to generate immortalized cell lines, it is important to understand the important proteins that regulate the cell cycle and the complex interplay that takes place between them to maintain cell homeostasis.

1.2 Cell cycle

DNA replication between cell generations occurs in an organised and orderly manner regulated by the cell cycle to ensure correct cell division. The standard cell cycle is comprised of four phases: the gap phase prior to mitosis, the gap phase post mitosis, the synthesis phase and the mitotic phase, known as G_1, G_2, S and M respectively (Vermeulen, Van Bockstaele et al. 2003) . G_1 , G_2 and S phases collectively comprise the 'interphase' part of cell division, at times including periods of inactivity termed Gap phase zero (G_0), wherein the cell is constantly synthesizing RNA, producing protein and growing in size prior to advancing into M phase where it divides (Vermeulen, Van Bockstaele et al. 2003). The cell cycle is regulated tightly by key regulatory proteins called cyclin-dependent kinases (cdks), a family of serine/threonine protein kinases that are activated at specific points of the cell cycle (Kahl and Means 2003). Cdks regulate the cell cycle by inducing downstream processes and phosphorylating selected proteins and are constantly being activated and deactivated by association with regulatory subunits known as 'cyclins' (Denicourt and Dowdy 2004) . It is this sequential activation and inactivation of cdks through the periodic synthesis and destruction of cyclins that provides the primary means of the cell cycle regulation (Johnson and Walker 1999); (Fig 1.1) and the various functions (table 1.1)

Cyclin	CDK	Function
Cyclin D1,2,3	CDK2,6	Required for cell entry into G_1 phase
Cyclin E	CDK 2	Progression from G_1 into S phase
Cyclin A	CDK1	Permits entry into M phase
Cyclin B	CDK1	Regulation of G2/M phase
Cyclin C	CDK8	Assumed to be involved in mammalian transcription apparatus

Table 1.1: Functions of cyclin-CDK complexes within the cell cycle.

All cyclins contain a common region of homology involved in binding and activating cdks, known as the cyclin box (Johnson and Walker 1999). Apart from regulating progression through the phases of the cell cycle, some cyclins form complexes that regulate their own proteolysis, for example cyclins A and E contain a 'destruction box' whilst cyclins D and E contain a PEST sequence rich in proline, glutamic acid, serine and threonine residues, which is required for efficient ubiquitin-mediated cyclin proteolysis at the end of a cell cycle phase (Vermeulen, Van Bockstaele et al. 2003). Not all cyclin-CDK have cell cycle regulatory functions, however, and other roles include regulation of transcription, DNA repair, differentiation and apoptosis for example; several cyclin-cdk complexes such as cyclin C-cdk8 and cyclin H-cdk7 have been found to be components of the basal transcription machinery (Johnson and Walker 1999).

Cdk activity is regulated by cdk inhibitors (CKI) which bind to cdk-cyclin complexes or cdk alone and inhibit their function. Based on their sequence homology and functions within the cell cycle, CKI are divided into two distinct families; the CIP/KIP family that includes p21 and the INK4 family that includes $p16^{INK4a}$ (Denicourt and Dowdy 2004). The INK4 family includes p15 (INK4b), p16 (INK4a), p18 (INK4c) and p19 (INK4d), which specifically interact with cdk4 and cdk6 but not the other cdks (Sherr 2000). Binding of INK4 proteins prevents the association of cdk4 and cdk6 with the D type cyclins thereby preventing entry into G_1 phase of interphase. The second family of inhibitors, the Cip/Kip family includes p21 (Waf1, Cip1), p27 (Cip2), p57 (Kip2) (Johnson and Walker 1999). Whilst the INK4 family of CKI form stable complexes with the CDK enzyme before cyclin binding, thereby preventing association with cyclin D, the Cip/Kip CKI inactivate CDK-cyclin complexes by acting on a wider spectrum of cyclin-CDK complexes (Denicourt C, 2004).

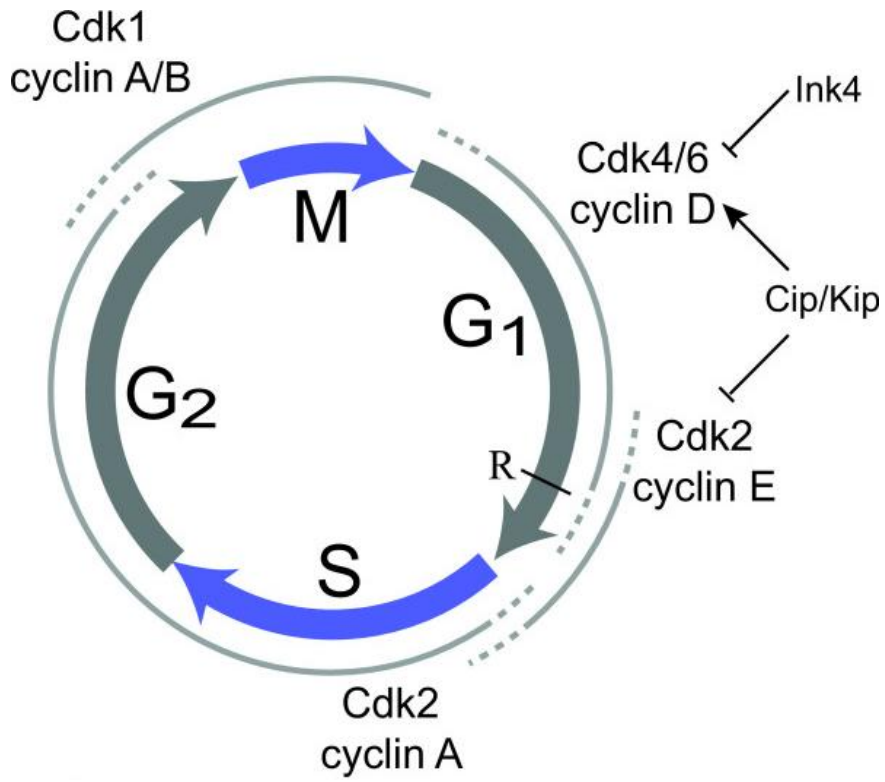

Figure 1.1: **Role of cdk-cyclins and CKI in cell cycle regulation.**

Each phase of the cell cycle is regulated by a particular cdk-cyclin complex. G_1, G_2 and S are part of 'interphase', regulated predominantly by cyclin D and E, followed by cellular division in M under regulation of cyclin A. CKI from INK4 family interact specifically with cdk4 /6, preventing association with cyclin D and subsequent entry into G_1, whilst members of the Cip/Kip family act as negative regulators of G_1 by acting upon a wider spectrum of cyclin-cdk complexes (Figure obtained from Johnson and Walker 1999).

1.3 INK4a locus: $p16^{INK4a}$ and $p14^{ARF}$

The CDKN2A locus on human chromosome 9p21 (mouse chromosome 4) encodes two distinct proteins translated from alternatively spliced mRNAs. The products of the α transcript is $p16^{INK4a}$, a recognized tumour suppressor and inhibitor of G_1 through cyclin D-dependent kinases cdk4 and cdk6. $p16^{INK4a}$ is responsible for inducing a G_1 cell cycle arrest by inhibiting the phosphorylation of the retinoblastoma protein (protein Rb) through the actions of cdk4 and cdk6 (Sherr 2000). In contrast, the product of human CDKN2A β transcript, designated as originating from the 'Alternative Reading Frame' (ARF), $p14^{ARF}$, activates a p53-dependent response causing cell cycle arrest in both G_1 and G_2/M through its actions on MDM2 and $p21^{WAF1}$ (Sherr 2001). $p14^{ARF}$ requires a functional p53 gene to exert its cell cycle regulatory effects and seems to work by affecting p53 stability, causing it to accumulate, resulting in cell cycle arrest. $p14^{ARF}$ has also been shown in the direct accumulation of p53 in response to senescence induced by oncogene activation (Zuckerman, Wolyniec et al. 2009). Although functionally similar, the primary amino acid sequences of both $p16^{INK4a}$ and $p14^{ARF}$ are completely unrelated and bear no homology, with $p14^{ARF}$ functioning as a distinct gene (Sherr 2006). As the coding regions of these two genes have been found to overlap, homozygous deletions of $p16^{INK4a}$ simultaneously appear to disrupt $p14^{ARF}$ functions as well, emphasizing the importance of the INK4a locus in carcinogenesis.

The involvement of $p16^{INK4a}$ in the development of human tumours was implied by the observation that the INK4a locus is mutated in many tumour derived cell lines and maps to a chromosomal region frequently altered in human malignancies (Serrano, Lee et al. 1996). One of the main and critically important substrates of the cyclin D-dependent kinases is the retinoblastoma protein (pRb) that is able to prevent entry into the S phase of the cell cycle by blocking the E2F transcription factors (Sherr 2001). Phosphorylation of pRb, catalysed by cdks D and E, allows the progression into S phase by disrupting the suppression of the E2F transcription factors and permitting activation of genes needed for DNA replication and

nucleotide metabolism, thereby allowing G_1 exit (Sherr 2001). $p16^{INK4a}$ directly inhibits the activities of cdk4 and cdk6 that maintain pRb in its active and non-proliferative state. The functional disruption of these tumour suppressors along with the over-expression of cyclin D1 and cdk4, occurs in many human cancers (Geradts and Wilson 1996, Tanaka, Fujii et al. 1998, Chen, Chen et al. 2001). The majority of point mutations found in the INK4a locus are nonsense whilst a second type of $p16^{INK4a}$ inactivation consists of large homozygous deletions that eliminate the INK4a locus with INK4b partly involved in some cases (Serrano, Lee et al. 1996).

$P16^{INK4a}$ is now recognized as a major tumour suppressor because of its regulation of the oncogene cyclin D1 and loss of INK4a function seems to provide cells with a proliferative advantage and $p16^{INK4a}$ is frequently inactivated in a variety of human cancers (Azechi, Nishida et al. 2000). Furthermore, inherited INK4a mutant alleles that inactivate $p16^{INKa}$ predispose individuals to the development of malignancies (Serrano, Lee et al. 1996) . $p16^{INK4a}$ has also been shown to accumulate when primary cells are propagated in culture, suggesting that it participates in the G_1 cell cycle arrest in replicative senescence.

1.4 p53 tumour suppression pathway

The importance of the p53 protein in suppressing tumour development is illustrated by the fact that it is disrupted in approximately 50% of human cancers (Hofseth, Hussain et al. 2004) and acts to prevent aberrant cell proliferation. p53 is one of the most extensively studied tumour suppressors and acts in response to various DNA stressors, such as DNA damage and hypoxia, to mediate many anti-proliferative processes (Levine 1997). Owing to a relatively short half life, p53 levels are usually low within the cell and rapidly increase in response to intra and extra cellular stress signals. This in turn promotes the stabilization and activation of p53 bringing about tumour suppressive processes such as cell cycle checkpoints, cellular senescence and apoptosis. Conversely, disruption in p53 regulation promotes checkpoint defects, cellular immortalization, genomic instability and inappropriate cell survival by allowing continued proliferation and evolution of damaged cells (Levine 1997). Furthermore, it is important to note that apart from inactivation, chronic activation of p53 is also deleterious since hyperactivation of p53 is associated with many degernative diseases such arthritis and multiple sclerosis (Michael and Oren 2002). Considering the lethal affects of incorrect p53 levels, it is not surprising that there is a tightly regulated system in place that is responsible for maintaining p53 homeostasis.

As mentioned, p53 expression is induced by both intra and extra cellular stress signals however both these utilize different pathways to bring about p53 expression. In response to DNA damage and strand breaks following ionizing or ultraviolet radiation, p53 is activated via the ataxia telangiectasia mutated (ATM) pathway. ATM is an kinase whose substrates include CHK1 and CHK2 proteins, which, upon phosphorylation by ATM, phosphorylate their own targets, including p53 (El-Deiry 1998). Activated p53 transactivates downstream target genes including $p21^{WAF1}$, responsible for inhibiting CDK2 and obstructing the activity of CDK2-Cyclin E complexes, thereby preventing the cell cycle progression from G_1 to S phase (Meek 2004).

Apart from ATM pathway, p53 is also activated by the $p14^{ARF}$-MDM2-p53 pathway (Fig 1.2) where internal aberrations such as abnormal oncogene activation stabilizes and activates p53. The cyclin-dependent kinase inhibitor $p21^{WAF1}$ is encoded in humans by the CDKN1A gene, located on chromosome 6 and it binds to and inhibits the activity of CDK1, thereby functioning as a regulator of cell cycle progression at G_1 checkpoint. The expression of $p21^{WAF1}$ is tightly controlled by p53 and it mediates cellular senescence by directly inhibiting the activity of cyclin E /cdk2 and cyclin D cdk4/6 complexes and blocking cell cycle progression from G_1 into S (Itahana, Dimri et al. 2001). $p21^{WAF1}$ is thought to be a major executor of the p53-dependent cell cycle arrest in response to DNA damage and past studies have shown that disruption of $p21^{WAF1}$ extends the lifespan of human diploid fibroblasts (Kaul, Reddel et al. 2000). p53 also transcribes its own negative regulator called MDM2 (referred to as HDM2 in humans) that is responsible for terminating the p53 response. Overexpression of certain oncogenes can induce expression of $p14^{ARF}$, which inactivates MDM2 and blocks the degradation of p53, thereby activating it and inducing either cell cycle arrest or apoptosis (Itahana, Dimri et al. 2001). The binding of MDM2 to p53 induces its ubiquitylation, followed by its exportation from the nucleus to the cytoplasm and subsequent degradation, thus preventing unnecessary cell death by antagonizing its transcriptional activity (Kamijo, Weber et al. 1998). MDM2, in turn, is subject to negative control by $p14^{ARF}$ that directly associates with MDM2, blocking its ability to interact with p53 through the localization of MDM2 within the nucleolus and inhibition of its ubiquitin protein ligase activity (Sherr 2001). This negative feedback loop blocks progression of the cell cycle until the DNA can be repaired or alternatively, if the damage is extensive then the cell enters apoptosis. Loss of $p14^{ARF}$ by homozygous mutation of the INK4a gene will lead to elevated levels in MDM2 and therefore loss of p53 function and cell cycle control (Kamijo, Weber et al. 1998).

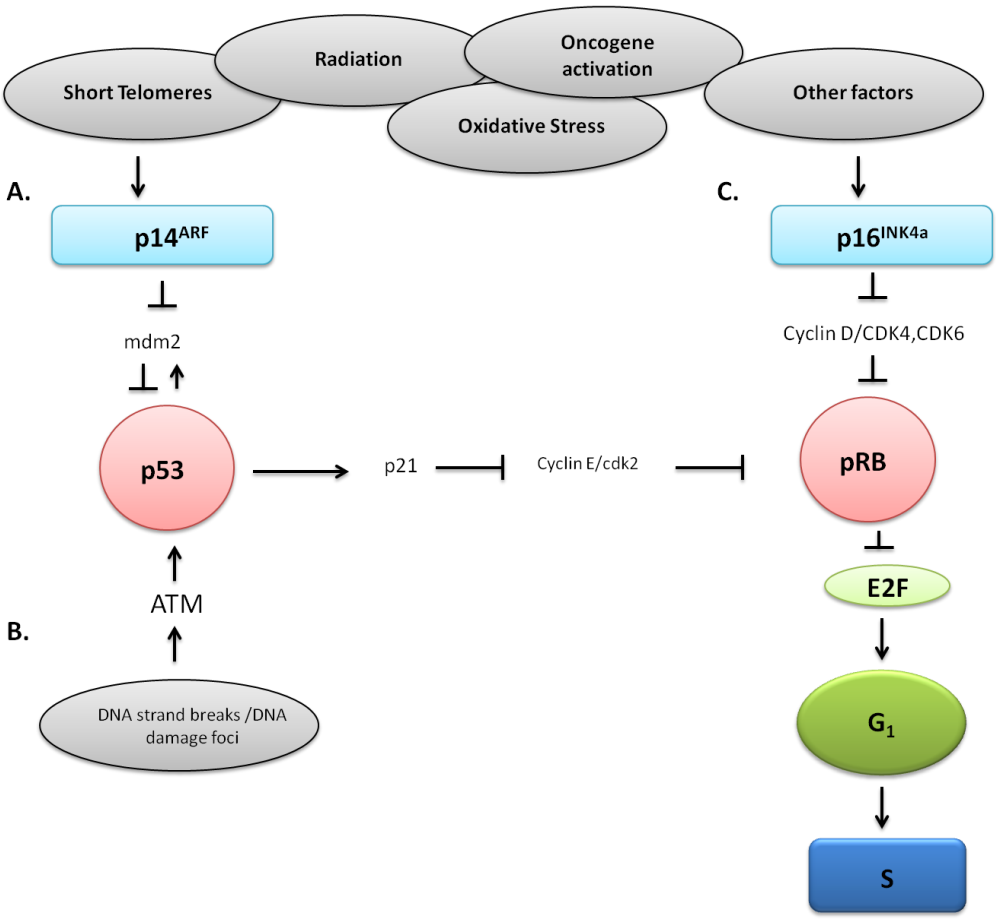

Figure 1.2 : Cell cycle arrest via the INK4a/ARF tumour suppressive pathway.

Tumour suppressive activity of p53 and pRb is regulated by the products of the INK4a/ARF locus. **A)** Under normal cellular conditions p53 is maintained at relatively low levels but rapidly accumulates in response to cellular stress, triggering either cell cycle arrest or cell suicide. (Levine 1997). p53 is negatively regulated by p53-responsive gene MDM2 which in turn is under regulation by $p14^{ARF}$, that gets activated in response to DNA damage signals and blocks the ability of MDM2 to bind to p53 **B)** In response to stimuli such as telomere shortening, ATM/Chk2 is activated to phosphorylated p53 and its downstream targets, mainly $p21^{WAF1}$ tumour suppressor to inhibit cyclin E/Cdk2 complex that prevents phosphorylation of pRb, resulting in a G_1 cell cycle arrest. **C)** Phosphorylation of pRb by cyclin-D dependent kinases permit the cell to progress into S phase. The up regulation of $p16^{INK4a}$ in response to DNA signals and its subsequent inhibition of cyclin-D dependent kinases prevents pRb phosphorylation and thus results in G_1 cell cycle arrest.

In relation to cancer, MDM2 is over expressed in 5%-10% of human cancers whereas ARF is silenced or deleted in many others, highlighting the importance of the ARF-MDM2-p53 signalling pathway (Michael and Oren 2002). ARF is induced by oncogenes such as *Myc*, mutated *Ras* and *v-Abl* which results in p53 activation, re-routing cells that have acquired oncogenic damage to alternative fates such as growth arrest or apoptosis. Subsequently, the loss of ARF or p53 eliminates this 'tumour surveillance' mechanism , instead allowing oncogenes to drive proliferation in a manner that favours uncontrolled cell growth and rapid tumour formation (Sherr 2001).

1.5 Bmi1

B-cell-specific moloney murine leukemia virus integration site 1, Bmi1, is part of the polycomb group of genes that are epigenetic suppressors of gene expression and play a central role in mammalian development (Lee, Adhikary et al. 2007). Bmi1 is expressed in the basal and suprabasal layers of the epidermis and is located in the nucleus of cultured keratinocytes where it promotes cell survival and protects against stress mediated apoptosis (Ross, Parker et al. 2008). Bmi1 appears to work by suppressing the INK4a/ARF locus expression, increasing levels of cyclin D1 and selected cdks at the same time as reducing caspase activity. Disruption of Bmi1 action has profound effects on development, for example; it has been suggested that Bmi1 may enhance tumour cell proliferation/cell survival by repressing transcription of $p16^{INK4a}$ and $p14^{ARF}$ (Dimri, Martinez et al. 2002). Bmi1 has also been shown to induce telomerase activity, suggesting a role in the regulation of normal cell physiology as well as a pro-survival proliferation factor in hyperproliferative diseases and epithelial cancer (Dimri, Martinez et al. 2002). A study conducted by Kang *et al* (2007) demonstrated enhanced levels of Bmi1 protein and RNA expression in cells of oral squamous cell carcinomas when compared to normal human oral keratinocytes, thus reinforcing its role in carcinogenesis (Kang, Kim et al. 2007).

1.6 Senescence

Senescence is the permanent, irreversible state of growth arrest wherein cells lose the ability to proliferate and divide yet remain metabolically active. Senescent cells display altered morphological and physiological properties and are part of the tumour suppression mechanism (Campisi and d'Adda di Fagagna 2007).

1.6.1 The hayflick limit

Normal cells have a limited ability to proliferate in culture and after initial cell division the growth rate gradually starts to decline until all cells in the culture lose their ability to divide, and this is referred to as the 'hayflick limit' (Campisi and d'Adda di Fagagna 2007). The hayflick limit is named after Lenoard Hayflick who demonstrated in 1961 that embryonic stem cells can divide only a finite number of times in culture with an average of 50 cumulative population doublings (CPD) whereby they were termed as having reached replicative senescence (RS) (Campisi and d'Adda di Fagagna 2007). Although senescence was initially demonstrated in fibroblasts, it has since been observed and characterized in a variety of other cell types such as keratinocytes, lymphocytes and endothelial cells (Erusalimsky and Kurz 2005). Senescence appears to have been derived as a tumour suppressive mechanism along with a simultaneous role in cellular ageing where it slows down tissue regeneration. This phenomenon is known as antagonistic pleiotropy, wherein genes or processes that were selected to benefit the health and fitness of young organisms can have unselected, deleterious effects that manifest in older organisms and promotes ageing (Campisi and d'Adda di Fagagna 2007).

One of the main hallmarks of senescence is the inability to progress through the cell cycle as the cells fail to initiate DNA replication despite adequate growth conditions. Senescent cells also acquire resistance to certain apoptotic signals such as those caused by growth factor deprivation and oxidative stress but are not able to resist apoptosis caused by the engagement of the FAS death receptors (Higami

and Shimokawa 2000). The senescence phenotype is induced by multiple stimuli, also known as 'stressors', that include dysfunctional telomeres, non-telomeric DNA damage, excessive mitogenic signals and non-genotoxic stress (Lloyd 2002). Despite such a tightly regulated senescence mechanism, cells have been found to evade senescence and exhibit an infinite lifespan. These cells are termed 'immortal' and are generally thought to have been derived from tumours.

1.6.2 Replicative senescence

Replicative senescence (RS) is an fundamental feature of all somatic cells and the number of division a cell undergoes is determined by species, age, genetic background and cell types, for example human keratinocytes generally have a replicative lifespan of between 30–50 population doublings (PD) whilst human foetal cells have been shown to reach upto 60-80 PD before senescing (Harley and Sherwood 1997). The senescence growth arrest occurs with a G_1 DNA content and cells are prevented from entering the S phase of the cell cycle, turning unresponsive to growth-promoting stimuli yet remain metabolically active for long periods (Cristofalo and Pignolo 1993). Morphologically, senescent cells demonstrate a large and flattened morphology with enlarged nucleoli and an increased number of lysosomes and golgi apparatus (Cristofalo, Lorenzini et al. 2004). Senescent cells have been shown to express acidic β galactosidase (β gal) enzymatic activity and express high levels of cell cycle inhibitory proteins, used as markers of senescence activity within cells (Dimri, Lee et al. 1995).

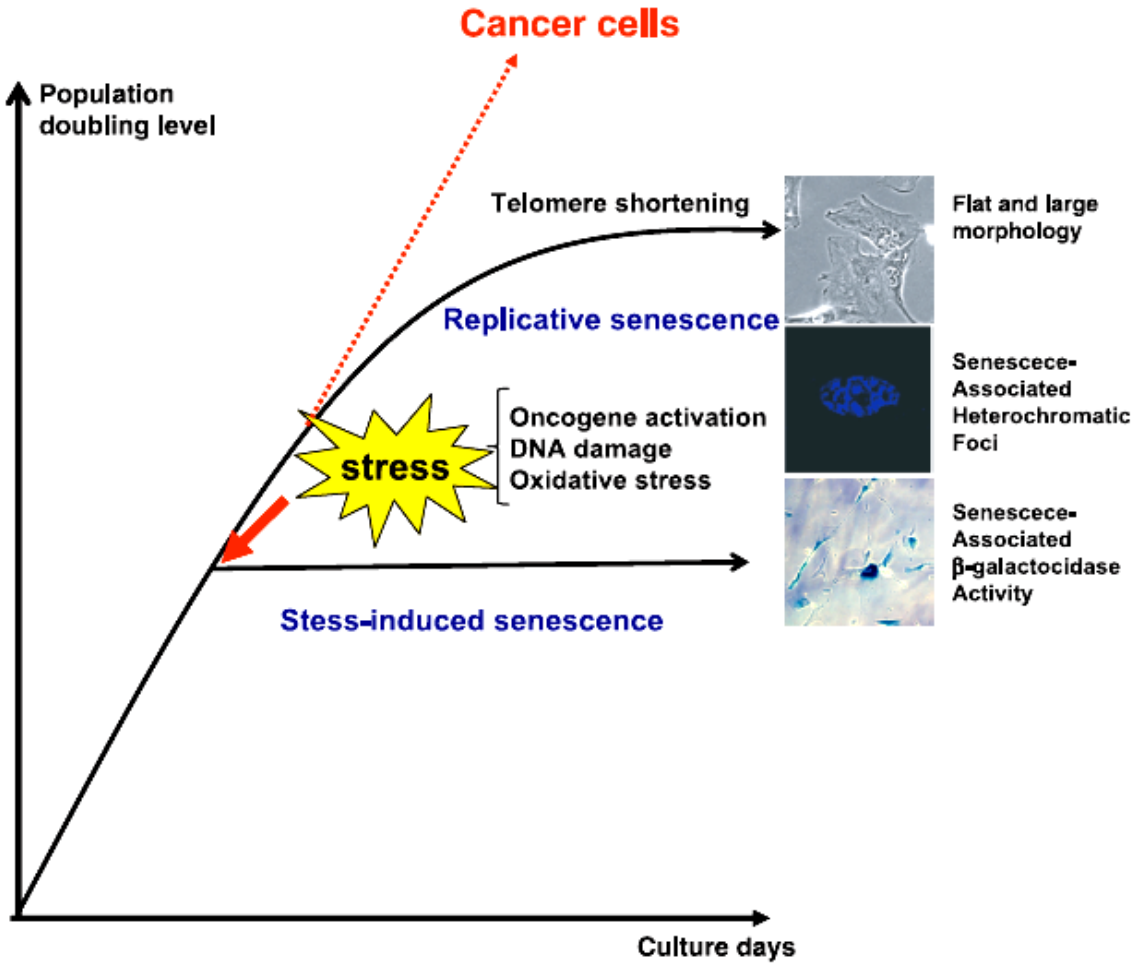

Figure 1.3 : Relationship between population doublings and cellular Senescence.

As cells are sub-cultured *in vitro*, they undergo a finite number of cell divisions before entering a state of irreversible growth arrest termed as senescence, caused by telomere shortening with each cell division. Senescence can also be induced prematurely by cellular stress on the cell such as oncogene activation, DNA damage and oxidative stress. Senescent cells can be recognised in a mixed population by their large and flat morphology; senescence associated heterochromatin foci (DAPI foci in blue); and senescence associated β gal staining (blue). Immortal cells such as cancer cell lines are capable of by-passing senescence and proliferating indefinitely (image obtained from (Ohtani, Mann et al. 2009).

1.6.3 Telomere dependent senescence

Telomeres are stretches of repetitive DNA and associated proteins that cap the ends of linear chromosomes and allow for the cell to distinguish between a chromosome end and a potentially catastrophic double strand break (DSB) (Bailey, Meyne et al. 1999). In the absence of telomeres, chromosomes tend to be highly unstable thus leading to potential loss of heterozygosity, chromosomal deletions and translocations, hence telomeres act to stabilize chromosomes by protecting them from degradation, recombination or random fusion by cellular DNA repair systems (Campisi, Kim et al. 2001).

Telomere-dependent senescence is the inevitable result of the progressive shortening of telomeres that occurs after each cell division. Mammalian telomeres are thought to end in large circular structures termed the 't-loop' due to the 'end replication problem', wherein standard DNA polymerases cannot completely replicate these DNA ends and cells end up losing 50-200 base pairs of telomeric DNA in each S phase of cell cycle (Bolzán and Bianchi 2006). These 'critically short' telomeres are able to trigger the DNA damage response (DDR) by forming DNA damage foci containing γH2AX, enabling cells to sense damaged DNA and respond by arresting cell-cycle progression to repair the damage. These foci, when co-localised with dysfunctional telomeres, are called telomere dysfunction induced foci, (TIFs) (Takai, Smogorzewska et al. 2003). Other proteins involved in the DDR include protein kinase ataxia telangiectasia mutated (ATM) and adaptor proteins such as p53 binding protein 1 (53BP1), with many of these proteins localising to the DNA damage foci detected in senescent cells (Campisi and d'Adda di Fagagna 2007).

It was first proposed in the early 70's by Olovnikov that chromosomal ends are unable to proliferate without the presence of the specific enzyme telomerase (Olovnikov 1996) but it was not until later that senescent cells were shown to have shorter telomeres as compared to their pre-senescent counter parts (Harley and

Sherwood 1997). As mentioned, RS is a feature of somatic cell lines, and in contrast germ lines exhibit longer telomeres due to the presence of telomerase, thus accounting for their long telomeric length despite rapid cell turnover rates (Kim, Kaminker et al. 2002). Evidence that telomere shortening can induce RS was provided by the introduction of the human telomerase catalytic protein unit, hTERT, into normal human cells resulting in telomerase activity, telomere maintenance and indefinite cell proliferation (Campisi, Kim et al. 2001, Kim, Kaminker et al. 2002, Minty, Thurlow et al. 2008, Cesare and Reddel 2010) . Evidence has also been provided *in vivo*, with telomerase deficient mice supporting the idea that short telomeres promote senescence (Campisi 2003). In keeping with the idea of short telomeres determining cellular lifespan, studies have also suggested a link between senescence and ageing, with studies showing a correlation between *in vitro* lifespan of cells with the age of the donor, the correlation between *in vitro* lifespan with the average life expectancy of the species and the reduced *in vitro* life span of cells from patients afflicted with premature ageing syndromes (Sedivy 1998).

It is important to distinguish senescence from quiescence, which is the normal physiological withdrawal of the cell from the cell cycle that is displayed by almost all cells. Unlike senescence, quiescence is a reversible process whereby stimulation with proper growth factors results in resumption of proliferation (Sedivy 1998).

1.6.4 Telomere-independent senescence

Although extensive evidence has confirmed the presence of a 'mitotic clock' monitoring cell divisions and initiating senescence, it is clear that senescence is not simply the end result of shortened telomeres. A variety of physiological stimuli can also provoke a cell to enter senescence independent of telomere length including extensive passage in culture, exposure to oxidative DNA damage or activation of an oncogene (Hanahan and Weinberg 2000). Furthermore, telomere shortening is not

a consistent measure of senescence as the rate of telomere erosion varies between cells during *in vitro* culture and there is no consistent telomere length at which senescence occurs (Hanahan and Weinberg 2000). Perhaps major evidence in support of an alternative senescence mechanism came from studies with hTERT, in which ectopic expression of hTERT in keratinocytes and other epithelial cell types restored telomerase enzymatic activity and telomere length but still did not allow the cells to evade senescence (Sharpless 2004). Apart from the factors mentioned above, non-telomere related inducers of senescence include DNA damage such as ultraviolet radiation, oxidative damage resulting in the generation of ROS as well as oxygen tension whereby the culture of cells in conditions of mild hyperoxia shortens replicative lifespan and conversely cells cultured in low oxygen exhibit extended lifespan and delayed senescence (Ben-Porath and Weinberg 2005). In keeping with its proposed role in tumour suppression, activation of oncogenes such as *Ras* has been shown to illicit a senescent-like state in cells wherein the cells are phenotypically similar to senesced cells with a flattened morphology and presence of β gal activity along with the induction of cell cycle inhibitory proteins (Cristofalo, Lorenzini et al. 2004).

A number of regulatory proteins have been proposed to be involved in the non-telomere dependent senescence mechanism. In keratinocytes and other epithelial cell types, senescence has been found to be associated with the expression and accumulation of $p16^{INK4a}$ during culture and indicates an increase in $p16^{INK4a}$ levels with passage in culture. Studies of cells that have bypassed senescence demonstrate loss of $p16^{INK4a}$ expression and have established that immortalization of human skin keratinocytes cannot be achieved by expression of telomerase alone, but requires the additional inactivation of the $p16^{INK4a}$/pRb pathway (Rheinwald, Hahn et al. 2002). Another gene implicated in senescence is $p14^{ARF}$ and as discussed previously, $p14^{ARF}$ contributes to senescence by directly binding to and sequestering MDM2 and inhibiting its capacity to induce degradation of tumour suppressor p53, inducing a p53-mediated growth arrest or apoptosis. Bmi1 over expression has

been shown to down regulate both $p16^{INK4a}$ and $p14^{ARF}$, resulting in the immortalization of mouse embryonic fibroblasts and suggesting that Bmi1 may co-operate with hTERT in immortalization of human epithelial cells (Haga, Ohno et al. 2007). The involvement of the $p16^{INK4a}$ and pRb pathway is brought about in response to cellular stresses and signalling imbalances irrespective of telomere status (Guney, Wu et al. 2006). The important role of the INK4a locus in senescence and cell immortalization is illustrated by repeated findings in cancers and human immortalized cell lines wherein this locus is frequently deleted or silenced and both the $p16^{INK4a}$/pRb and the $p14^{ARF}$/p53 pathways are inactivated in a single event, promoting unlimited cell proliferation.

1.7 Oral Mucosa

Human epithelia are tissues composed of cells which line the surfaces of the body and are classified into different groups according to their structural properties and the amount of layers they are composed of. The oral mucosa consists of squamous (flat and thin) epithelial cells arranged in a multilayer and therefore classified as a stratified squamous epithelium (SSE) (Squier and Kremer 2001). The main cell type of the oral mucosa is the keratinocyte, cells filled with cytokeratins and tightly linked with each other by desmosomes. The complex, multilayered epithelia part of this SSE is a direct result of the cell proliferation and differentiation pattern across the multiple cell layers. This proliferation occurs mainly in the cells located at the lowermost layers of the epithelium and is gradually restricted as cells migrate upwards towards the outermost epithelial layers (Squier and Brogden 2011). Differentiation is said to be initiated as soon as the cells start migrating upwards throughout the layers of the SSE, ultimately giving rise to terminally differentiated squames which line the outer visible surfaces of the tissue (Squier and Kremer 2001).

The oral mucosa has two layers: the oral epithelium and the lamina propria, also known as oral connective tissue. In certain areas of the oral cavity such as the lips and cheeks there is a layer of loose fatty or glandular connective tissue called the submucosa. This contains the major blood vessels and nerves of the oral mucosa and therefore determines the flexibility of its attachment to the underlying structures (Squier and Brogden 2011). In contrast, other areas of the oral mucosa such as the gingival lack the submucosa thus creating a firm and inelastic attachment to the surface of the bone, the periosteum, which is called the mucoperiosteum (Liu, Bian et al. 2010).

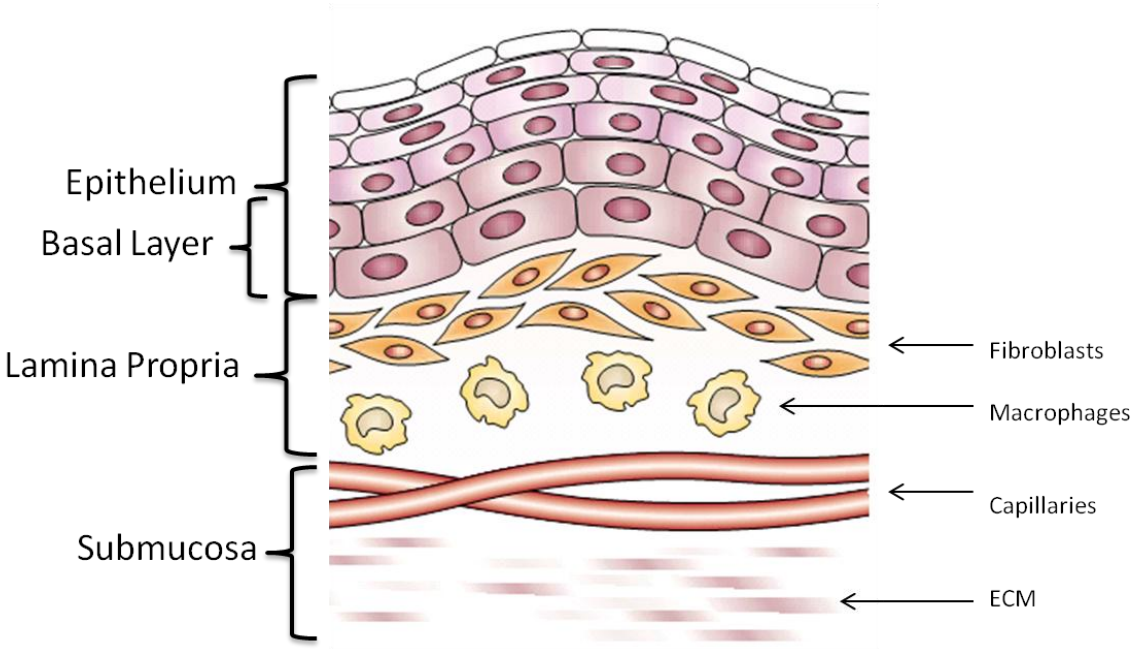

Figure 1.4 : The structure of the oral mucosa.

The diagram illustrates the multi layered human oral epithelium consisting of the epithelium, the lamina propria and in some subtypes, the submucosa (Image obtained from Squier and Brogden 2011).

The human oral mucosa can be divided into three functionally and structurally different subtypes:

1. **Masticatory Mucosa** (keratinized): found in areas that come into primary contact with food and therefore subjected to mechanical forces associated with mastication, such as the hard palate and gingival. The keratinized masticatory mucosa is tightly attached to the underlying tissues by the collagenous lamina propria.

2. **Lining Mucosa** (non-keratinized): found in areas that require flexibility for proper functioning such as the mouth and cheeks (buccal), the non keratinized lining mucosa consists of elastic connective tissue to facilitate functions such as chewing and swallowing.

3. **Specialized Mucosa** (keratinized and non-keratinized): Located on the dorsum of the tongue, the specialized mucosa consists of more specialized structures such as taste receptors.

The average surface area of the oral mucosa is 214 cm^2, of which the lining mucosa represents ~ 60% , while masticatory and specialized mucosa cover ~25% and ~15% respectively (Collins and Dawes 1987). The anatomical distribution of the oral mucosa is shown in Figure 1.5.

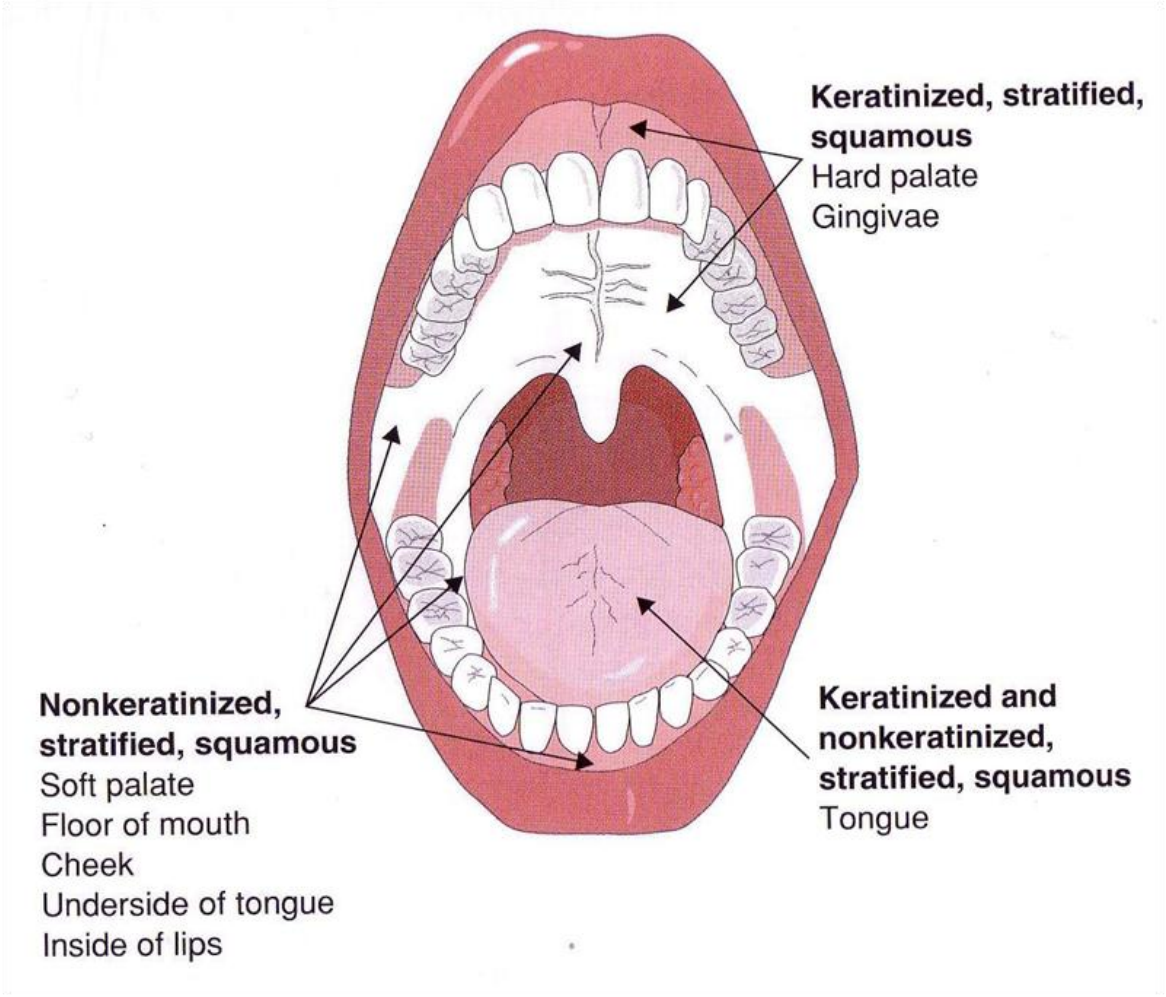

Figure 1.5 : The distribution of the different types of oral mucosal epithelium within the oral cavity.

The diagram shows the anatomic locations and extent of the masticatory (keratinized epithelium), lining (non-keratinized epithelium) and specialized mucosa (keratinized and non-keratinized) in the oral cavity (Allam, Stojanovski et al. 2008) .

Apart from epithelial cells, many regions of the oral epithelium contain other cell types including melanocytes, langerhans cells and inflammatory cells such as lymphocytes (table 1.2). These cell types represent approximately 10% of the cell population in the oral epithelium (Allam, Stojanovski et al. 2008).

Cell Type	Location within Oral Mucosa	Function
Melanocytes	Basal layer	Specialized pigment cells that produce melanin which contribute to the colour of the oral mucosa and blood haemoglobin.
Langerhans' Cells	Suprabasal layer	These are dendritic cells originating from the bone marrow with the ability to penetrate the oral mucosa and migrate to lymph nodes. They are immune cells that recognise and process antigens which enter the epithelium and present them to helper T-lymphocytes.
Merkel Cells	Basal layer	These are sensory cells responding to touch and are characterized by small, membrane-bound vesicles in their cytoplasm.
Inflammatory Cells	Nucleated cell layers	These include mainly lymphocytes along with macrophages, leukocytes and mast cells.

Table 1.2: Functions of different cell types present in the oral epithelium (Squier and Kremer 2001).

1.7.1 Epithelium Differentiation

The differentiation process of the human oral mucosa shares many similarities with the human epidermis in terms of structure and sequential differentiation and hence oral epithelial differentiation is often understood with reference to the epidermal model of epithelial cell renewal.

The human oral SSE is composed of four distinct cell layers which show considerable site and type-related variability between the different mucosal linings (table 1.3). The cell layers include the basal layer (stratum basale, or SB), spinal layer (stratum spinosum, or SS), granular layer (stratum granulosum, or SG) and the surface cornified layer (stratum corneum, or SC) (Fig 1.6). All epithelial cells mature to terminally differentiated squames although the differentiation paths can vary between the types of mucosa (Squier and Kremer 2001).

Type of Epithelium	Differentiation Pattern	Stratification
Masticatory Mucosa **eg: hard palate, gingival**	Keratinized	4-layered; SB, SS, SG, SC The cuboidal/columnar SB cells are separated from the connective tissue by basal lamina membrane; the SS is characterized by many layers of oval to polygonal cells; the cells of the SG contain keratohyalin granuoles; the SC has thin flat cells devoid of nuclei and filled with soft keratin.
Lining Mucosa **Eg; buccal**	Non keratinized	3-layered; SB,SS, SF SB and SS cells (as above); cells of the SF are small with flat oval nuclei with a papillary and recticular layered filled lamina propria.
Specialized Mucosa **Eg; tongue**	Non keratinized	Epithelial papillae organization; vast majority of papillae is filiform papillae (thread-like extensions of the epithelium); fungiform papillae (few mushroom shaped structures near tip of tongue); foliate papillae (approximately 4-11 located on the lateral posterior side of the tongue and these contain taste buds).

Table 1.3: The differentiation pattern of human oral epithelia according to their anatomical site (Squier and Brogden 2011).

The multi layered oral epithelium represents a progressive process of cell maturation. As cells move upwards through the layers they undergo a constant process of maturation and differentiation with the keratinocytes in the basal layer of the SSE retaining the ability for DNA synthesis and mitosis (Squier and Brogden 2011). As soon as the basal cells start to migrate upwards through the suprabasal layers towards the outer epithelial tissue surfaces there is the onset cessation of cell proliferation through the layers. This process of keratinization is called epithelial turnover that begins with mitotic division of basal keratinocytes and continuously occurs within the epithelial tissue (Liu, Bian et al. 2010). The turn over time varies between the different mucosal surfaces with the lining mucosa having a turnover time of approximately 10 days, the masticulatory mucosa slightly more than 10 days and the specialized mucosa having turnover of around 5 days (Shellis and Berkovitz 2009).

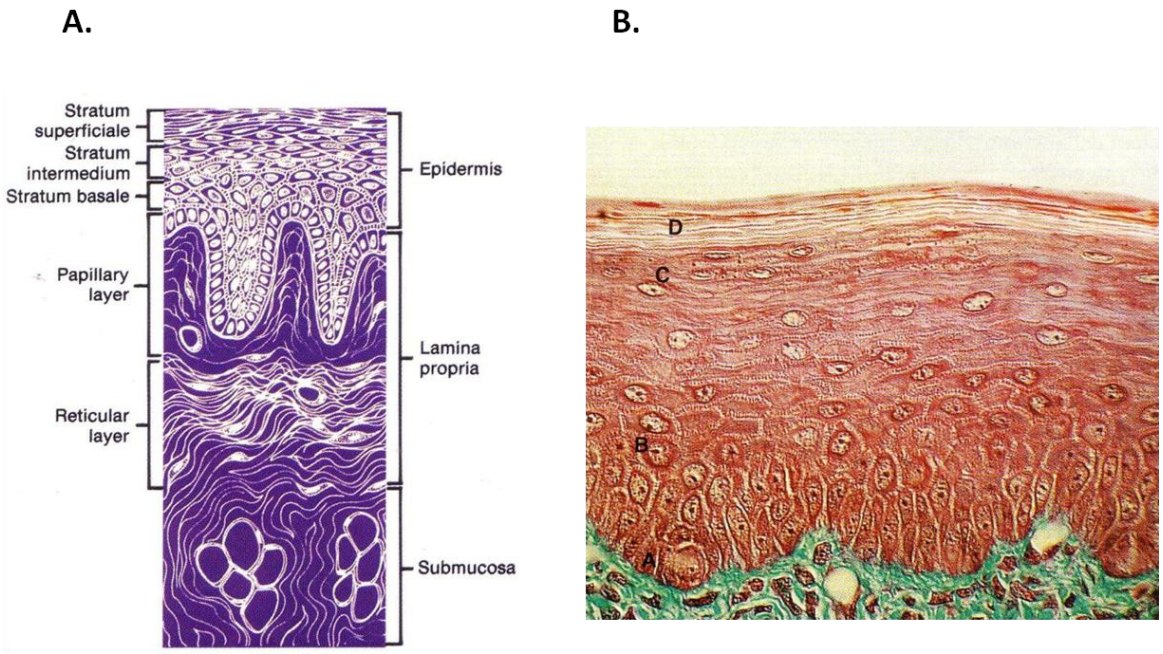

Figure 1.6 : The structure of the oral mucosa.

a) The diagram shows the structure of the oral mucosa and the different layers of the oral epithelium.

b) Stratum Basale (SB) **(A)**, Stratum Spinosum (SS) **(B)**, Stratum Granulosum (SG) **(C)**, Stratum Corneum (SC) **(D)**. The basal layer contains the keratinocytes that retain the ability for continuous DNA mitosis and synthesis (Fuchs, 1993).

1.8 Epidermis

The mature epidermis is a SSE, composed of proliferating basal and differentiated suprabasal keratinocytes which form the outermost skin surface. This outer covering of the skin contains the hair follicles, sebaceous glands and sweat glands and functions as a waterproof protective barrier against environmental pathogens as well as regulating the body's water release into the atmosphere through transepidermal waterloss (TEWL) (Alonso and Fuchs 2003). The epidermis is composed of four main type of cells; the keratinocyte, which is the predominant cell type, melanocytes, langerhans cells and merkel cells (Moll, Moll et al. 1984). The epidermis is divided into many layers and as the cells move up the strata from the innermost levels they differentiate and undergo changes in shape and composition and become keratin filled (Fig 1.7). Upon reaching the topmost layer, the cells slough off and are replaced by inner cells moving outwards in a process called keratinization, with the outermost layer of the epidermis consisting of approximately 25-30 layers of dead skin (Jones, Harper et al. 1995). As in the case for the oral mucosa, the keratinization process time can vary between species, with the average time for humans being 28-30 days compared to 14 days in mice (Morgan and Mulligan 1989).

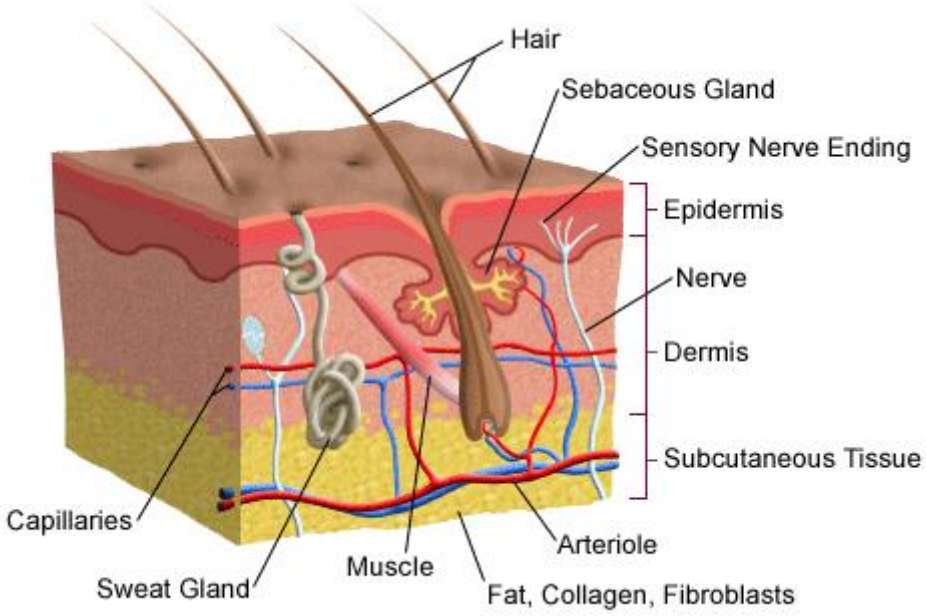

Figure 1.7 : Epidermis structure.

Diagram showing multi layered structure of human epidermis

http://www.rci.rutgers.edu/~uzwiak/AnatPhys/APFallLect7.html

The epidermis is maintained by epidermal stem cells which reside in the basal layer and generate daughter cells that move upward towards the surface of the skin (Koster 2009). Keratinocytes undergoes a complex process of differentiation through a series of cellular layers to provide its protective barrier function (Koster 2009). The epidermis is composed of four to five layers, depending on the region of skin being considered (Fig 1.8). The five layers of the skin are the stratum basale (SB, or basal layer) and the suprabasal layers consisting of the stratum spinosum (SS, or spinal layer), stratum granulosum (SG, or granular layer), stratum lucideum (SL, or clear layer) and the outermost stratum corneum (SC, or cornified layer) (Alonso and Fuchs 2003). Whilst the clear layer is only found in thicker areas of the epidermis which lack hair follicles such as the soles of the feet and palm of the hands, the other four layers are found in both thick and thin skin (Montagna and

Ellis 1960). The single layer of undifferentiated cells known as the stratum basale, contains the epidermal stem cell population that provides a continuous supply of new cells for epidermal differentiation (Eckert, Efimova et al. 2002). Following division, cells migrate upwards towards the stratum spinosum, characterized with extensive network of desmosomal connections between the cells and early markers of differentiation (Eckert, Efimova et al. 2002). The third layer, the stratum granulosum, is distinguished by the presence of granules containing products of keratinocyte differentiation to be used subsequently in the assembly of the corneocyte membrane (Koster 2009). The stratum lucidum is a layer of intense enzymatic activity in which cellular organelles and nucleic acid are destroyed by the actions of proteases, nucleases and other enzymes (Liu, Bian et al. 2010). The development of the cornified envelop represents the terminal stage in keratinocyte differentiation in the stratum corneum, forming a mass of dead, flattened cells that are uniquely adapted to provide a protective surface, constantly being shed and replaced (Eckert, Efimova et al. 2002).

a.

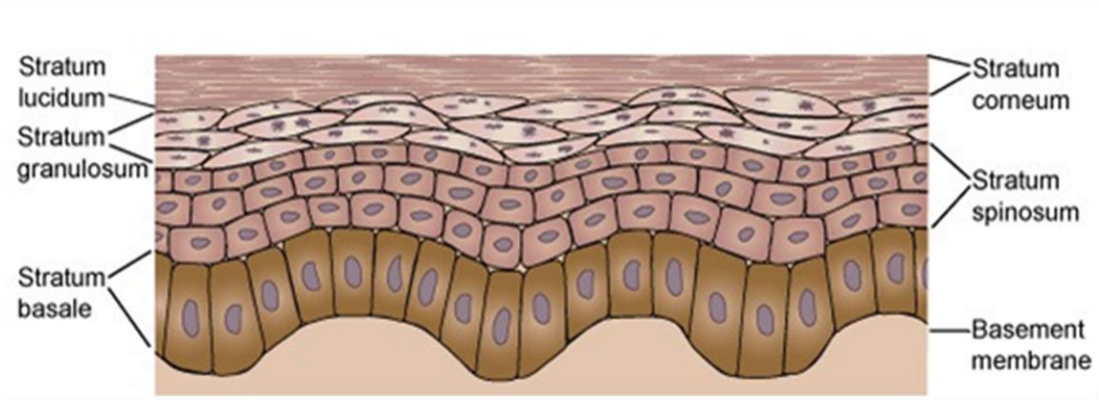

b.

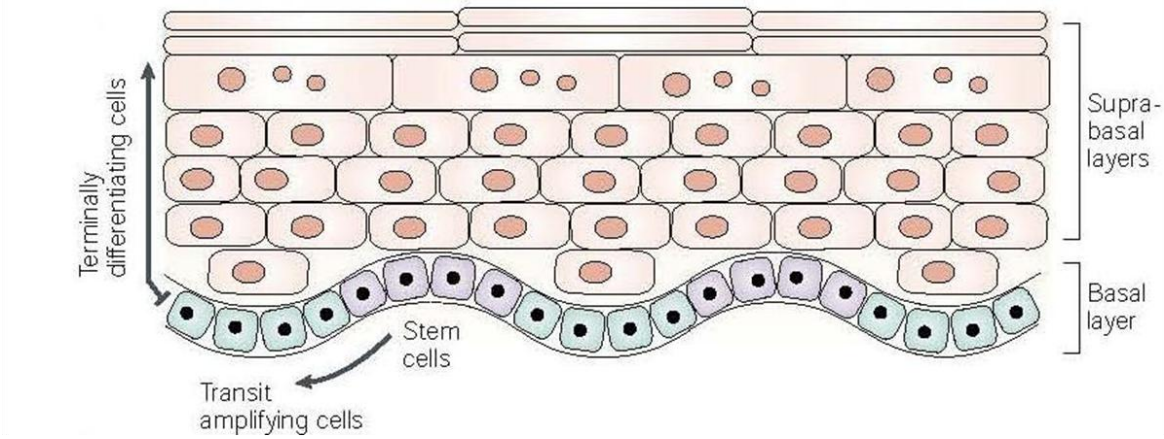

Figure 1.8 : Keratinization of the epidermis.

a) The epidermis consists of five different layers of keratinocytes

b) The keratinization process whereby the cells move upwards throughout the layers of the epidermis is associated with a series of morphological and biochemical changes as cells migrate from the proliferative and mitotic basal layer through the non-proliferative suprabasal layers, at the end of which maturation is complete. In each layer keratinocytes express different molecular markers such as keratins, involucrin, filaggrin and loricrin (Image obtained from (Liu, Bian et al. 2010).

1.8.1 The keratinocyte

The most abundant cell type of the epidermis, the keratinocyte, undergoes a complex process of differentiation through a series of cellular layers to provide its protective barrier function in the production of hair follicles, sweat and sebaceous glands (Eckert, Crish et al. 1997). Keratinocytes are named after the filamentous keratin family of proteins that make up a major part of its distinctive cytoskeleton. This network of keratin intermediate filaments (IFs) is a useful marker of epidermal differentiation as the expression of keratins change in each of the stratified epidermal layers (Eckert, Crish et al. 1997). The basal layer is typified by the expression of K4 and K14 as well as keratin K5 (expressed in the embryo), whilst the intermediate suprabasal layers express K1 and K10 (Lloyd, Yu et al. 1995).

1.8.2 Dermis

The layer beneath the epidermis is formed of connective tissue and known as the dermis, and its main role is to provide support to the epidermis and cushion the body from stress and strain (Eckert, Crish et al. 1997). Dermal tissue is made up of 80% water, elastin fibres and collagen and is heavily vascularised with blood vessels, enabling it to regulate body temperature, store much of the body's water supply as well as provide both the dermis and epidermis with nutrient-rich blood and waste removal (Koster 2009). The dermis is tightly connected to the epidermis by a basement membrane and contains many nerve endings and mechanoreceptors that allow for the sense of touch and heat. Collagen fibres compose of upto 70% of the dermal proteins, providing characteristic resistance to strain and mechanical injury whilst the presence of elastin fibres allow for elasticity (Koster 2009).

The dermis is divided into two layers, the superficial area adjacent to the epidermis called the papillary region and a deep, thicker area known as the reticular dermis (Sorrell and Caplan 2004). The papillary region is composed of loose connective tissue with elastic fibres, and it contains the dermal papillae filled with finger –like

fibrous, vascular nerve projections called the papillae filled with blood-rich capillaries that extend towards the epidermis (Eckert, Crish et al. 1997). This specialized surface at the junction with the epidermis acts to strengthen the connection between the two layers of the skin. The second layer of the dermis is the much thicker reticular layer, situated below the papillary and composed of dense, irregular connective tissue with bundles of collagen and some elastic fibres that weave through it (Sorrell and Caplan 2004). Together these protein fibres provide the dermis with its properties of strength, elasticity and extendibility. The reticular region is also the location of hair follicles, sebaceous glands, sweat glands, blood vessels and nerve endings (Kanitakis 2002). The dermis contains most of the skins specialized cells including adipose cells, mast cells, schwan cells and its main cell type, the fibroblast (Eckert, Crish et al. 1997). The most common cell type of connective tissues in animal cells, fibroblasts, specialize in producing collagen and elastin fibres which constitute the extracellular matrix (ECM) and have a key role in tissue maintenance and metabolism as well as in wound healing (Marionnet, Pierrard et al. 2006). The main function of the fibroblast is to maintain the structural integrity of the connective tissue by secreting ECM precursors and a variety of protein fibres. In the dermis, fibroblasts are primarily located in the dermal papillary layer, although they can be found in lesser amounts in the reticular region as well (Cha and Purslow 2010).

1.8.3 Keratinocytes *in vitro*

Human diploid epidermal cells were first serially cultivated by James Rheinwald and Howard Green in 1975, prior to which cultivation of mammalian cells *in vitro* was difficult, and numerous attempts to culture disaggregated epidermal keratinocytes in monolayer had proved unsuccessful. Rheinwald and Green demonstrated that epidermal cells were dependent on fibroblast products to initiate colony formation and subsequent co-culture with the fibroblast 'feeders' resulted in keratinocyte growth and differentiation. Furthermore, these studies concluded that for optimum keratinocyte growth, fibroblasts must be lethally irradiated to inhibit proliferation and they must be present at the correct density to prevent overpopulation of the epidermal cells. Upon inoculation of epidermal cell suspension with lethally irradiated fibroblasts, the feeder cells quickly formed a monolayer on the dish surface whilst epidermal cells took several days to attach but upon making contact with the dish they grew as expanding colonies on the vessel surface, pushing away the feeders at the periphery (Green, Rheinwald et al. 1977, Rheinwald and Green 1977).

In the absence of fibroblast feeders and despite high seeding densities, human keratinocytes could not initiate colony formation and the use of medium conditioned by the growth of 3T3 cells could not substitute for the cells themselves (Green, Rheinwald et al. 1977). In contrast, another study by Rheinwald and Green on a tumourigenic keratinocyte cell line showed successful proliferation in 3T3 conditioned medium, highlighting the fact that tumourigenic cell lines are less dependent on growth factors (Rheinwald and Green 1975). Irradiated mouse-3T3 cells were found to be more effective then irradiated human diploid fibroblasts in supporting growth of human epidermal keratinocytes since in the presence of human fibroblasts, keratinocyte growth was slow and the cells did not stratify as much. 3T3 cells were established in 1962, when they were derived from Swiss mouse embryo by Howard Green, and since then it has become a standard fibroblast cell line. It is spontaneously immortalized with stable growth rates and its

name is derived from the protocol established for its generation, an abbreviation for '3-day transfer, inoculums 3 x 10^5 cells' (3T3) (Green, Rheinwald et al. 1977).

The successful culture of keratinocyte *in vitro* showed that, like most cells, keratinocytes also exhibit a finite replicative lifespan as a result of the Hayflick limit, ceasing growth between 20-50 population doublings and senescing. Improvement in cell culture conditions can extend lifespan although it still cannot compare to the proliferative potential of cells *in vivo,* as the removal of cells from the dividing population affects its maximum growth potential. The age of the donor from which the cell population was obtained also affects replicative lifespan as the use of epidermal cells from older donors have reduced growth potential with keratinocytes of donors of ages 3-34 years growing through a total of 20-27 generations, whereas newborn cells grew through 25-51 generations (Green and Rheinwald 1975b).

The plating efficiency also differs between donors as those cells from older donors have a plating efficiency of less than 1% whilst cells from younger donors are in the range of 2%-10%. Prior to human diploid epidermal cell culture, only fibroblasts were readily available for experiments and the pioneering work of Rheinwald and Green illustrated that previous limitations in epidermal cell culture were due to the complex relation of epidermal cells to fibroblasts and in doing so revolutionalized the way into mammalian cell-based research.

Keratinocytes are heterogeneous in their proliferative potential and three classifications have been established (Barrandon and Green 1987b):

i) **Holoclone**; Cells forming part of the holoclone have the highest reproductive capacity. Less than 5% of colonies formed by the cells of the holoclone abort and terminally differentiate.

ii) **Paraclone**; Cells in this subset have short replicative lifespan, rarely exceeding 15 cell generations before aborting and terminally differentiating.

iii) **Meroclone**; This is often the stage between holoclone and paraclone and consists of cells with a variety of replicative potentials.

The relative proportion of different clonal types is affected by aging as cells originating from the epidermis of older donors subsequently give rise to a lower proportion of holoclones and a higher proportion of paraclones (Barrandon and Green 1987). Each of the keratinocyte colonies ultimately forms a SSE in which the dividing cells are restricted to the lower layer (Rheinwald and Green 1977).

The addition of hydrocortisone, cholera toxin and epidermal growth factor (EGF) contribute to increased cell growth rates and proliferation in culture. Hydrocortisone makes keratinocyte colonies more orderly and distinctive, maintaining proliferation at a slightly higher rate whilst the use cholera toxin causes an increase in cyclic AMP levels, again increasing rates of cellular proliferation and increasing number of cells in smaller colonies (Rheinwatd and Green 1975). The addition of EGF extends the culture lifespan of epithelial cells from neonatal foreskin (Rheinwald and Green 1977) by contributing to the rate of migration of the cells that is essential for sustained growth of the keratinocyte colonies (Barrandon and Green 1987). Intracellular levels of calcium are important for keratinocyte stratification and adhesion (mediated by calcium-dependent desmosomes and non-disjunction cadherins) and standard tissue culture concentrations of calcium range

from 1.2 – 1.8 mM in which keratinocytes are able to stratify in contrast to levels ranging between 0.05 – 0.10 mM wherein keratinocytes proliferate but are unable to stratify or form a monolayer (Hennings, Michael et al. 1980).

1.9 Serum free culture

Despite good culture conditions and increased rates of proliferation, the fibroblast feeder system is complicated and time consuming, as well as difficult to adapt universally. The problems associated with the feeder layer approach led to the development of a well defined serum free culture system for cell culture. The presence of animal serum in cell medium is believed to be a source for nutrients and other 'factors' essential for cell growth *in vitro.* Perhaps the main drawback of animal serum is that by nature, serum is largely undefined, complex mixture of multiple constituents and the effects of many of these on cultured cells remain unclear, with suggestions that cytotoxins present in the serum have a detrimental effect on primary and established cell lines (Mujaj, Manton et al. 2010). Due to high batch to batch inconsistency of serum, laboratories have to undergo a highly costly and time consuming screening process before use, with such variation making it hard to control culture conditions and different serum batches can illicit varying effects in different cell assays (Do 2003). High costs, presence of contaminants such as virus, bacteria and mycoplasma and ethical concerns for animal welfare add to the disadvantages associated with animal sera and highlight the importance of developing and using a well defined and consistent serum free system. The switch over from serum to serum free can vary between cell types but in general cells can be gradually weaned to grow in a serum free system with relative ease and some companies offer their own cells already adapted to grow in serum free media (Do 2003). Such systems are suggested to have better comparable cell growth rates and produce higher yields of end products since they allow for more control of culture conditions, elimination of contaminants and serum cytotoxicity, improved reproducibility between cultures and consistency of media that avoids the need to screen batches (Gstraunthaler 2003).

1.10 DNA damage response

The DNA of eukaryotic cells is constantly exposed to endogenous and exogenous DNA-damaging agents. To prevent accumulation of genomic damage and retain normal genome integrity, cells have evolved a complex response mechanism known as the DNA Damage Response (DDR) (Nyberg, Michelson et al. 2002). This inhibition of further DNA synthesis following DNA damage is critical for avoiding genetic lesions that may later contribute to cellular transformation and results in premature cell growth arrest (Kastan, Onyekwere et al. 1991). If DNA damage is not repaired prior to the cell entering mitosis, the use of a damaged DNA template results in the permanent fixation of the mutated lesion, ultimately leading to cellular transformation in cells deficient in this inhibitory process (Kastan, Onyekwere et al. 1991). The different types of DNA damage as a result of acute or chronic stress on cells include oxidation of bases, DNA single strand breaks (SSBs) and DNA double strand breaks (DSBs), with the latter considerably more lethal, resulting in senescence via the p53 and $p21^{WAF1}$ tumour suppressors (Funayama and Ishikawa 2007). Oxidative stress and radiation-induced DNA DSBs can also lead to chromosomal instability by erroneous joining of DNA ends or the deletion or amplification of tumourigenic mutations (Banin 1998). In response, the cell recruits primary DNA damage proteins ataxia telangiectasia mutated (ATM) and Rad3-related protein (ATR) to the site of damage. Upon recruitment of ATM and ATR, the histone protein variant, H2AX, is phosphorylated to γH2AX that facilitates the assembly of DNA repair factors such as 53BP1 and MDC1, in turn leading to the phosphorylation of p53 activating proteins, Chk1 and Chk2 (Fernandez-Capetillo, Lee et al. 2004). Stabilization of p53 is achieved through phosphorylation of p53 at ser-15 by ATM and at ser-20 by Chk2 and thus prevents the binding of p53 with MDM2 (Khanna, Lavin et al. 2001) .

1.10.1 Markers of DNA damage

The DNA damage response involves a large number of checkpoint and repair proteins that are responsible for damage detection, check point activation, damage repair and post repair resumption of the cell cycle. In eukaryotic cells these multi protein complexes are organized into centres called 'foci' and such DNA damaged induced foci formation is a tightly regulated multi-step process involving diverse protein-protein interaction, post-translational modifications and enzymatic reactions (Lisby and Rothstein 2004).

One such protein involved in the DNA damage response is p53 binding protein 1, (53BP1), initially identified as a protein that binds to the central DNA binding domain of p53 thereby enhancing p53 mediated transcriptional activation (Ward, Minn et al. 2003). Inconjunction with ATM, 53BP1 creates a positive feedback loop that is activated upon DNA damage whereby 53BP1 phosphorylates ATM at ser-25 and in return is a target of phosphorylation by ATM itself. 53BP1 is essential for DNA repair through nonhomologous end joining (NHEJ) and has been shown to influence chromatin mobility around DNA damage-induced foci, allowing for separated DNA ends to come together for repair (Dimitrova, Chen et al. 2008). Consequently, knock out studies of 53BP1 have demonstrated an increase in genomic instability and chromosomal aberrations as well as accumulation of chromatin breaks (Fitzgerald, Grenon et al. 2009).

In response to genomic stress 53BP1 becomes hyperphosphorylated and has been shown to co-localise with *γ*H2AX into distinct nuclear foci at sites of DNA lesions, suggesting its involvement in DNA damage response (Kastan, Onyekwere et al. 1991)(Fig 1.9). H2AX becomes rapidly phosphorylated upon exposure of cells to DNA damage due to a highly conserved serine residue located 4 amino acids from the COOH terminus and has been shown to rapidly form ionizing radiation induced foci (IRIF) in the chromatin surrounding the DSB and to co-localise with other

proteins involved in the DNA response such as ATM, BRCA1 and 53BP1 (Fernandez-Capetillo, Lee et al. 2004). Presence of γH2AX has been shown to be essential for the recruitment of repair/signalling proteins to DNA damage and in the formation of foci for numerous factors including 53BP1. It has been suggested that phosphorylation of H2AX increases the likelihood of assembling a functional repair complex by increasing the local concentration of repair factors near the lesion (Fernandez-Capetillo, Lee et al. 2004). The DNA damage response is crucial to the proper functioning of the cell and a defect in this pathway results in chromosomal instability disorders and genetic diseases such as ataxia telangiectasia wherein a defective ATM leads to immunodeficiency and severe disability.

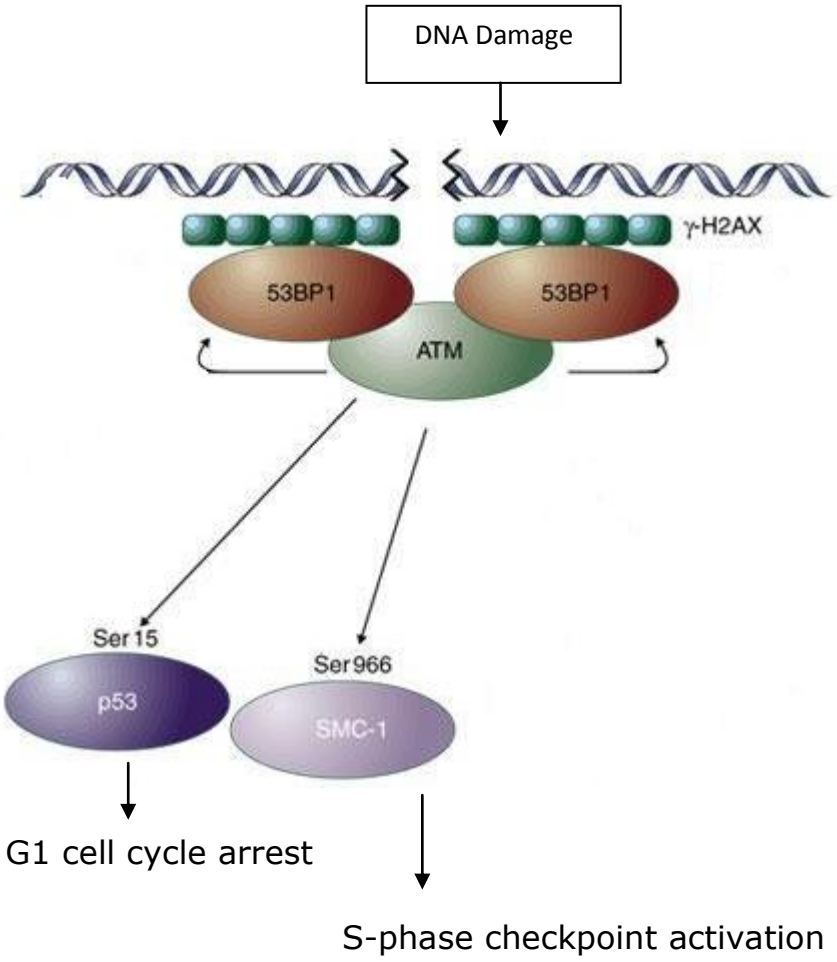

Figure 1.9 : Involvement of 53BP1 and γH2AX in DDR.

In response to double strand breaks following DNA damage, H2AX is phosphorylated by the checkpoint kinase ATM and acts as a marker for DNA damage. After its subsequent phosphorylation, 53BP1 co-localizes with γH2AX to form nuclear foci and is responsible for coupling ATM with downstream targets such as p53 and SMC1 (Abraham 2002). Following damage, ATM targets the ser-15 residue of p53 for phosphorylation and leads to p53 mediated G_1 cell cycle arrest. Structural maintenance of chromosome protein 1, SMC-1, is involved in DNA repair and is a downstream effector of ATM-dependent S –phase checkpoint pathway. Following recruitment of 53BP1 to γH2AX nuclear foci, ATM phosphorylates serine 966 *in vivo* that activates the S-phase checkpoint in response to DNA damage leading to a decrease in the rate of DNA synthesis (Yazdi, Wang et al. 2002) (Figure modified from (Abraham 2002).

1.10.2 Oxidative Damage to DNA

Living cells are constantly exposed to potentially damaging free radical species that may arise from normal cellular metabolism or be produced following exposure to ultra violet or ionizing radiation (Cooke et al., 2004). Oxidative stress has been established as the source of endogenous reactive species (ROS) resulting in DNA base damage and strand breaks, both of which, unless repaired, may be mutagenic, cytotoxic or both to the cell (Cooke, Evans et al. 2003). In view of the damage caused by ROS and the significance in cancer and ageing, oxidative DNA damage and its repair pathways have attracted much research (Cheng, Cahill et al. 1992). ROS are the by-products of oxygen metabolism, cell injury, phagocytosis and environmental oxidants and are released from the mitochondria during cellular respiration or generated by ionizing or ultraviolet radiation. The most important ROS includes the relatively unreactive superoxide anion radical ($O2^{\cdot -}$) which is converted by superoxide dismutase into hydrogen peroxide ,H_2O_2, that in turn can take part in the fenton reaction to produce the very reactive hydroxyl radical, $^{\cdot}OH$ (Halliwell 2003). Additionally, endogenous and exogenous stimuli can also accelerate the generation of ROS, altering the redox balance and causing oxidative stress to cells.

One of the most frequently occurring base modification in mammalian DNA in response to oxidative stress is the guanine analogue, 8-oxyguanine, formed spontaneously by reaction of ROS with DNA either by oxidation of guanine basis or incorporation of oxidised dGTP into the DNA during DNA synthesis. The oxidized guanine has altered base pairing properties wherein adenine (A) tends to be incorporated into the daughter strand during DNA replication in place of cytosine (C). The enzymes and processes involved in the repair of 8-oxo-Gua are the most intensively studied amongst those enzymes that repair oxidative DNA damage due to the abundance of this lesion, its mutagenic potential and its use as a biomarker of oxidative DNA damage (Cook, Gius et al. 2004).

1.10.3 Repair of oxidative DNA damage

It is assumed that ROS, in particular hydroxyl radical, is formed close to the DNA and that as little as 1% of the oxygen passing through the respiratory chain may undergo single electron transfer to superoxide and hence the potential for DNA damage is enormous (Collins 1999). Oxidative DNA damage greatly increases the potential for mutations in mammalian cells and elevated levels of oxidative DNA lesions have been noted in many tumours, strongly implicating a role of oxidative stress-induced DNA damage in the etiology of cancer (Collins 1999). The removal of oxidative DNA lesions is important for the limitation of mutagenesis, cytostasis and cytotoxicity and therefore is not surprising that the cell has evolved multiple and overlapping repair mechanisms to prevent lesion formation and should an lesion occur, to ensure rapid removal and repair (Evans, Dizdaroglu et al. 2004).

The first line of defense against ROS is enzymatic inactivation by antioxidants such as superoxide dismutase (SOD (inactivation of superoxide), catalase (breaks down H_2O_2 into water and oxygen), glutathione (GSH) which is abundant in the nucleus and glutathione peroxidase (catalyses the breakdown of peroxides via reaction with GSH) (Collins 1999). The second line of defense addresses the misincorporated 8-OH-Gua, and is via specialized enzymatic activities by a homologue of the enzyme MutY (MYH), a special adenine DNA glycosylase which removes the mispaired adenine from opposite 8-OH-Gua, and MutT homologue 1 (MTH1), which catalyses the hydrolysis of 8-OH-Gua by preventing its incorporation in the DNA template followed by base excision repair that is initiated by OGG1, eliminating 8-oxo-guanine (Collins 1999). At the proof reading step the misincorporated adenine is removed by MUTYH, a special adenine DNA glycosylase, which initiates base excision repair (Cook, Gius et al. 2004). The third line of defense for oxidized DNA base lesions is by an intricate network of DNA repair mechanisms such as base excision repair (BER), mismatch repair (MMR), homologous recombination (HR) and non-homologous end-joining (NHEJ) (Cook, Gius et al. 2004). Lesions are removed by BER which involves removal of a single lesion by a glycosylase action and a more

complex process involving the removal of a lesion-containing oligonucleotide by nucleotide excision repair (NER) (Collins 1999).

1.10.3 Oxidative DNA damage in disease

One of the main consequences of oxidative lesions is DNA mutations and hence the role of oxidative lesions in cancer is extensively studied. Oxidative mechanisms have been implicated in carcinogenesis due to its ability to introduce spontaneous mutations in the genes encoding for tumour suppressors and proto-oncogenes, and incorrectly activating or silencing them. ROS are constantly generated within the cell and one of the crucial cellular targets of these radicals is DNA, showing specificity for guanine bases and corresponding to mutations in the tumour suppressor genes *Ras* and p53 (Cook, Gius et al. 2004). Oxidative free radicals have the ability to continuously activate transcription factors and consequently give rise to an increase in genomic instability, thereby creating selection pressure for malignancy (Cook, Gius et al. 2004). Apart from DNA base modifications, oxidative stress-induced lesions can also occur at chromosomal level whereby deletions and rearrangements can alter expression in key genes through single point mutations or rearrangements of the promoter/enhancer regions (Evans, Dizdaroglu et al. 2004). Despite circumstantial evidence establishing the role of oxidative stress in carcinogenesis, there have been conditions wherein increased levels of oxidative stress does not increase incidence of cancer. The reasoning behind such observations remain unclear, however it has been suggested that it could result from mutations being present in the non-coding regions of DNA and as such would have very little significance in terms of cancer mutations (Bohr, Anson et al. 1998). Alternative reasoning includes the theory that oxidative DNA damage is an epiphenomenon and elevated levels do not have any physiological role within the body. There is also the belief that the detection of elevated levels of oxidative DNA damage is not indicative of carcinogenesis and it may be due to increased cell proliferation and metabolic activity within the tumour itself (Bohr, Anson et al. 1998).

The role of oxidative stress in the pathology of non-cancer related disorders has been widely reported. Firstly, the association between oxidative stress and inflammation has been widely documented with cellular DNA damage occurring as a result of the 'respiratory burst' from immune cells such as macrophages and neutrophils in response to infection (Cook, Gius et al. 2004). This can further lead to chronic inflammation in which ROS-damaged tissues release cytokines, further promoting infiltration by inflammatory cells. Such chronic inflammation and oxidative stress has been linked to the pathogenesis of autoimmune disorders such as rheumatoid arthritis and systemic lupus erythematosus and these autoimmune disorders are a result of the free radicals altering the non-immunogenic DNA whereby they are viewed as antigens and elicit an immune response and cross-reactivity (Cooke, Evans et al. 2003).

The 'free radical theory of ageing' suggests a link between gradual accumulation of free radical damage and ageing. The concept behind the theory is that with age, the antioxidants defenses fail to detect, eliminate or repair all of the potentially damaging radical species resulting in accumulation of damage and gradual loss of function (Bohr, Anson et al. 1998). Other diseases in which oxidative stress has been implicative include neurodegenerative disorders such as Parkinsons Disease and cardiovascular disorders such as atherosclerosis and myocardial infarctions as a result of its involvement in artherosclerotic plaque development (Cook, Gius et al. 2004).

1.11 The Telomere and telomerase: functions and regulation

1.11.1 The telomere

The concept of the telomere was first proposed by Hermann Muiller in 1938 through his work on x-ray induced chromosomal damage in *Drosophila* wherein he described the presence of a specialized terminal structure responsible for chromosome stability (Zakian,1989). Barbara McClintock advanced the theory on telomeres through her work on *Zea Mays* when she demonstrated the difference between the behavior of chromosomes with broken ends that often fused and mispaired with other broken ends as compared to natural chromosome ends that were stable and did not attempt to fuse with other chromosomes (Zakian, 1989). In molecular terms, telomeres are specialized nucleoprotein structures providing a protective 'cap' for the ends of chromosomes, in the absence of which, 'broken' chromosomes and free DNA ends are susceptible to end-to-end fusions and exonucleolytic degradation (Olovnikov 1996). By protecting against these events the telomere acts to prevent the formation of highly unstable, dicentric chromosomes and potential loss of genetic information.

An important feature of telomeres was discovered to be their role in what is known as the 'end replication problem' wherein telomeric DNA cannot be added by normal DNA synthesis because of a lack of DNA template (Olovnikov, 1996). Telomeric DNA is added by a telomere-specific reverse transcriptase, the telomerase, which itself contains the RNA template required for the synthesis of telomeric DNA (Rhodes and Giraldo 1995). This conserved feature seems to have come about to prevent the gradual loss of genetic information from the chromosome ends which became apparent with the gradual understanding of the role of telomeres in both ageing and tumour formation.

A comparison of telomeric DNA sequence across distantly related eukaryotes show highly conserved features consisting of short sequence motifs which typically contain a G-rich and a C-rich strand respectively (Rhodes and Giraldo 1995). In humans, telomeres are typically composed of tandem repeats of the base sequence 'TTAGGG' between 3 to 20 kb in length although this differs with cell types and between individuals. In skin keratinocytes, for example, mean telomere length varies from approximately 10 kb in samples from infant foreskin to approximately 6-7 kb after 30 cell divisions when the cells start to senesce (Krunic, Moshir et al. 2009). Most of the telomere is double stranded DNA but each telomere ends with a short single stranded 3' overhang, which acts as the substrate for telomerase to add telomeric DNA to the ends of chromosomes in elongation (Rhodes and Giraldo 1995). Apart from their role in chromosomal stability, the conserved telomeric sequences have been suggested to allow for the telomeres to fold into specialized structures called the 't-loop' which acts to protect chromosome ends and prevent them from being exposed to degradation enzymes (de Lange 2005). The importance of conserved telomeric sequences have been reinforced by studies in yeast which have shown telomeric DNA to not only be essential in chromosome stability but also demonstrated that mutations within telomeric DNA impair or prevent nuclear division (Rhodes and Giraldo 1995).

1.11.2 Role in senescence

The main function of telomeres has been widely studied since it was originally proposed that there was a correlation between the Hayflick limit and the end-replication problem in the early 1970s by Olovnikov. As mentioned previously, the function of the telomere is to ensure that the end of the chromosome is not interpreted by the cell as a DSB which can lead to chromosome instability and cell cycle arrest (Rhodes and Giraldo 1995). This illustrates a tightly regulated system in place to ensure that only cells which are supposed to be in a continuous proliferative state such as stem cells or cells in the germline, avoid telomere shortening and cell death.

In contrast, somatic cells need to senesce in order to maintain the correct homeostasis of the tissue that they belong to, and that of the whole organism (Blackburn 2001). Human telomeres in somatic cells undergo progressive shortening with cell division through replication dependent sequence loss at DNA termini, culminating in cellular senescence. Despite undergoing progressive shortening, the integrity of telomeres in somatic cells is maintained by the involvement of specific binding proteins, collectively termed the 'shelterin complex' (Xin, Liu et al. 2008). These proteins work together with others to recognize the telomeric DNA sequence and form a protective cap structure, thereby protecting the chromosome ends from degradation and attempted DNA repair (Reddel 2003). This is necessary as without the protective cap the exposed telomeric ends are subject to DNA repair processes and to prevent this, the telomeres of normal and telomerase positive cells along with the specific binding proteins, form a loop, effectively hiding the chromosome ends from repair processes (Reddel 2003).

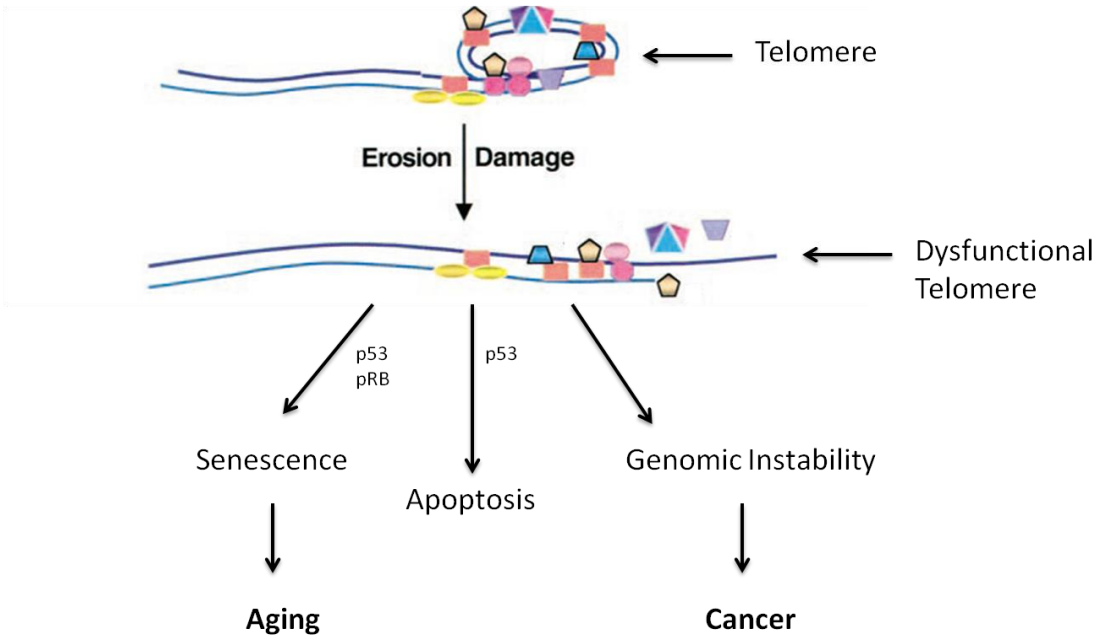

Figure 1.10 : Cellular consequences of telomere dysfunction.

Telomere structure can be disrupted by direct damage, critically short telomeres or through defects in telomere associated proteins. In response to critically short telomeres, normal cells usually undergo senescence via the pRb/p53. In the presence of a pRb checkpoint, however, cells undergo p53-mediated cell death only. In the absence of both pRb and p53, cells survive and accumulate genomic rearrangements leading to genetic instability and this can lead to cancer. (Figure modified from (Kim, Kaminker et al. 2002).

1.11.3 Telomere regulation

The protection of the telomere is achieved by a complex formed of six telomere specific proteins, named 'shelterin', which directly or indirectly bind telomeric DNA sequences and protect chromosome ends. The shelterin subunits include TRF1, TRF2 and POT1, together which directly recognize the tandem repeats sequences of telomeres at chromosome ends, and these are interconnected by three additional shelterin proteins, TIN2, TPP1 and RAP1, forming a complex which allow cells to distinguish telomere ends from sites of DNA damage (de Lange 2005). Amongst the shelterin proteins, TRF2 has been proposed to have a central role in conceding telomere ends from being recognized as DSBs and exposed to repair processes. The introduction of dominant negative alleles of TRF2 *in vitro* in human cells triggers rapid changes atypical of DSBs with the initiation of apoptosis and induction of end to end chromosome fusion. The shelterin complex works to arrange the human telomere into the 't-loop' (Griffith, Comeau et al. 1999), formed by strand invasion of 3' overhang into the preceding telomere tract thereby effectively hiding the natural end of the DNA and protecting it from the DNA repair machinery constantly scanning for broken chromosome ends (Stansel, De Lange et al. 2001).

In the absence of shelterin complex, telomeres are no longer hidden from the cells surveillance machinery and are inappropriately recognized as DNA damage (de Lange 2005). Research has shown that the shelterin complex has reversible DNA remodeling activity that, together with several associated DNA repair factors, acts to change the structure of telomeric DNA and thereby protects chromosome ends (de Lange 2005). This 'capping' is generally a temporary state and is generally lost when the structure of telomere needs to be accessible for the replicating machinery to proceed (Blackburn 2001).

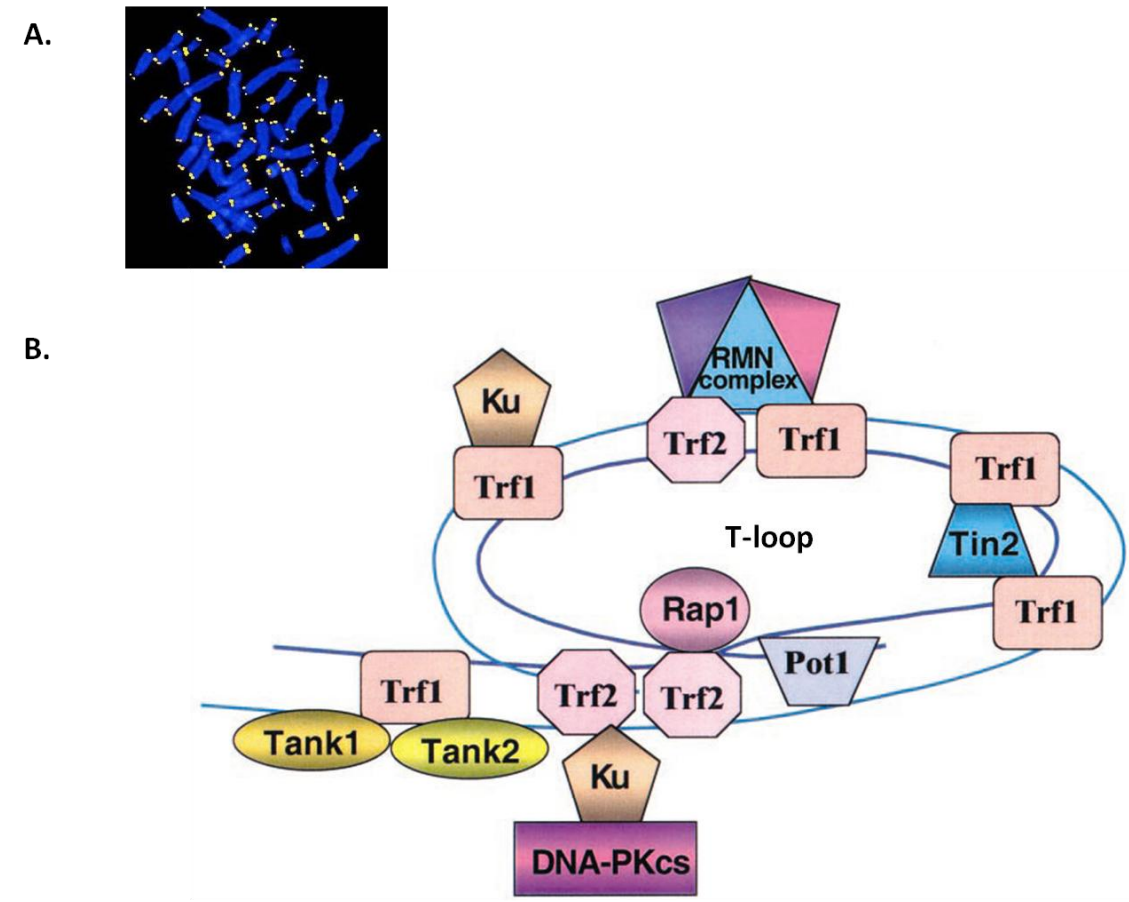

Figure 1.11 : Structure of telomeres.

A). Telomeres visualized by fluorescence *in situ* hybridization (FISH). Telomeres are located at the end of linear chromosomes and composed of hundreds to thousands of tandem DNA repeated sequences and protect the chromosome ends from degradation or random fusion events (Image from N Engl J Med; 2009; 361:2353-2365).

B). The schematic diagram shows the human telomeric complex. The human telomeres end in 100-200 nucleotide protrusion of single TTAGGG repeats which are thought to end in a large 't-loop'. The structure and stability of the t-loop depends on a number of proteins such as POT1, which binds to single strand TTAGGG repeat DNA, and TRF1 and TRF2 that are associated with the duplex repeats and form part of the shelterin complex protecting the ends of the chromosomes. Proteins involved in the maintenance of the t-loop include TIN2 and RAP1 and proteins which indirectly interact with the proteins of the shelterin complex include TNAK1 and TANK2, which that associate with telomeres through their association with TRF1. TRF1 and TRF2 also recruit a number of proteins which participate in telomere repair processes such as the RMN complex, the DNA pKcs. (image modified from (Kim, Kaminker et al. 2002)

1.11.4 Telomerase

A specialized ribonucleoprotein complex, telomerase activity was first characterized biochemically in 1985 in *Tetrahymena* (Blackburn and Greider 1985) and four years later in the immortal hela cell line (Morin 1989). Telomerase directs the synthesis of telomeric repeats at chromosome ends and is required for the maintenance of telomeric repeats throughout many cycles of cell division. As previously mentioned, maintenance of telomere length is essential for the continued viability of proliferating cells as in normal human cells telomeres gradually shorten with each round of cell division (Collins and Mitchell 2002). Critically short telomeres are able to induce proliferative senescence, apoptosis or continued proliferation accompanied by genomic instability (Stewart and Weinberg 2000). In contrast, immortalization of human cells correlates with stabilization of telomere length, suggesting that human cancer cells achieve immortalization, atleast in part, through the illegitimate activation of telomerase expression (Masutomi, Yu et al. 2003). As mentioned previously, telomere shortening occurs in somatic human cells and this is because telomerase activity is strongly repressed in these cells (Kim, Piatyszek et al. 1994) but it is to be found in germ-line cells as well as weak expression in bone marrow, gastrointestinal tissues and basal layer of skin (Fujimoto, Kamata et al. 2001). Despite being repressed, some somatic cells exhibit detectable levels of telomerase activity and it is possible that this could be compensating for the shortening of telomeres that occurs with cell division and thus increasing the proliferative capacity of cell populations in tissues that require a high cell turnover (Reddel 2003). In addition, telomere lengthening may also occur in normal cells for example, the telomere length of B lymphocytes appear to increase during their transit through the germinal center of the lymph nodes (Toouli, Huschtscha et al. 2002). Human telomerase is composed of RNA template encoded by the TERC gene and a catalytic protein subunit called hTERT. It is a reverse transcriptase which works by copying a template sequence carried within its integral RNA (provided by the catalytic subunit hTERT) and adds single-stranded telomeric repeats to the chromosome 3’ ends (Collins 2000) and in doing so compensates for the loss of telomeric sequences during DNA replication. The catalytic subunit hTERT is

implicated as the rate limiting component of the telomerase holoenzyme as telomerase activity in cells directly correlates with levels of hTERT (Masutomi, Yu et al. 2003) . Most cancer cells and immortalized human cell lines express detectable levels of telomerase activity and exhibit stable telomere lengths in cell culture (Kim, Piatyszek et al. 1994). As most malignant tumours and some precancerous lesions have been reported to have higher levels of telomerase activity than normal tissue, this is now considered to be a marker of malignancy (Fujimoto, Kamata et al. 2001).

It is important to note that whilst the majority of cancer and immortalized cells maintain telomere lengths by illegitimate activation of telomerase, a smaller subset of these cells do not show detectable levels of telomerase activity yet maintain telomere lengths (Reddel 2003). An alternative lengthening of telomeres (ALT) system, a recombination-like process that allows for rapid elongation of shortened telomeres, was proposed to overcome the Hayflick limit by these cells (Reddel 2003). The ALT process can proceed in two separate ways and results in the presence of highly heterogeneous telomere lengths in cells performing ALT (Cesare and Reddel 2008). The ALT process involves the DNA strand of an ALT cell annealing with the complementary strand of a nearby telomere and thereby priming the synthesis of new telomeric DNA using the complementary strand as a copy template (Reddel 2002). The ALT pathway has been observed in a variety of tumours and tumour-derived cell lines including breast carcinoma, glioblastoma, osteosarcoma and adrenocortial carcinoma and it has also been identified to be present in approximately 28% of immortalized cell lines *in vitro* (Bryan, Englezou et al. 1997). Experimental evidence has indicated the possibility of both ALT and telomerase activity co-existing together with *in vitro* data suggesting certain tumour types to exhibit both telomerase activity and extreme telomere length heterogeneity, typical of ALT pathway.

It has been suggested that this is either due to intratumoural heterogenicity with some areas of the tumour being telomerase positive and others possessing a ALT activity or, more unlikely, that both processes may reside within the same cell together (Reddel 2003).

1.12 Primary cell culture and cellular immortalization

The use of primary human cells for research, biotechnology and therapeutic purposes has been restricted mainly due to their limited replicative potential. Whilst epithelial cells can provide *in vitro* systems to investigate many biochemical and physiological mechanisms, they are limited due to their restricted replicative life span and the distortion in morphological features and gene expression that start to accumulate with age in culture, including increase in cell size and development of multiple nuclei alongside activation of tumour suppressors (Hanahan and Weinberg 2000). Such limitations often led to the need to re-establish fresh cultures from explanted tissues, not only a tedious task but one which can also add variation from one preparation to another as well as disrupting experimental data, particularly for long term experiments. For many applications, it is ideal to have either an extended replicative capacity or unlimited numbers of characterized cells with the genotype and phenotype of the parental tissue as this would result in consistency throughout the research application and eliminate variation due to the use of different strains. The limitations posed to research by primary cells have since been overcome through the establishment of tumour-derived cell lines or through the generation of immortal cell lines by various methods, reviewed below.

1.12.1 Tumour-derived cell lines

For years, tumour-derived cell lines have been used in research for their ability to proliferate indefinitely, an ability which likely stems from the fact that p53 is inactivated in over 80% of tumours, thereby allowing abnormal cells to overcome cell cycle checkpoints, as well as their ability to synthesize telomerase activity (Harvey and Levine 1991). Downregulation of the cells' tumour suppressors can account for the highly volatile and unstable characteristics displayed by cancer cell lines. One of the main irregularities cancer cells display is lack of contact inhibition when cultured on culture vessels and continue to proliferate after encountering neighboring cells, not appearing to co-operate with other cells in the environment. Cancer cell lines can also be grown in simpler growth mediums as they have a reduced dependence on the presence of growth factors in the culture environment compared to their normal counterparts. Another major feature of cancer cells which make them undesirable for research is their abnormal karyotypes, with cells being either polyploidy or aneuploid and their chromosomes appear very unstable with abnormal structure due to chromosomal translocations, deletions, duplications and inversions (Shay, Wright et al. 1991).

One prime example of a commonly used tumour derived cell line is the HeLa cell line, derived in 1951 from a malignant cervical biopsy of Henrietta Lacks and it was also the first human cell line to prove successful *in vitro*. HeLa cells were deemed immortal as they are capable of unlimited proliferation in culture as long as they are maintained in a suitable culture environment and to date are used in multiple applications from testing of the first polio vaccine through to cancer research (Shay, Wright et al. 1991). Although immortal, HeLa cells have been characterized as having abnormal rates of cell proliferation, they appear to proliferate extremely rapidly even for cancer cells and have constantly activated telomerase activity. Many chromosomal aberrations have also been characterized in HeLa cells and they are highly unstable with gene transfer from the HPV18, an average of 82

chromosomes with four copies of chromosome 2 and 3 copies each of chromosomes 6, 8 and 17 (Shay, Wright et al. 1991).

As mentioned, HeLa cells are highly unstable and so far many strains exist as they continuously evolve. Another issue that has arisen in the culture of HeLa is that of contamination, with HeLa cells often being branded as difficult to control and a 'lab weed' that interferes with research, invalidating data by infecting other cells in the same lab (Harvey and Levine 1991).

1.12.2 Spontaneous immortalization

Cells capable of overcoming cellular growth restraints, bypassing senescence in the absence of deliberately added exogenous agents and acquiring the ability to proliferate indefinitely are deemed to have undergone spontaneous immortalization. As mentioned previously, the cell division potential of any particular culture appears to be dependent on many factors such as the age of the donor and it has been suggested that the frequency at which cells escape senescence is species dependent (Harvey and Levine 1991). Most rodent cells show frequent spontaneous immortalization in comparison to human cells in which this event is a rarity. This is likely due to the longer lifespan of humans which has led to the evolvement of efficient control mechanisms for prevention of such events for example; less error prone replication machinery, more efficient repair systems and molecules being better adapted to react with free radicals (Shay, Wright et al. 1991). A number of studies have suggested that spontaneous immortalization occurs by the selection of rare cells in the cell population carrying mutations in key genes to inactivate their tumour suppressive activity and cell cycle regulators (Shay, Wright et al. 1991). In keeping with this idea, it is not surprising that many of these spontaneously derived cell lines illustrate mutations at the p53 locus with the inactivation of p53 widely reported as a key event in cellular immortalization (Harvey and Levine 1991).

1.12.3 DNA tumour viruses

For years one of the most common methods to generate immortal cells was to transduce human cells with genes from DNA tumour viruses such as simian virus 40 (SV40), human papillomavirus (HPV) , adenoviruses and the epstein-barr virus (EBV) (Shay, Wright et al. 1991). DNA tumour viruses appear to increase the frequency of human cell immortalization as they encode proteins that interact with the cells tumour suppressive gene products and efficiently over-ride the cell cycle regulatory proteins (Linder and Marshall 1990). Although useful, such methodology has its limitations as virus induced transformation often results in loss of some aspect of differential cell phenotype. As mentioned, several families of DNA viruses appear to induced immortalization in human cells and some will be briefly reviewed below.

1.12.3.1 Simian virus 40 (SV40)

Infection of human cells with SV40 early region genes by transfection of an expression plasmid remains a very common immortalization technique for extending the replicative life span of almost any human cell type. It has now been recognized that the major SV40 oncoprotein encoded by early region DNA, the large T antigen, is responsible for the immortalization of rodent and human cells (Linder and Marshall 1990). The cells infected with SV40 and expressing the large T antigen develop altered morphology, show a reduced serum requirement for growth as well as acquiring extended life span *in vitro (Shay, Wright et al. 1991)*. SV40 achieves this by random integration of viral DNA into host genome and inactivating the p53 and pRb proteins, hence cells expressing SV40 oncoproteins proliferate for many population doublings beyond the point at which their normal counterparts senesce (Linder and Marshall 1990). During this extended replicative lifespan, the cells continue to proliferate as their telomeres continue to shorten, and ultimately the cell population stops proliferating and enters into ‘crisis’. In some cultures, a rare dividing cell population which has acquired a spontaneous genetic change gives rise to an established cell line although such an event is rare, approximately 1 per 10^7 and all cells evading crisis in this way always have a

activated telomere maintenance mechanism, either through activated telomerase or ALT (Shay, Wright et al. 1991).

An example of a SV40 transformed cell line displaying altered features is the normal human uroepithelial cells (HUC) which were transformed with SV40 *in vitro* (Reznikoff, Loretz et al. 1988). Although SV-HUC seemed to achieve immortalization, they displayed altered growth characteristics. In comparison to HUC, SV-HUC had altered ability to grow on plastic vessels, seemed to lose dependence on medium supplements for optimal growth as well as lack of requirement on feeder cells for optimal growth at clonal density. Additionally, SV-HUC had irregularly shaped nuclei and nucleoli, a lack of cell surface marker glycocalyx and a inability to stratify and differentiate in culture (Reznikoff, Loretz et al. 1988). Another phenotype associated with SV40 transformed cells is an ability to induce tumours with time in passage (Reddel, Salghetti et al. 1993).

1.12.3.2 Human papilloma virus (HPV)

HPV are small DNA tumour viruses that induce epithelial proliferation and cause benign lesions such as warts and papillomas, as well as possible malignant tumours of cutaneous and mucosal epithelia (Shay, Wright et al. 1991). HPV oncogenes E6 and E7 from high risk strains 16 and 18 have been shown to assist in the immortalization of a number of cell types and are found in approximately 70% – 80% of cervical cancers and cell lines derived from them (Shay, Wright et al. 1991). E6 oncogene causes degradation of p53 and an upregulation of *c-myc* expression as well as partially activating telomerase activity whilst the E7 oncogene is known to degrade pRb (Yeager and Reddel 1997). As is the case with SV40 transformed cells, these cells also undergo a two step immortalization process with cells first undergoing crisis and then a rare population emerging.

A study by Shay *et al* (1991) showed that transfection of human foreskin keratinocytes with a plasmid containing HPV16 DNA produced immortalized cell lines, however the cells had heteroploid karyotypes and were not anchorage dependent (Shay, Wright et al. 1991)

1.12.3.3 Epstein Barr virus (EBV)

EBV has proved to be a very efficient method for extending proliferative capacity of B lymphocytes and the path to immortalization by EBV is different from those of SV40 and HPV (Shay, Wright et al. 1991). Experimental data has indicated that in some lymphoblastoid cell generations transformed with EBV, there is a significant increase in pre-crisis lifespan of upto 160 population doublings, exhibiting strong telomerase activity and hence these cell lines are more likely to become immortalized then those that show weaker telomerase expression. The proliferative capacity of these lymphoblastoid cell lines, regardless of whether they immortalize, makes them useful for a wide variety of applications especially as an essentially unlimited source of DNA for genetic studies (Yeager and Reddel 1997).

Infection of human EBV-negative B lymphoma cell line by gene transfer of EBV resulted in increased cell size, acid production, plasma membrane ruffling and villous projections (Wang, Liebowitz et al. 1988).

1.12.3.4 Limitations of DNA tumour viruses

Studies with viral oncogenes have been extremely insightful for the senescence and immortalization processes over the years, as well as generating many useful cell lines, either immortalized or displaying a greatly enhanced proliferative capacity (Yeager and Reddel 1999). One of the main problems encountered with immortalizing cells using tumour viruses, however, is that the proteins that they encode disrupt many cellular pathways, in particular p53 and pRb, and possibly

many others which as yet remain unknown. These oncogenes also cause many undesirable changes within the cell line such as loss of differentiated properties and loss of normal cell cycle checkpoint controls (Reddel, Salghetti et al. 1993).

Cell Line	Cell Type	Characteristics
HaCat	keratinocyte	Spontaneously derived from adult skin; initially hypodiploid leading to aneuploid and multiple chromosome alterations; ability to differentiate
Hela	Epithelial of cervix origin	Tumour derived ; highly unstable *in vitro* ; chromosome aberrations and unstability
N-TERT	keratinocyte	Spontaneous loss of $p16^{INK4a}$
N-TERT1	keratinocyte	Reduced expression of $p16^{INK4a}$
N/Bmi/Tert1	keratinocyte	$P16^{INK4a}$/$p14^{ARF}$ repressed
K107	keratinocyte	Inherited loss in $p16^{INK4a}$; deficient p53

Table 1.4: List of commonly used epidermal immortalized epithelial cells and their characteristics.

Cell line	Cell type	Characteristics
OKF4	keratinocyte	Viral oncogene knockdown of $p16^{INK4a}$ and p53
OKF6	keratinocyte	Spontaneous loss of $p16^{INK4a}$
TR146	Buccal carcinoma cells	Tumour derived
SCC25	SCC	Tumour derived
POE9N	keratinocyte	Dysplasia derived, deletion of $p16^{INK4a}$ and loss of p53

Table 1.5: List of commonly used oral immortalized epithelial cells and their characteristics.

1.12.4 Activation of hTERT

Critically short telomeres activate senescence through the $p16^{INK4a}$/pRb and/or $p53/p21^{WAF1}$ pathways to block cell cycle progression and inhibit cell division. Viral oncogenes such as SV40 large T antigen and the E6 and E7 proteins of HPV have been shown to effectively extend cell lifespan by inactivating $p16^{INK4a}$ and p53, albeit by altering cellular phenotype and gene expression patterns. It is important to note that apart from the cellular aberrations induced by viral oncogene transformations, this method alone merely extends the replicative lifespan of the cells and does not result in immortalization. Following extended cell divisions, these cells inevitably enter into a crisis state, characterized with extreme cell death, unless spontaneous immortalization occurs. The inability of viral proteins to successfully immortalize cells is due to the presence of the second type of senescence, one that is telomere-controlled.

In respect to immortalization, the cell life cycle can be analyzed by the three separate stages of mortality known as M1, M2 and M0 and the different factors required to overcome the senescence barriers (Figure 1.12) (Lustig 1999).

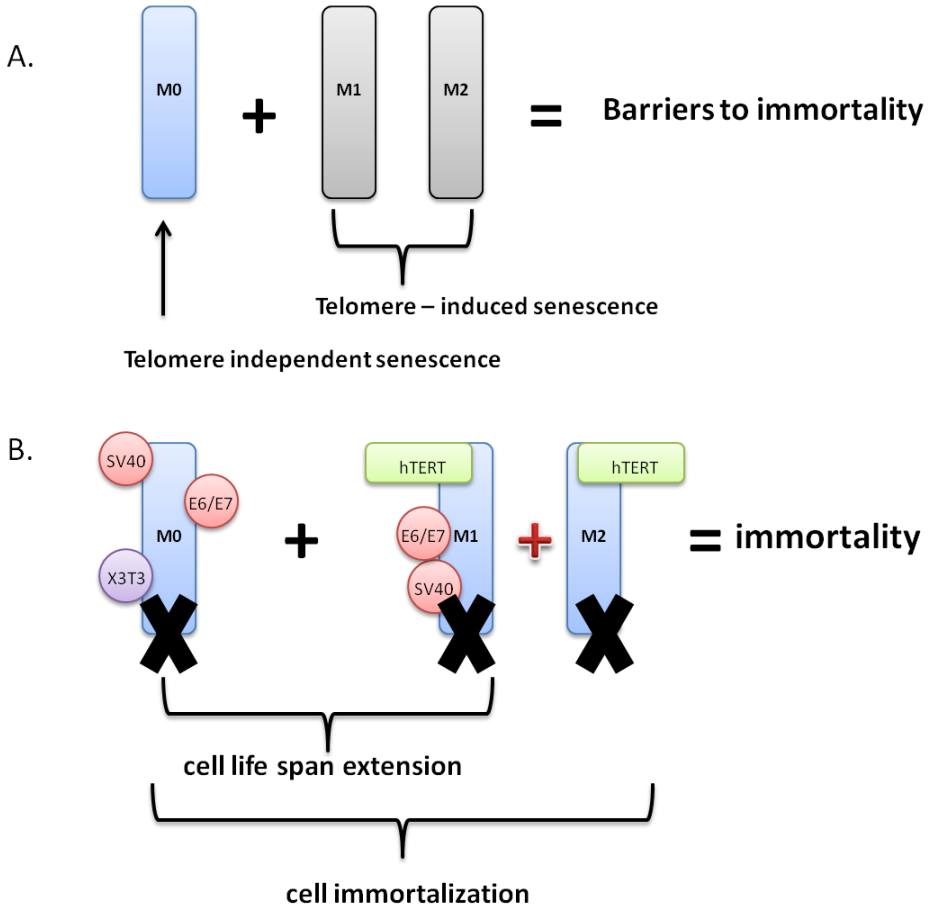

Figure 1.12 : Barriers to mortality of primary cells.

Primary cells derived from non-cancerous tissues display a finite lifespan when cultivated *in vitro*. Research into senescence for generation of immortalized cell lines has revealed two distinct forms of senescence, each representing a separate obstacle to cellular immortality. **A)** The two obstacles to all human cells preventing immortality consists of the shortening of telomeres and stress related factors , mainly the induction of $p16^{INK4a}$ through different stimuli. **B)** In order to achieve immortality it is vital for the cells to overcome these barriers. M0 stage can be overcome either by rare spontaneous changes in the cell or by the introduction of viral proteins such as the SV40 large T antigen or HPV proteins E6/E7. The second obstacle is the shortening of telomeres with cell division which can be overcome by introduction of exogenous hTERT, catalytic subunit of telomerase holoenzyme , responsible for maintain telomere length. Whilst hTERT introduction can effectively bypass the barrier without causing abnormal phenotypic changes in the cells, it is important to note that hTERT alone is not sufficient to cause immortalization in all cell types. Overcoming M0 by viral proteins in the absence of telomerase activation will result in cell lifespan extension but the cells will eventually enter crisis and cell death. Similarly, introduction of hTERT alone, whilst sufficient to immortalize cell types such as fibroblasts, alone they will extend replicative life span of certain cell types, notably the keratinocyte , prior to entering crisis.

An alternative method for cellular immortalization and life span extension whilst avoiding direct interference in cell regulatory pathways which has come to light in recent years is induction of telomerase activity from the cloning of the catalytic subunit of the telomerase gene; hTERT (Hahn and Meyerson 2001). As mentioned previously, telomerase activity is determined by levels of hTERT and this reverse transcriptase works by stabilizing telomere length and thereby greatly extends proliferative capacity of the cells. In most human cell types, hTERT and telomerase activity is either absent or present at insufficient levels for telomere maintenance and hence expression of hTERT in these cells suffice to reconstitute telomerase activity by maintaining telomere size and preventing the onset of M1 and M2 (Harley, Kim et al. 1994). Primary cells in general are very hard to transfect and so hTERT is introduced into the cells by use of retroviral vectors encoded with a selection marker and consequently cells are selected and assayed for telomerase expression and lifespan extension (Shay and Wright 2005). Primary human cells that have so far being successfully immortalized with the introduction of hTERT include fibroblasts, retinal pigmented epithelial cells and endothelial cells.

Despite the success of bypassing crisis and extending life span in some cell types, it appears that hTERT alone is not always sufficient for immortalization of primary cells. The main example of this is the human keratinocyte, wherein expression of hTERT alone was found to be insufficient to extend proliferative lifespan (Rheinwald, Hahn et al. 2002). Further research demonstrated that exogenous hTERT expression has no effect on lifespan limits of keratinocytes unless accompanied by downregulation of $p16^{INK4a}$ expression, by methods such as the use of viral proteins or by DNA methylation. These studies highlighted the fact that additional changes apart from hTERT are required to increase proliferative potential in cells such as keratinocytes. An important factor to consider here is that since these cells require disruption of the $p16^{INK4a}$ and/or p53 pathways, it is important to obtain a method of extending cellular lifespan and immortalizing cells whilst inducing the least amount of damage as possible. The use of common methods

such as viral proteins has multiple limitations and disadvantages, and it is desirable to disrupt the senescence pathways by other means such as use of dominant negative proteins or gene targeting.

1.13 Project summary

In cell based research, immortalized cell lines offer substantial benefits over primary or transformed cell lines. Normal primary cell lines have a finite lifespan in culture, limiting long term research whilst transformed lines exhibit abnormal gene expression and impaired metabolism thus greatly limiting their effectiveness for drug testing and screening. Whilst conventional methods to immortalize human cell lines using viral oncogenes and tumour biopsies have been successful in generating most of the immortalized cell lines currently used in medicine and research, it has various limitations and disadvantages. The use of these methods almost invariably gives rise to cells that display cancer associated changes such as loss of contact inhibition, reduced growth factor requirements, inhibition of differentiation, genomic instability, aneuploidy and disruptions of cell cycle checkpoints. As such, the presence of these characteristics pose significant limitations in the analysis of many cellular functions, in particular to those related to genomic integrity and cell cycle regulations as well as evaluation of potential drugs and pharmaceutical products. A novel immortalized cell line that is well characterized and does not show such phenotypic changes would be extremely useful for applications in tissue engineering and as a model for cancer research.

The testing and optimization for new drug compounds/oral healthcare products usually involves a complex process utilizing both *in vitro* and *in vivo* models. The process commonly begins *in vitro* using primary, immortalized and/or transformed cell lines, followed by the use of a '3D' organotypic culture model and ending with extensive *in vivo* tests prior to human clinical trials. Each of these systems have their own strengths and limitations.

Organotypic cultures reconstructed from dissociated cells were first developed in the 1980's and the best characterized reconstructed organotypic culture is the living skin equivalent. Developed in 1980, the epidermal model is still being used today, where one of its main uses is in replacing damaged skin as well as to study, amongst others, antioxidant protection against photodamage, drug metabolism, differentiation, gene therapy and the immune system. Apart from the skin model, organotypic models are currently being used for studies of cardiovascular function, angiogenesis, thymus, bone, cornea and oral mucosa. The advantages and disadvantages of primary cell lines have been described above and some of the commonly used immortalized cell lines reviewed in table 1.4 and 1.5.

Cells grown in monolayers on tissue culture dishes lack 3D cell-cell plus cell-matrix contacts and communications present in intact native tissue. Monolayer cultures are important for high throughput screening of compounds plus can provide information on the molecular mechanisms of drugs and are at high risk of providing results that might not hold true in the 3D environment of the tissues or whole bodies and discoveries have already emerged that would not have been apparent if only monolayer cultures had been used. Organotypic cultures provide a 3D model of functional tissue and can be easily made from human cell lines and the main aim of using these 3D models is to get a response as close as possible to normal human response. The major issue with each model is its relevance to the human body, thus highlighting the importance for developing and characterizing a primary cell line with minimal genetic changes which would have the potential to be used for *in vitro* studies in addition to as a base in the development of 3D cell models. This could potentially prevent or minimize the differences in toxicity and efficacy between *in vitro* studies as compared to animal studies and clinical trials and reduce the need for multiple systems that are used to increase the likelihood of accurate translation to human trials and avoid artifact.

With respect to the oral mucosa, a well characterized, normal immortalized cell line would be extremely valuable with many benefits in research and healthcare. A major benefit of such a model would be for permeability and metabolism studies in drug development. For the development and optimization of drug delivery systems it is vital to have knowledge of permeability barriers, transport pathways and transport mechanisms of the human mucosa. Current models for the testing of oral drugs, delivery methods and pharmaceutical products involve cell lines which are genetically altered, either cancer-derived or spontaneously arisen with unknown genetic constituents. Such cell lines can be undesirable to work with when testing healthcare products such as toothpastes and mouthwashes as well as potential therapeutic drugs and currently studies need to use multiple systems to validate data due to lack of confidence in such systems. Present 'immortalized' models of the oral mucosa includes one that is derived from the cell line TR146 (manufactured by Skin Ethics) that is a useful and valuable model for studies of drugs intended for buccal delivery as well as for the testing of oral healthcare products. Having been derived from a squamous cell carcinoma of the buccal mucosa, it cannot be expected to be a accurate representation of an *in vivo* response and hence it would be beneficial to have an equivalent fully characterized and non tumourigenic derived, easily reproducible cell line. The need for a system which utilizes a reproducible and easy to culture, genetically defined immortal cell line in a well defined culture system is very much evident in the current pharmaceutical and commercial setting. This cell line would ideally retain cell cycle check points and be able to reproduce accurately the responses of normal cells in relation to the DDR. Much of the research into immortalization methodology has been done using epithelial cells and there is a need for an equivalent in the oral system.

1.14 Hypothesis

Immortalized cells derive their benefits by suppressing cell cycle regulatory processes and consequently immortal cells are often genetically unstable having lost cell integrity as a direct result of cell cycle compromise. The cells main tumour suppressor, p53, regulates the progression from the G_1 phase into the S phase of the cell cycle and most immortalized cells have a mutated p53 gene or else downregulated p53 expression. Changes in p53 expression and/or regulation leads to genomic instability and abnormal cellular phenotypes since DNA damage within the cell is replicated and the cell permitted to progress through the cell cycle. Initially p53 suppression was thought essential for lifespan extension of human keratinocytes however it has since been shown dispensable with the use of oncogenes such as Bmi1 to drive cell proliferation and over ride cell inhibitory processes.

This study was therefore designed to test the hypothesis that a cell line immortalized by the novel method of Bmi1 alongside human telomerase, hTERT, will extend replicative lifespan of oral keratinocytes without disrupting p53 activity through indirect suppression of the $p16^{INK4a/ARF}$ locus. Since the cells will retain p53 expression, there will be increased genetic stability alongside responsiveness to DNA damage stimuli in comparison to cell lines with dysfunctional p53.

1.15 Aims and Objectives

This project aims to develop an oral keratinocyte cell line with a significantly extended cellular lifespan and the potential to be developed into a well defined, reproducible and user friendly culture system. This will be beneficial in industry and clinical research for the testing and development of new drugs and oral health care products.

The specific objectives are as follows:

- Generation of retrovirus for the infection of Normal Human Oral Keratinocytes (NHOK) by an optimized, 2 step retroviral infection protocol for the successful transduction of keratinocytes. The combination of extensive studies on lifespan and characterization *in vitro* of epidermal keratinocytes as well as being the best reconstructed organotypic culture made epidermal keratinocytes a highly desirable control to use alongside the primary study of oral cells. Normal Human Epidermal Keratinocytes (NHEK) will be used alongside NHOK in infection and culture studies, providing a basis for measuring successful infection of NHOK. Immortality of keratinocytes in culture will be assessed by calculating population doublings. Cells are deemed immortal if they continue to proliferate for a minimum of 50 population doublings beyond the lifespan of parental control.

- The cell lines will then be analyzed for various variables and be compared to the commonly used OKF6 and OKF4 immortalized oral cell lines.

- Optimization of the culture system for the cell line and adaptation to serum free system.

- Assessing ability of cells to stratify in the optimized culture conditions and on organotypic substrate.

Chapter 2:

Materials and Methods

Chapter 2

Materials and Methods

2.1 Cells and Medium

Cells	Supplier	Medium and Culture
Normal Human Oral Keratinocytes (NHOK) Early passage cells taken from oral mucosa -NHOK 810 -NHOK 882	Cells kindly donated by Dr. Angela Hague (University of Bristol, UK)	**Keratinocyte FAD medium** (Flavin Adenine Dinucleotide) medium supplemented with 10% (v/v) FCII (fetal serum clone II), 2 mM L-Glutamine, 0.4 µg/ml hydrocortisone, 5 µg/ml insulin, 5 µg/ml transferrin, 10^{-10} M cholera toxin, 1.8×10^{-4} M adenine and 10 ng/ml epidermal growth factor (added after first medium change , donated as **FAD^{+}**)
NHEK (Normal Human Epidermal Keratinocytes) taken from neonatal foreskin and released from the epidermis by digestion with trypsin-EDTA	CDOS, BICMS	
NHEK 92 (Early passage keratinocytes)	CDOS, BICMS	

3T3 Swiss albino mouse fibroblasts ; used as 'feeders' after irradiation	CDOS, BICMS	**10C Fibroblast Medium** DMEM (Dulbecco's Modified Eagle Medium) supplemented with 10% (v/v) FCII, 2mM L-glutamine, pen/strep and 10 mM HEPES.
OKF4-TERT Immortalized Oral Keratinocyte cell line with compromised p16 and p53 activity	Kindly donated by Dr. James Rheinwald , Harvard University, Boston.	**Keratinocyte Serum Free Medium (KSFM)** supplemented with Bovine pituitary extract, undiluted EGF, calcium chloride and pen/strep
OKF6-TERT Immortalized Oral Keratinocyte cell line with spontaneous down regulation of p16		
Phoenix E (E, Ecotropic Receptor) Phoenix E cells are based on the human embryonic kidney cell line 293T and are highly transfectable	CDOS, BICMS	**Phoenix Growth Medium (GM)** 10% (v/v) FCII in DMEM supplemented with pen/strep, and glutamine. Serum free GM for part of infection study
PT67 (NIH-3T3 based retroviral packaging cell line with ecotropic receptors)	CDOS, BICMS	**10C Medium** 10% Medium (v/v) FCII and 2 mM L-Glutamine **,** pen/strep and 10 mM

	CDOS, BICMS	HEPES in DMEM
SCC-25 Tumourigenic keratinocyte cell line derived from Squamous Cell Carcinoma of the oral cavity		**Keratinocyte Growth Medium (KGM).** Keratinocyte Basal Medium (KBM) (Cambrex) supplemented with bullet kit hydrocortisone, insulin, bovine pituitary extract, EGF) (Cambrex) and pen/strep to make KGM.
SVFHK SV40 virus transformed epidermal keratinocyte cell line	CDOS, BICMS	**Keratinocyte Serum Free Medium (KSFM)** supplemented with Bovine pituitary extract, undiluted EGF, calcium chloride and pen/strep

Table 2.1: List of cell lines and culture medium used throughout this study.

2.2 Tissue Culture

All tissue culture was undertaken inside a laminar flow hood using aseptic technique with retroviral infection conducted in a health and safety approved category II containment suite. All cells were incubated at 37^{o}C in a humid atmosphere containing 5% CO_2, except when incubation at 32^{o}C was required during retroviral infection. 1 x phosphate buffered saline (PBS) was used throughout cell culture for adequate washing.

Cells were trypsinized using 0.1% trypsin (Worthington, USA) prepared either in PBS for fibroblasts or in PBS and 0.02% ethylenediaminetetraacetic acid (EDTA) (Sigma Aldrich, UK) for keratinocytes.

Tissue culture plastic was supplied by BD Falcon.

2.2.1 Swiss 3T3 Feeder Preparation

Swiss 3T3 fibroblasts were cultured in 10C medium (Table 2.1) until 80% confluent in 10 cm dishes. The cells were trypsinized with 0.1% trypsin and centrifuged at 800 rpm for 5 min at 20^{o}C and resuspended at a density of 1 x 10^6 per ml of 10C in a universal. The cells were then γ irradiated with a 60 Gy dosage and snap frozen for storage in vapour phase. When required for keratinocyte culture, a vial was thawed and after plating unused feeders were maintained at 4^{o}C and used for up to one week before discarded and a fresh vial thawed.

2.2.2 Cryopreservation and Recovery of Cells

Cell lines were cryopreserved to maintain stock for future experiments. Cells were trypsinized and between 1–2 million cells were resuspended in freezing medium, consisting of 10% dimethyl sulfoxide (DMSO) (Sigma, Poole, Dorset, UK) in neat serum appropriate for the cell line and transferred into cryotubes. Ampoules were stored in Mr. Frosty and subjected to gradient freezing overnight at -80^{o}C before transferring to liquid nitrogen tanks.

Cells were recovered from liquid nitrogen tanks by thawing the vials instantly after removal from tanks in 37^{o}C water bath. Once completely thawed, cells were transferred to a universal containing 9 ml of warm serum-containing medium and centrifuged at 800rpm, 4^{o}C for 5 min. The DMSO-containing supernatant was aspirated immediately and cell pellet resuspended in culture medium and re-seeded accordingly.

2.2.4 Keratinocyte Culture

Cells were retrieved from liquid nitrogen as per routine cell recovery protocol and plated at the appropriate density along with feeders (Table 2.2). Epidermal growth factor (EGF) was added to the culture medium from next medium change.

Plating Diameter	Keratinocyte	Feeder
60 mm plate	1×10^5	1.5×10^5
100 mm plate	$1 \times 10^5 – 1 \times 10^6$	1×10^6
4 well chamber slide	5×10^4	25×10^4

Table 2.2: Keratinocyte and Feeder Seeding Densities.

2.2.5 Feeder Layer Removal from Keratinocytes

Feeders were removed prior to cell harvesting using PBS: 0.02% EDTA (PE) with force applied against the plate using a bulb attached to the pipette in a clock-wise motion for a total of 30 seconds. The plates were checked under microscope to ensure total feeder removal and washed twice with PBS and trypsinized with trypsin/EDTA (T/EDTA) at 37^{o}C before being neutralized with 9 ml of a serum containing medium. This cell suspension was centrifuged for 5 min at 4^{o}C, 800 rpm and resuspended and re-plated according to the recommended seeding density (table 2.2).

2.3 Rhodamine B staining

Rhodamine B is a red/violet staining dye used as a histopathological stain for cornification and keratinization and therefore is a valuable *in vitro* marker of epidermal keratinocytes (Liisberg, 1968). In this study, keratinocyte cell lines were stained with rhodamine B in order to determine the colony forming efficiency and visualize colony morphology of cells in culture.

Cells were fixed with 10% formalin in PBS for 30 min at room temperature. The cells were washed several times with PBS before being stained with aqueous 1% rhodamine B for 30 min at room temperature. Plates were then washed with tap water until cell colonies were clearly visible and then left to air dry.

Keratinocyte	Feeder
1×10^3	1.5×10^5
1×10^2	1.5×10^5

Table 2.3: Seeding Densities for rhodamine B staining.

2.4 Immunofluorescence Protocols

Cell lines were cultured in 4 well chamber slides up to approximately 70%-80% confluence to evaluate the expression of DNA and oxidative damage markers 53BP1 and γH2AX by immunofluorescence.

2.4.1 53BP1 and γH2AX

Cells were fixed with 4% formalin in PBS for 15 min, rinsed with PBS and permeabilized using Triton-X 100 buffer (0.5% triton-X 100 in PBS (Sigma-Aldrich, Dorset, UK) for 15 min at RT. Cells were then rinsed with 0.05% PBS-Tween 20 and blocked for 1 hour with 1% (w/v) BSA in PBS (Sigma-Aldrich, Dorset, UK) followed by incubation overnight at 4^oC with primary antibody (table 2.4). The next day, cells

were washed three times with 0.05% Tween 20 in PBS for 5 min each and then incubated with the secondary antibody solution for 1 hour, RT in the dark (table 2.4). After incubation, cells were washed with 0.05% Tween 20 and counter stained with 0.2 μg/ml Hoechst (Invitrogen, UK) constituted in PBS, in the dark for 15 min. Cells were then washed twice with 0.05% Tween 20 and then twice with PBS for 5 min each before being mounted with an aqueous mounting medium Immunmount (Invitrogen, UK). Stained cells were then analysed using the Lecia Epifluorescence microscope with the appropriate filters for Alexa Fluor and Hoestch.

Antibody	Dilution
53BP1 (Upstate, Millipore)	1: 1000 in PBS containing 1% BSA
γH2AX (Upstate, Millipore)	1: 1000 in PBS containing 1% BSA
Goat anti-mouse IgG Alexa Fluor 488 (Sigma Aldrich, UK)	1:500 in 1% BSA

Table 2.4: Primary and Secondary Antibodies.

2.5 Retrovirus Mediated Gene Transfer

Retroviral vectors are used to efficiently induce long term, stable expression of genes of interest in human keratinocytes instead of routine, ineffective plasmid transfection methods. Retroviral vectors allow for the efficient integration of retroviral DNA into actively transcribing regions of the host genome, produce reliable and long term expression of gene of interest as well as subsequent expression of the protein encoded by the gene. (Watt, Broad et al. 2004).

Replication-incompetent retroviral vectors have been used in this study for the one-time infection of target cells to minimize safety hazards from the continuous

spreading of replication competent retroviruses. This is achieved by incapacitating the self-replicating machinery of the retrovirus by removing the viral packaging genes from the retroviral backbone (Levy, Broad et al. 1998). To replace the requirement for viral packaging proteins needed for retrovirus production, retroviral packaging cell systems are used such as Phoenix and PT67 which provide the viral packaging proteins *in trans* (Kotani, Newton III et al. 1994).

2.5.1 DNA amplification

shp53 and shp16 (Kindly donated by Dr Emilios Gemenetzidis (CDOS, Blizard Institute of Cell and Molecular sciences, Queen Mary, UK), along with the empty vector control, were cloned into pRetrosuperior vector (Fig 2.1) for subsequent retroviral transductions. pBabe Tert-neo and the empty vector-neo control were kindly donated by Professor Ken Parkinson, CDOS. Bmi1 was a gift from Prof. Judith Campisi (LBL, University of California).

2.5.1.1 Cloning

A standard cloning protocol was followed. For ease of understanding, all the vectors will be termed as DNA for the cloning protocol. 10 ng/µl of DNA was added to 100 µl of XL1 Blu bacteria and incubated on ice for 15 min. Bacterial cells were immersed in a pre-heated 42^{o}C water bath for 2 min to heat shock the cells before incubating on ice for a further 10 min. Bacterial cells were then transferred to universals and 400µl of LB broth was then added per universal and incubated for 1 hour at 37^{o}C. If no bacterial growth had occurred after 1 hour, a further 5 ml LB broth was added per universal and left to incubate for a further 24 hours.

2.5.1.2 Preparation of bacterial colonies

0.5 ml of the LB broth was then spread onto ampicillin resistant plates and incubated over night at 37^{o}C. Bacterial colonies were then selected and expanded

in 1 ml of LB-containing ampicillin with incubation in a shaking incubator at 200 rpm for 4 hours at 37^{o}C.

The DNA was then purified from the XL1 blu competent cells using the maxi prep protocol (Qiagen Plasmid Maxi Kit #12163). Glycerol stocks were prepared for each construct and stored at -80^{o}C.

2.5.1.3 DNA Quantification

Isolated and purified DNA was quantified using the NanoDrop^{TM} ND-1000 spectrophotometer (ThermoScientific, Cambridgeshire, UK). Instrument was blanked with 2µl of nuclease-free H_20 (Sigma-Aldrich, Dorset, UK) and a sample volume of 2µl of DNA was used. The concentration of sample DNA is provided in ng/µl at 260 nm absorbance whilst the quality (purity) of DNA content was estimated by the nuclei acid : protein (260 : 280) ratio, with values of 1.8–2.0 considered of good quality and subsequently samples with this ratio was used for retroviral transduction.

2.6 Retroviral Infection of Keratinocytes using a 3T3 based Feeder System

A modified, 2-step infection protocol was devised based on the work of Fiona Watt to obtain a high number of cells expressing the vectors of interest (Levy, Broad et al. 1998) .

2.6.1 Retrovirus Production

In the first part, the Phoenix E retroviral producer cell line was used for the production of retroviral particles containing the genes of interest. Phoenix cell line (supplied by Nolan lab, CA) was originally created by stable transfections of the 293T cells with constructs expressing gag-pol and envelope proteins for ecotropic and amphotropic viruses. Second, a 3T3 fibroblast-derived retroviral packaging cell

line PT67 was infected using the supernatant harvested from phoenix E transfections and infected PT67 were used to infect human keratinocytes.

2.6.2 Phoenix E Transfections

Cells were cultured in 10% FCII medium (Growth Medium or GM). Phoenix E cells adhere poorly to tissue culture plastic, so during routine tissue culture the cells were subcultured by detaching them from the plates using fresh medium with slight force applied against the plate. In instances where single cell suspensions were required, such as cell counting, cells were trypsinized using 0.1% trypsin. Any cell clumps were broken up by pipetting the cell suspension up and down many times before centrifugation for 5 min at 800 rpm and re-plating according to the confluency required (table 2.2).

Phoenix E cells were transfected using Fugene^{6} (Invitrogen, UK) with pRetrosuperior empty vector, shp53, shp16 and pBabe empty vectors, tert-neo and bmi1. Transfection was carried out in duplicates per vector with a seeding density of 2 x 10^{5} cells per 6 cm dish and a Fugene^{6} : DNA ratio of 2.5 : 1. Transfection mix was prepared with 25 µl of Fugene^{6} added drop wise into 1 ml of serum free growth medium, tapped gently to mix and left to incubate for 5 min at RT. 10 µg of construct was added per eppendorf and again left to incubate for 20 min at RT. Media was then aspirated off the surface of the phoenix E cells and the Fugene-DNA mix added to the cells and left to incubate at RT for 10 min before adding 1 ml of serum free GM and leaving to incubate at 5% CO_2, 37^{o}C . After 5 hours, 2 ml of growth medium was added and cells left to incubate for a further 48 hours.

The cells were then pooled together from the duplicate 6 cm dishes and incubated in Phoenix E GM containing 2 µg/ml puromycin into a single 10 cm dish per construct. Drug selection was continued and media refreshed regularly until cells

reached approximately 80% confluency at which point media was removed and cells were washed with PBS. 10 ml of serum free growth medium was then added and cells incubated over night at 32^{o}C. Supernatant was then collected for infection of PT67 cells and stored in 1 ml aliquots at -80^{o}C until ready for infection.

2.6.3 Infection of PT67

3T3 fibroblast-derived retroviral packaging cell line PT67 was infected using the supernatant harvested from phoenix E transfections. PT67s were cultured in standard 3T3 10C medium (table 2.1). Cells were subcultured using 0.1% trypsin and the trypsin neutralized with addition of 10C and centrifuged for 5 min at 800 rpm prior to re-plating.

PT67 cells were plated at 2.5 x 10^4 per well of a 6 well plate and left to incubate over night at 37^{o}C. Cells were washed with PBS and treated with 5 µg/ml of polybrene (Sigma, UK) in 10C medium and incubated for 15 min at 37^{o}C. Cells were then treated with 2 ml of the 10C/supernatant/ polybrene (1:1:1) mix and the plates centrifuged for 1 hour at 350 rpm at 32^{o}C. The media was then removed and the cells washed with PBS before the addition of 2 ml of 10C medium. The cells were incubated at 37^{o}C, in 5% CO_2 for 48 hours after which they were transferred to a 10 cm dish (one dish per construct) and once over 80% confluent, subjected to drug selection. pRetrosuperior constructs were selected with 2.5 µg/ml puromycin and pBabe constructs with 1.2 mg/ml neomycin. After the mock cells (positive control cells with polybrene/media only) were dead, infected PT67 cells were frozen down and stored in liquid nitrogen until ready for keratinocyte infection.

2.6.4 Retroviral Transduction of Human Keratinocytes

2.6.4.1 γ Irradiation of iPT67

Once confluent, infectious PT67 cells were trypsinized, resuspended in fresh 10% FAD medium and given a 60 Gy γ-IR dose. Cells were then re-plated at the same confluent density with keratinocytes (e.g. 1 x 10^6 keratinocyte with 1 x 10^6 infectious PT67 / 10 cm dish) and cells co-cultured for 48 hours. Infectious PT67 were then removed from the plate in the way normal feeders would be. The medium was replaced with FAD^{+EGF} and fresh feeders containing the relevant drug resistant maker were applied.

2.6.5 Keratinocyte Transduction

Infected PT67 were cultured in 10C until confluent and treated with 60 Gy dosage of γ radiation. The freshly irradiated infectious cells were plated at 1 x 10^6 with a keratinocyte seeding density of 1 x 10^5 per 10 cm dish and medium changed at 72 hours at which point drug selection was started with puromycin (1 μg/ml) and G418 (7 μg/m). The irradiated infectious PT67 feeders were replaced with freshly thawed feeders at 72 hours post drug selection and cells subcultured and subjected to drug selection until confluent. Feeders were then removed and cells cultured until confluent and stocks frozen down. Cells were cultured long term and population doublings recorded.

2.7 Telomere Repeat Amplification Protocol (TRAP)

2.7.1 TRAP assay

The Telomeric Repeat Amplification Protocol, or TRAP, is a two-step PCR based methodology originally developed to determine telomerase activity *in* vitro (Kim, Piatyszek et al. 1994). The first step of the assay comprises of telomerase adding telomeric repeats (TTTAGG) to a template substrate and in the second step there is amplification of these products using specific forward and reverse primers, together with the amplification of an internal standard PCR control (with separate forward and reverse primers) (Herbert, Hochreiter et al. 2006). The internal control can be used to check equal loading of the lysates as the amount of telomeric products detected is inversely correlated with the amount of telomeric product as well as to identify false-negative samples due to Taq polymerase inhibitors (Herbert 2009).

Telomeric repeats representing enzymatic activity are subsequently shown on a polyacrylamide gel as a ladder pattern of PCR products with a spanned size of 6 bp, starting from a size of 50 bp. The internal control band is shown at 36 bp and the higher the telomerase activity, the stronger the signal of the ladder will be. A non-radioactive TRAP assay was adapted for use in this study (Herbert, Hochreiter et al. 2006).

2.7.2 Preparation of samples

Semi confluent cells were trypsinized as per routine and cell extracts were prepared by lysing half a million cells per sample in 200 µl Chaps buffer (Sigma Aldrich) and incubating on ice for 20 min. Lysates were separated from cell debris by centrifugation at 12,000 rpm for 20 min at 4^{o}C and 160 µl of the supernatant was used to determine the protein concentration. BCA protein assay was used to determine the protein concentration of the lysates as per the manufacturer's instructions. A standard protein curve was prepared with a known Bovine Serum

Albumin (BSA) concentration using the CHAPS lysis buffer and following this the protein concentration in the samples was determined according to the standard and scanned for absorbance at 650 nm in a plate reader. Aliquots of the lysates were stored at -80^{o}C in RNAse-free tubes until subsequent use and from which appropriate dilutions were made. The optimal protein concentration was estimated to be 100 ng/µl.

2.7.3 Positive and negative controls

The cell pellet for the positive control was provided in the Chemicon TRAPeze kit (Chemicon Europe Ltd, Chandlers Ford, UK) and suspended in 200 µl of CHAPS lysis buffer to prepare lysate for the positive control following the same protocol for sample preparation. The lysate was diluted 1:1 with RNAse-free water before loading into the assay to avoid over-loading of the system.

A specific negative control for the absence of telomerase activity was obtained by the cell lysate of GM847 cells, which possess ALT phenotype and lacks detectable telomerase activity. A chaps buffer only negative control was utilized to check the presence of primer-dimer PCR artefacts or the presence of PCR contamination.

As telomerase is heat sensitive, each sample extract was heat treated and used as a third negative control. Samples were incubated at 85^{o}C for 10 min prior to the assay to inactivate telomerase.

2.7.4 Cy5 fluorescent-based PCR reaction

The fluorescent dye Cy5 (fluorescent in the red region (~650 nm excitation/670 nm emission), was attached to the 5'-end of the primer TS to permit final quantification of the PCR products on the gel. Primer details are shown in table 2.6.

2.7.5 PCR

Sample lysates were amplified by PCR in a five-stage reaction: incubation at 30°C for 1 hour, where telomerase is allowed to add repeats to the substrate; telomerase inactivation at 95°C for 5 min; 24 cycles at 95°C for 30 sec (denaturation), 52°C for 30 sec (annealing) and 72°C for 30 sec (extension); final elongation at 72°C for 2 min; hold at 4°C.

2.7.6 Visualization of PCR products

A 12% polyacrylamide gel was cast in a disposable plastic cassette (Invitrogen, Paisley, UK) by mixing 12% of PolyPAGE-40 Acrylamide/Bis (19:1) (Polysciences, Eppelheim, Germany) with 6% of 1 x TBE (89 mM Tris base, 89 mM boric acid, 2 mM EDTA), 0.01% of 10% ammonium persulfate, 0.001% of TEMED and dH_2O.

Following PCR samples were visualized by adding 5 µl of loading dye (0.25% bromophenol blue, 50% glycerol, 50 mM EDTA) to each sample and 25 µl of this mix was loaded into the gel. The gel was run in 0.5X TBE for 1 hour at 140V and protected from external light. To avoid DNA diffusion the gel was fixed by incubation in 0.5 M NaCl, 50% (v/v) ethanol and 40 mM sodium acetate (pH 4.2) for 15 min at room temperature (RT) in the dark. The TRAP ladder on the gel was visualized using a Phosphorimager scanner (Typhoon 9400 scanner, GE Healthcare, Chalfont, UK) reading Cy5 fluorescence at 633 nm.

Component	Supplier	Concentration	Volume (ul) per reaction Total 50 ul
Rnase-free H_2O	Qiagen, Crawley,UK	-	37.7
TRAP buffer	-	10X	5
dNTP mix	New England Biolabs, Hitchin, UK	10 mM each primer	0.5
Cy5-TS	Eurofins, MWG Operon, London, UK	100 ng/µl	1
NT primer	Eurofins MWG Operon, London, UK	100 ng/µl	1
ACX primer	Eurofins MWG Operon, London, UK	100 ng/µl	1
TSNT template	Sigma-Aldrich, Poole, UK	10^{-20} mol/µl	1
BSA	Ambion, Huntingdon, UK	50 mg,ml	0.4
Taq polymerase	New England Biolabs, Hitchin, UK	5U/µl	0.4
Sample	-	100 ng/µl	2

Table 2.5: Components of PCR reaction for TRAP assay.

The main components of the PCR reaction of the TRAP assay are the 10X TRAP buffer (200mM Tris-HCL pH 8.3, 15 mM $MgCL_2$, 630 mM KCL, 10 mM EGTA, 0.5% Tween-20) to lyse the cells of the sample and collect TERT; the different primers (see table 2.6); the substrate TS to which telomerase adds the telomeric repeats; and the TAG polymerase to amplify the product added by telomerase in the first step of the reaction.

Primer name	Sequence	Function
Cy5-TS	5'-Cy5-AATCCGTCGAGCAGAGTT-3'	Substrate oligonucleotide/forward primer
ACX	5'-GCGCGGCTTACCCTTACCCTTACCCTAACC-3'	Reverse primer
TSNT	5'-AATCCGTCGAGCAGAGTTAAAAGGCCGAGAAGCGAT-3'	Template for internal control
NT	5'-ATCGCTTCTCGGCCTTTT-3'	Reverse primer for internal control

Table 2.6: **Role of the primers used in the PCR reaction for TRAP assay.**

Each of the four primers utilized in the PCR reaction have got specific functions that allow the addition of the telomeric repeats and the following amplification for further detection and correlation with telomerase activity. Active telomerase binds to the TS substrate and a number of telomeric repeats (TTTAGG) are added to TS according to the degree of activity of the enzyme. In the PCR step of the assay, the products generated are amplified with the TS primer, that is attached to a fluorophore for the following detection, and with the reverse primer ACX. In addition, the sequence TNST serves as a template for an internal control which is amplified with the reverse primer NT and the forward primer TS. Therefore, using the same TS primer, this internal control competes with the telomeric repeats in the amplification process and its expression will be inversely correlated with the amount of telomeric products, thus with the activity of telomerase.

2.8 Western Blotting

2.8.1 Whole Cell Extraction

Cell pellets were washed twice with PBS and lysed with Radio-Immunoprecipitation Assay (RIPA) buffer (1% NP-40, 0.1% SDS, 50 mM Tris pH 7.3, 150 mM NaCl) (Sigma,UK) with protease inhibitors (cOmplete cocktail tablets, Roche Diagnostics) and incubated on ice for 20 min. The lysates were separated from cell debris by centrifugation at 15,000 rpm for 20 min and approximately 160 µl of supernatant transferred into new eppendorfs on ice. Total protein concentration was measured using the DC protein assay kit (BioRad, Hemel Hempsted, UK) following manufacturers protocol. The protein concentration in each sample was calculated using a standard curve calculated from BSA standards. 4x sample buffer was mixed with the protein sample to dilute the lysate to get the final loading concentration of 20 µg. The lysates were boiled for 5 min at 100^{o}C and stored at -80^{o}C.

2.8.2 Gel Electrophoresis

Cell lysates were prepared as above and total cellular protein was separated from the lysate on 4%-12% gradient SDS-PAGE gels (NuPage novex bis-tris pre cast gels, Invitrogen, UK) under denaturing and reducing conditions at 130 V. The 20 x NuPage sodium dodecyl sulphate (SDS) running buffer (Invitrogen) was diluted 1 in 20 to make 1x running buffer. The dual colour marker (dual colour, BioRad) was used to visualize respective band sizes.

2.8.3 Western Blotting

The proteins were then transferred to a 0.45 µM Immobilin PVDF membrane (Millipore, Watford, UK) that had been soaked first in neat methanol (VWR, Lutterworth, UK) and then in transfer buffer (25 mM Tris, 190 mM glycine and 20% methanol) for 3 min. Protein transfer took place at 100 V for 90 min. The membrane was then blocked in 5% (w/v) skimmed milk powder (Marvel, Bristol, UK) prepared in wash buffer saline and tween-20 (TBS-T) (1 M Tris pH 8.0, 5 M NaCl,

0.05% tween-20 for 1 hour at RT. The membrane was then probed in 5% milk in TBS-T with the appropriate primary antibody overnight at 4^{o}C. The following day the membrane was washed extensively with TBS-T and then incubated with an appropriate secondary solution, prepared in 5% milk TBS-T, for 1 hour at RT. The membrane was washed again four times in one hour with TBS-T before being developed as described below.

2.8.4 Developing Western Blots

Membranes were dried and developed firstly with Amersham ECL plus (GE Healthcare Life Sciences) or, if the signal was weak and required > 30 min development time, it was washed briefly with TBS-T and then incubated with Supersignal West Femto maximum sensitivity substrate (Pierce, Thermo Fisher Scientific) on Amersham Hyperfilm ECL (GE Healthcare Life Sciences).

2.8.5 Stripping Blots

If a second protein of a similar weight to the first protein was being examined, the membrane was stripped using stripping buffer for 30 min at RT. The membrane was then washed three times with TBS-T for a total of 30 min and re-incubated with the secondary antibody used (as above) to detect the first protein, before being washed and developed. If the first antibody had been satisfactorily stripped, the membrane was re-probed. If it had not, the procedure was abandoned.

2.9 Senescence Associated β Galactosidase expression

Cells were cultured and at 50%-60% confluency they were stained for β galactosidase (β gal) activity using the BioVision Senescence detection kit (Cambridge Biosciences, Cambridge) as per manufacturers protocol. The plates were incubated in dark for 16 hours at 37^{o}C, washed with water, photographed using a light microscope and the number of senescent cells counted. The presence

of β gal activity was evidenced by dark green colour in the perinuclear cytoplasmic region and 500 individual cells were counted and the percentage of positive cells for each cell line was quantitated. Early and late passage cells were incorporated into the experiment as positive and negative controls respectively.

2.9.1 Nuclear Fast Red Staining

Cells were counterstained with nuclear fast red (NFR) (BDH Chemicals, Poole, UK) as per manufacturer's instructions to easily distinguish cells that were negative for β gal from the dark green positively-stained cells.

2.10 Metaphase Spreads with hypotonic KCL

Cells were cultured to 70%–80% confluence, cells were medium changed as per routine and incubated overnight. The following day 37 µl of 10 mg/ml demecolcine colchizine (Sigma, UK) was added directly to the cells and culture dishes incubated for 3 hours at 37^{O}C, following which medium was collected from the plates and cells trypsinized, followed by neutralization using the previously collected medium and transferred to a 15 ml centrifuge tube and centrifuged for 5 min at 800 rpm. The pellet was resuspended drop wise in warm hypotonic KCL solution (0.075M) with constant gentle agitation and incubated for 45 min at 37^{O}C. Cold methanol-acetic acid fixative (3:1 ratio) , freshly prepared, was then added drop wise to the cell suspension at 20% of the total volume of the 15 ml tube with constant agitation and centrifuged for 3 min at 800 rpm. This fixative step was repeated 3 times to form turbid cell suspensions. For metaphase spreads an aliquot of cell suspension was added drop-wise onto a humidified slide, pre-chilled overnight, from a height of approximately 1 metre and the slides allowed to air-dry. Slides were photographed with light microscopy.

2.11 UVB treatment of cells for detection of apoptosis by Annexin V assay

2.11.1 UVB Treatment

UVB induced DNA damage is a crucial event in UVB-mediated cellular apoptosis (Kulms, Pöppelmann et al. 1999). Medium was aspirated from semi-confluent cells (50%–60% confluent) and culture dishes placed in a U.V cross-linker (UVP, Cambridge, UK) with the lids removed. Cells were irradiated with UVB at different doses (10 mj/cm^2 and 20 mj/cm^2) and fresh medium was replaced immediately following UVB exposure and cells incubated at 37^{o}C, 10% CO_2 for 24 h, 48 h and 72 h. Non UV treated cells were used as controls and cultured under the same conditions. Following incubation, treated and untreated cells were either used for whole protein extraction followed by western blot analysis for markers of apoptosis and senescence (p53 and p16^{INK4a}) or used for Cy ^{TM}5 annexin V antibody staining followed by FACS analysis to check apoptosis and cell death.

2.11.2.1 Annexin V Apoptosis Assay

In the early stages of apoptosis cells undergo a variety of structural and biochemical events which lead to changes on the cell surface. One of these altercations involves the translocation of the plasma membrane protein phosphatidylserine (PS) from the inner side of the plasma membrane to becoming exposed on the outer surface of the cell membrane (Vermes, Haanen et al. 1995). Annexin V is a Ca^{2+} dependent binding protein which has high affinity for PS and is fluorescein-conjugated to use as a probe in detection of cell apoptosis (Vermes, Haanen et al. 1995). Since the intermembrane translocation of PS is not unique to apoptotic cells but also a prominent feature of cells undergoing necrosis, due to loss of membrane integrity, a DNA stain such as DAPI is utilized to differentiate between the two cell types.

Cells were trypsinized as per usual and cell pellets washed in PBS with centrifugation at 1000 rpm for 6 min RT. Each pellet was resuspended in 500 µl of Annexin V binding buffer (beckton Dickinson), 4µl/ml of Annexin V FLUOS (Roche Diagnostics) and 200 ng/ml of DAPI . Cell suspension was gently vortexed and transferred into sterile 5 ml round bottom FACS tubes and incubated at RT for 15 min. FACS analysis was carried out by flow cytometer (LSRII BD Biosciences), collecting 10,000 events per cell sample. The remaining cell suspension was fixed in 70% ETOH for cell cycle analysis.

2.12 Organotypic Stratification

2.12.1 Polycarbonate Membrane

For the most part of this study cells were cultured, transduced and assessed for population doublings on a monolayer culture system. *In vivo* however, keratinocytes are part of a stratified epithelium and to determine stratification of transduced cell lines the cells were cultured on top of 0.5 cm^2 polycarbonate inserts and raised to the air-liquid interface in both serum free medium and FAD for 7 and 14 days.

Cells were gently applied to the polycarbonate epithelial surface at a density of 5 x 10^4 in 150 µl of appropriate medium and incubated overnight at 37^oC in humidified 10% CO_2. The next day cells were raised to air-liquid interface by aspirating medium off from membrane surface. Cells were medium changed every 2 days and cultured for the set time interval and at each time point the inserts were analyzed for cell viability.

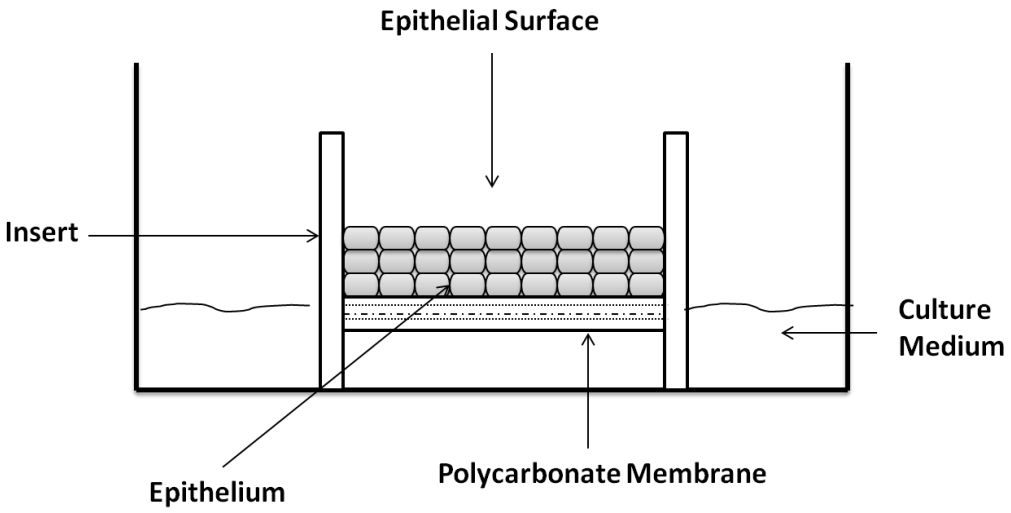

Figure 2. 1: Diagram of reconstitute epithelium cultured on polycarbonate membrane insert.

Keratinocytes were cultured atop the polycarbonate membrane surface and allowed to differentiate over time prior to being assessed for stratification.

2.12.2 MTT Assay

The Thiazolyl Blue Tetrazolium Bromide (MTT) assay (Sigma) is a rapid colorimetric assay which is based on the use of [3-(4,5-dimethylthiazol-2-yl)-2,5-diphenyltetrazolium bromide] to measure cell survival and proliferation (Mosmann 1983). It is based on mitochondrial reductase activity in metabolically viable cells to convert the yellow tetrazolium salt, MTT, into dark blue forazan crystals (Gerlier and Thomasset 1986). As the cultured cells proliferate, a reduced cellular environment is maintained causing the yellow MTT to change from its yellow oxidized form to reduced blue formazan form. This reduction only takes place in the presence of mitochondrial reductase activity and hence the number of surviving cells is directly proportional to the level of formazan product generated (Mosmann 1983).

This assay was used to determine the number of viable cells after culture on polycarbonate membranes. $5x10^4$ cells were plated onto the polycarbonate membrane in 100 µl of appropriate medium and the membranes were themselves placed in 12-well plates and 2 ml of appropriate medium was added to each well, enough to cover the well but not overflow the membrane. The next day cells were brought to air-liquid interface by removing medium from the surface of the membrane. The wells were medium changed every 2 days and MTT assay performed every 5 or 7 days upto 1 month. As MTT is highly toxic to cells it was not possible to use the same cells throughout the time course to measure proliferation and so the same number of cells had to be plated separately for each additional time point.

An MTT solution (5 mg/ml) was prepared in sterile PBS and stored at 4ºC and was used to prepare the working concentration of 0.5 mg/ml of MTT solution as required and filter sterilised. Using sterile forceps, polycarbonate membranes were

transferred to a new 24-well plate and 500 µl of MTT working solution was added into the membrane and plate was incubated in the dark for 1 hour in a CO_2 incubator at 37°C. MTT solution was then aspirated off and the blue formazan dye was dissolved adding 500 µl of isopropanol in each well and the plate sealed with parafilm and incubated for a further 1 hour at 37°C to elute any formazan crystals that had formed. Cell membrane was then punctured with sterile pipette tip to allow contents to mix together and DMSO solution mixed thoroughly to ensure complete solubilization of formazan crystals. Triplicates of 200 µl dissolved coloured aliquots from each well were transferred to a 96-well plate along with DMSO only control (Nunc-VWR).

The absorbance (optical density) was measured at 570 nm optical density (OD) using a 96 microplate reader well on FLUOstar OPTIMA BMG Labtech plate reader. For each cell line, 6 replicates were prepared per time point and DMSO-only as control. The OD of the blank (just 200 µl DMSO) was subtracted from the sample OD. Cell viability was expressed as a percentage of the control cultures as: Viability = OD (570nm) Treated / OD (570nm) Control*100.

2.12.3 Stratification

Membrane was cut out from the polycarbonate insert and sent for sectioning and histology examination by the Blizard Institute of Cell and Molecular Sciences Pathology Group, Queen Marys, University of London.

2.13 Statistical Analysis

A two tailed T-test was used throughout this study unless stated otherwise.

Chapter 3:

Results 1

Chapter 3

Results 1

Prior to starting the retroviral transduction process, a number of pilot experiments were performed to establish culture conditions for the optimum growth and infection of keratinocytes, with established growth conditions maintained for the duration of the study. Carbon dioxide is an essential requirement for the culturing of cells *in vitro* as CO_2 deficient environments inhibit cell growth (Maurel and Pareilleux 1985) and culture environments have since been established to adversely affect cell growth and viability (Hu and Aunins 1997). The CO_2 level at incubation during retroviral transfection is important for the optimum growth of cells and usually 5% – 10% CO_2 is commonly used for cell growth with a level of 14% deemed as growth inhibitory (Hu and Aunins 1997), although previous studies have also found transfection efficiency to be better at a lower CO_2 percentage of 3% (Chen and Okayama 1987). To enhance growth and minimize time in culture, particularly for primary cells, it is important to obtain the correct seeding density as cultivation of cell lines on tissue culture plastic is known to be affected by high seeding densities (Watt 1988) . When seeded at high seeding densities, cells often fail to differentiate properly whilst too low a density will result in very slow growth rates and prolonged exposure *in vitro*, in both cases there is a decrease in cell growth, emphasizing the need for optimization.

The aim of this study was to develop a well characterized oral epithelial cell line that has a significantly extended replicative lifespan and can be used in place of the current tumour-derived or tumourigenic cell lines as a monolayer or for the development of organotypic cultures. To do this, keratinocytes at early passage were used (table 2.1) as these are characteristically devoid of genetic mutations, DNA damage and other changes that accumulate with age.

Population doubling times have been shown to vary as a function of cell seeding density, growth medium and serum supplement and desirable conditions should allow independent growth of cell lines with multiple subcultures, maintenance of differentiation properties and characteristic responsiveness.

The results in the chapter will be described in following sections:

i) The effect of culture conditions on early passage keratinocytes
ii) Optimization of retroviral infection protocol for successful transduction of keratinocytes.

3.1 The effect of culture conditions

Prior to starting retroviral transductions, early passage oral and epidermal keratinocytes were assessed for optimal growth conditions. Cells were grown for 14 days and clonogenicity evaluated using rhodamine B staining and the number and size of colonies quantitated. CO_2 levels along with seeding density were shown to influence the number of colonies formed (Appendix 1).

Serum concentrations used in cell culture media are known to affect cell kinetics and metabolism and a direct link has been shown between media serum levels and cell viability (Elsayed, Demellawy *et al.* 2009). The serial culture of early passage NHOK and NHEK in an *in vitro* environment generated nuclear foci when stained for DNA damage markers 53BP1 and γH2AX across three culture mediums (Fig 3.1). The data indicates that keratinocytes cultured in medium supported with feeders, FAD^+ had the highest levels of positively stained cells for 53BP1 when cultured in feeder supported medium (NHOK 69% ± 7.1%, NHEK 68% ± 3.8%) compared to the two serum free mediums KGM (NHOK 64% ± 6.5% , NHEK 61% ± 5.5%) and KSFM (NHOK 61% ± 6.7%, NHEK 59% ± 7.4%). Similar trends were observed when stained for γH2AX, with higher numbers of positive cells for FAD^+ (NHOK 69% ±4.5%, NHEK 70% ± 5%) compared to KGM (NHOK 59% ± 8.1% , NHEK 63% ± 6.6%) and KSFM (NHOK 52% ± 3.6% , NHEK 58% ± 8.5%). The results are the averages of three independent experiments that were performed.

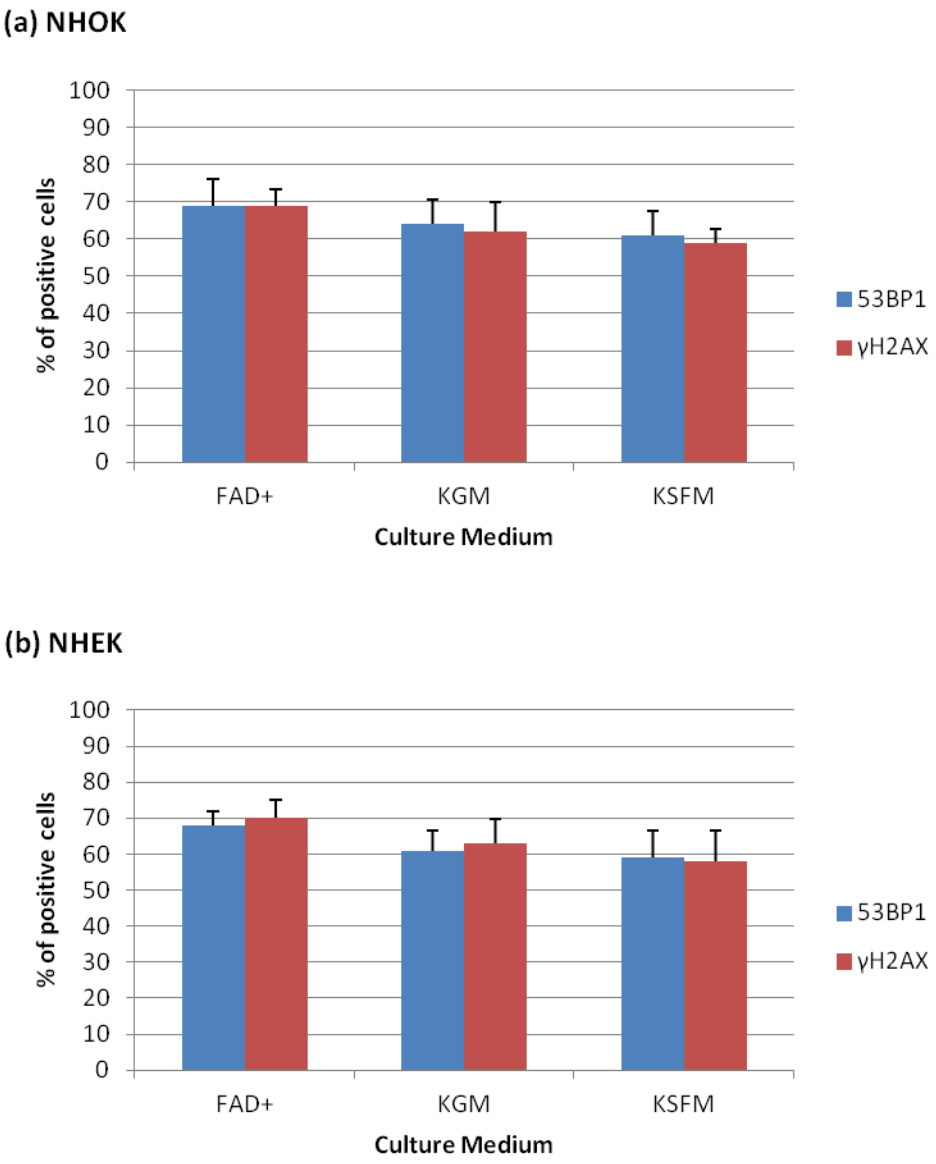

Figure 3. 1: Percentage of (a) NHOK and (b) NHEK cells stained positive for DNA damage markers 53BP1 (blue) and γH2AX (red).

Extent of DNA damage in non-transduced (a) NHOK and (b) NHEK cells after culture across the different culture mediums was determined by 53BP1 and γH2AX staining. A cell was classified as positive if it contained 3 or more nuclear foci. The percentage of positive cells was based on a counting of 300 cells in total per culture medium for each antibody. Means of 3 independent experiments are shown.

3.2 Retroviral Infection

A two-step retroviral infection protocol based on the study of Fiona Watt's group for the infection of keratinocytes was optimised for the successful transfection of DNA into phoenix E cells (Fig 3.2). Infection of PT67 fibroblasts with phoenix E derived supernatant successfully generated high numbers of infectious, drug resistant cells. The co-culture of keratinocytes with γ irradiated infectious PT67 generated drug resistant, infected cells.

3.2.1 Optimization of retroviral protocol for keratinocyte transduction

Retroviruses are an efficient means to transfer DNA expression constructs to a wide range of mammalian cell types and is a preferred method for manipulating gene expression in keratinocytes due to the ease with which they rapidly deliever genes stably to mammalian cells (Cepko and Pear 2001). A two-step retroviral protocol was followed using a phoenix retrovirus producer cell line (Levy, Broad *et al.* 1998). Phoenix expression vectors are highly transfectable with either calcium-phosphate mediated transfection or lipid based transfection protocols and is used worldwide for delievery of genes to cells for use in biomedical research (Morita, Kojima *et al.* 2000). Based on Moloney Murine Leukemia Virus (MMLV), it allows for the deleivery of genes to most dividing mammalian cell types and produces virus within a few days. The phoenix expression system is available in two vector types and for the purposes of this study the Ecotropic packaging system was used and hence will be referred to as phoenix E and these are capable of delivering genes to dividing murine and rat cells. The Amphotropic packaging system is capable of delivering genes to dividing cells of most mammalian species including humans (Kessels, Wolkers *et al.* 2005). Phoenix cells generate helper free retrovirus which allows for the production of replication defective retrovirus vectors in the absence of a helper virus and these vectors can infect and integrate into cells but cannot replicate and spread. These helper free vectors make it possible for a variety of studies to be conducted in which virus spread would make it difficult to interpret results and the

absence of helper virus prevents occurance of new integration sites and avoids virus spread (Kessels, Wolkers *et al.* 2005).

Early attempts to achieve long term gene expression in retrovirally transduced human epidermal keratinocytes remained largely unsuccessful (Levy, Broad *et al.* 1998). Keratinocytes are difficult to stably transfect with plasmid constructs but close to 100% infection can be achieved using retroviral vectors and there is stable expression of transduced gene during repeated passaging (Levy, Broad *et al.* 1998).

Although retroviruses are easier to work with, one limitation is that the percentage of cells infected is not as high as with the commonly used adenovirus infections and hence tradionally antibiotic drug selection is used for a minimum of one week to ensure a pure population of cells expressing the gene of interest. Prior to commencing experiments, a stock of primary keratinocytes were expanded and frozen down at between 5.5-6.6 mpd and since each experiment used a fresh ampoule, keratinocytes had undergone a total of between 7-9 mpd at the time of infection.

Following a previously established retroviral infection protocol, phoenix E cells were transfected for infection of PT67 but this did not prove straightforward. Phoenix E supernatant was used to infect PT67 but cells failed to survive drug selection. The following protocol was established and optimized following a series of pilot experiments.

The optimization process for infecting keratinocytes began with transfected DNA vectors into phoenix E using lipid based fugene 6 transfection reagent protocol. The phoenix E cells were plated in the afternoon at an optimized density of 2 x 10^4

instead of the previously recommended 1 x 10^6 and this was denoted as day 1. On morning of day 2 they were washed and fed with medium and drug selection was introduced to select for a pure phoenix E population containing the vector of interest. Once selected, phoenix E cells were cultured to approximately 80% confluency, upon which the transfected phoenix E cells were maintained in a 32^{o}C incubator overnight as the half life of the retrovirus is greater when stored at this lower temperature. Supernatant from phoenix E was collected and filter sterilized and used to infect PT67 cells. Drug selection was started with PT67 cells at 2 days post infection as this was found to allow for the cells to adhere to the tissue culture plastic thus allowing for better infection rates. Once selected, stocks were frozen and confluent PT67s were trypsinized and subjected to a lethal 60 Gy irradiation dose to prevent further replicaton prior to replating with keratinocytes and feeders at confluent levels.

Keratinocytes were co-cultured with lethally irradiated PT67 and feeders in medum without epidermal growth factor o/n at 37^{o}C. The inclusion of feeders alongside infectious PT67 allowed for better proliferation of keratinocytes rather than if they were cultured alone, as previously recommended. The medium was then supplemented with EGF and refreshed every other day. EGF is not added until the cells have attached to the tissue culture plate as this aides cloning efficiency (Rheinwald and Green 1977). Keratinocytes were co-cultured with infectious PT67 for a minimum of 24 hours and a maximum of 72 hours. If drug-resistant feeders were used then selection could be started immediately otherwise resistant feeders were added immediately after removal of PT67s and drug selection started. Co-culturing proved an effective way of introducing the constructs into the cells as the contact between the PT67 and the keratinocytes allows the virus to pass straight from one cell to the other which is considered to be more efficient than direct retroviral infection of keratinocytes using viral supernatants.

Once the mock cells were dead , drug selection was stopped and cell subculture continued with analysis of cell population doublings.

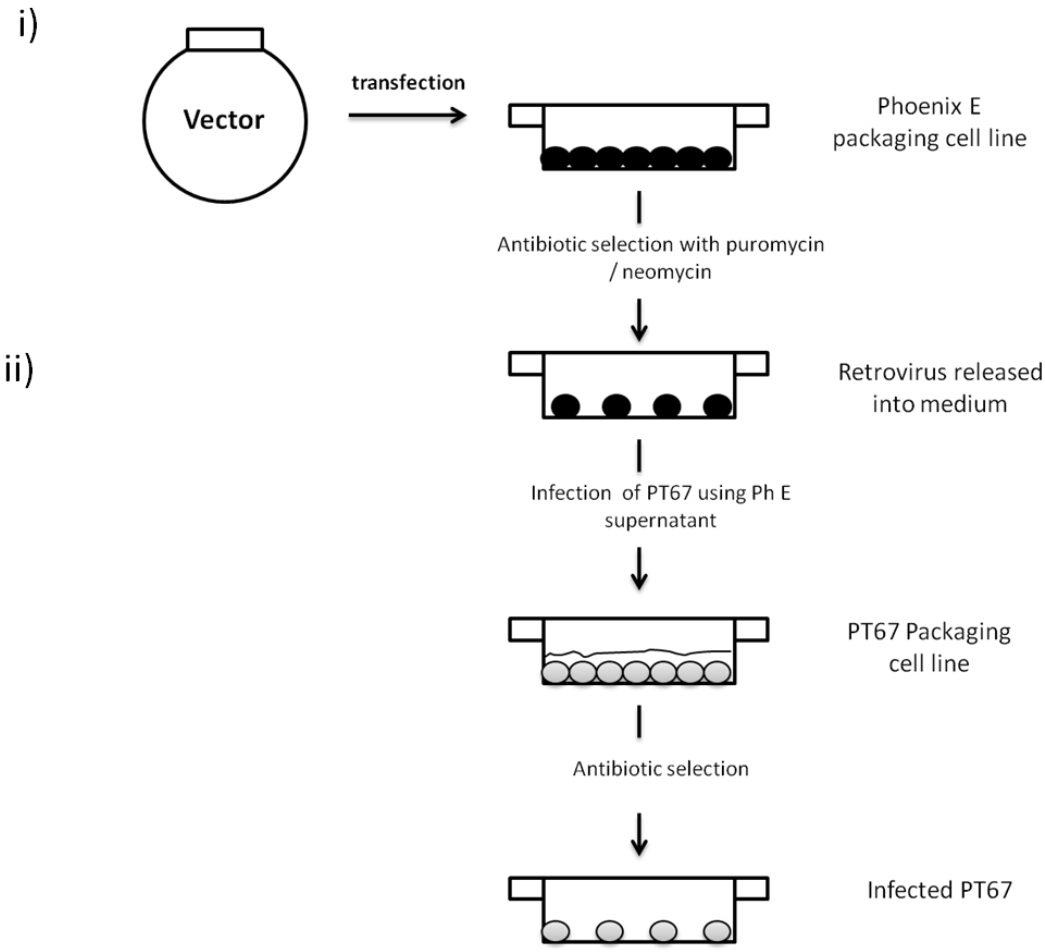
i)
Vector
transfection
Phoenix E
packaging cell line
Antibiotic selection with puromycin
/ neomycin
ii)
Retrovirus released
into medium
Infection of PT67 using Ph E
supernatant
PT67 Packaging
cell line
Antibiotic selection
Infected PT67

iii)

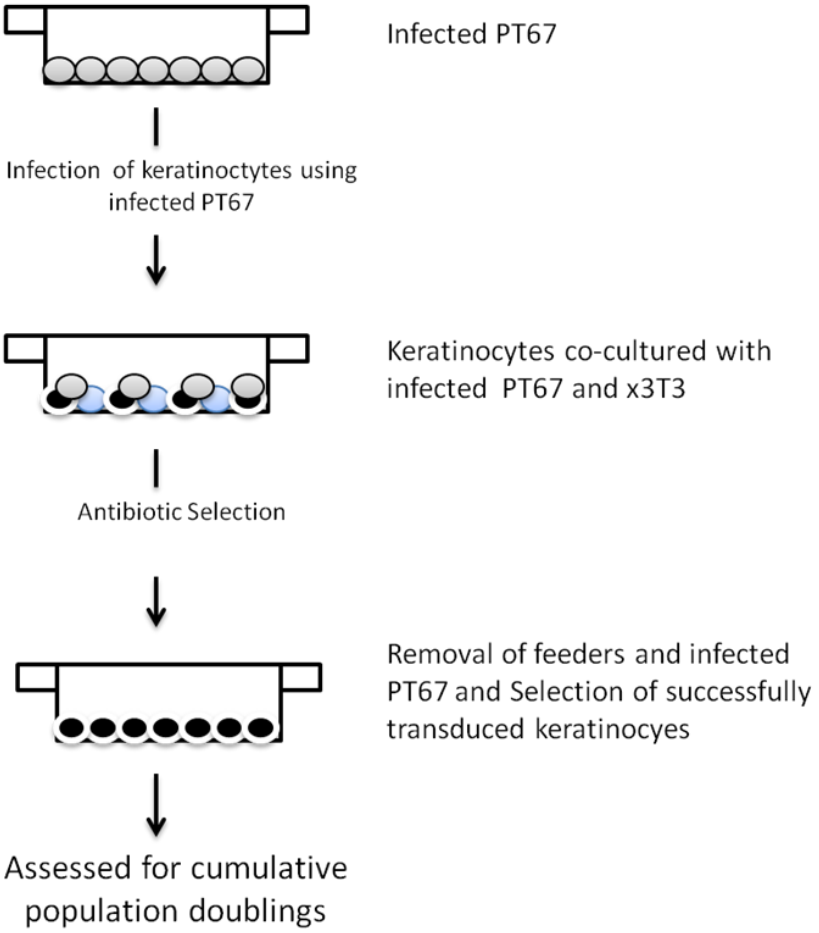

Figure 3. 2: Retroviral infection of keratinocytes.

(i) Phoenix E retroviral producer cells were plated at 2 x 10^5 a day prior to start of transfection. pRetro superior vectors and pBabe vectors were transfected on day 2 using fugene[6] at a fugene : DNA ratio of 2:1. Cells were then drug selected from day 4 until approximately 80% confluent. Cells were subjected to regular medium change throughout the selection process.

(ii) Medium containing retrovirus was then harvested from the phoenix E cells and used to infect PT67 cells, an NIH-3T3 amphotropic packaging cell line. Remaining retroviral supernatants were frozen as 1 ml aliquots at -80^{o}C. PT67 were subjected to drug selection two days post transfection until mock cells died.

(iii) Infections PT67 lethally irradiated with 60 Gy of *y*-IR and used as feeder layer for keratinocytes.

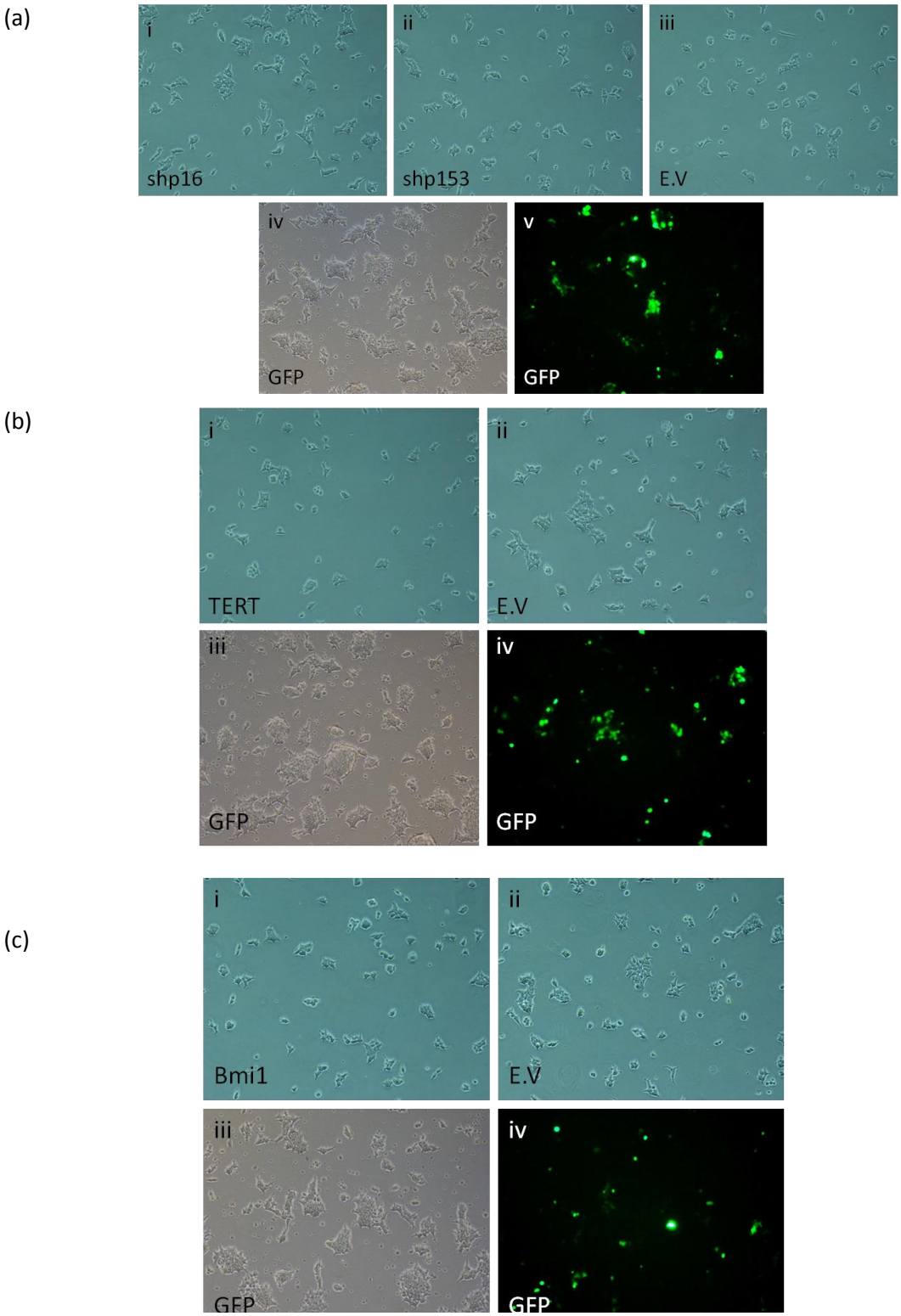

Figure 3. 3: Transfected Phoenix E cells.

Representative colonies of successfully transfected Phoenix E cells for the shp16/hTERT infections (a and b) and Bmi1/hTERT infections (c). GFP used as positive control throughout.

3.3 Discussion

Keratinocytes were grown in a feeder system to optimize culture conditions in relation to CO_2 percentage and optimal seeding density for subsequent retroviral infections. Cell growth was visibly enhanced and colonies better defined when cultured at 10% CO_2 and consequently it was decided to culture keratinocytes at a 10% CO_2 for the duration of the study.

Keratinocytes have typically been hard to stably transfect directly with plasmid constructs and it has been shown that the use of retroviral vectors results in high infection rates despite repeated passage in culture (Levy, Broad *et al.* 1998). This protocol was adapted and modified for the purposes of this study to infect early passage NHOK and NHEK cells with the vectors of choice.

An initial seeding density of 1 x 10^6 was used for phoenix E transfection after which infection of PT67 was carried out using phoenix E-derived supernatant and cells subjected to drug selection. At such a high starting density cells become over confluent on day of transfection in relation to the diameter of the 60 mm tissue culture dish. A series of pilot experiments were carried out to optimise the protocol to suit the current set of experiments. For successful transfection, phoenix E cells should be approximately 50% – 60% confluent at time of transfection and to determine this, cells were plated at five different seeding densities and cultured for five days. It was observed that a seeding density of 2 x 10^5 results in cell confluency of approximately 60% and when used for subsequent transfection, it greatly enhanced transfection efficiency. Additionally, to obtain a purer culture of transfected cells, drug selection was started two days post-transfection and cells were subcultured until 80% confluency was achieved. The phoenix E cells that were selected with 5 μg/ml of puromycin failed to survive and optimal puromycin dose was calculated to be at 2.5 μg/ml (for pRetrosuperior vectors). The GFP control

included in the study demonstrated high levels of phoenix E transfection and the subsequent infection of PT67 was successful. For transduction of keratinocytes, infected PT67 were subjected to a 60 Gy dosage of γ radiation prior to co-culturing with cells. It was important to culture the irradiated PT67 with the keratinocytes as soon as possible after irradiation, (rather than vapour phase storage), to avoid any reduction in the infectious ability of PT67 as a result of storage in liquid nitrogen. Furthermore, although the protocol originally states to use PT67 as a substitute for feeder cells during infection, the addition of feeders to the cultures alongside PT67 resulted in higher infection rates for the keratinocytes, possibly by providing additional growth factors. A high initial seeding density of keratinocytes at transduction was used, exposing higher number of initial cells available to be transduced and two days post transduction keratinocytes were subjected to drug selection prior to being assessed for PD. It was important to lower the dose of both puromycin and G418 for keratinocyte selection as the cells are more sensitive and less robust compared to fibroblasts and cannot withstand high drug doses. Drug selection successfully generated pure, transduced populations whereas cells allowed to proliferate in the absence of drug selection senesced earlier than their non-selected counterparts.

3.4 Chapter Conclusions

Early passage NHOK and NHEK were grown in presence of feeders and tested for optimal growth conditions which were maintained post transduction. PT67 cells were successfully infected from phoenix E supernatant after optimizing the retrovirus infection protocol and were irradiated for the transduction of NHOK and NHEK which were assessed for population doublings over an extended period of time (chapter 4, 5).

Chapter 4:

Results 2

Chapter 4

Results 2

4.1 Keratinocyte transductions and analysis of replicative life span

Cellular immortalization occurs when the cell acquires the ability to over-ride critical cell cycle regulatory mechanisms such as suppression of tumour suppressors 16^{INK4a} and p53 and/or escaping telomere regulation by upregulating telomerase expression. Keratinocytes were successfully cultured and immortalized by Rheinwald *et al.*, (1992) in a study which demonstrated that apart from down regulating $p16^{INK4a}$ along with introduction of telomerase, knock down of p53 is also required in order to extend lifespan of keratinocytes (Rheinwald, Hahn *et al.* 2002). Many studies have since, however, achieved life span extension of cells using varying infection protocols and demonstrated that p53 suppression is not required for immortalization of epithelial cells. The next part of this study aimed to reproduce that experiment in oral keratinocytes with an established and improved retroviral infection protocol, in hope of extending cellular lifespan with $p16^{INK4a}$ knockdown combined with telomerase without silencing p53. Many studies have stated that keratinocytes do not respond well to drug selection and to test whether this has any effect on replicative potential each infection was carried out in two sets, with one selected with antibiotics.

The Biovision senescent detection cytochemical assay was used to detect the activity of senescence-associated β galactosidase (β gal) activity (Dimri et al 1995)

within transduced cells that had ceased proliferation. B gal is a hydrolase enzyme that catalyzes the hydrolysis of β galactosides into monosaccharides and is commonly used in molecular biology as a reporter marker to detect the presence of an active β gal. The assay is based on the production of a blue-green dye precipitate resulting from the cleavage of β gal substrate X gal, a colourless compound which produces an insoluble, blue product when cleaved by β gal, thereby providing a means to distinguish the presence or absence of an active β gal enzyme.

Following successful optimization of the retroviral infection protocol, keratinocytes were transduced and subsequently assessed for replicative lifespan over an extended time frame with appropriate controls (table 4.1) and under different conditions. Two different methods were utilized to transduce keratinocytes: shp16 with hTERT (see below) and Bmi1 with hTERT (chapter 5). The results of these two methods will be presented under the different cell types (oral vs epidermal) and under the different selective conditions (drug-selected vs non-selected). Results from keratinocyte transductions on strains wherein cells failed to extend lifespan are not discussed here (Appendix 2).

Control Abbreviation	Controls
Parental	Non-transduced NHOK or NHEK cells at same PD as transduced cells
pRs E.V puro	pRetrosuperior Empty Vector control; cells transduced independently with pRs vector to confer puromycin resistance
pBabe E.V neo	pBabe Empty Vector Control; cells transduced independently with pBabe vector to confer neomycin resistance
shp53	shp53 only control ; cells transduced independently with shp53 to downregulate expression of p53
shp16	shp16 only control ; cells transduced independently with shp16 to downregulate expression of $p16^{INK4a}$
hTERT	hTERT only control ; cells transduced independently with hTERT to induce telomerase expression

Table 4. 1 List of controls used in the transduction of $NHOK^{shp16+hTERT}$ and $NHEK^{shp16+hTERT}$.

Extensive controls were used throughout the study to ensure validity of results. NHOK and NHEK cells were transduced separately with each of the controls mentioned above and cultured until they senesced.

4.1.2 Method Summary

Successfully infected PT67 cells were irradiated to act as infectious feeders and co-cultured with keratinocytes alongside normal feeders. Each cell line was assessed for population doublings (PD) under the two different selective conditions and the results presented herein.

4.2 NHOK $^{shp16+hTERT}$

NHOK strain 810 was transduced at early passage with shp16 and hTERT alongside appropriate controls (table 4.1) and assessed for proliferative capacity under two

conditions, with one set subjected to drug selection. Two independent experiments with similar results were obtained using shp16+hTERT (data not shown).

4.2.1 NHOK$^{shp16+hTERT}$ (selected)

NHOK$^{shp16+hTERT}$ continued to proliferate for an additional 7 PD up to a total of 27 PD compared to the parent NHOK control which plateaud after reaching 20 PD (Fig 4.1). Controls all ceased proliferation between 15 to 21 PD. As expected, NHOK$^{shp16+shp53+hTERT}$ continued to proliferate indefinitely until end of experiment at which point it had reached 95 PD. To determine senescence, cells were analyzed for β Gal activity (Fig 4.2 a and Fig 4.2 b). NHOK$^{shp16+hTERT}$ alongside controls exhibited high levels of senescence as evident from the presence of blue cell colonies (Fig 4.2 a) with 93% of NHOK$^{shp16+hTERT}$ cells positive for β gal as compared to 5% of NHOK$^{shp16+shp53+hTERT}$ (Fig 4.2 b).

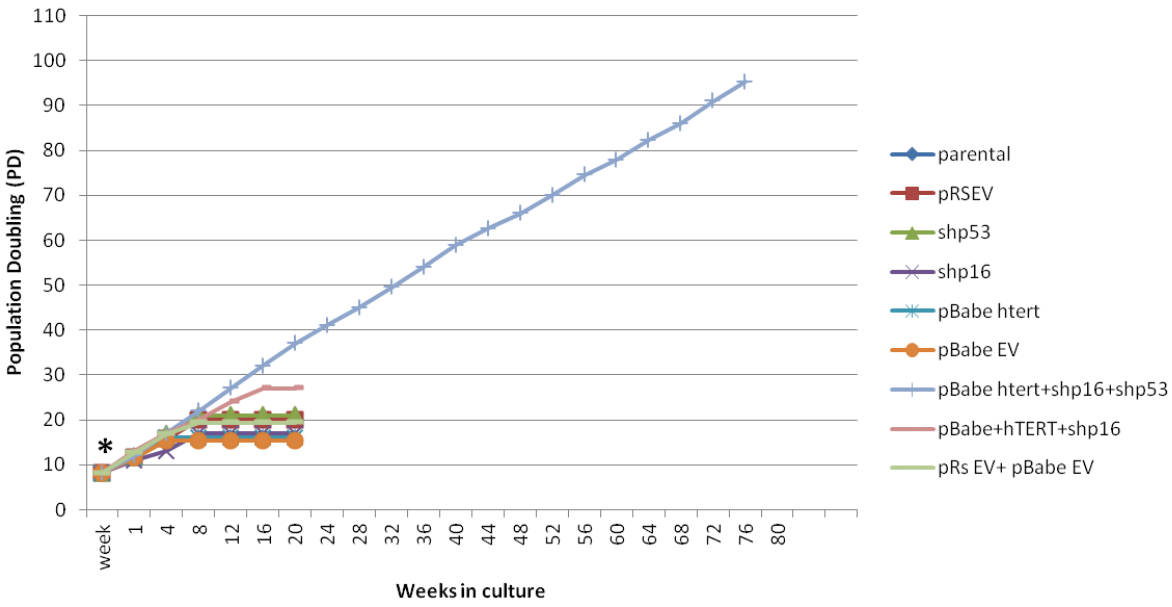

Figure 4. 1: NHOKshp16+hTERT (selected).

Early passage NHOK cells were transduced with shp16 and hTERT and subjected to drug selection with population doublings assessed (* indicates point of transduction). Appropriate controls were used (table 4.1).

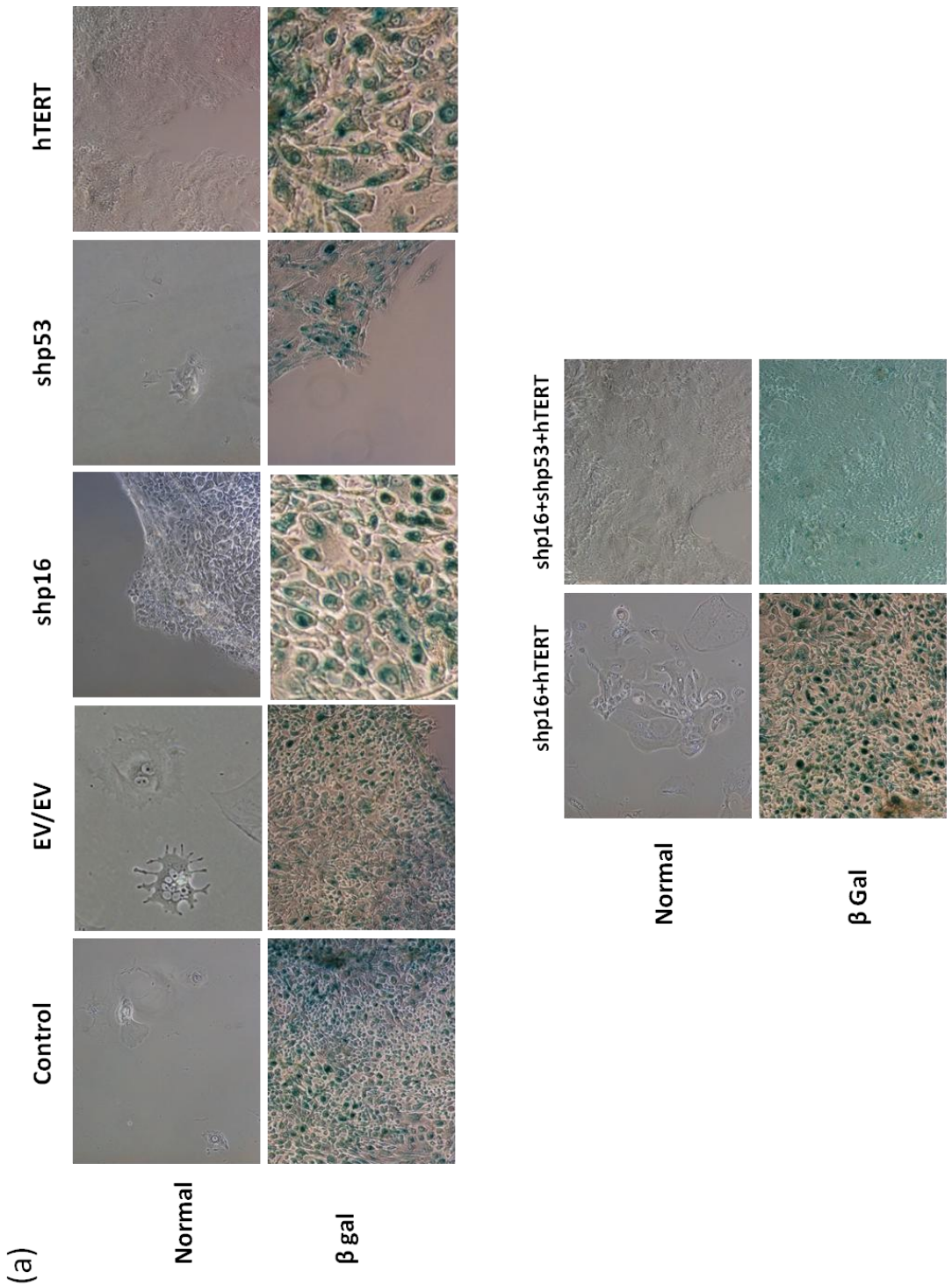
(a)
Control
EV/EV
shp16
shp53
hTERT
Normal
β gal
shp16+hTERT
shp16+shp53+hTERT
Normal
β Gal

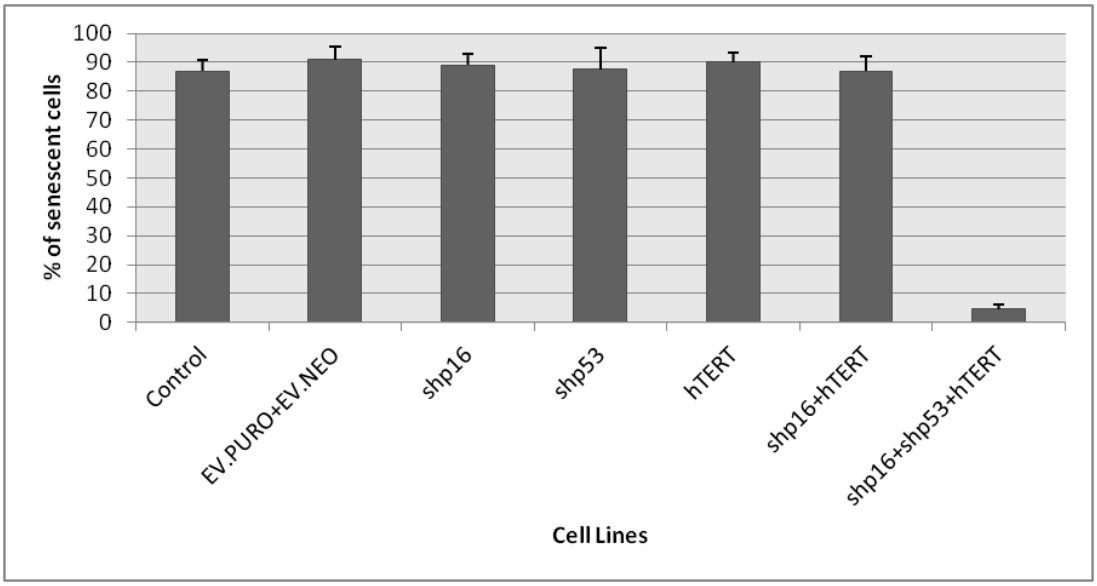

Figure 4. 2: Expression of Beta-galactosidase in NHOKshp16+hTERT (selected).

(a) Control plates all contained large, blue-green colonies positive for β Gal. $NHOK^{shp16+hTERT}$ ceased to proliferate indefinitely and the majority of cells were positive for β Gal. $NHOK^{shp16+shp53+hTERT}$ continued to proliferate and plates contained large colonies without extensive β Gal staining although did contain some small, naturally occurring senescent colonies.

(b) Quantification of senescent colonies. Cells were analyzed for β gal activity using the Biovision senescence detection kit. A total of 300 cells were counted and cells deemed positive if stained blue. Means of 3 independent experiments are shown.

4.2.2 NHOK$^{shp16+hTERT}$ (non-selected)

NHOK$^{shp16+hTERT}$ continued to proliferate for an additional 3 PD upto a total of 23 PD compared to the parent NHOK control which ceased to proliferate at 20 PD (Fig 4.3). Controls all ceased proliferation between 15.4 to 23 PD. Interestingly, however, it was noted that in the absence of drug selection NHOK$^{shp16+SHP53+hTERT}$ did not proliferate indefinitely, rather continued to proliferate for an additional 17 PD as compared to parental control and plateauing at 37 PD (Fig 4.3). To determine senescence, cells were analyzed for β Gal activity (Fig 4.4 a and Fig 4.4 b). All transduced cell lines exhibited high levels of senescence as evident from the presence of blue cell colonies (Fig 4.4 a) with 88% positive cells for NHOK$^{shp16+hTERT}$ and 91% positive for NHOK$^{shp16+shp53+hTERT}$ (Fig 4.4 b), whilst control cell lines were in the ranges of 85% - 91% positive cells.

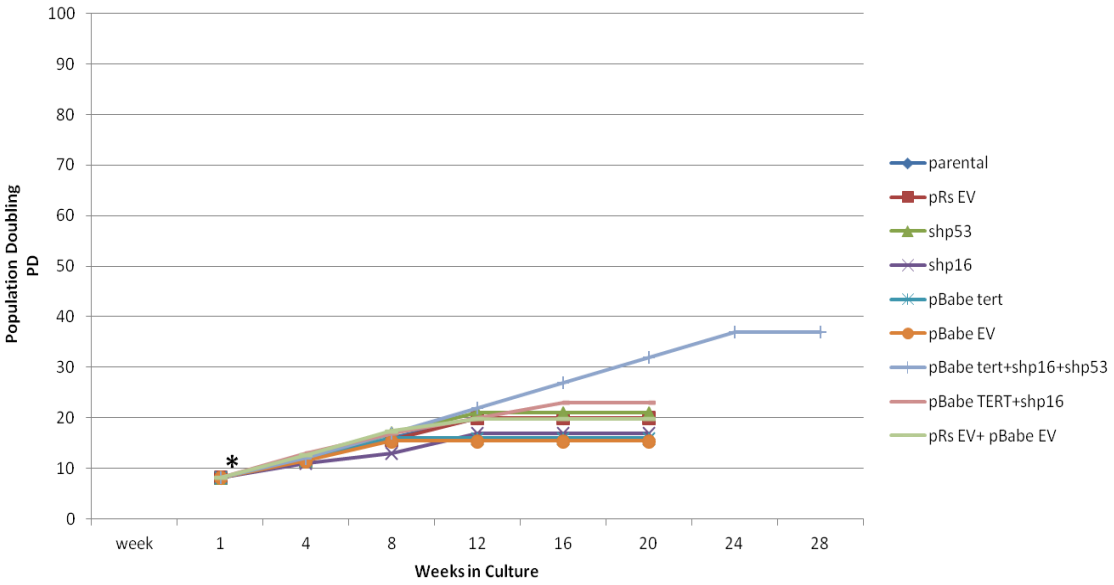

Figure 4. 3: NHOKshp16+hTERT (Non-selected).

Early passage NHOK cells were transduced with shp16 and hTERT and assessed for population doublings in the absence of drug selection (* indicates point of transduction). Appropriate controls were used (table 4.1).

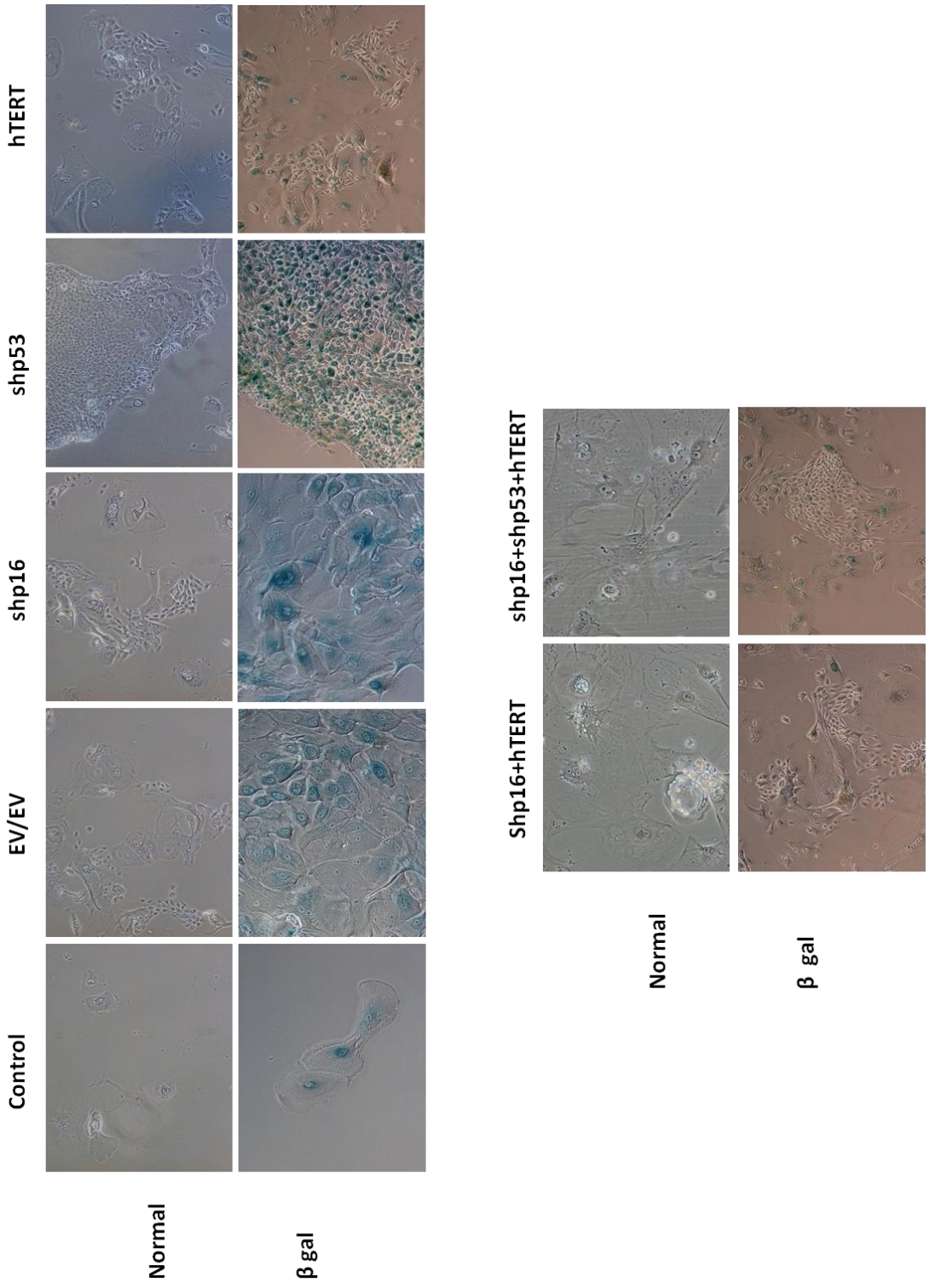
Control
EV/EV
shp16
shp53
hTERT
Shp16+hTERT
shp16+shp53+hTERT
Normal
β gal
Normal
β gal

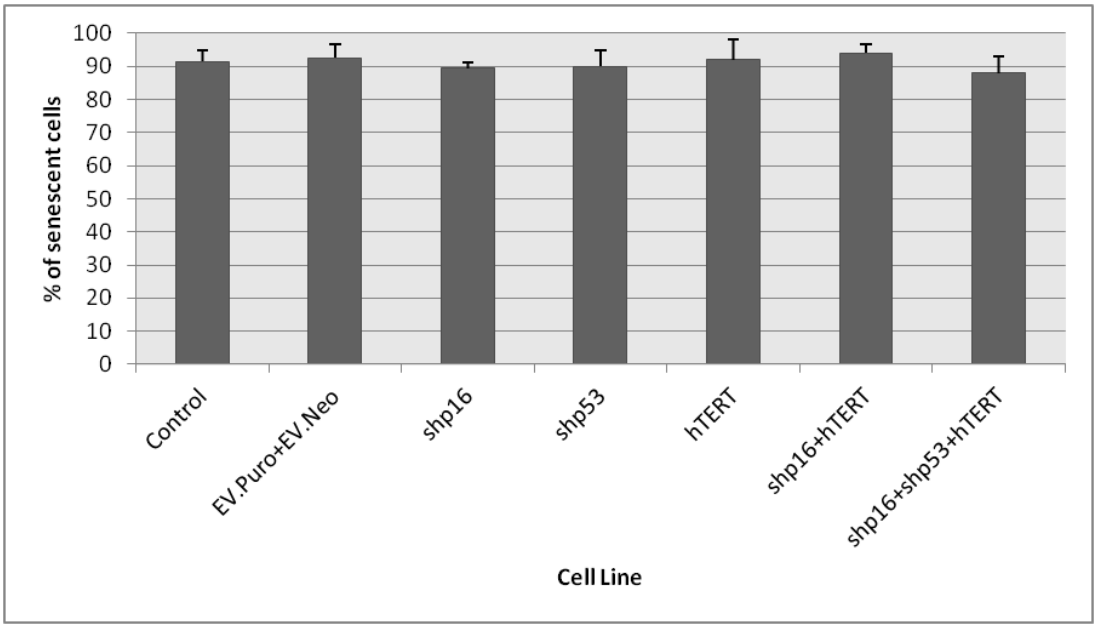

Figure 4. 4: Expression of Beta-galactosidase in NHOKshp16+hTERT (Non-selected).

(a) Control plates all contained large colonies positive for β gal. $NHOK^{shp16+hTERT}$ and $NHOK^{shp16+shp53+hTERT}$ ceased to proliferate indefinitely in absence of drug selection with majority of cells stained positive for β gal.

(b) Quantification of senescent colonies. Cells were analyzed for β gal activity using the Biovision senescence detection kit. A total of 300 cells were counted and cells deemed positive if stained blue. Means of 3 independent experiments are shown.

4.3 NHEK $^{shp16\ +hTERT}$

Early passage NHEK were transduced with shp16 and hTERT alongside appropriate controls and assessed for proliferative capacity under two conditions, with one set subjected to drug selection. Two independent experiments with similar results were obtained using shp16+hTERT (data not shown).

4.3.1 NHEK$^{shp16+hTERT}$ (selected)

NHEK$^{shp16+hTERT}$ continued to proliferate for an additional 3 PD up to a total of 19 PD as compared to the parent NHEK control that appeared to plateau after reaching 15 PD (Fig 4.5). Controls all ceased to proliferate between 13 to 19 PD. As expected, NHEK$^{shp16+shp53+hTERT}$ continued to proliferate indefinitely until end of experiment at which point it had reached 92.4 PD (Fig 4.5). To determine senescence, cells were analyzed for β gal activity (Fig 4.6 a and Fig 4.6 b). NHEK$^{shp16+hTERT}$ alongside control cells exhibited high levels of senescence as evident by the presence of positive cells (blue colonies) (Fig 4.6 a) with 91.8% of NHEK$^{shp16+hTERT}$ positive for β gal compared with 11% of positive cells for NHOK$^{shp16+shp53+hTERT}$(Fig 4.6 b).

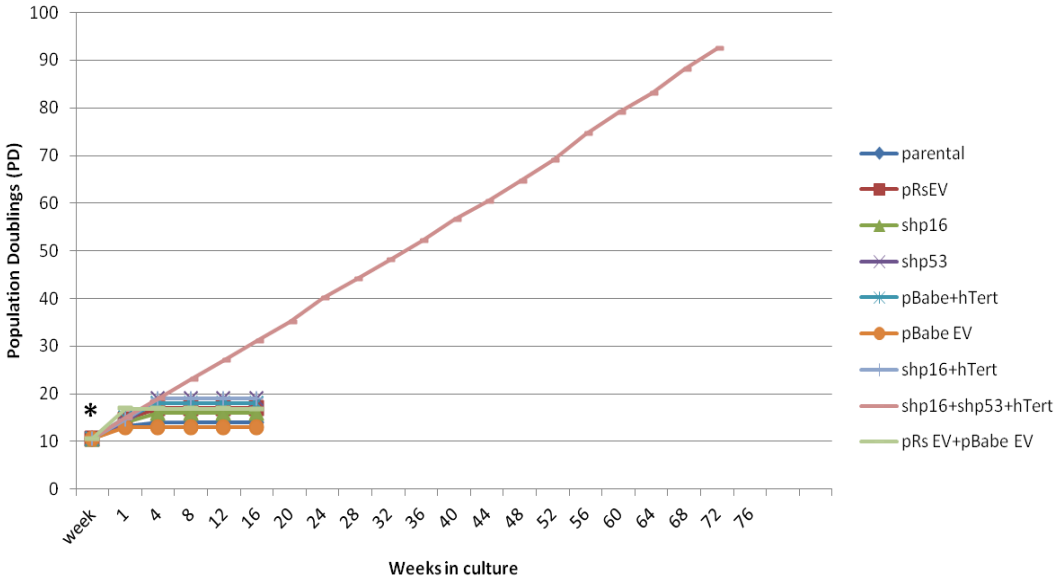

Figure 4. 5: NHEKshp16+hTERT (selected).

Early passage NHEK cells were transduced with shp16 and hTERT and subjected to drug selection with population doublings assessed (* indicates point of transduction). Appropriate controls were used (table 4.1).

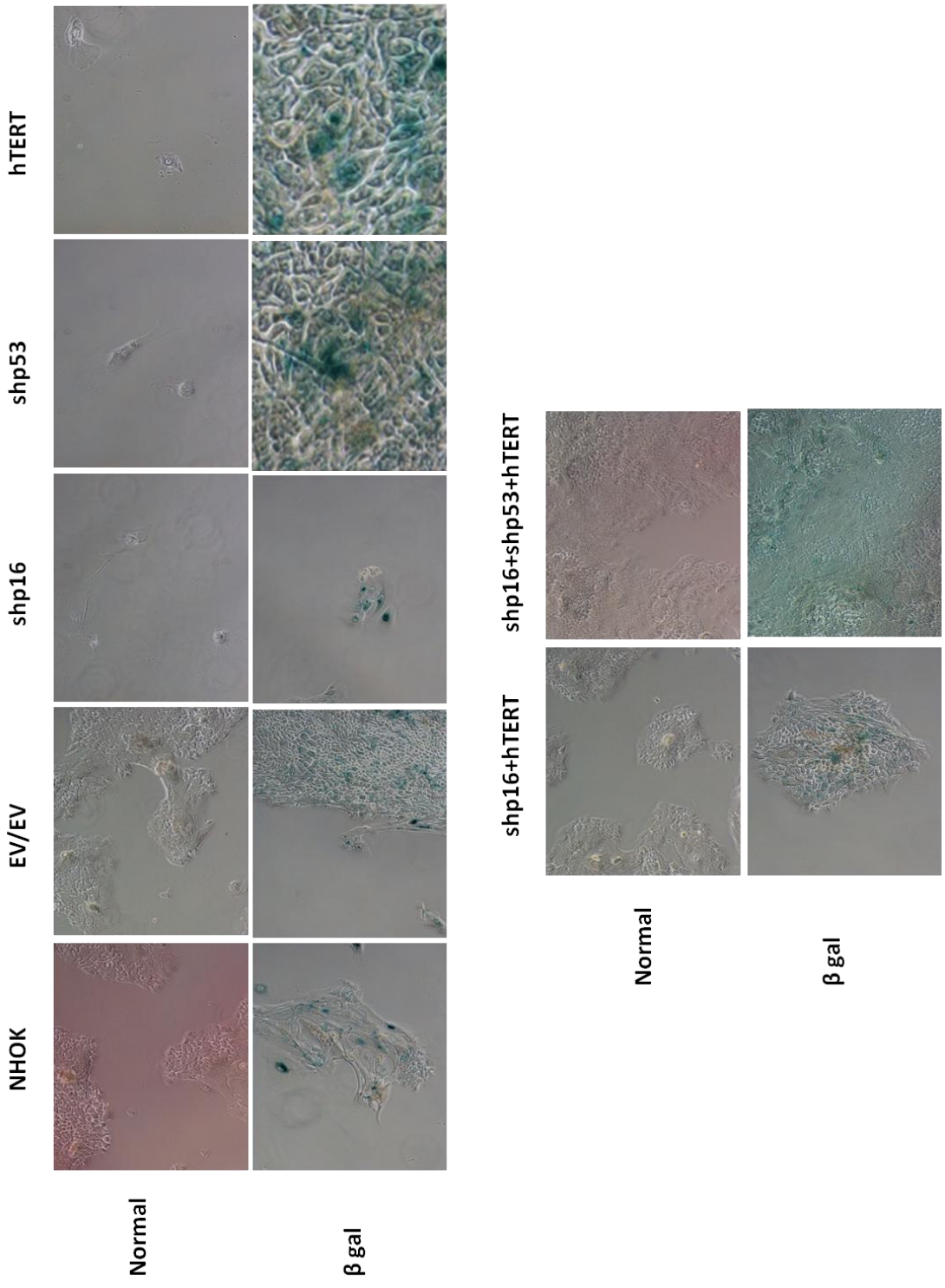
NHOK
EV/EV
shp16
shp53
hTERT
shp16+hTERT
shp16+shp53+hTERT
Normal
β gal
Normal
β gal

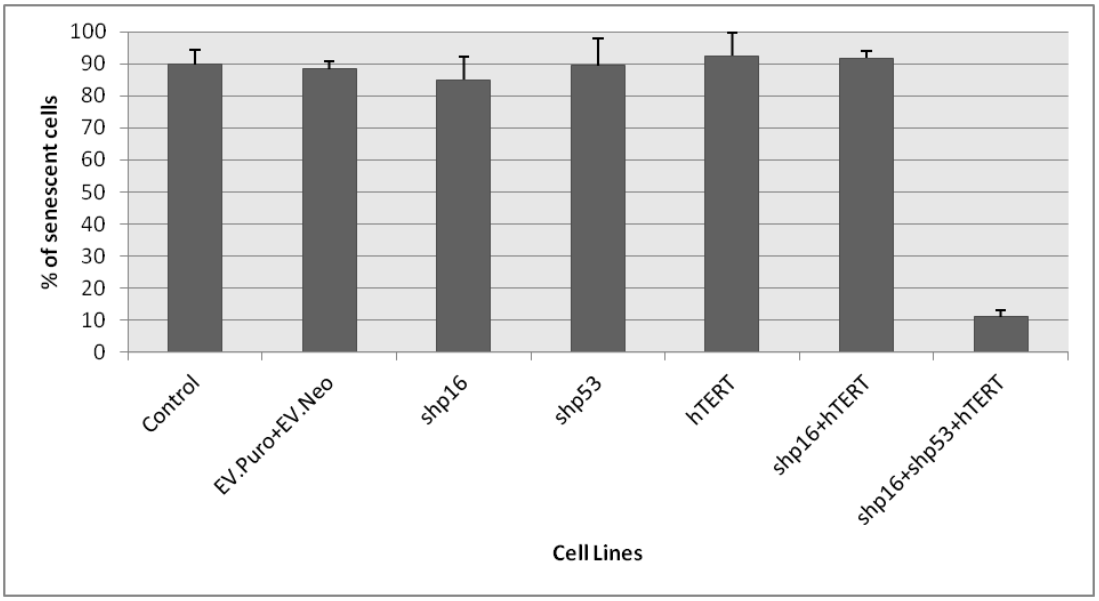

Figure 4. 6: Expression of Beta-galactosidase in NHEKshp16+hTERT (selected).

(a) Control plates all contained large, blue-green colonies positive for β gal. $NHEK^{shp16+hTERT}$ ceased to proliferate indefinitely and the majority of cells were positive for β gal. $NHEK^{shp16+shp53+hTERT}$ continued to proliferate and plates contained large colonies without extensive β gal staining although did contain some small, naturally occurring senescent colonies.

(b) Quantification of senescent colonies. Cells were analyzed for β gal activity using the Biovision senescence detection kit. A total of 300 cells were counted and cells deemed positive if stained blue. Means of 3 independent experiments are shown.

4.3.2 NHEK$^{shp16+hTERT}$ (non-selected)

NHEK$^{shp16+hTERT}$ continued to proliferate for an additional 4 PD upto a total of 18 PD compared to the parent NHEK control which ceased to proliferate at 14 PD (Fig 4.7). Controls all ceased to proliferate between 15 to 19 PD. Interestingly, however, it was noted that in the absence of drug selection NHEK$^{shp16+shp53+hTERT}$ only proliferated for an additional 24 PD compared to the parental control prior to plateauing at 39 PD (Fig 4.7). To determine senescence, cells were analyzed for β gal activity (Fig 4.8 a and Fig 4.8 b). All transduced cell lines exhibited high levels of senescence as evident from the presence of blue cell colonies (Fig 4.8 a). When tested for β gal activity, all cell lines showed high levels of activity with 88% of NHEK$^{shp16+hTERT}$ cells and 91% of NHEK$^{shp16+shp53+hTERT}$ cells positive for β gal (Fig 4.8 b). Control cell lines were in between ranges of 87% to 93% positive cells (Fig 4.8 b).

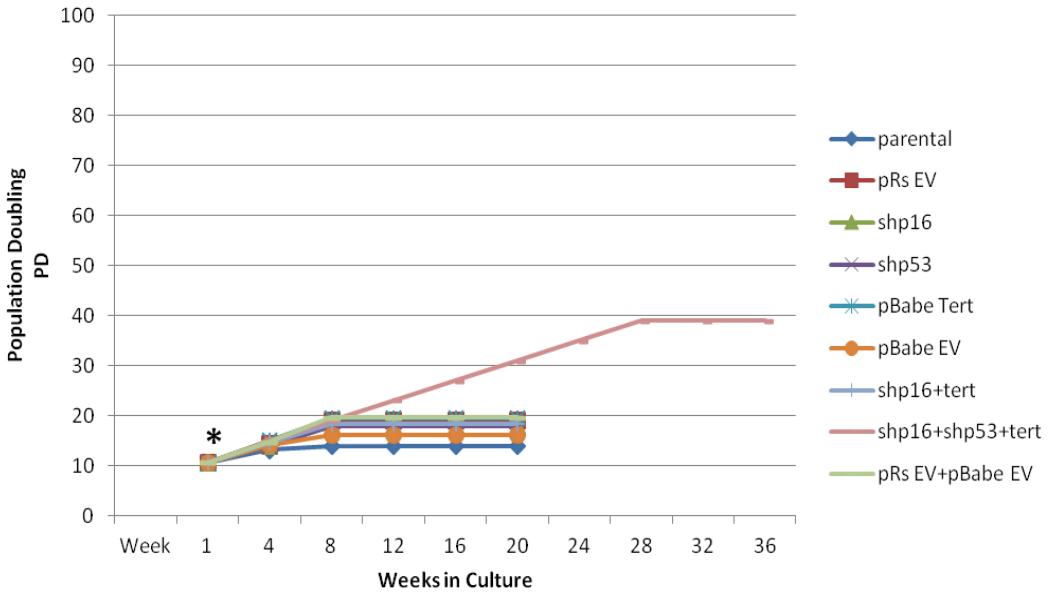

Figure 4. 7: NHEKshp16+hTERT (non-selected).

Early passage NHEK cells were transduced with shp16 and hTERT and assessed for population doublings in the absence of drug selection (* indicates point of transduction). Appropriate controls were used (table 4.1).

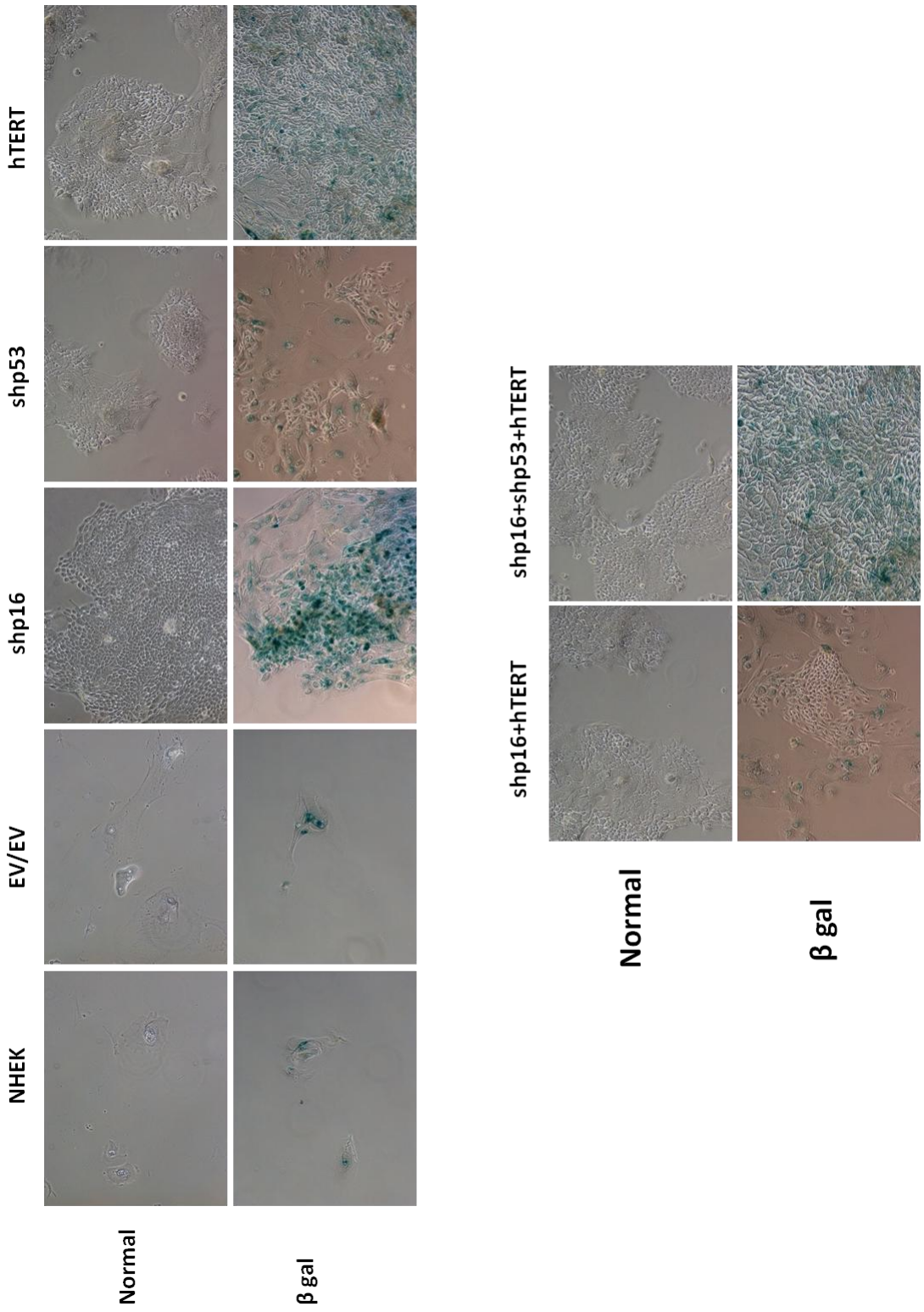
NHEK
EV/EV
shp16
shp53
hTERT
shp16+hTERT
shp16+shp53+hTERT
Normal
β gal

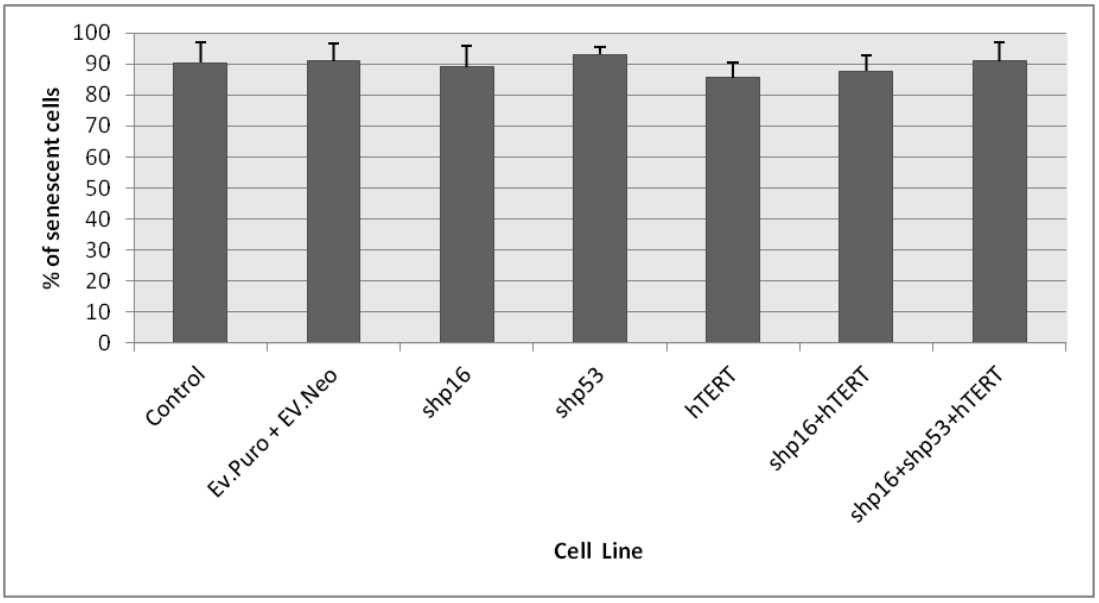

Figure 4. 8: Expression of Beta galactosidase in NHEKshp16+hTERT (non-selected).

(a) Control plates all contained large colonies positive for β gal. $NHEK^{shp16+hTERT}$ and $NHEK^{shp16+shp53+hTERT}$ ceased to proliferate indefinitely in absence of drug selection and stained positive for β gal.

(b) Quantification of senescent colonies. Cells were analyzed for β gal activity using the Biovision senescence detection kit. A total of 300 cells were counted and cells deemed positive if stained blue. Means of 3 independent experiments are shown.

4.4 Discussion

Early passage oral and epidermal keratinocytes were transduced with shp16 and hTERT and assessed for population doublings with appropriate controls. In the set subjected to drug selection, cells transduced with shp16+hTERT did not extend replicative lifespan significantly more than the control group and cells senesced within an additional 20 PD after parental controls senesced. Cells transduced with shp53 alongside shp16 and hTERT were found to proliferate indefinitely and were negative for β gal expression. Similarly, for the set assessed in the absence of drug selection, cells transduced with shp16 and hTERT did not extend replicative lifespan and senesced alongside controls. Surprisingly, however, even the addition of shp53 did not extend cell lifespan indefinitely, suggesting the importance of drug selection when selecting for pure populations of transduced cell lines.

There have been many conflicting reports into the role of p53 in the immortalization of human cells with some stating it is essential (Rheinwald *et al.* 2002) and others claiming it is not necessary (Kiyono, Foster *et al.* 1998, Dickson, Hahn *et al.* 2000, Haga, Ohno *et al.* 2007). The results of the study confirmed the findings of Rheinwald and group, that despite using an optimized retroviral infection protocol, down regulation of $p16^{INK4a}$ alongside telomerase did not sufficiently extend cell lifespan and in both NHOK and NHEK, downregulation of p53 was also required to extend cell growth. No rare, spontaneously immortalized cell clones appeared as in the case with cells such as OKF6 and NTERTs, reinstating the fact that spontaneously arisen cell lines are not reproducible.

Imaging studies have provided evidence *in vivo* of 'cross-talks' between $p16^{INK4a}$ and p53 (Yamakoshi, Takahashi *et al.* 2009) , indicating that p53 normally holds $p16^{INK4a}$ in check and it is possible that the knockdown of $p16^{INK4a}$ alone is insufficient at extending replicative lifespan of keratinocytes due to a direct signalling mechanism

between $p16^{INK4a}$ and p53 that 'alerts' p53 when $p16^{INK4a}$ is directly silenced, resulting in a p53-mediated cell cycle arrest. Studies that have downregulated $p16^{INK4a}$ indirectly have had higher success rates at extending cell lifespan whilst retaining p53 expression (Dickson, Hahn *et al.* 2000, Haga, Ohno *et al.* 2007) .

When tested for expression of β gal activity, close to 90% activity was found in transduced cells that ceased proliferation, in accordance with data from studies using β gal as a biomarker for senescent cells. It is important to note, however, that although initially senescence-associated β gal activity was thought to be expressed specifically in senescent cells, since then studies have established that expression of β gal in these cells is due to the over-expression and accumulation of the lysosomal endogenous β gal. Furthermore, it was noted that its expression is not essential for senescence but despite this it still remains the most widely used biomarker for senescence and aging cells since it is reliable and easily detectable.

4.5 Chapter Conclusions

The findings from keratinocyte transductions reveal that, interestingly, the direct method of downregulating $p16^{INK4a}$ does not allow for cellular immortalization in oral and epidermal keratinocytes except arising spontaneously after periods of crisis in culture, an unfortunate event from the perspective of reproducibility in research. Cells did not witness cell growth expansion of more than 3-5 PD beyond controls in the absence of p53.

Chapter 5:

Results 3

Chapter 5

Results 3

5.1 Bmi1+hTERT transductions

Bmi1 is an oncogene found to be over expressed in many cancers, promoting cell survival and proliferation. In 2007, Haga *et al* demonstrated that in human mammary epithelial cells, bmi1 along with telomerase sufficiently immortalized cells without crisis or growth arrest whilst retaining near-normal chromosomal ploidy (Haga, Ohno *et al.* 2007). The next method used to transduce keratinocytes was by over expressing bmi1 alongside telomerase to extend cellular replicative lifespan whilst retaining tumour suppressive activity and cell cycle checkpoints.

Transductions were repeated as previously (chapter 4) with a combination of Bmi1+hTERT and assessed for replicative lifespan over an extended time frame with appropriate controls (table 5.1) and under different conditions. Transduced cells were drug selected to elicit pure cell populations, however, as it has been reported that cells do not respond well to drug selection, separate transductions were also performed in the absence of drug selection. The results will be presented under the different cell types (oral vs epidermal) and under the different selective conditions (drug-selected vs non-selected).

Control Abbreviation	Controls
Parental	Non-transduced NHOK or NHEK cells at the same PD as transduced cells
Bmi1 + E.V neo	pBabe neo empty vector control and Bmi1 only; conferring resistance to both selection markers
hTERT + E.V puro	pBabe puro empty vector control and hTERT only; conferring resistance to both selection markers

Table 5. 1 List of controls used in the transductions of NHOK and NHEK with Bmi1+hTERT.

Extensive controls were used throughout the study to ensure validity of results. To save time, NHOK and NHEK cells were transduced with empty vectors alongside either Bmi1 or hTERT and selected for both selection markers simultaneously.

5.1.1 Method Summary

Successfully infected PT67 cells were irradiated to act as infectious feeders and co-cultured with early passage keratinocytes alongside normal feeders. Each cell line was assessed for PDs under the two different selective conditions and the results presented herein.

5.2 NHOK$^{bmi1+hTERT}$

NHOK strain 810 was transduced at early passage with Bmi1 and hTERT alongside appropriate controls and assessed for proliferative capacity under two conditions, with one set subjected to drug selection. Two independent experiments with similar results were obtained using Bmi1+hTERT (data not shown).

5.2.1 NHOK$^{Bmi1+hTERT}$ (selected)

NHOK$^{Bmi1+hTERT}$ continued to proliferate indefinitely until the end of the experiment at which point it had reached 86 PD as compared to the parent NHOK control which plateaued at 16 PD (Fig 5.1). Surprisingly, NHOK$^{Bmi1+EV}$ showed significant lifespan extension even in the absence of hTERT, proliferating upto 35 PD before plateauing (Fig 5.1). With the exception of NHOK$^{Bmi1+EV}$, controls all ceased proliferation between 16 to 19 PD. To determine senescence, cells were analyzed for β gal activity (Fig 5.2 a and Fig 5.2 b). NHOK$^{Bmi1+hTERT}$ exhibited low levels of positively stained cells (12%) as compared to controls (between 87% to 92%).

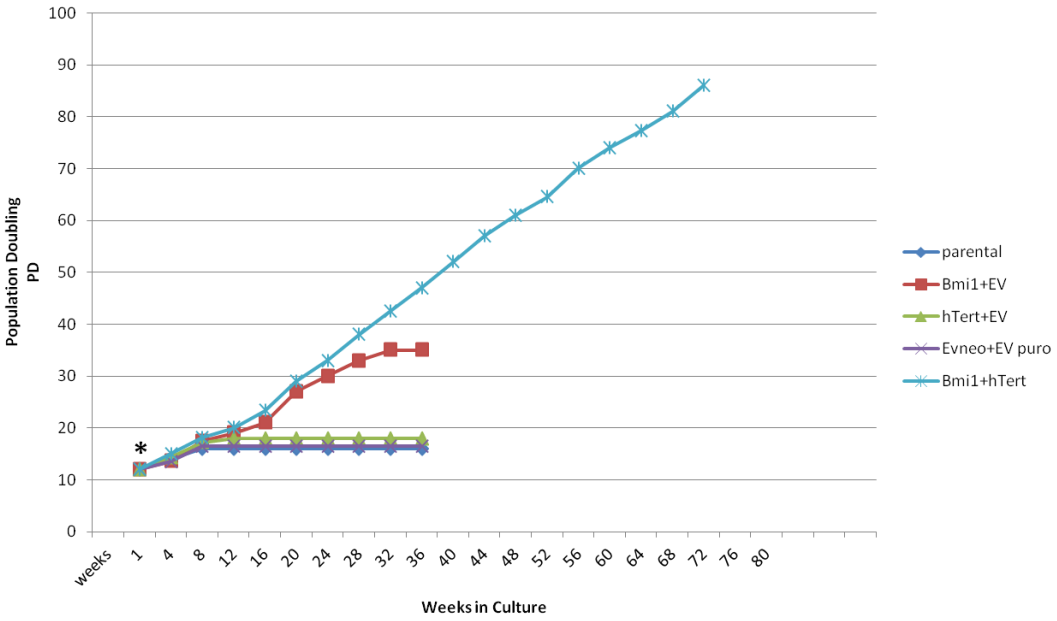

Figure 5. 2: NHOKBmi1+hTERT (Selected).

Early passage NHOK were transduced with Bmi1 and hTERT and subjected to drug selection with population doublings assessed (* indicates point of transductions). Appropriate controls were used (table 5.1).

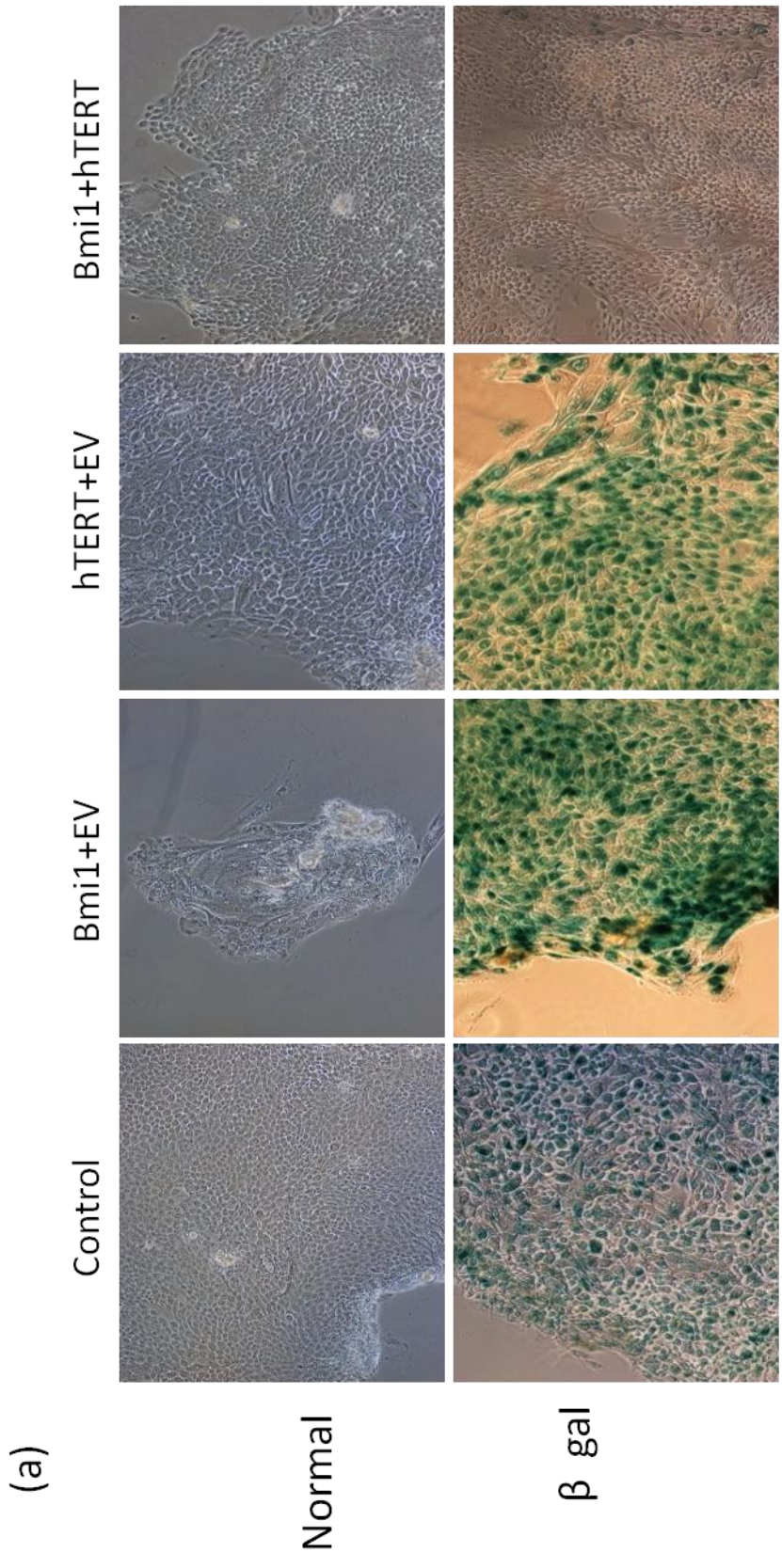
(a)
Normal
β gal
Control
Bmi1+EV
hTERT+EV
Bmi1+hTERT

(b)

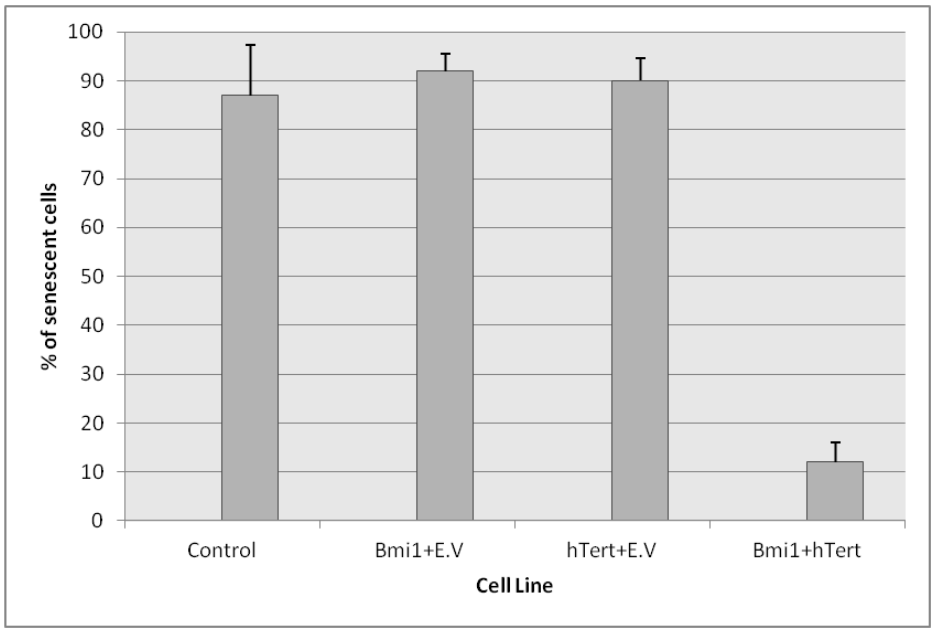

Figure 5. 3: Expression of β galactosidase in NHOKbmi1+hTERT.

(a) Control plates all contained large, blue-green colonies positive for β gal. NHOK$^{Bmi1+hTERT}$ continued to proliferate and plates contained large colonies without extensive β gal staining although did contain some small, naturally occurring senescent colonies.

(b) Quantification of senescent colonies. Cells were analyzed for β gal activity using the Biovision senescence detection kit. A total of 300 cells were counted and cells deemed positive if stained blue. Means of 3 independent experiments are shown.

5.2.2 NHOK$^{Bmi1+hTERT}$ (non-selected)

In the absence of drug selection NHOK$^{Bmi1+hTERT}$ continued to proliferate upto 45 PD before exhibiting plateau level compared to the parental NHOK control which reached plateau at 18 PD (Fig 5.3). All other controls ceased proliferation between 17 to 20 PD with the exception of NHOK$^{Bmi1+EV}$ that continued to proliferate until 33 PD (Fig 5.3). To determine senescence, cells were analyzed for β gal activity (Fig 5.4 a and Fig 5.4 b). All transduced cell lines exhibited high levels of senescence as evident from the presence of blue colonies (Fig 5.4 a) with 95% of NHOK$^{Bmi1+hTERT}$ cells positive for β gal and between 93% - 96% of control cells positive cells for β gal (Fig 5.4 b).

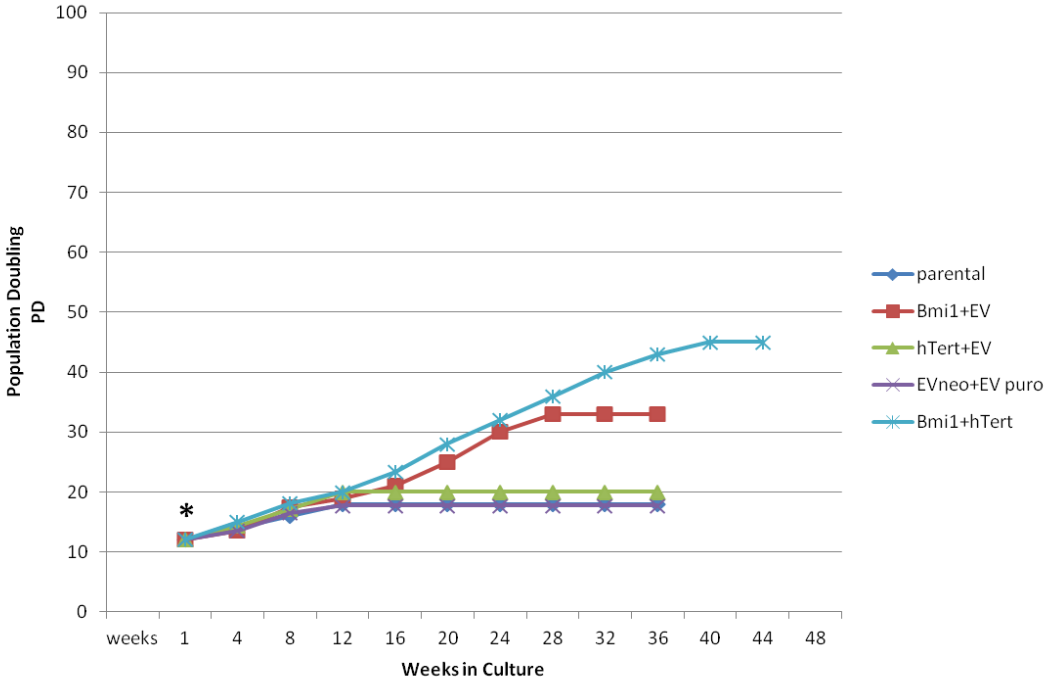

Figure 5. 4: NHOKBmi1+hTERT (Non-selected).

Early passage NHOK were transduced with Bmi1 and hTERT and assessed for population doublings in the absence of drug selection (* indicates point of transduction). Appropriate controls were used (table 5.1).

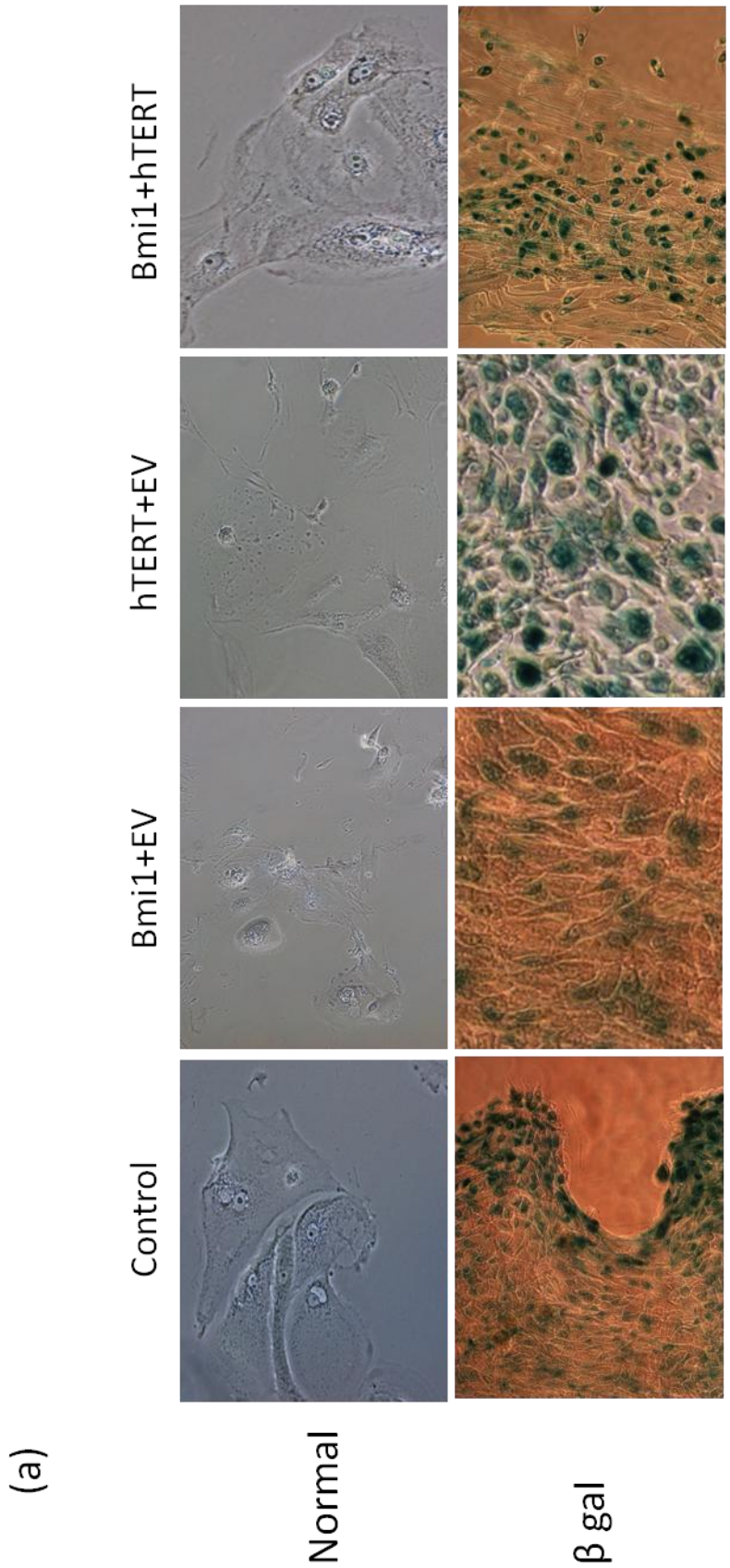
(a)
Normal
β gal
Control
Bmi1+EV
hTERT+EV
Bmi1+hTERT

(b)

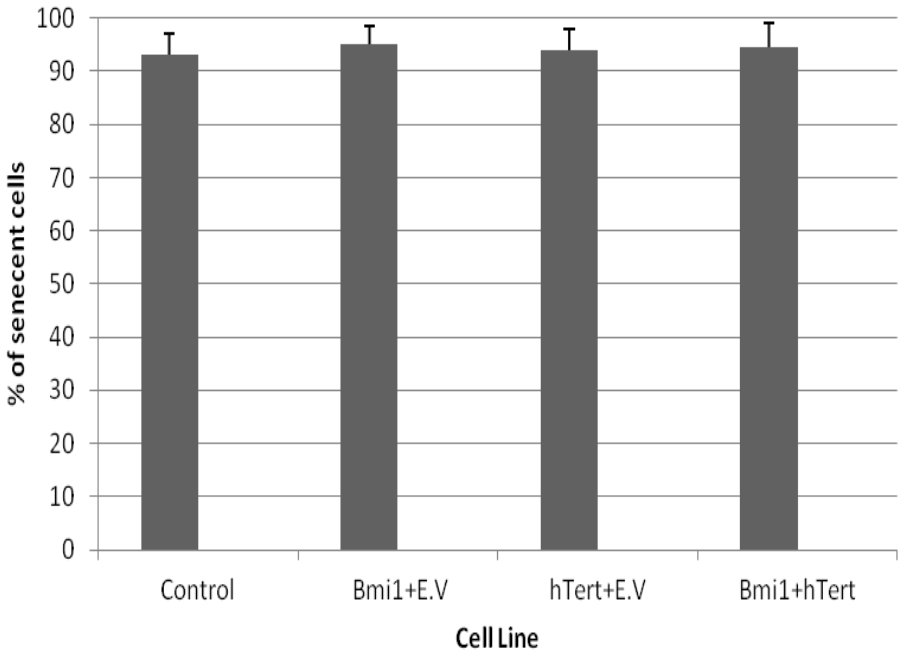

Figure 5. 5: Expression of Beta galactosidase in NHOKBmi1+hTERT.

(a) Control plates all contained large, blue-green colonies positive for β gal. NHOK$^{Bmi1+hTERT}$ ceased to proliferate indefinitely and majority of cells stained positive for β gal.

(b) Quantification of senescent colonies. Cells were analyzed for β gal activity using the Biovision senescence detection kit. A total of 300 cells were counted and cells deemed positive if stained blue. Means of 3 independent experiments are shown.

5.3 NHEK $^{Bmi1+hTERT}$

Early passage NHEK were transduced with Bmi1 and hTERT alongside appropriate controls (table 5.1) and assessed for proliferative capacity under two conditions, with one set subjected to drug selection. Two independent experiments with similar results were obtained using bmi1+hTERT (data not shown).

5.3.1 NHEK$^{Bmi1+hTERT}$ (selected)

NHEK$^{Bmi1+hTERT}$ continued to proliferate indefinitely until the end of the experiment at which point it had reached 96 PD as compared to the parent NHEK control that plateaud at 18 PD (Fig 5.5). As with the NHOK transductions, NHOK$^{Bmi1+EV}$ showed lifespan extension even in the absence of hTERT, proliferating upto 30 PD before plateauing (Fig 5.5). With the exception of NHEK$^{Bmi1+hTERT}$, all controls ceased proliferation between 18 to 21 PD. To determine senescence, cells were analyzed for β gal activity (Fig 5.6 a and Fig 5.6 b). NHEK$^{Bmi1+hTERT}$ exhibited low levels of β gal activity (15%) as compared to controls (between 86% - 93%) of positive cells (Fig 5.6 b).

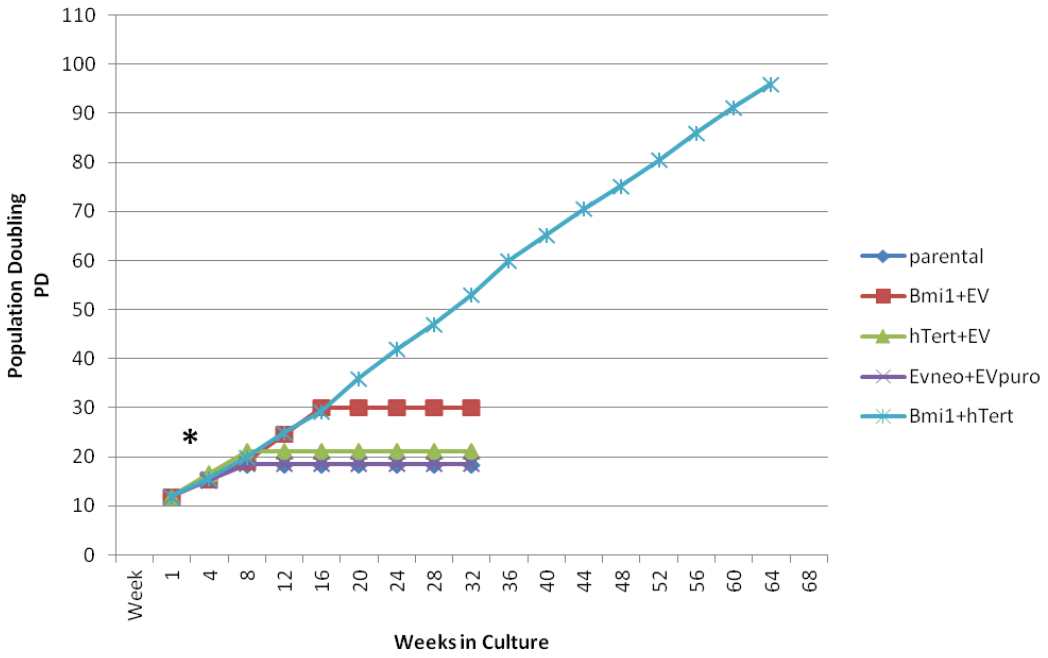

Figure 5. 6: NHEKBmi1+hTERT (Selected).

Early passage NHEK were transduced with Bmi1 and hTERT and subjected to drug selection with population doublings assessed (* indicates point of transductions). Appropriate controls were used (table 5.1).

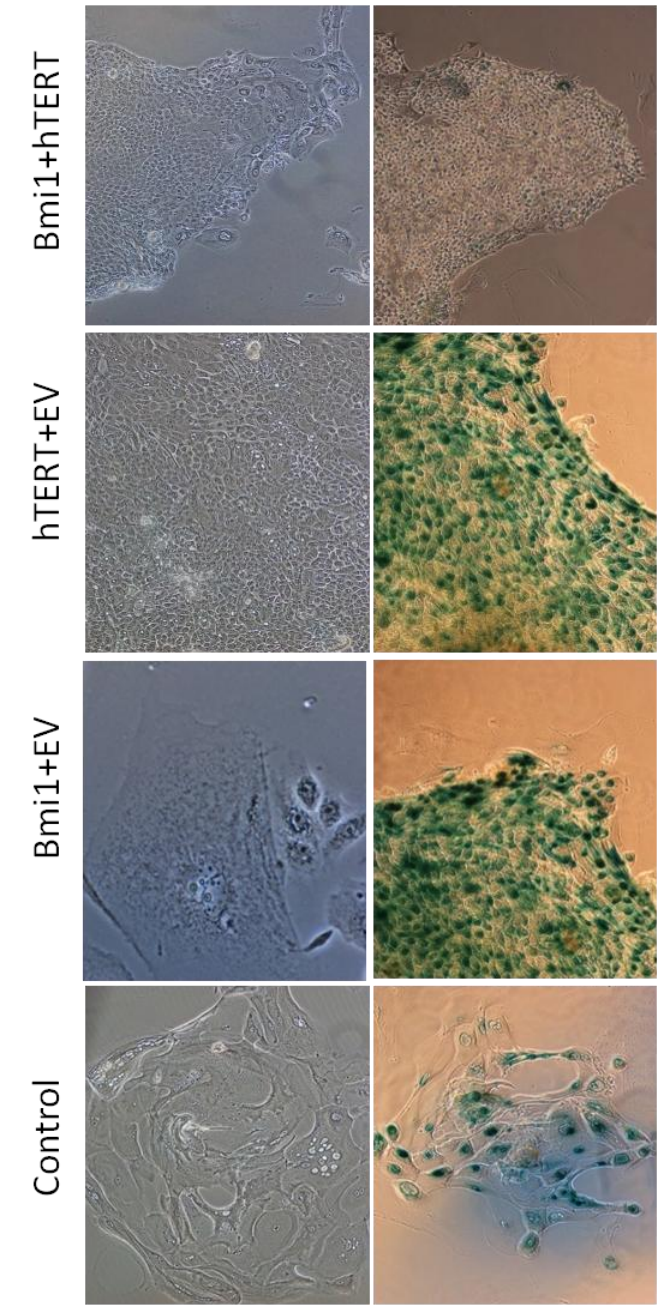
(a)
Normal
β gal
Control
Bmi1+EV
hTERT+EV
Bmi1+hTERT

(b)

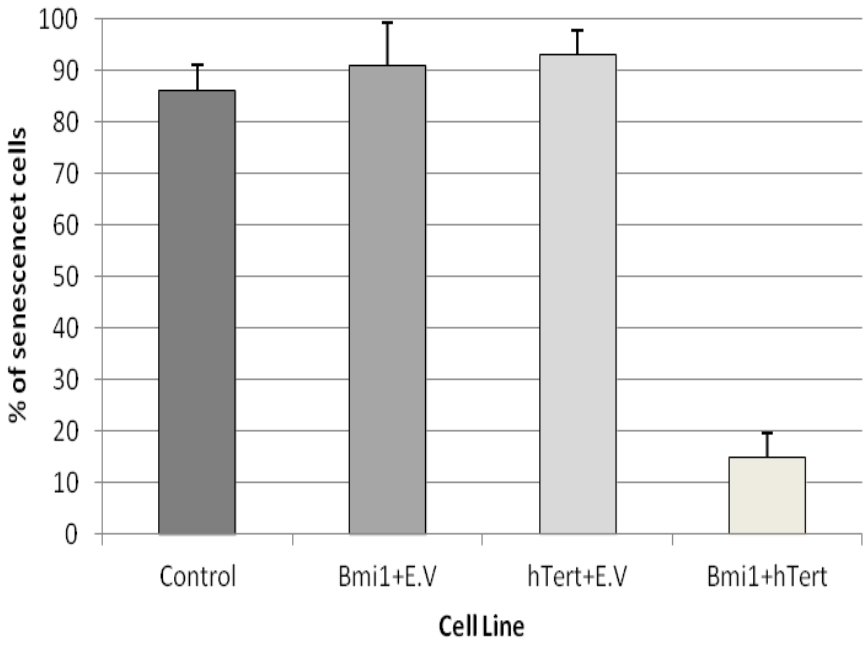

Figure 5. 7: Expression of β galactosidase in NHEKBmi1+hTERT.

(a) Control plates all contained large, blue-green colonies positive for β gal. $NHEK^{Bmi1+hTERT}$ continued to proliferate and plates contained large colonies without extensive β gal staining although did contain some small, naturally occurring senescent colonies.

(b) Quantification of senescent colonies. Cells were analyzed for β gal activity using the Biovision senescence detection kit. A total of 300 cells were counted and cells deemed positive if stained blue. Means of 3 independent experiments are shown.

5.3.2 NHEK$^{Bmi1+hTERT}$ (non-selected)

In the absence of drug selection, NHEK$^{Bmi1+hTERT}$ continued proliferation upto 53 PD before exhibiting plateau compared to parent NHEK which ceased proliferation at 16 PD (Fig 5.7). All other controls ceased proliferation between 16 to 19 PD with the exception of NHEK$^{Bmi1+EV}$, that continued proliferation until 27 PD (Fig 5.7). To determine senescence, cells were analyzed for β gal activity (Fig 5.8 a and Fig 5.8 b). All transduced cell lines exhibited high levels of senescence as evident from the presence of blue , positively stained cells (Fig 5.8 a) with 89% of NHEK$^{Bmi1+hTERT}$ cells positive for β gal and 89% - 94% of positive control cells (Fig 5.8b).

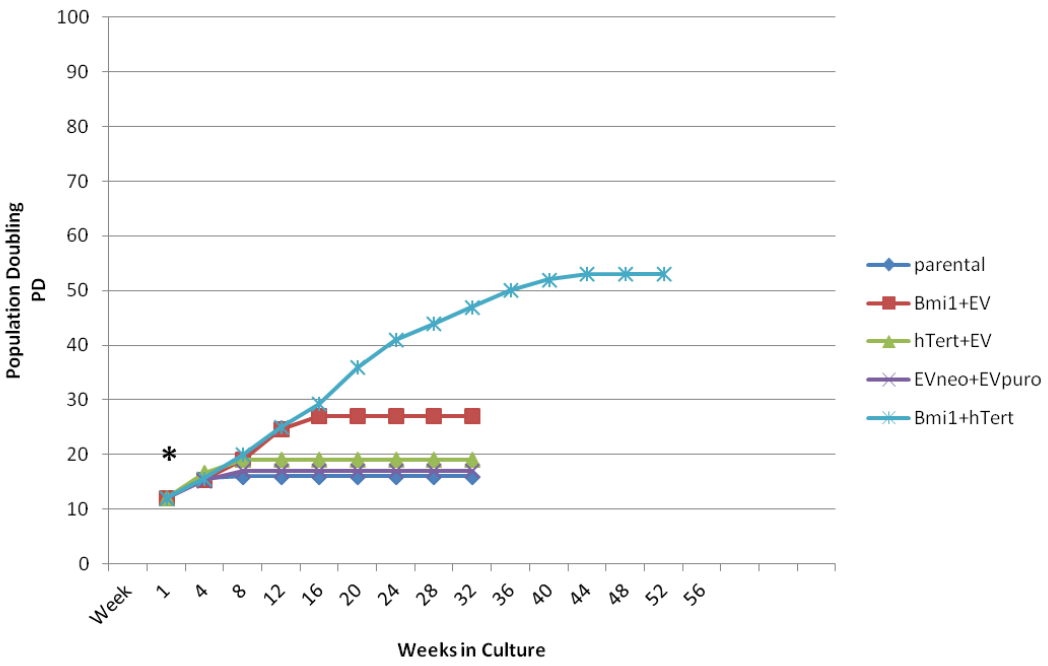

Figure 5. 8: NHEKBmi1+hTERT (Non-selected).

Early passage NHEK transduced with Bmi1 and hTERT and assessed for population doublings in absence of drug selection (* indicates point of transduction). Appropriate controls were used (table 5.1).

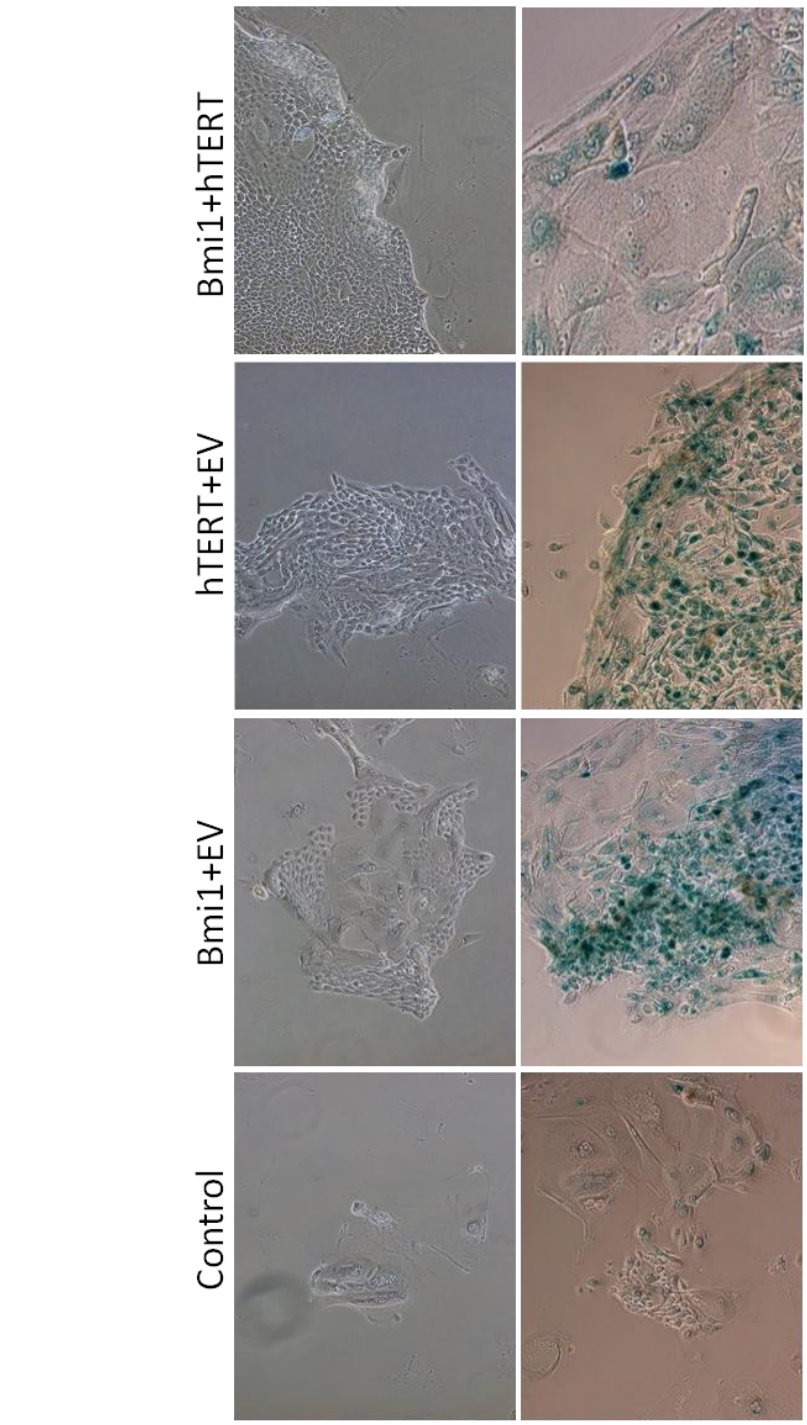
(a)
Normal
B gal
Control
Bmi1+EV
hTERT+EV
Bmi1+hTERT

(b)

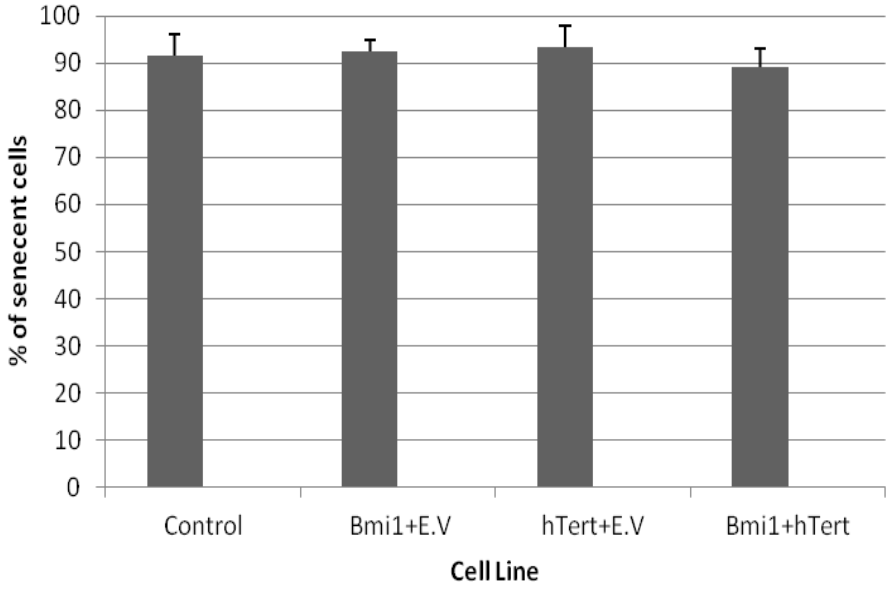

Figure 5. 9: Expression of β galactosidase in NHEKBmi1+hTERT.

(c) Control plates all contained large, blue-green colonies positive for β gal. $NHEK^{Bmi1+hTERT}$ ceased to proliferate indefinitely and majority of cells stained positive for β gal.

(d) Quantification of senescent colonies. Cells were analyzed for β gal activity using the Biovision senescence detection kit. A total of 300 cells were counted and cells deemed positive if stained blue. Means of 3 independent experiments are shown.

5.4 Discussion

Early passage oral and epidermal keratinocytes were transduced with Bmi1 and hTERT and assessed for population doublings with appropriate controls (table 5.1). In the set subjected to drug selection, cells transduced with Bmi1+hTERT reached 90 PD (NHOK) and 94 PD (NHEK) compared to parental controls that proliferated upto 16 PD (NHOK) and 18 PD (NHEK), respectively. Similarly, in the set assessed in the absence of drug selection, cells transduced with Bmi1 and hTERT did extend replicative lifespan however eventually senesced after 50 PD and furthermore, when tested for β gal expression all control cells tested positive.

Interestingly, cells transduced with bmi1 alone also continued to proliferate for an additional 19 PD in NHOK and 12 PD in NHEK and studies into mammary cells lines have shown over expressing Bmi1 alone leads activation of telomerase (Dimri, Martinez *et al.* 2002), although with regards to this study transient telomerase expression was not enough to maintain cell growth indefinitely. When tested for expression of β gal activity, all cells apart from those transduced with bmi1+hTERT stained over 90% positive for senesce associated β gal activity, in accordance with data from studies using β gal as biomarker for senescent cells.

5.5 Chapter Conclusions

The data suggests Bmi1 alongside hTERT to be an effective method of extending replicative lifespan of keratinocytes as compared to downregulating $p16^{INK4a}$ directly alongside hTERT. A comparison of cell proliferation in presence and absence of drug selection suggests the importance of antibiotic selection in eliciting pure cell populations without which cells ultimately senesce despite conditions favouring proliferation.

Chapter 6:

Results 4

Chapter 6

Results 4

6.1 Characterization

Following successful lifespan extension of cells, $NHOK^{Bmi1+hTERT}$ and $NHEK^{Bmi1+hTERT}$ lines were assessed and compared with $NHOK^{shp16+shp53+hTERT}$ and $NHEK^{shp16+shp53+hTERT}$ as well as the commonly used OKF6 and OKF4. Cell lines were analyzed for $p16^{INK4a}$ expression, p53 activity and telomerase expression to characterize the expression levels of these key elements responsible for cellular immortalization and compare it to non transduced cell lines alongside the OKF4 and OKF6 cells. Following this, the $NHOK^{Bmi1+hTERT}$ cell line was cultured in a serum free environment for culturing onto organotypic substrates.

The results of this chapter will be described in five sections:

(i) Western Blot analysis of cell lines for $p16^{INK4a}$ and p53 expression

(ii) TRAP analysis

(iii) Apoptosis response

(iv) DNA damage effects in different culture media

(v) Adaption of cell line into a serum free environment

6.2 Western blot analysis

It is well established that knockdown of $p16^{INK4a}$ is essential for immortalization of cells and that accumulation of $p16^{INK4a}$ in cells is indicative of senescence (Reznikoff, Loretz et al. 1988, Serrano, Lee et al. 1996, Lin, Barradas et al. 1998, Rheinwald, Hahn et al. 2002). $p16^{INK4a}$ has been shown to accumulate in cells with time in culture and cause senescence alongside telomere shortening, whilst immortal cells usually have suppression of $p16^{INK4a}$, allowing them to override the cell cycle regulation and continue to proliferate. Lysates made from cells at progressive PD were analyzed by western blotting to show levels of 16^{INK4a} progression and allow comparison between normal cells and immortalized cells to observe expression levels over time in culture. It is expected that normal, non-transduced parent cells will show an increase in $p16^{INK4a}$ with time in culture whilst the transduced counterparts will not.

Western blotting allows the assessment of protein expression from a cell extract with denatured cell lysates separated based on size on a acrylamide gel and are transferred to a suitable membrane prior to being recognized with an appropriate antibody. Although transduced cell lines were drug selected, as an additional control and to determine level of protein expression, cell lysates from each cell line were obtained post transduction and assessed for $p16^{INK4a}$ and p53. Tubulin was used as a loading control along with SVFHK and SCC.25 for positive and negative controls. SVHFK is a SV40 virus-transformed epidermal keratinocyte cell line that is not tumourigenic at early passage (Brown & Gallimore, 1987) with normal cellular tumour suppressive mechanisms along with functional p16 and p53. SCC.25 is a tumourigenic keratinocyte cell line derived from the tongue (Rheinwald & Beckett, 1981) with deficient tumour suppressive mechanisms including dysfunctional p16 and downregulated p53.

As shown in Fig 6.1, both bmi1 and shp16 effectively reduced expression of $p16^{INK4a}$ as compared to control. Next, the cell lysates were examined for p53 expression and considering p53 levels generally remain low within the cell unless triggered by stress-inducing stimuli, the Bmi1+hTERT transductions appear to express normal levels of p53 as shown by the presence of a light visible band (Fig 6.1) . The absence of detectable band in the shp16+shp53+hTERT transductions compared to control demonstrated shp53 to be effectively downregulated in these cells (Fig 6.1).

Cell lysates were taken from progressing population doublings to illustrate levels of $p16^{INK4a}$ as cells age in culture. When tested for $p16^{INK4a}$ expression, normal NHOK and NHEK displayed a gradual increase in expression of $p16^{INK4a}$ (Fig 6.2a) whereas in contrast, there was no detectable change in $p16^{INK4a}$ levels in cell lysates of transduced cell lines Fig 6.2 b and c). Three independent experiments with similar results were obtained using cell lysates to analyze $p16^{INK4a}$ expression (data not shown).

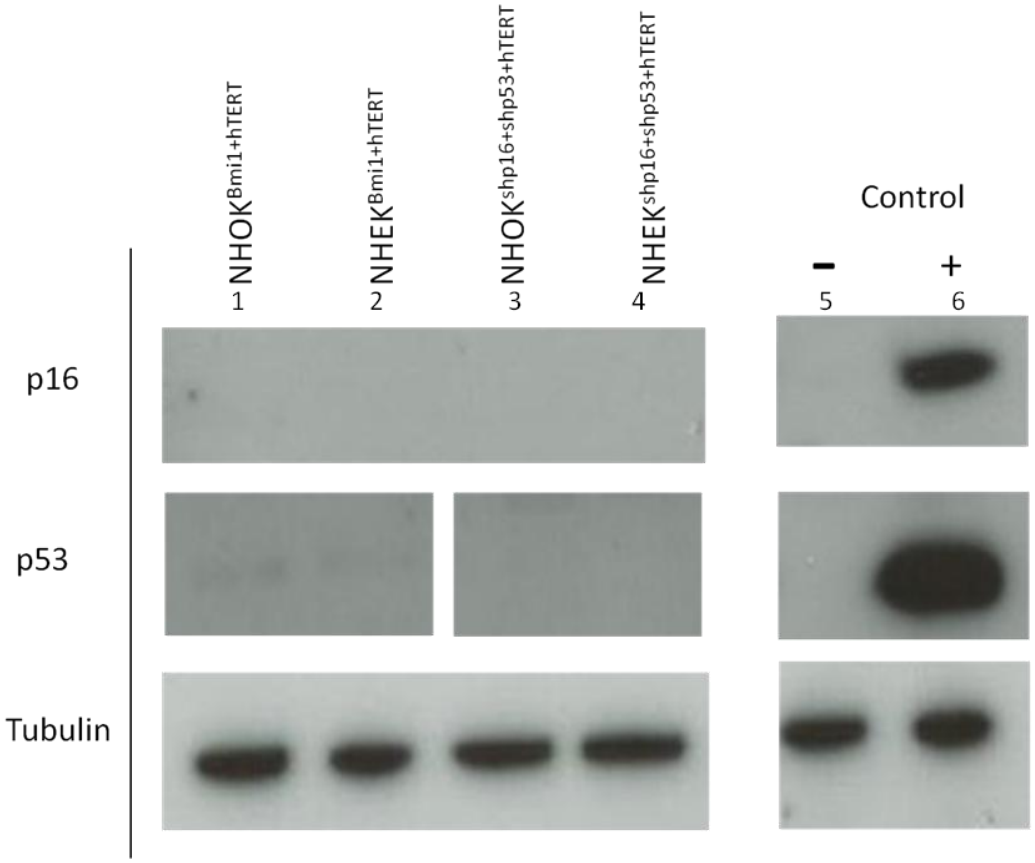

Figure 6. 1: Expression of p16INK4a and p53 in transduced cell lines.

Representative western blots showing expression of $p16^{INK4a}$ and p53 in NHOK and NHEK cell lines after transductions. Cell lysates were obtained at 30 PD for all cell lines and $p16^{INK4a}$ expression was effectively knocked down in both $NHOK^{bmi1+hTERT}$ and $NHEK^{bmi1+hTERT}$ (lanes 1 and 2) as well as in $NHOK^{shp16+shp53+hTERT}$ and $NHEK^{shp16+shp53+hTERT}$ (lanes 3 and 4). Weak expression of p53 is visible in $NHOK^{bmi1+hTERT}$ and $NHEK^{bmi1+hTERT}$ (lanes 1 and 2) but completely absent in $NHOK^{shp16+shp53+hTERT}$ and $NHEK^{shp16+shp53+hTERT}$ (lanes 3 and 4) as compared to controls. SVFHK and SCC.25 cell lysates were used for positive and negative controls respectively (lanes 5 and 6). Tubulin served as loading control.

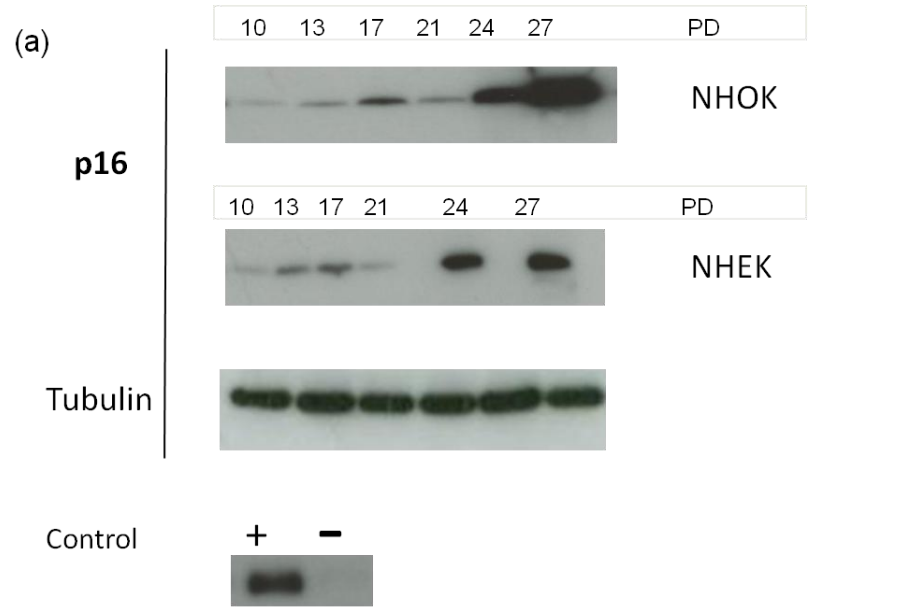

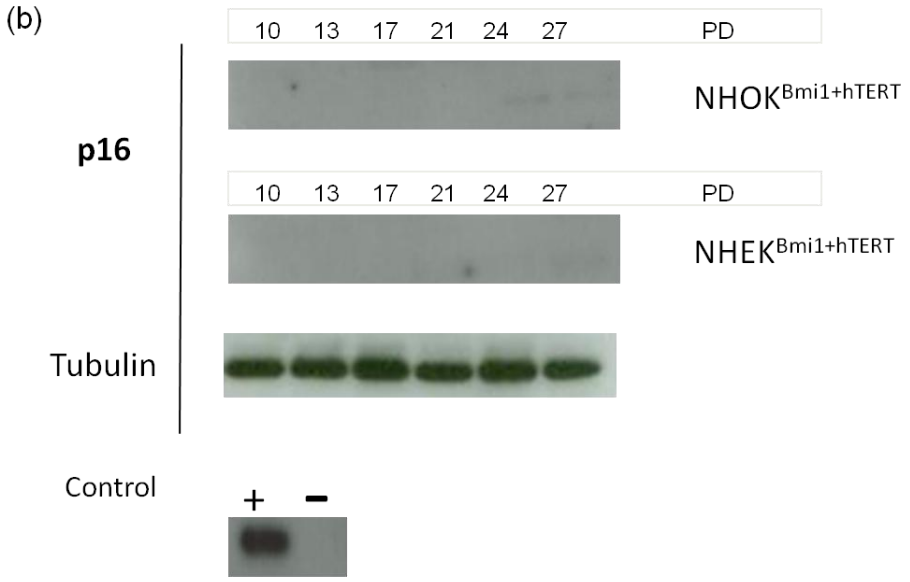

continued overelaf

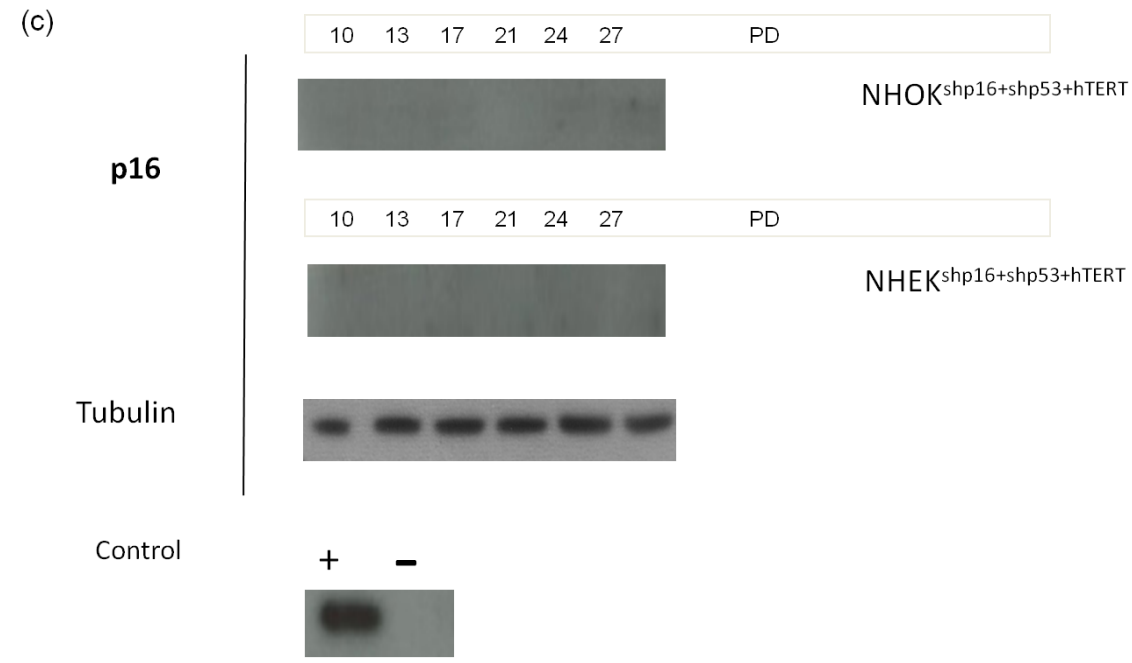

Figure 6. 2: Expression of p16INK4a with progressive population doublings in culture.

Representative western blots showing expression of $p16^{INK4a}$ over progressive population doublings in (a) normal NHOK and NHEK , (b) $NHOK^{bmi1+hTERT}$ and $NHEK^{bmi1+hTERT}$ and (c) $NHOK^{shp16+shp53+hTERT}$ and $NHEK^{shp16+shp53+hTERT}$. Cell lysates were obtained over time in culture and the data showed that in normal NHOK and NHEK, expression of $p16^{INK4a}$ increased progressively with time in culture (a). No evident change was seen in expression of $p16^{INK4a}$ in transduced cell lines (b) and (c).

SVFHK and SCC.25 cell lysates were used for positive and negative controls respectively (lanes 5 and 6). Tubulin served as loading control.

6.3 Characterizing telomerase activity in transduced cell lines

Extension of telomere length is required for the immortalization of all mammalian cells as well as to extend cellular lifespan by preventing telomere-dependent senescence in many cell types including fibroblasts, retinal epithelial cells, smooth muscle cells and keratinocytes (Milyavsky, Shats et al. 2003, Ramirez, Herbert et al. 2003, Vaughan, Ramirez et al. 2006, Zhu, Mouly et al. 2007, Wieser, Stadler et al. 2008).

Cell lines were tested for telomerase expression using a PCR based TRAP assay to show level of telomerase expression within cell samples, confirming successful transduction and allowing comparison with controls and other immortalized cell lines such as OKF4 and OKF6.

6.3.1 Methods

A cy5 based TRAP assay was used to measure the activity of the enzyme *in vitro* by introducing a primer that acts as a substrate for telomerase-mediated addition of TTAGGG repeats in a PCR reaction. If present, active telomerase from a cell extract extends this 50 base pair primer as if it were a telomere with the hexameric repeat (TTAGGG) and when run on a gel the activity of telomerase can then be judged by how many hexameric repeats were added as indicated by the extent of the 6bp ladder created within a set time and PCR cycle program. To determine levels of enzymatic activity in the cultures without transduction, TRAP analysis was performed at 10 PD compared to lysates from transduced cells which were analyzed for telomerase activity from lysates taken at 50 PD.

6.3.2 Results

Very little telomerase activity was found in both NHOK and NHEK without exogenous hTERT expression (Fig 6.3 b). Expression of the hTERT construct in these cells after transduction demonstrated far more telomerase activity, shown by stronger bands (Fig 6.3 a) demonstrating that telomerase activity is limited by hTERT expression. For each sample, a heat inactivated counterpart was included as an additional negative control and these were devoid of any visible bands. OKF6 and OKF4 were also tested for telomerase activity (Fig.6.3 b) and the bands appeared slightly darker than those for the transduced cell lines. Three independent experiments with similar results were obtained (data not shown).

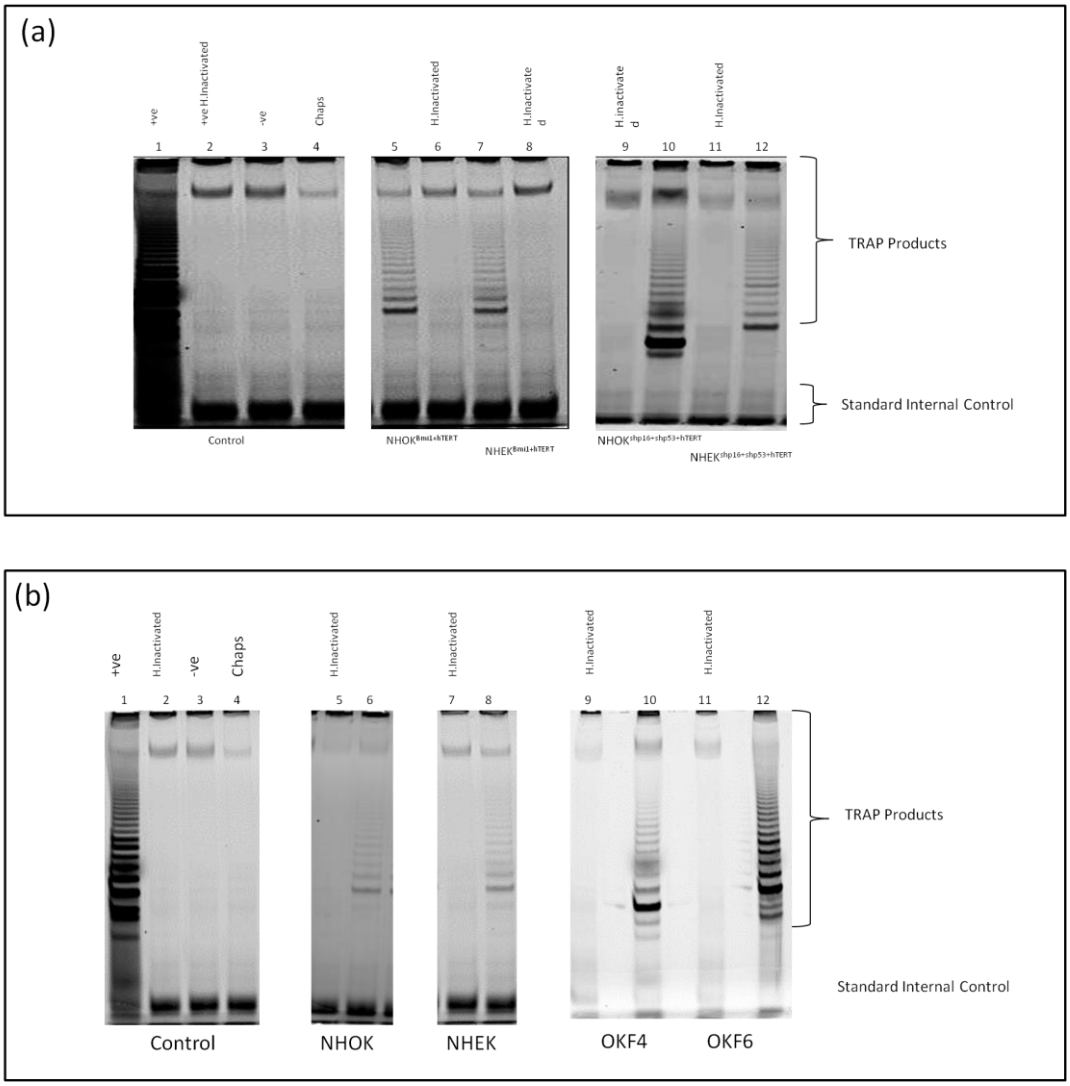

Figure 6. 3: Telomerase Repeat Amplification Protocol (TRAP) analysis of telomerase levels in (a) NHOKbmi1+hTERT , NHEKbmi1+hTERT, NHOKshp16+shp53+hTERT and NHEKshp16+shp53+hTERT and (b) untransduced NHOK and NHEK, OKF6 and OKF4.

(a) TRAP analysis was undertaken on cell lysates obtained at 19 PD from the transduced cell lines for detection of telomerase activity within cells. Positivity for telomerase activity is shown by the 6-bp incremental TRAP ladder. All cells transduced with hTERT showed telomerase expression (lanes 5,7,10 and 12) which was absent in the negative controls (lanes 2, 3 and 4) as well as after heat inactivation of each sample (lanes 6,8,9 and 11).

(b) TRAP analysis was undertaken on cell lysates obtained from non-transduced cell lines at 10 PD and from OKF6 and OKF4 cells lines and assessed for expression of telomerase. Non-transduced cells showed weak telomerase expression (lanes 6 and 8) as compared to OKF6 and OKF4 cell lines which had strong expression (lanes 10 and 12). Telomerase expression was absent in the negative controls (lanes 2,3 and 4) as well as after heat inactivation of each sample (lanes 5, 7, 9 and 11).

A positive control available with the TRAPeze kit was used as a positive and negative control (by heat inactivation) respectively. A separate negative control was also used from a telomerase-negative cell line, GM847. The 36-bp internal standard control (IC) is indicated at bottom of gel to confirm equal loading of the samples.

6.4 Induction of p53-dependent apoptosis response by UVB

Due to its pivotal role in the cells ability to respond to a range of environmental and intra-cellular stresses, including agents which cause DNA strand breaks, ultraviolet radiation, hyperproliferation and hypoxia, it is imperative for cells to have a functioning and intact p53 gene (Meek 2004). The role of p53 in apoptosis has been well documented and the two outcomes of p53 activation include apoptosis and cellular senescence and both of these responses require a functional p53. There are many mediators of p53 induced apoptosis including the Bax protein which is part of the bcl-2 protein family and the cells death receptors, such as FAS that work by directly stimulating mitochondria to produce an excess of highly toxic ROS (Borlon, Vankoningsloo et al. 2008). In keeping with its regulating role in genes governing the cell cycle and DNA errors, presence of a functional p53 is crucial for genetic stability, by not only preventing replication errors but also by inducing genes that regulate nucleotide excision repair of DNA (Kastan, Onyekwere et al. 1991).To investigate the response of the cells to UVB, cells were analyzed via FACS analysis for protein expression after exposure to different UVB doses and cells were assessed for viability . Cells with some tumour suppressive activity will undergo apoptosis and the cell population will have lower levels of viable cells as compared to cells with silenced p53, hence the total cell population from these cell lines are expected to have higher levels of viable cells since they will continue to proliferate past the G_1 cell cycle checkpoint governed by p53. Therefore these experiments will give an idea of level of p53 expression in the transduced cell lines and allow comparison with OKF4 and OKF6 controls.

Increased p53 levels lead to cell cycle arrest in the G_1 phase of the cell cycle through the upregulation of $p21^{WAF1}$, which in turn binds to cdks and induces the G_1 cell cycle arrest (Athar, Kim et al. 2000). In this way, cells ensure that they maintain the integrity of the genome and are protected from accumulating mutations. In cell lines derived from malignant tissues, p53 is often dysfunctional or mutated thereby permitting the cells to proliferate in the presence of cellular damage. Studies have

shown a decrease in the apoptotic response of immortalized cells with a mutated or dysfunctional p53 in response to treatment with DNA damaging UVC radiation (Latonen and Laiho 2005) . It is not clear whether the vast majority of immortalized cells illicit similar responses with regard to p53-linked apoptosis, however for the purposes of this study and its long term goals, it was important to determine a normal p53-dependent apoptotic response.

6.4.1 Method

Cells were treated to 10mj/cm^2 and 20mj/cm^2 UVB and cultured for 24h and 48h prior to analysis alongside appropriate controls. To allow for a comparative study, OKF6 and OKF4 were also investigated for their apoptotic response. Flow cytometric annexin V / dapi assay was performed in order to determine whether the transduced cell lines demonstrated apoptotic cell death following UVB exposure. The annexin V assay is a high sensitivity assay with the ability to detect early apoptosis as the annexin V antibody binds with high affinity to PS (chapter 2). The results are the averages of three independent experiments that were performed, analyzing 10,000 cells.

A representative FACS analysis experiment is shown in Figure 6.4. The scatter plot (A) is shown for the untreated control where SSC=side scatter and FSC= forward scatter and the fluorescence plots are shown for each sample (B, C, D). Untreated control cells are shown in (B). Cells were treated with 10mj/cm^2 (C) and 20mj/cm^2 (D) for both 24h and 48h. Q3 shows the viable cell population (annexin V -ve, DAPI -ve), Q4 shows early apoptotic cells (annexin V +ve DAPI –ve), Q2 shows late apoptotic and necrotic cells (annexin V +ve, DAPI +ve) and Q1 shows only necrotic cells (annexin V –ve, DAPI +ve).

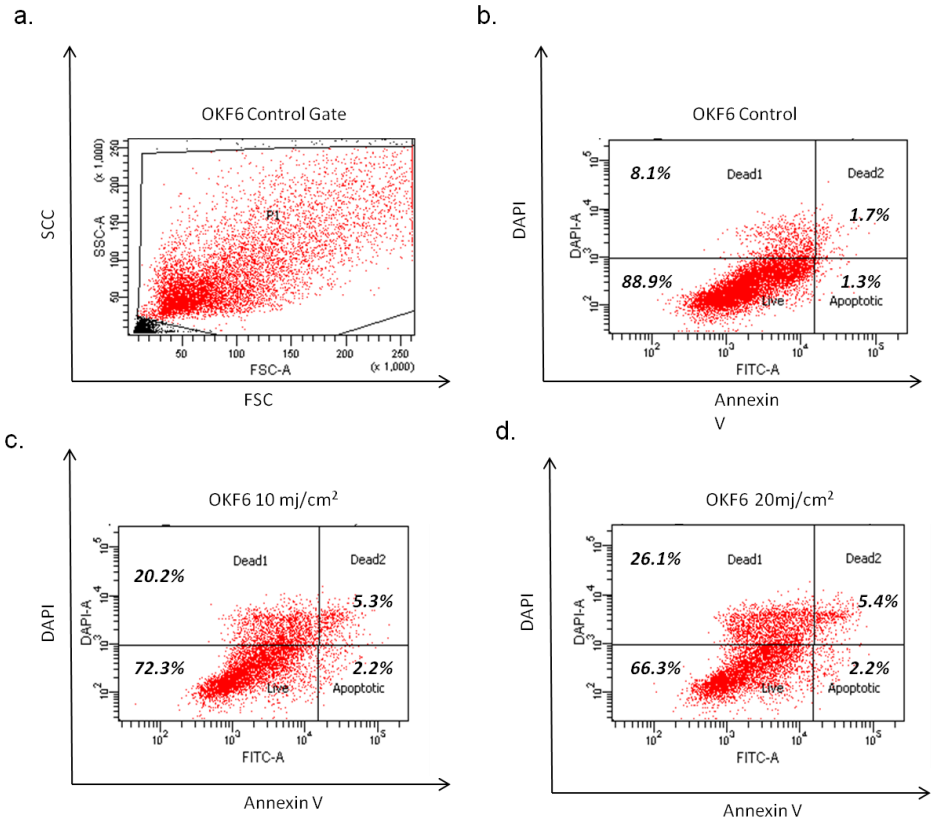

Figure 6. 4: Apoptosis assay.

Representative flow cytometry plots for annexin V FITC/DAPI for cellular viability. The scatter plot (A) is shown for the untreated control where SSC=side scatter and FSC= forward scatter and the fluorescence plots are shown for each sample (B, C, D). OKF6 cells were used in this example.

6.4.2 Results

The assay showed a marked difference in the percentage of viable cells between untreated and treated cells for both NHOK$^{Bmi1+hTERT}$ and NHEK$^{Bmi1+hTERT}$ and OKF6 and OKF4 at 24 h and 48 h post UVB treatment (Fig 6.5 - Fig 6.7).

6.4.2.1 NHOK transductions

As shown in Figure 6.5, NHOK$^{Bmi1+hTERT}$ cells showed a marked decrease in number of viable cells at 24 h between control (88% ± 3.5%) compared to cells treated to 10mj/cm^2 (82% ± 3.1%) and 20mj/cm^2 (61% ± 4.1%) UVB with the latter being significantly different when compared to the untreated control. After 48 h, a further decrease in viable cell numbers was observed in the untreated control (83% ± 4%) compared to 10mj/cm^2 (54% ± 6 %) and 20 mj/cm^2 (39% ± 8%) , both of which were significant when compared to the untreated control (Fig 6.5).

Percentage of viable cells was higher in cell lines with silenced p53 expression compared to those for bmi1+hTERT transductions (Fig 6.5). At 24 h post UVB treatment, percentage of viable cells for NHOK$^{shp16+shp53+hTERT}$ control cells were slightly higher (92% ± 1.5 %) than those treated with 10mj/cm^2 (83% ± 6%) and 20mj/cm^2 (72% ± 4.6%) of UVB, with the latter being significantly different compared to the untreated control. At 48h a slight decrease in numbers of viable cells was observed in the control (89% ± 5.5%), as well as with treatment at 10mj/cm^2 (72% ± 8%) and at 20mj/cm^2 (63% ± 6.4%), both of which were significantly different when compared to untreated controls (Fig 6.5).

Early apoptotic/late apoptotic cell percentages also increased with time and UVB dose with NHOK$^{Bmi1+hTERT}$ untreated control 5.3% ± 2.8% (early apoptotic) and 5.1% ±2.6% (late apoptotic) after 48 h , compared to 15.5% ±2.4% (early apoptotic) and 29% ±2.7% (late apoptotic) for 10mj/cm^2 and 21.8 ± 5.9% (early apoptotic) and 30.5% ± 2.5% (late apoptotic) for 20mj/cm^2 (Fig 6.8). In the case of untreated NHOK$^{shp16+shp53+hTERT}$ control cells, the viable cell percentages at 24 h post treatment

were 1.9% ± 1.2% (early apoptotic) and 2.5% ±1.4% (late apoptotic) and at 48h 2.2% ± 0.5% (early apoptotic) and 3.5% ± 1.1% (late apoptotic). When treated to 10mj/cm^2, a slight increase was observed in percentage of apoptotic cells with 14.8 %± 2.3% (early apoptotic) and 15.6% ± 2% (late apoptotic) after 48h. Similarly, when treated to 20mj/cm^2, apoptotic cell percentages were 20.4% ± 4.4% (early apoptotic) and 27.5% ± 3.6% (late apoptotic) at 48 h (Fig 6.8).

6.4.2.2 NHEK transductions

As shown in Figure 6.6, NHEK$^{Bmi1+hTERT}$ cells also showed a similar pattern at 24 h, with a decrease observed in viable cells at 10mj/cm^2 (60% ± 11%) and 20mj/cm^2 (54% ± 6%) with the latter being significantly different when compared to the untreated control (85% ± 4.6%). Again, a similar decline in viable cells was observed after 48 h at 10mj/cm^2 (59% ± 5%) and 20mj/cm^2 (41% ± 8%) and both were significantly different when compared to untreated controls (83% ± 4%).

Similarly for the NHEK$^{shp16+shp53+hTERT}$ cells, viability at 24 h for control cells (91% ± 3.2%) was higher than in cells treated to 10mj/cm^2 (79% ± 6.6%) and 20mj/cm^2 (74% ± 7%) , although there was no significant difference between the cells. At 48 h post UVB treatment percentages of viable cells were still higher than the Bmi1+hTERT transductions of untreated control cells (88% ± 5.1%) as well as cells treated to 10mj/cm^2 (76% ± 4.6%) and 20mj/cm^2 (67% ± 6.2%), with the latter being significantly different when compared to untreated controls (Fig 6.6).

When assessed for early and late apoptotic cell percentages, NHEK$^{bmi1+hTERT}$ control cells were 4.1% ± 1.7 % (early apoptotic) and 2.7% ± 1% (late apoptotic) compared to the treated cells at 48 h , 19.4% ± 3.65% (early apoptotic) and 22.5% ± 4.9% (late apoptotic) at 10mj/cm^2 and in response to 20mj/cm^2 UVB dose, these levels

increased to 29.4% ± 4.9% (early apoptotic) and 30% ± 5.3% (late apoptotic) cells (Fig 6.9).

In the case of NHEK$^{shp16+shp53+hTERT}$ cells, untreated control percentages at 24 h were 2.7% ± 2% (early apoptotic) and 2.5% ± 1.1% (late apoptotic) and at 48 h 2.8% ±0.4% (early apoptotic) and 6% ± 3.2% (late apoptotic). Similarly, when treated to 10mj/cm^2 viable cell percentages were 6.6% ± 2.9% (early apoptotic) and 11.4% ±4.3% (late apoptotic) at 48 h and when treated to 20mj/cm^2 cell percentages were 11% ± 3.5% (early apoptotic) and 11.5% ± 5.6% (late apoptotic) at 48 h (Fig 6.9).

6.4.2.3 OKF6 and OKF4

As a control, the commonly used OKF4 and OKF6 cells were assessed for their apoptotic response and having a dysfunctional p53, these cell lines will provide a good comparison for the bmi1+hTERT transduced cell lines. As shown in Figure 6.7, the percentage of viable OKF6 cells at 24h for the untreated control was 89% ± 5.6% compared to 63% ± 4.2% at 10mj/cm^2 UVB and 58% ± 7% at 20mj/cm^2 with both cell lines displaying significant differences when compared to untreated controls. After 48 h, a slight decrease in number of viable cells was observed with 61% ± 8% at 10mj/cm^2 and 59%±3.6% at 20mj/cm^2, with the latter being significantly different when compared to the untreated control at 82% ± 5.7% (Fig 6.7). Similarly for OKF4 cells, at 24 h the viable cell percentage for the untreated control was 86% ± 8% compared to 81% ± 7% at 10mj/cm^2 and 72% ± 6.2% at 20mj/cm^2, neither of which are significantly different from the untreated controls. After 48 h, a slight decrease in percentage of viable cells was observed with 67% ± 8% when treated to 10mj/cm^2 UVB and 62% ± 3.1% when treated to 20mj/cm^2 UVB, with the latter significantly different when compared to the untreated control at 87% ± 2.5%.

When assessed for the percentages of early and late apoptotic cells, cell percentages were similar to those observed for shp16+shp53+hTERT transductions rather than the Bmi1+hTERT transductions. As shown in Figure 6.10 , cell

percentages for OKF6 untreated control at 24 h were 4% ± 1% (early apoptosis) and 3% ± 1.5% (late apoptosis) whilst after 48 h a slight increase was observed at 7% ±3% (early apoptosis) and 6% ± 1.1% (late apoptosis). As shown in Figure 6.10, even after treatment with UVB at 10mj/cm^2 , cell percentages remained low at 13% ± 3.2% (early apoptosis) and 28% ± 3.3% (late apoptosis). When treated to 20mj/cm^2 UVB, cell percentages were 26% ± 9% (early apoptosis) and 11% ± 3.5% (late apoptosis). Similar results were obtained for OKF4 cells with untreated control percentages after 24 h of 3% ± 1% (early apoptosis) and 3% ± 1.2% (late apoptosis) compared to 4.5% ± 2.2% (early apoptosis) and 3.5% ± 1.3% (late apoptosis) after 48 h. Percentage of cells increased slightly after treatment with 10mj/cm^2 UVB at 8% ± 1.2% (early apoptosis) and 8.2% ± 3.5% (late apoptosis) and similarly when treated to 20mj/cm^2 UVB at 11% ± 2% (early apoptosis) and 10% ± 5% (late apoptosis) after 48h (Fig 6.10).

It is obvious that lack of p53 causes an altered apoptotic response to DNA damaging agents and in this case, NHOK$^{Bmi1+hTERT}$ and NHEK$^{Bmi1+hTERT}$ cells demonstrate responsiveness to such agents. The results suggest UVB is cytotoxic to the cells and in order to confirm expression of p53 following UVB exposure, lysates were obtained for each cell line treated with 10mj/cm^2 and 20 mj/cm^2 UVB at 24 h and 48 h. Western blot analysis showed an increase in p53 levels in Bmi1+hTERT cells following exposure to UVB as expected in cells with functional p53 activity (Fig 6.11), whilst there was no detectable p53 expression in cells with silenced p53. SVHFK and SCC25 were used as positive and negative controls and tubulin served as loading control.

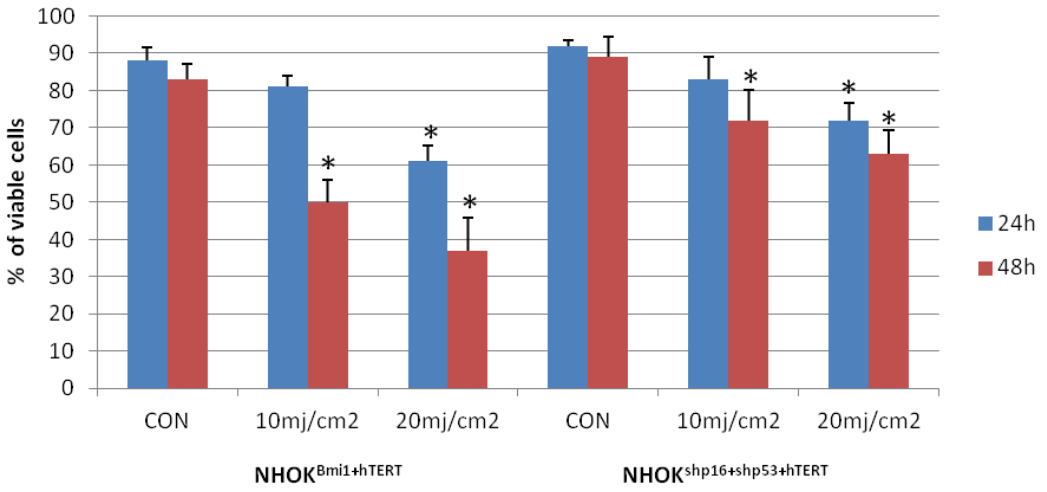

Figure 6. 5: Proportion of viable a) NHOKBmi1+hTERT and b) NHOKshp16+shp53+hTERT in the apoptosis assay.

Means± S.E.M of 3 independent annexin V/DAPI experiments. NHOK$^{Bmi1+hTERT}$ and NHOK$^{shp16+shp63+hTERT}$ were incubated for 24 h and 48 h following exposure to 10mj/cm^2 and 20mj/cm^2 doses of UVB prior to trypsinisation. The cells were then stained with annexin V and DAPI and analyzed by flow cytometry with the percentage of viable cells shown above. * is significantly different from the mean value of untreated control of each cell line.

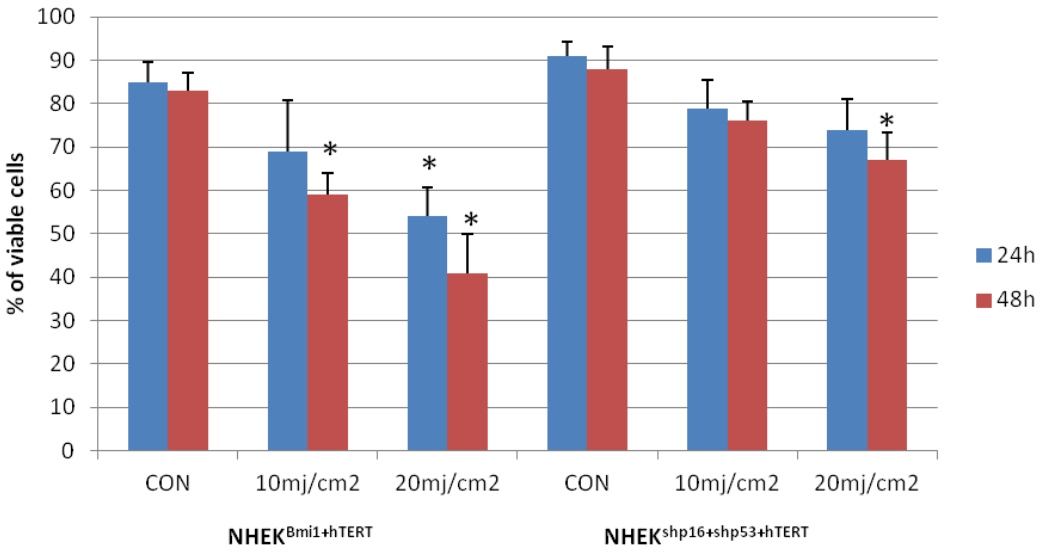

Figure 6. 6: Proportion of a) NHEKBmi1+hTERT and b) NHEKshp16+shp53+hTERT in the apoptosis assay.

Means± S.E.M of 3 independent annexin V/DAPI experiments. NHEK$^{bmi1+hTERT}$ and NHEK$^{shp16+shp63+hTERT}$ were incubated for 24 h and 48 h following exposure to 10mj/cm^2 and 20mj/cm^2 doses of UVB prior to trypsinisation. The cells were then stained with annexin V and DAPI and analyzed by flow cytometry with the percentage of viable cells shown above. * is significantly different from the mean value of untreated control of each cell line.

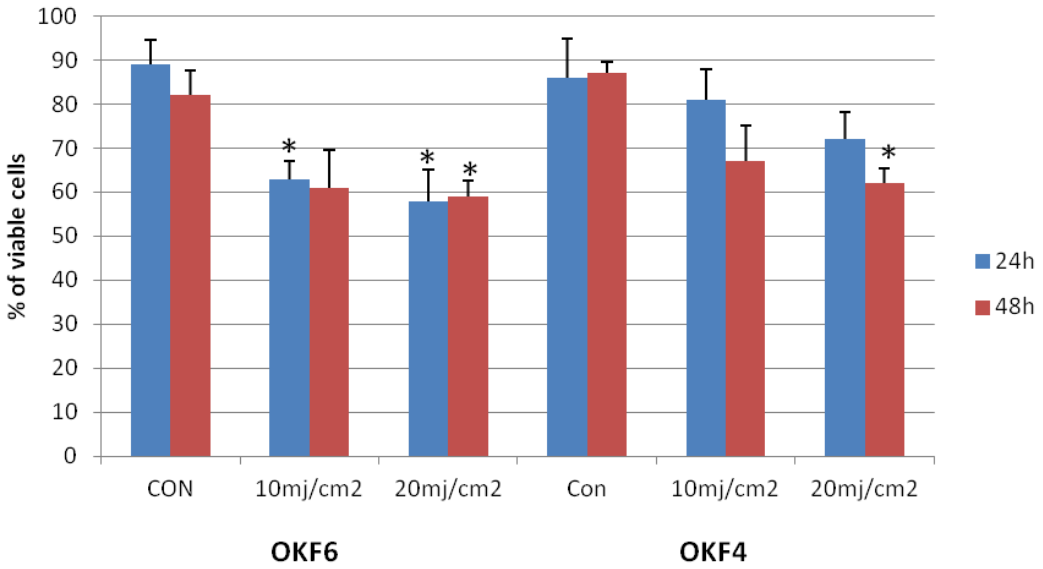

Figure 6. 7: Proportion of a) OKF6 and b) OKF4 in the apoptosis assay.

Means± S.E.M of 3 independent annexin V/DAPI experiments. OKF6 and OKF4 were incubated for 24 h and 48 h following exposure to 10mj/cm^2 and 20mj/cm^2 doses of UVB prior to trypsinisation. The cells were then stained with annexin V and DAPI and analyzed by flow cytometry with the percentage of viable cells shown above. * is significantly different from the mean value of untreated control of each cell line.

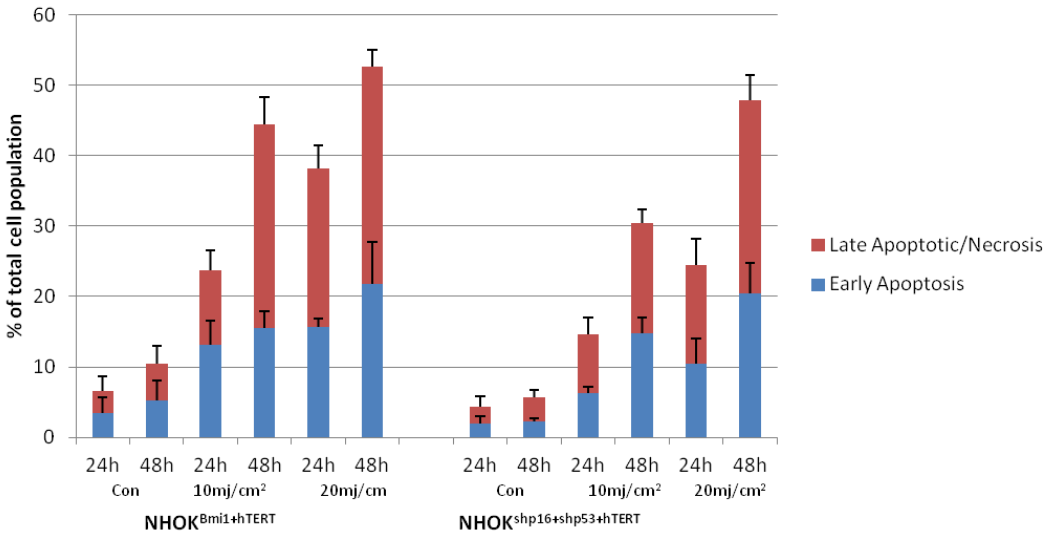

Figure 6. 8: Proportion of early apoptotic and necrotic cells in a) NHOKBmi1+hTERT and b) NHOKshp16+shp53+hTERT

Means± S.E.M of 3 independent annexin V/DAPI experiments. $NHOK^{Bmi1+hTERT}$ and $NHOK^{shp16+shp53+hTERT}$ were incubated for 24 h and 48 h following exposure to 10mj/cm^2 and 20mj/cm^2 doses of UVB prior to trypsinisation. The cells were then stained with annexin V and DAPI and analysed by flow cytometry. The percentages of early apoptotic and necrotic cells are shown. * is significantly different from the mean value of untreated control of each cell line.

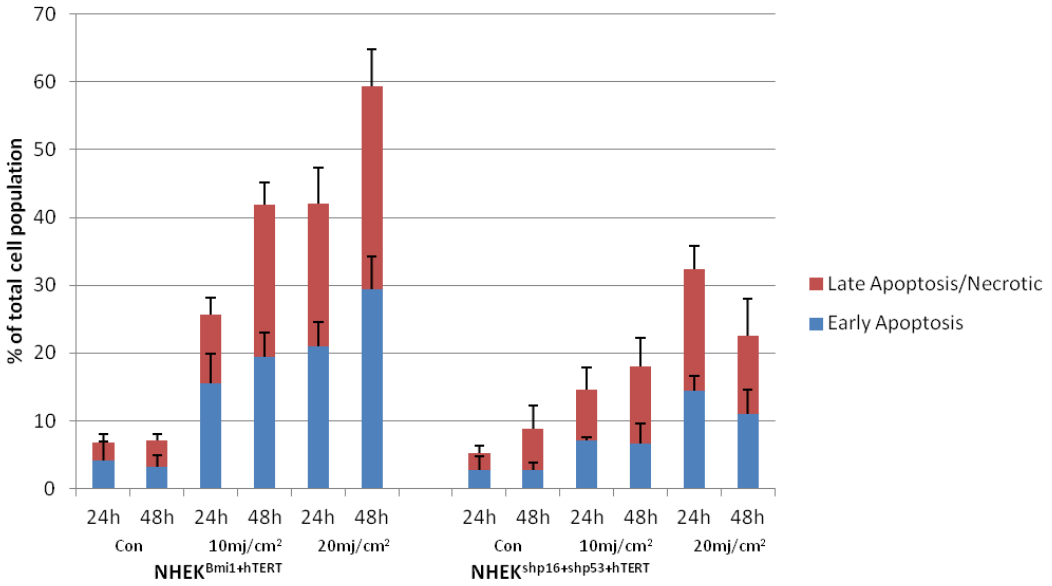

Figure 6. 9: Means Proportion of early apoptotic and necrotic cells in a) NHEKBmi1+hTERT and b) NHEKshp16+shp53+hTERT

Means± S.E.M of 3 independent annexin V/DAPI experiments. NHEK$^{Bmi1+hTERT}$ and NHEK$^{shp16+shp53+hTERT}$ were incubated for 24 h and 48 h following exposure to 10mj/cm^2 and 20mj/cm^2 doses of UVB prior to trypsinisation. The cells were then stained with annexin V and DAPI and analysed by flow cytometry. The percentages of early apoptotic and necrotic cells are shown. * is significantly different from the mean value of untreated control of each cell line.

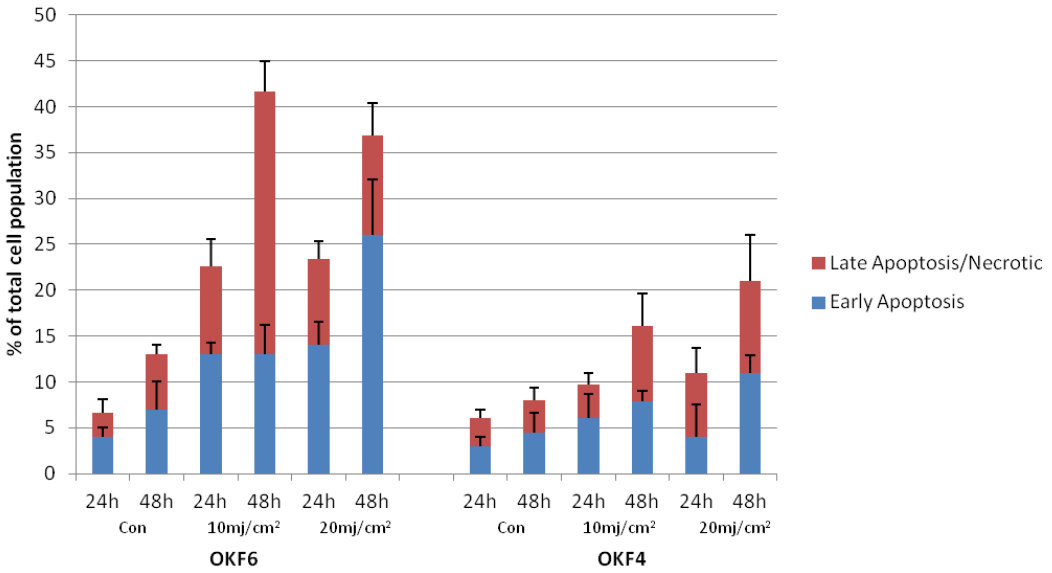

Figure 6. 10: Proportion of early apoptotic and necrotic cells in a) OKF6 and b) OKF4

Means± S.E.M of 3 independent annexin V/DAPI experiments. OKF6 and OKF4 were incubated for 24 h and 48 h following exposure to 10mj/cm^2 and 20mj/cm^2 doses of UVB prior to trypsinisation. The cells were then stained with annexin V and DAPI and analysed by flow cytometry. The percentages of early apoptotic and necrotic cells are shown. * is significantly different from the mean value of untreated control of each cell line.

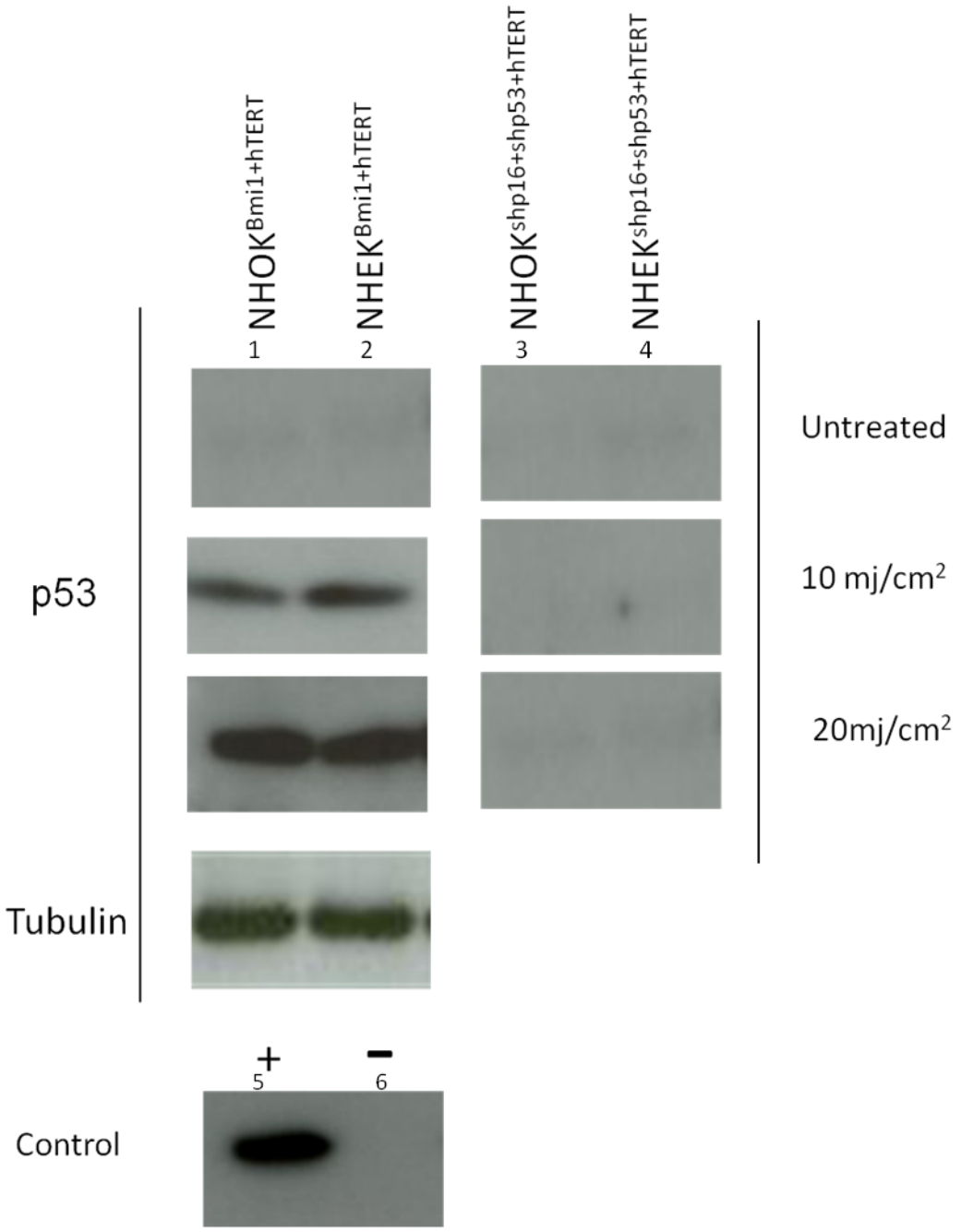

Figure 6. 11 : Upregulation of p53 in test cell lines in response to UVB.

Representative western blots showing expression of p53 in NHOK$^{Bmi1+hTERT}$ and NHOK$^{shp16+shp53+hTERT}$ following UVB treatment at 10mj/cm^2 and 20mj/cm^2 after 12 h. As expected, p53 is not visibly expressed in untreated controls since it is activated in response to DNA damage or cellular stress, as shown by the rapid rise of p53 levels following UVB treatment at 10mj/cm^2 and a further increase in expression levels at 20mj/cm^2. Comparably, there is no change of p53 expression in NHOK$^{shp16+shp53+hTERT}$ or NHEK$^{shp16+shp53+hTERT}$ when compared to untreated control. SVFHK and SCC.25 cell lines served as positive and negative controls respectively. Tubulin served as the loading control.

6.5 Evidence of DNA damage

Culture conditions and the stress which they impose on cells *in vitro* remains an underappreciated problem. Cell culture is invaluable, allowing for studies on metabolism, signal transduction, regulation of gene expression, cell proliferation, senescence and cell death. It is essential to remember that cells in culture behave differently to cells *in vivo* in many ways, most importantly by imposing a state of oxidative stress on cells (Halliwell 2003). The 'foreign' culture conditions that the cells find themselves in during *in vitro* culture is pronounced by the difficulty of culturing primary cells *in vitro*; approximately 10% of cells manage to adapt and survive when cultured whilst the remainder enter senescence or undergo apoptosis (Halliwell 2003) . Consequently, and perhaps worrisome, this can lead to effects in cells that are in fact due to oxidation products and under certain circumstances lead to misleading conclusions. Hence, cells that survive and grow in culture are not always representative of cells *in vivo*, in terms of metabolism, gene expression and enzyme levels and there is a profound need for caution when obtaining data in cell culture relevant to *in vivo* situations. For example; it can be problematic when interpreting what appears to be cellular senescence in cultured cells as rarely are culture conditions adequate to permit cells to reach the replicative senescence of the cells original *in vivo* (Halliwell 2003). DNA damage response factors 53BP1 and *γ*H2AX have been shown to bind DNA following cellular stress (Takai, Smogorzewska et al. 2003) and co-localise to form nuclear foci. 53BP1 and γH2AX staining was carried out in keratinocytes cultured in the fibroblast feeder system and two types of commercially available serum free medium, KGM and kSFM. The number of DNA damage induced foci formed per cell in each culture medium is an indication of the level of DNA damage and stress caused to cells as a result of the culture environment.

Supplementation of culture media with undefined components of serum has many disadvantages and there is a growing demand to develop improved serum free

mediums for use in research as well as for industrial applications. Serum concentrations used in cell medium has been shown to have an effect on cell kinetics and metabolism and a direct link has been shown between serum levels in cell media and cell viability. A study on HeLa cells demonstrated low serum levels slowing cell growth rates whilst increasing serum levels results in a significant reduction in viable cell numbers (Elsayed, Demellawy et al. 2009).

6.5.1 Method

NHOK$^{Bmi1+hTERT}$ and NHEK$^{Bmi1+hTERT}$ were cultured in three different culture mediums consisting of 10% serum plus EGF (FAD^{+}) and two serum free mediums; KGM and KSFM. Cells were stained for DNA damage markers 53BP1 and γH2AX following a standard immunofluorescence protocol as outlined in chapter 2 and assessed for generation of nuclear foci in response to cellular stress as a result of culture environment.

6.5.2 Result

The serial culture of early passage NHOK$^{Bmi1+hTERT}$ and NHEK$^{Bmi1+hTERT}$ in an *in vitro* environment generated nuclear foci when stained for DNA damage markers 53BP1 (Fig 6.12, NHOK and Fig 6.13, NHEK) and γH2AX (Fig 6.14, NHOK and Fig 6.15, NHEK) in all three culture mediums. As shown in Fig 6.17, when stained for 53BP1, NHOK$^{Bmi1+hTERT}$ had highest levels of positively stained cells when cultured in FAD^{+} (69% ± 7 %) and this was followed by KGM (64% ± 6.5%) and KSFM (61% ± 6.6%). Similarly, when stained for γH2AX, there was a slight decrease in the percentage of nuclear foci of NHOK$^{Bmi1+hTERT}$ cells positive when cultured in FAD^{+} (67% ± 4%) , KGM (62% ± 8%) and KSFM (59% ± 3%) (Fig 6.17). NHOK$^{Bmi1+hTERT}$ fixed and processed in the absence of staining showed little or no immunofluorescence (Fig 6.16).

A scoring system set up to determine percentage of positively stained cells illustrated that NHEK$^{Bmi1+hTERT}$ stained for 53BP1 had highest percentage of positive cells when cultured in FAD^{+} (68% ± 4%) compared to KGM (61% ± 5%) and kSFM

(59% ± 7%) (Fig 6.17). Similarly, $NHEK^{Bmi1+hTERT}$ stained for γH2AX demonstrated highest percentage of positive cells when cultured in FAD^{+} (70% ± 5%) compared to KGM (63% ± 6%) and kSFM (58% ± 8%) (Fig 6.17). Taken together, the data indicates that cells cultured in the presence of serum had higher levels of stress induced nuclear foci. To eliminate the possibility of false positives due to the use of lethally irradiated feeders, a feeder only control was also incorporated (Fig 6.16).

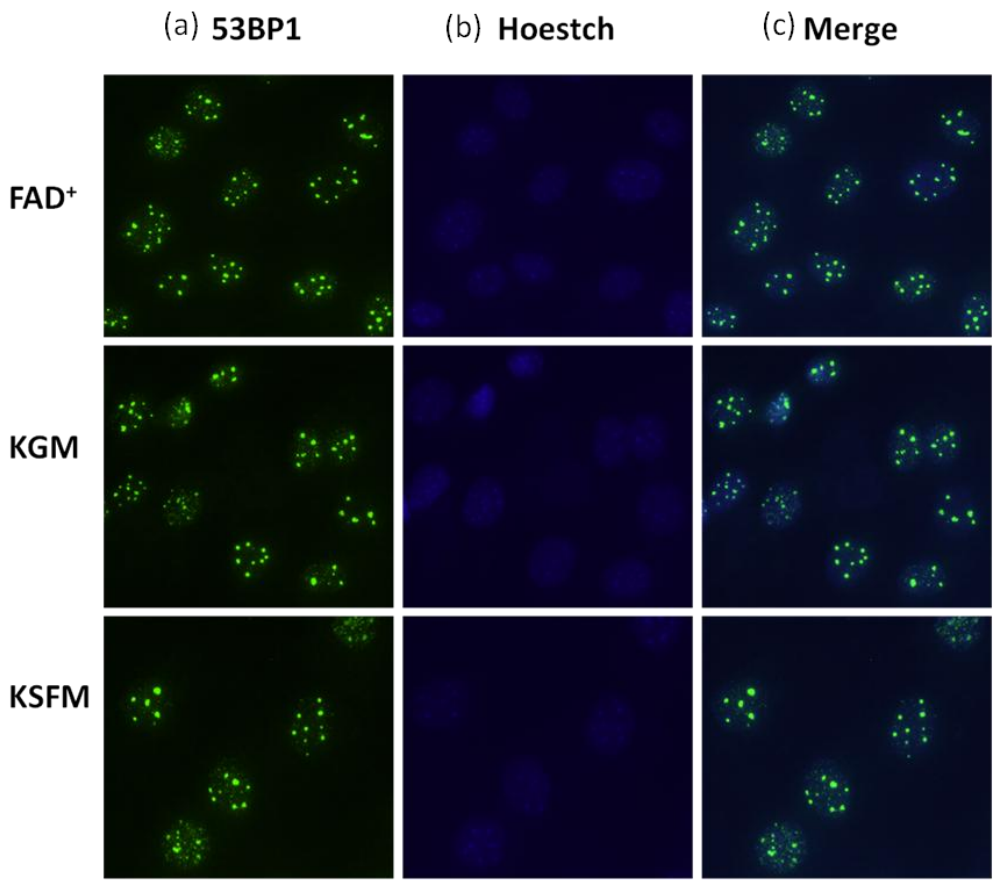

Figure 6. 12: Representative image of 53BP1 activation in NHOKBmi1+hTERT exposed to different culture conditions.

Representative images of NHOK$^{Bmi1+hTERT}$ cells staining positive with the 53BP1 antibody. Cells were incubated in FAD^{+}, KGM and KSFM for 5 days prior to staining. (a) shows 53BP1 staining (green) , (b) shows nuclear staining with Hoechst 33258 (blue) and (c) is an overlay of the two. (Magnification at 65x).

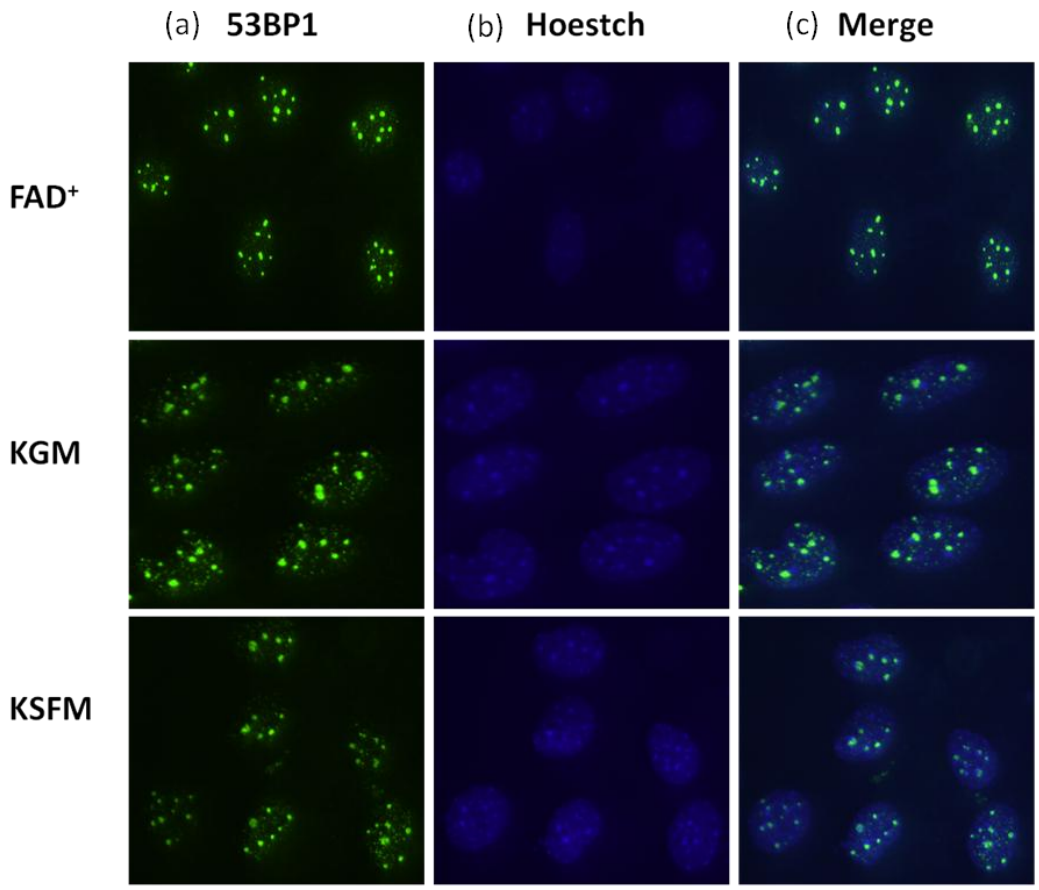

Figure 6. 13: Representative image of 53BP1 activation in NHEKBmi1+hTERT exposed to varying culture conditions.

Representative images of NHEK$^{Bmi1+hTERT}$ cells staining positive with the 53BP1 antibody. Cells were incubated in FAD^{+}, KGM and KSFM for 5 days prior to staining. (a) shows 53BP1 staining (green) , (b) shows nuclear staining with Hoechst 33258 (blue) and (c) is an overlay of the two. (Magnification at 65x).

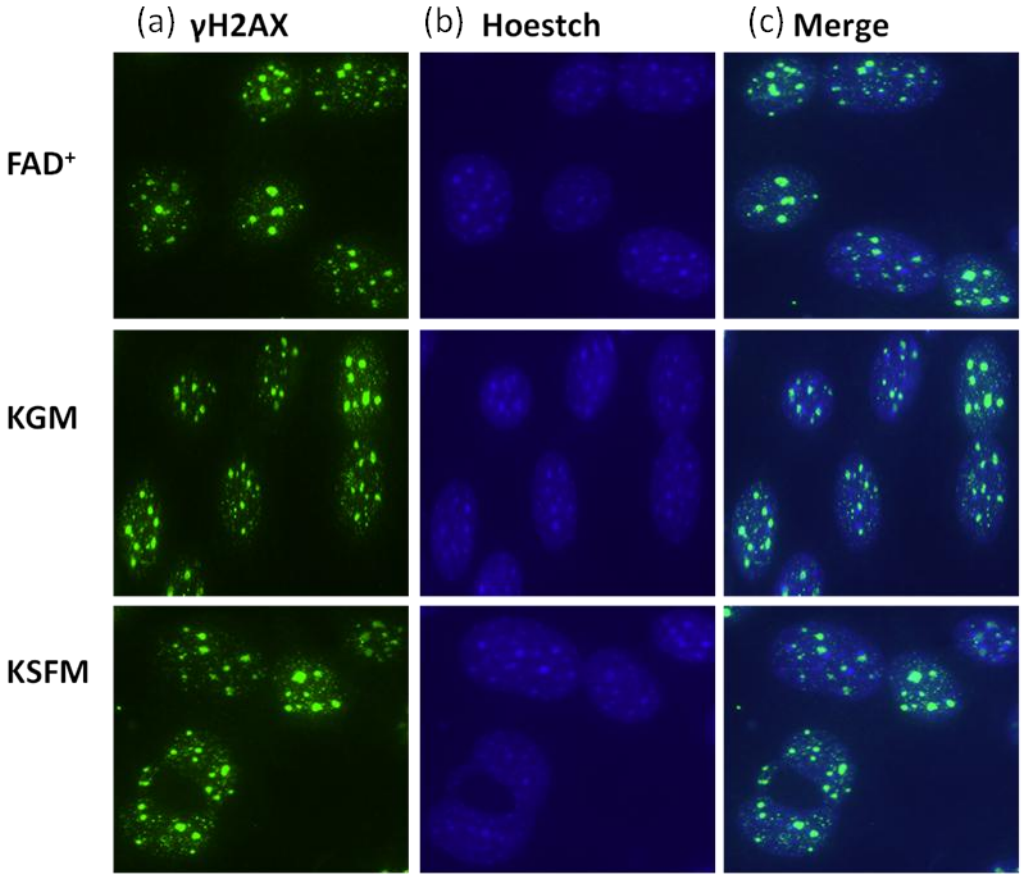

Figure 6. 14: Representative image of γH2AX activation in NHOKBmi1+hTERT exposed to varying culture conditions.

Representative images of NHOK$^{Bmi1+hTERT}$ cells staining positive with the γH2AX antibody. Cells were incubated in FAD^{+}, KGM and KSFM for 5 days prior to staining. (a) shows γH2AX staining (green) , b) shows nuclear staining with Hoechst 33258 (blue) and c) is an overlay of the two. (Magnification at 65x).

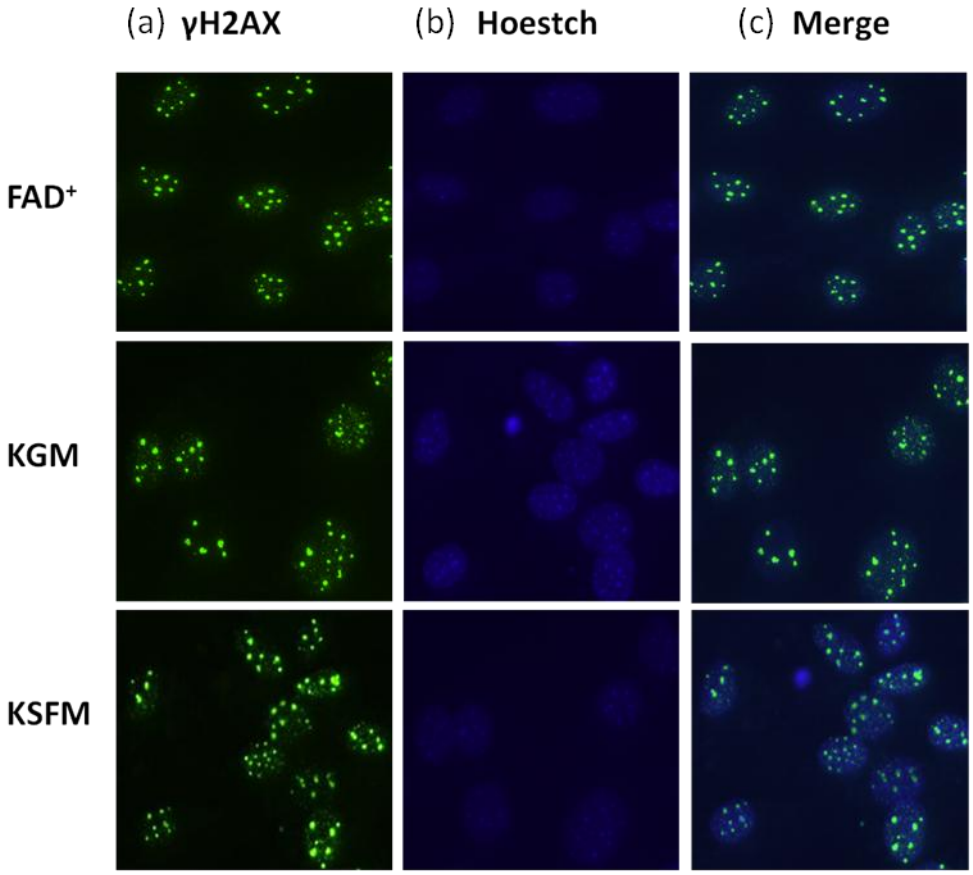

Figure 6. 15: Representative image of γH2AX activation in NHEKBmi1+hTERT exposed to varying culture conditions.

Representative images of $NHEK^{Bmi1+hTERT}$ cells staining positive with the γH2AX antibody. Cells were incubated in FAD^{+}, KGM and KSFM for 5 days prior to staining. (a) shows 53BP1 staining (green) , (b) shows nuclear staining with Hoechst 33258 (blue) and (c) is an overlay of the two. (Magnification at 65x).

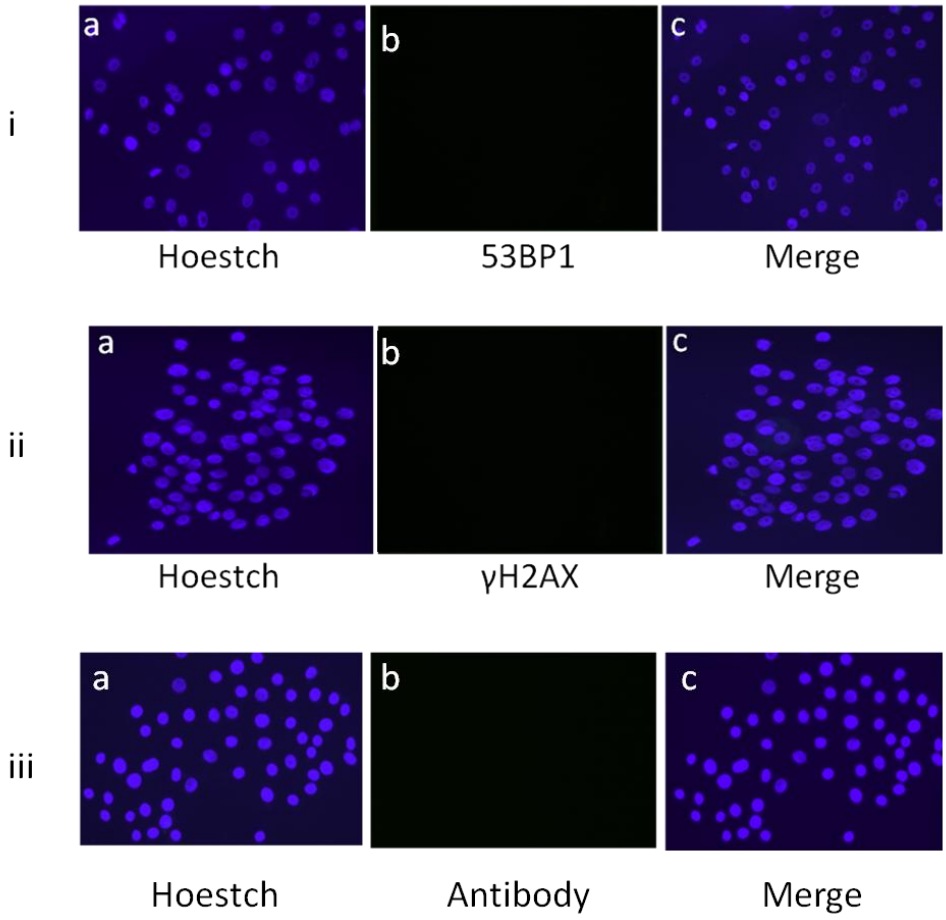

Figure 6. 16: Representative image of Immuofluorescence Antibody Controls.

Representative images of NHOK$^{Bmi1+hTERT}$ cells staining. Cells were incubated in FAD, KGM and KSFM for 5 days prior to staining. i) shows 53BP1 antibody control ii) shows γH2AX antibody control iii) shows feeder only control. (Magnification at 65x).

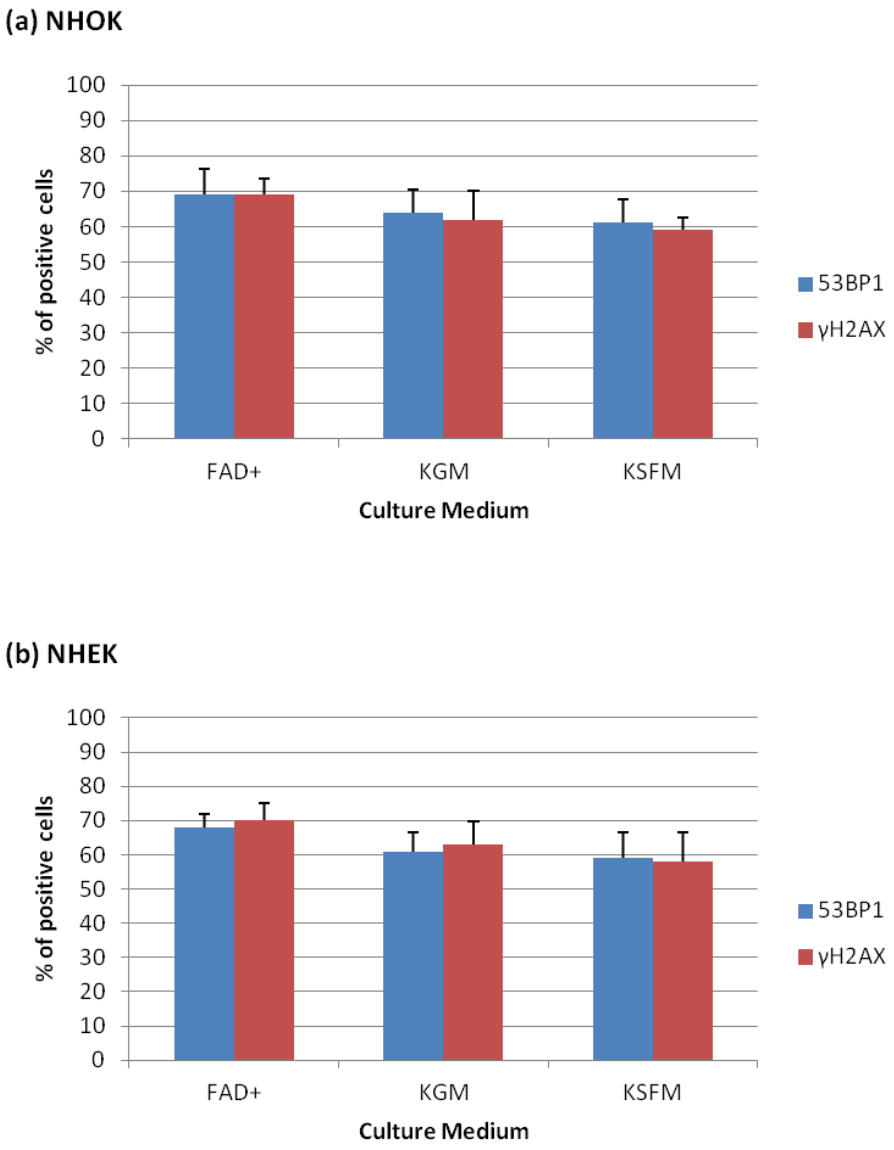

Figure 6. 17: Percentage of NHOKBmi1+hTERT and NHEKBmi1+hTERT cells stained positive for DNA damage markers i) 53BP1 (blue) and ii) γH2AX (red).

A cell was classified as positive for 53BP1 or γH2AX if it contained 3 or more nuclear foci. The percentage of positive cells is based on a counting of 300 cells in total per culture medium for each antibody. * is significantly different from the mean value of untreated control of each cell line. There was no significant difference observed in the number of positive cells cultured in serum free media from those cultured in the presence of feeders in 10% serum (FAD^+).

6.7 Adaptability of cell lines to serum free system

As discussed previously, the benefits of using cells capable of successful culture in a serum free medium are multiple and researchers find it beneficial to either use cells that already adapted for successful serum free culture or they try and adapt their cells to it. The absence of animal-derived medium components in the culture eliminates the potential for contamination by adventious agents such as viruses in cell culture (Do 2003). Other benefits include economics, as generating and screening large stocks of sera is very expensive and the culture process is greatly simplified without the requirement of feeders. Studies that have attempted to adapt cells to a serum free culture have found that the adaptation process can lead to changes in growth performance of cells with a decline observed in cell growth rates and viability following serum withdrawal or, in some cases, activation of apoptotic pathways can also occur (Gstraunthaler 2003). These observations are hypothesized to take place because of a change in culture conditions and perturbation of events associated with cell cycle progression and entry into S phase, in turn triggering cycle arrest or apoptosis (Sinacore, Drapeau et al. 2000). In rare circumstances, there have also been reports of the emergence of rare and non-representative sub populations of cells as a result of culture stress imposed in the adaptation process, although this is more likely in cells going through crisis at time of adaptation (Song, Izumi et al. 2004). These cells have been reported to have altered characteristics in terms of growth rates, viability and density (Ozturk and Palsson 1991). Adapting cells to serum free culture is a long adaptation process and it is imperative that the structural and functional integrity of expressed proteins should be closely monitored throughout the adaptation process. Many cells have either been adapted to serum free conditions or grown normally in a serum free media supplemented with hormones, trace elements and defined serum components, and as yet there is no ‘standard’ serum free media and each cell type requires its own medium composition (Ozturk and Palsson 1991).

To adapt cells to KSFM, cells from two different PD were taken and immersed directly from the feeder system to KSFM and cell growth was found to be slow with cells proliferating to a total of 7 PD (for cell lysates obtained at 15 PD) and 6 PD (for cell lysates obtained at 30 PD).

The benefit of using cell lines capable of cultivation in a serum free environment has been outlined in chapter 1 and there are two methods through which to achieve this. The first is known as 'immersion' or direct adaptation, wherein cells are switched directly from serum-supplemented growth media to serum free media and the second is sequential adaptation or 'weaning', wherein cells are gradually and sequentially weaned into serum free cultivation (Sinacore, Drapeau et al. 2000). Both methods have been shown to result in successful transfer of cells from a serum supplemented culture environment to a serum free one, although some cells appear to adapt successfully using one method over the other.

6.7.1 Method

$NHOK^{Bmi1+hTERT}$ cells from 15 and 30 PD were transferred to KSFM using both the immersion and the weaning methods of adaptation and compared to OKF6 and OKF4 and the results are presented below.

6.7.2 Result

Cell morphology appeared normal and seemed similar to the OKF6 and OKF4 (Fig 6.18). $NHOK^{Bmi1+hTERT}$ at 15 and 30 PD were directly immersed into KSFM and assessed for cell population doublings. As shown in Figure 6.19, when compared to the cells cultured with feeders, those in KSFM proliferated for approximately 6 population doublings before slowing down and eventually reached a plateau and ceased proliferation.

In an attempt to increase cell growth rates, cell adaptation process was repeated but this time the cells were weaned off from serum supplemented media by introducing a gradual reduction in the media serum supplementation. Cells were initially cultured in routine 10% FBS, followed by a week of culture in 5% FBS prior to complete transfer into KSFM. This weaning process appeared to improve growth rate (Fig 6.20) by approximately 15 population doublings but after this cell growth slowed down and cells ceased to proliferate. Two independent experiments were performed with similar results obtained in adaptation of transduced cells to serum free medium (data not shown).

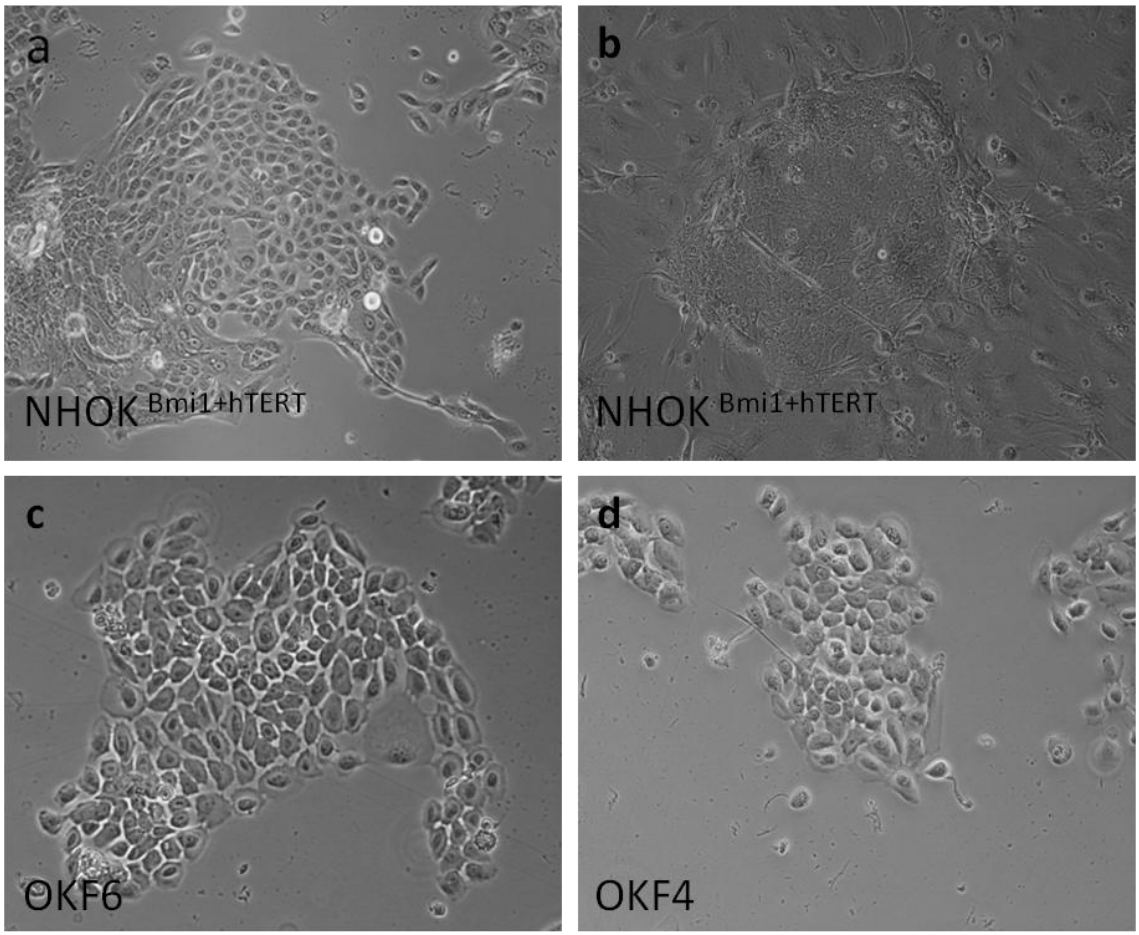

Figure 6. 18: Representative NHOKBmi1+hTERT colonies cultured in KSFM for adaptation to a serum free culture system.

Representative images of $NHOK^{Bmi1+hTERT}$ adaptation into serum free culture system. ($_a$) $NHOK^{Bmi1+hTERT}$ cultured in KSFM b) $NHOK^{Bmi1+hTERT}$ cultured in 10% serum with feeders c) OKF6 and d) OKF4. Cell morphology of $NHOK^{Bmi1+hTERT}$ appears similar to the established OKF6 and OKF4 cells lines already adapted to KSFM with normal morphology (d and c).

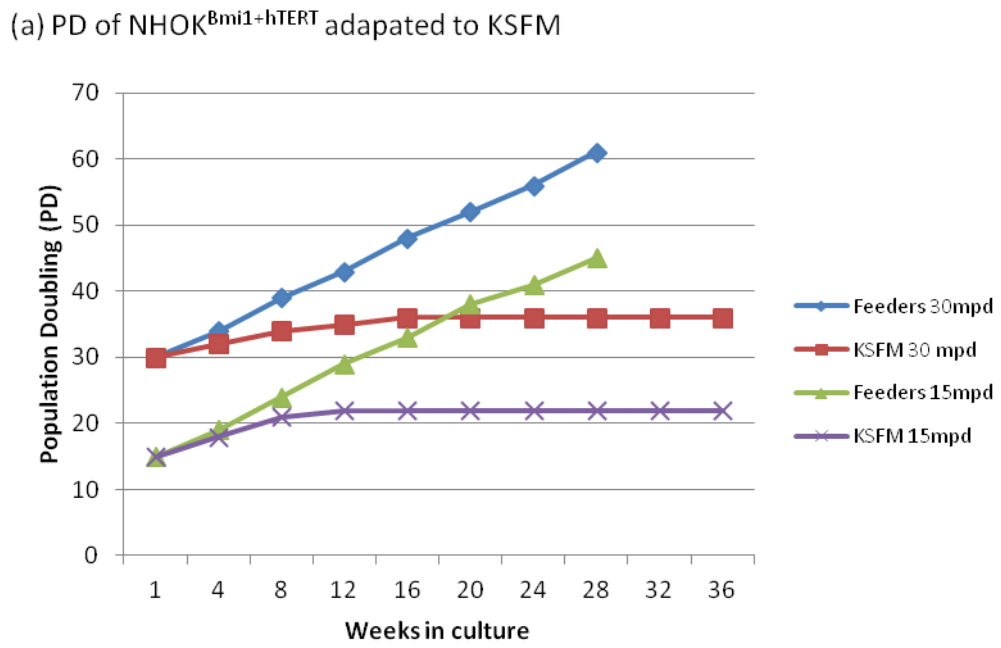

Figure 6. 19: Proliferation of NHOKBmi1+hTERT adapted to KSFM by immersion method.

NHOK$^{Bmi1+hTERT}$ were immersed in KSFM at 15 and 30 population doublings, respectively, and proliferation rates observed and compared to the same cells when grown with feeders in 10% serum. Cell proliferation rates declined for NHOK$^{Bmi1+hTERT}$ cultured in KSFM after approximately 6 PDs and ceased to proliferate further whereas the feeder control continued to proliferate indefinitely.

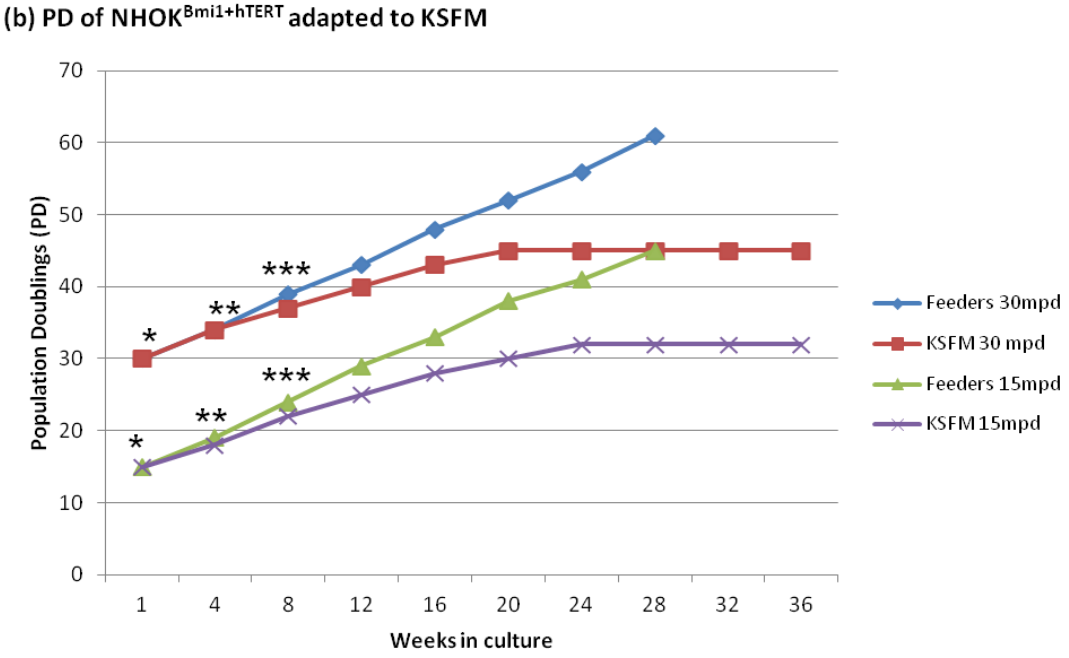

Figure 6. 20: Proliferation of NHOKBmi1+hTERT adapted to KSFM by gradual weaning.

NHOK$^{Bmi1+hTERT}$ cells were weaned into KSFM at 15 and 30 population doublings and proliferation rates compared to the same cells when grown with feeders in 10% serum. Cell rates declined after approximately 15 PD and ceased to proliferate further whereas the feeder control continued proliferation. (* indicates point of culture in 10% serum, ** indicates point of 5% serum and *** indicates start of complete serum free culture).

6.8 Discussion

Many studies have thus far reported and confirmed that overexpression of telomerase allows cells to bypass telomere-dependent senescence in many cell types including fibroblasts, retinal epithelial cells, smooth muscle cells and keratinocytes (Milyavsky, Shats et al. 2003, Ramirez, Herbert et al. 2003, Vaughan, Ramirez et al. 2006, Zhu, Mouly et al. 2007, Wieser, Stadler et al. 2008) . TRAP analysis confirmed presence of telomerase activity within the cells as compared to controls with normal keratinocytes demonstrating little telomerase activity, in accordance with current literature (Yasumoto, Kunimura et al. 1996, Kiyono, Foster et al. 1998, Kyo and Inoue 2002) .

Interesting, cellular immortalization has been reported in the absence of detectable telomerase despite displaying long telomeric length (Bryan, Englezou et al. 1995), indicating another mechanism of telomerase reactivation, whilst in some cell types, telomerase fails to overcome senescence (Kiyono, Foster et al. 1998, Dickson, Hahn et al. 2000).

Western blot analysis confirmed the presence of p53 with low expression, although it is important to consider that in normal cells p53 is often maintained at low, at times undetectable levels until a rapid rise following some stimuli such as DNA damage (Zuckerman, Wolyniec et al. 2009). This was confirmed by the UVB study on these cells which saw a rapid rise in p53 levels, discussed below. The results of this study coincides with those immortalization studies which state that downregulation of p53 is not a requirement for primary cell immortalization (Kamijo, Weber et al. 1998, Kiyono, Foster et al. 1998).

A comparison study to analyze $p16^{INK4a}$ expression in cell lines from progressing PD in culture revealed that in normal, non-transduced parent cells, $p16^{INK4a}$ expression increased with time in culture as compared to the test lines which showed no evidence of change in $p16^{INK4a}$ expression. Confirming down regulation of $p16^{INK4a}$ by bmi1 and $shp16^{INK4a}$, these results support the many studies reporting that knockdown of $p16^{INK4a}$ is essential for immortalization of cells and that accumulation of $p16^{INK4a}$ in cells is indicative of senescence (Reznikoff, Loretz et al. 1988, Serrano, Lee et al. 1996, Lin, Barradas et al. 1998, Rheinwald, Hahn et al. 2002). It must be noted that as an additional control, the use of normal, non-transduced cells for each cell line would have provided a comparable control in order to specifically conclude whether bmi1, shp16 and shp53 successfully downregulated the target proteins. A similar experiment to determine p53 levels with time in culture was not undertaken since physiological p53 levels remain low within the cell unless triggered by cellular stress of DNA damage and expression levels are not affected by progressive population doublings.

Due to its pivotal role in the cells ability to respond to a range of environmental and intracellular stresses, including agents which cause DNA strand breaks, ultraviolet radiation, hyperproliferation and hypoxia, it is imperative for cells to have a functioning and intact p53 gene (Meek 2004). In keeping with its regulating role in genes governing the cell cycle and DNA errors, presence of an functional p53 is crucial for genetic stability, by not only preventing replication errors but also by inducing genes that regulate nucleotide excision repair of DNA (Kastan, Onyekwere et al. 1991).

To investigate the response of the cells to UVB, cells were analyzed via FACS analysis for protein expression after exposure to different UVB doses. From the results there was a clear difference in percentages of viable cells between the cell lines with downregulated p53 and those with functional p53. The OKF4 and OKF6

cells also exhibited similar results to the test cell lines in which p53 was downregulated, and these results confirmed higher rates of apoptotic response in cells transduced with Bmi1 plus telomerase , coinciding with the increase in expression of p53 following UVB treatment in these cells.

Irradiation by UVB exposure has been shown to cause oxidative stress and DNA damage with p53 playing an important role in the cellular DNA damage response. A study on HaCat cells immortalized with viral oncoproteins E6 and E7 showed a significant reduction in apoptotic response to UVC irradiation and ,furthermore, analysis by western blotting did not reveal any changes in levels of p53 post treatment (Shnitman Magal, Jackman et al. 1998). In contrast, another study which immortalized uroepithelial cells (HUC) with HPV16 oncoprotein E6 did not undergo apoptosis in response to γ irradiation and had low to undetectable expression of p53 levels. Interestingly, in the same experiment, two independent HPV immortalized cell lines demonstrated stabilized p53 and subsequent p53-dependent apoptosis(Reznikoff, Yeager et al. 1996). It is interesting to note that two studies utilizing similar methods for immortalization responded differently to the same form of DNA damage.

Western blot analysis of cell lysate samples from the UVB irradiated cells also demonstrated elevated levels of p53 post treatment whilst the cells transduced with shp53 did not appear to have any protein expression at all. It is important to remember ,however, that apoptosis is not limited to p53 control, and this would explain the lower-than-expected percentage of viable cells despite downregulating p53 expression. A study by Bush *et al* (2001) demonstrated apoptosis in human melanoma cells independent of p53 by a FAS-receptor / caspase 8 pathway suggesting apoptosis activation through other pathways including caspase activation and via a membrane mediated mechanism through activation of death receptor pathways (Bush, Cheung et al. 2001). Another study on proliferating

lymphoid cells demonstrated that DNA damage induces apoptosis via p53 independent mechanisms and is inhibited by bcl-2 (Strasser, Harris et al. 1994).

Doses of UVB have also been shown to impact the response of a cell and keratinocytes have previously been shown to repair all of UVB induced DNA damage at low UVB doses and continue normal cellular functions. Similarly, in response to extremely high doses of UVB, there is extensive damage that cannot be repaired and cells respond by undergoing apoptosis, whilst with intermediate doses, keratinocytes have also been shown to undergo premature senescence (Lewis, Yi et al. 2008).

Comparison of early versus late apoptotic/necrotic cells further provided an accurate representation of 'true' apoptotic cells, essentially the proportion of cells irreversibly committed to programmed cell death. This is a result of the early p53-dependent apoptotic response being reversible and if the cells repair machinery is able to successfully repair DNA damage, early apoptotic cells can re-enter the cell cycle and continue as normal (FJ Geske, 2001). In contrast, late apoptotic cells are not permitted to re-enter the cell cycle and often transform into necrotic cells, in particular if the extent of cellular damage is severe. Consequently, late apoptotic and necrotic cells share many morphological and biochemical properties, often making it difficult to distinguish between the two using analytical techniques such as FACS, although other techniques such as complement binding can be used to differentiate between the two cell types since necrotic cells are known to activate complement components C3 and C4 early on in the process whereas this is a rather late even in apoptotic cells (US Gaipl, 2001).

Again, it must be noted that as an additional control, the use of normal, non-transduced cells for each cell line would have provided an additional comparative control in order to further conclude the extent of apoptotic response between normal cells and UVB-treated transduced cells alongside the untreated control.

DNA damage response factors 53BP1 and *γ*H2AX have been shown to bind DNA following cellular stress (Takai, Smogorzewska et al. 2003) and co-localise to form nuclear foci. 53BP1 and γH2AX staining was carried out in keratinocytes cultured in the fibroblast feeder system and two types of commercially available serum free medium, KGM and kSFM. The number of DNA damage induced foci formed per cell in each culture medium is an indication of the level of DNA damage and stress caused to cells as a result of the culture environment.

Using a standard immunofluorescence protocol where cells were fixed before being permeabilized, cells were stained for expression of 53BP1 and γH2AX. Analysis of cells using the lecia epifluorescence microscope revealed the formation of multiple nuclear foci in over 60% of the cells, therefore supporting the studies that tissue culture is a stressful environment for the nurturing of cells *in vitro*. It must be noted, however, that statistically there was no significant difference between the percentages of positive cells across the different culture mediums for both 53BP1 and γH2AX although there were some subtle differences observed. At a magnification of 65x, cells cultured with a feeder layer in a serum environment seemed to display, on average, higher numbers of nuclear foci per cell in comparison with the cells cultured in KGM or kSFM although foci were not detected in every cell. The difference in the number of nuclear foci numbers between the cells cultured in the two different serum free environments was less pronounced with a slightly higher number of nuclear foci in KGM when stained for γH2AX. For a more accurate analysis of the extent of DNA damage across the three different culture conditions, a foci scoring system was set up that was used as a standard throughout the quantification process. Assuming that three or more nuclear foci were present, the cell was rated as positive for DNA damage and scored

accordingly, with an aim of counting a minimum of 300 cells per marker. No nuclear foci were visibly detectable for the antibody controls staining therefore positive cells were scored with confidence.

In culture, cells in kSFM proliferated at a slightly faster rate than those cultured in KGM. This can be explained by the difference in the composition and varying concentrations of the growth factors, hormones and calcium used in the two mediums respectively, the proportions of which either promote proliferation and thereby limit differentiation or vice versa (Wille Jr, Pittelkow et al. 2005). Perhaps the main difference stems from the different calcium concentrations used of which KGM uses a concentration of 0.15mM whilst kSFM has a working calcium concentration of 0.09mM. It has been shown that at low levels of calcium keratinocytes tend to proliferate more rapidly, differentiate slowly and form fewer cornified envelopes (Song, Izumi et al. 2004) whilst as calcium concentrations exceed 1 mM , keratinocytes tend to differentiate more and express appropriate markers (Wille Jr, Pittelkow et al. 2005).

To adapt cells to KSFM, cells from two different PD were taken and immersed directly from the feeder system to KSFM and cell growth was found to be slow with cells proliferating a total of 7 PD (for cells taken from 15 PD) and 6 PD (for cells taken from 30 PD). Similarly, when serum was gradually eliminated from the culture medium, cells plateaued after proliferating for 17 PD (for cells taken from 15 PD) and 15 PD (cells taken from 30 PD). These results indicate that the direct immersion method was not suitable for the cells although the gradual weaning method appeared to show some potential. These results are in accordance with the supporting literature that cells prefer a gradual adaptation process to prevent culture shock, as when cultured gradually, there is a 2-fold increase in population doublings. It is possible that there would have been a more pronounced increase of population doublings had the adaptation process been longer and cells adapted gradually, however time restraints prevented that. Currently many cells have been

successfully adapted to serum free culture including keratinocytes, rat neuroblastoma cells (Darmon, Bottenstein et al. 1981) and fetal rat brain cells (Honegger, Lenoir et al. 1979).

6.9 Conclusion

After having established cell life span expansion, $NHOK^{Bmi1+hTERT}$ were characterized for a variety of variables. As expected, p53 expression was almost undetectable, as under normal circumstances p53 levels are low within the cell, rising rapidly following DNA damage or external stresses on the cell, as illustrated after UVB treatment. $p16^{INK4a}$ expression was low across increasing population doublings as compared to controls wherein it steadily increased with time in culture, in keeping with its role in cellular senescence. A p53-dependent apoptotic response was observed in cells following UVB treatment as compared to untreated controls. Cells were assessed for DNA damage across three different culture mediums and levels of DNA damage induced foci were lower in the absence of serum in culture media, following which $NHOK^{Bmi1+hTERT}$ cells were analyzed for growth in KSFM and demonstrated potential when weaned into a serum free system gradually.

Chapter 7:

Results 5

Chapter 7

Results 5

7.1 Evidence of cell viability on polycarbonate membrane

Keratinocytes *in vivo* stratify into multiple layers forming a stratified squamous epithelium and form distinct layers as they differentiate and mature through the layers, as described in chapter 1. Immortalized cell lines are often assessed for the ability to stratify as many studies require experiments to be done on multiple cell layers rather than monolayer experiments, for example drug permeation and delivery studies. It is essential to test cells for stratification and patterns of differentiation to ensure that the cell model has minimal differences from the native tissue, preventing results from constantly having to be reconfirmed by parallel studies using native tissue or primary cells, as found by a recent study of the growth of SV40-immortalized corneal cell on membrane tissue (Greco, Vellonen et al. 2010). The different organotypic substrates used to assess stratification of cells include DED, collagen gel and polycarbonate membranes.

Polycarbonate membranes provide an easy to culture membrane surface for cells to stratify and can be sectioned to assess stratification patterns. Assessment of cell viability by the colorimetric MTT assay indicated cellular activity levels since the amount of colour generated is a direct result of cellular mitochondrial activity. Cell lines were adapted to grow in serum free media prior to culture onto polycarbonate membrane inserts and assessed for cell viability using a standard MTT assay. Membranes were then sectioned for analysis of cell stratification.

Cells were plated at a pre-determined density and grown for 7 and 14 days prior to being analyzed for viability, as shown by MTT absorbance values. As shown in Figure 7.1 a, both cell lines showed little viability when cultured in accordance to a standard protocol with $NHOK^{Bmi1+hTERT}$ (absorbance 0.244 ± 0.01 at 7 days and 0.26 ±0.02 at 14 days) and $NHEK^{Bmi1+hTERT}$ (absorbance 0.24 ± 0.01 at 7 days and 0.25 ± 0.01 at 14 days) compared to blank control in the absence of cells (absorbance 0.2 ± 0.01). To improve growth rates, a variety of seeding densities were tested to determine optimal seeding density (data not shown) and cells were then reseeded and analyzed for viability, once again demonstrating little difference in cell growth despite the increase in seeding density and no significant difference was observed in the cell lines compared to the control (Fig 7.1 b).

To further improve cell viability, feeders were added to the culture vessels three days prior to culturing cells on membrane inserts and, as shown in Figure 7.2, when cultured in the presence of feeders, cell viability was significantly higher for both $NHOK^{Bmi1+hTERT}$ (absorbance 0.44 ± 0.01 at day 7 and 0.5 ± 0.03 at day14) and $NHEK^{Bmi1+hTERT}$ (absorbance 0.46 ± 0.02 at day7 and 0.48 ± at day 14) as compared to blank control (absorbance 0.2 ± 0.01). $NHOK^{shp16+shp53+hTERT}$ were also cultured on membrane inserts and once again demonstrated a similar increase in cell viability (Fig 7.2b), indicating a preference of the cells to a feeder culture environment and supportive growth environment. The results are the averages of three independent experiments that were performed.

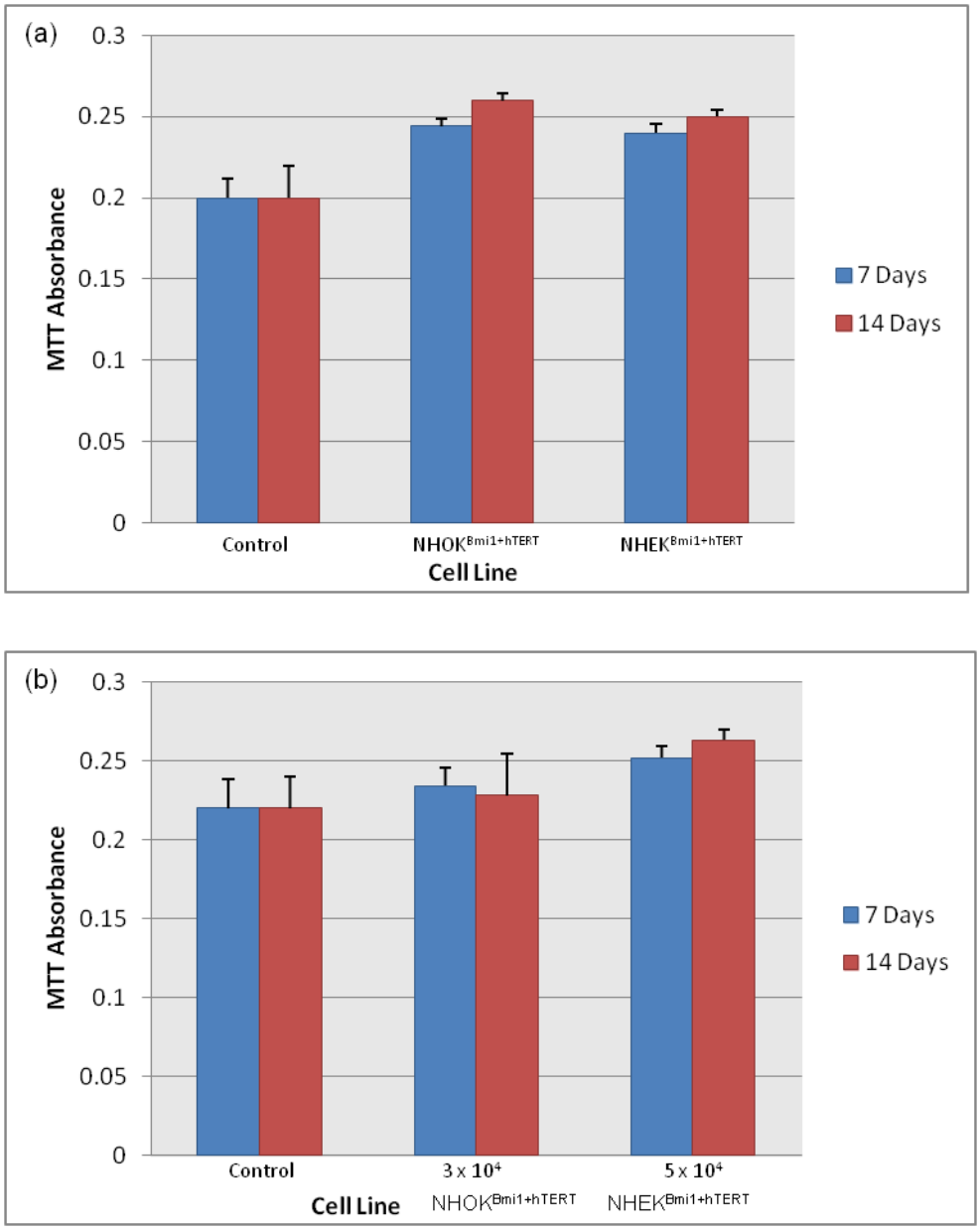

Figure 7. 1: Cell viability on polycarbonate membrane assessed by MTT assay.

a) NHOK$^{bmi1+hTERT}$ and NHEK$^{bmi1+hTERT}$ cultured on polycarbonate inserts show little viability and b) increasing seeding density did not increase cell viability significantly compared to control wells (no cells). * is significantly different from the mean value of the control. There was no significant difference observed between the cell lines and the control.

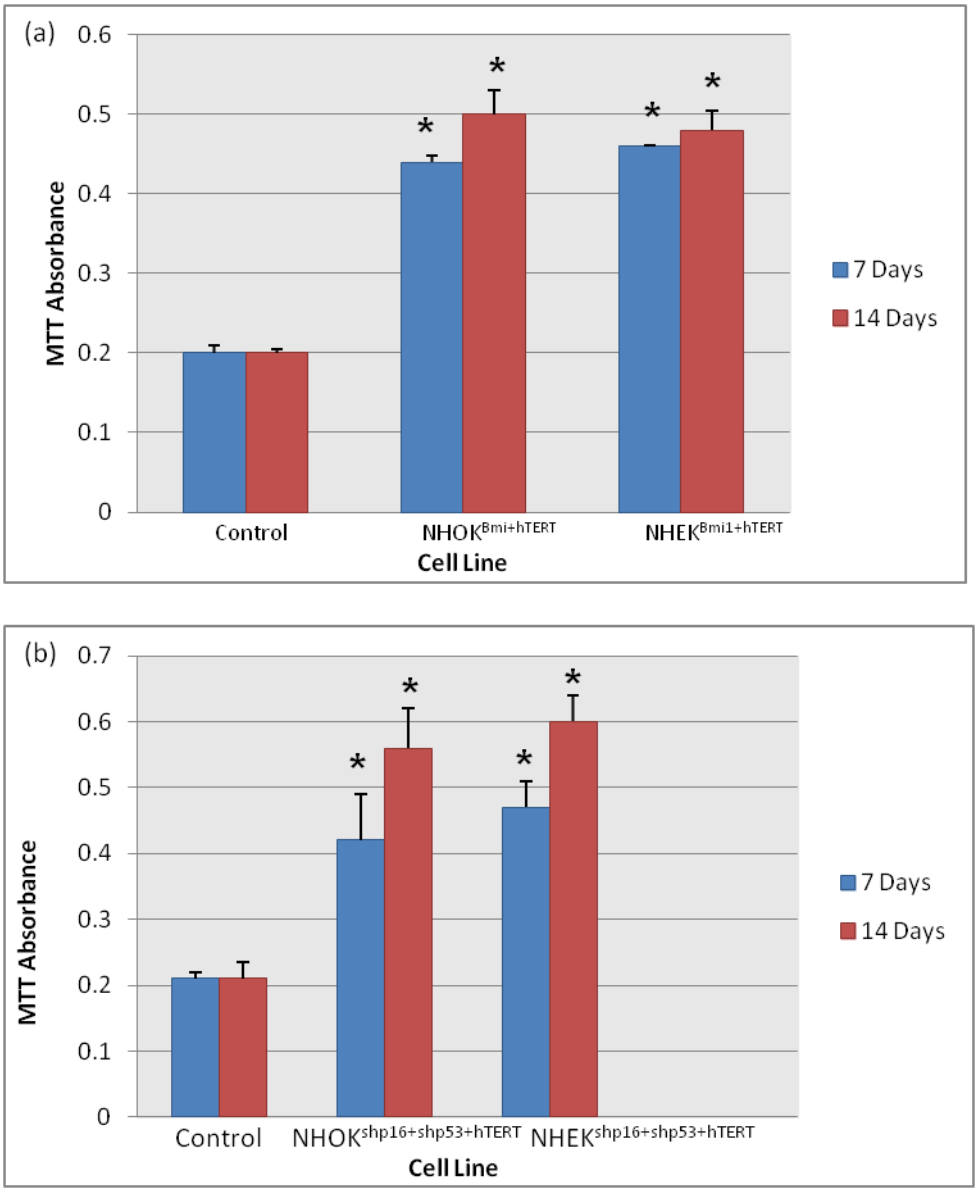

Figure 7. 2: Cell viability on polycarbonate membrane assessed by MTT assay.

a) NHOK$^{bmi1+hTERT}$ and NHEK$^{bmi1+hTERT}$ and b) NHOK$^{shp16+shp53+hTERT}$ and NHEK$^{shp16+shp3+hTERT}$ cultured on polycarbonate inserts show increased viability when cultured with feeders when compared to control (no cells). * is significantly different from the mean value of the control.

7.2 Stratification on polycarbonate membrane

The final part of this study aimed to get initial insight into whether these cell lines would stratify on membranes. Cells were placed onto polycarbonate membranes and assessed for viability by MTT assay prior to being sent for histopathological analysis. Cells that were seeded at the initially calculated seeding density did not grow on the membrane but after increasing seeding destiny cell viability seemed to increase slightly and this increase was also observed after membrane sectioning (Fig 7.3, Fig 7.4, Fig 7.5 and Fig 7.6).

To increase levels of stratification, feeders were used and plated on the tissue culture vessel three days prior to the cells being placed onto polycarbonate membrane inserts at the higher seeding density of 5×10^4. Cells appeared to respond to the supportive culture environment provided by the fibroblasts feeders and a significant increase in stratification was observed with the cells forming multiple layers (Fig 7.3, Fig 7.4 Fig 7.5 and Fig 7.6).

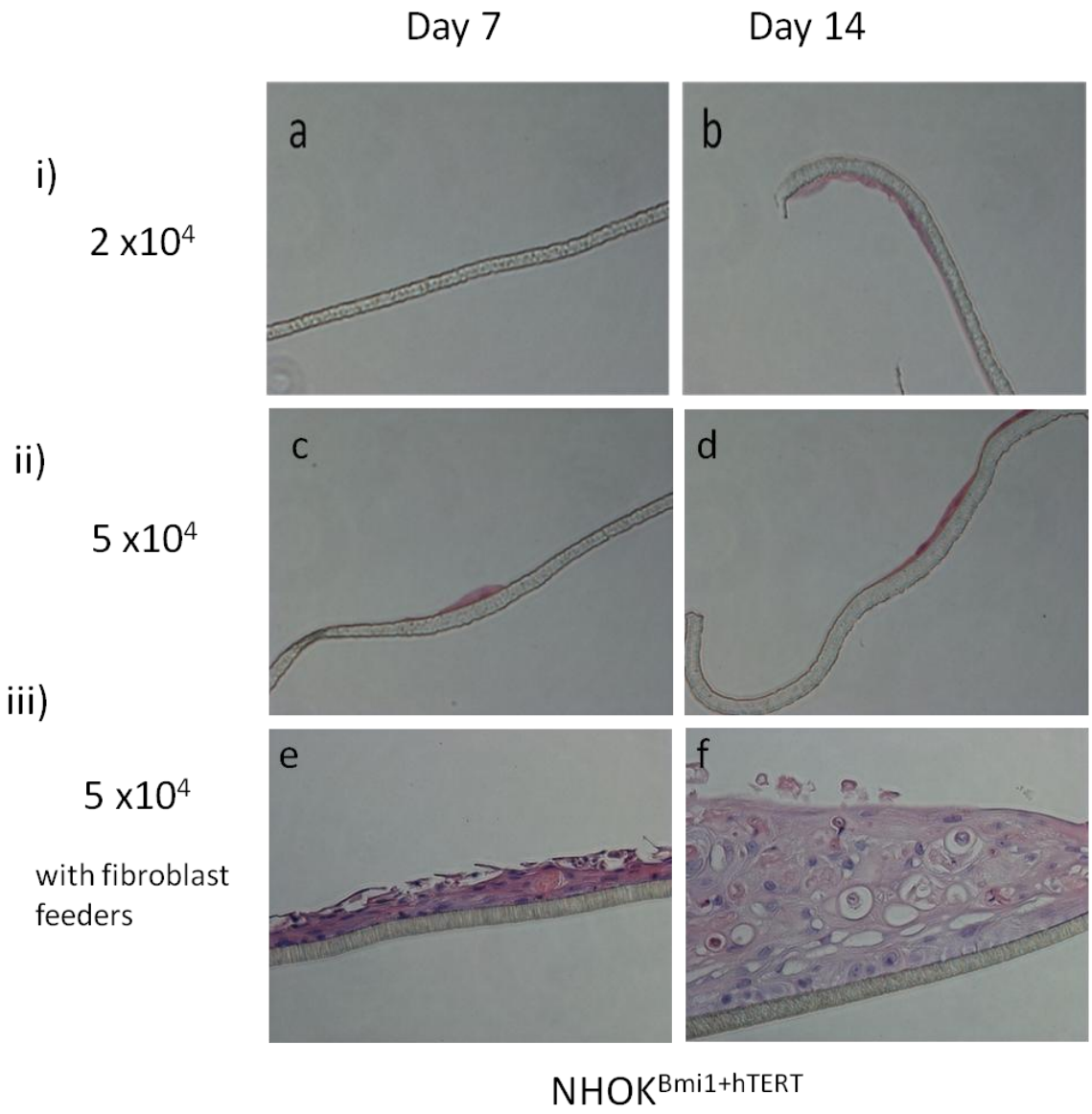

Figure 7. 3: Stratification of NHOKBmi1+hTERT on polycarbonate membranes after 7 and 14 days in culture i) KSFM at 2x104 ii) KSFM at 5 x 104 and iii) with feeders at 5 x 104.

$NHOK^{Bmi1+hTERT}$ cells were cultured on top of polycarbonate membranes under different conditions and seeding densities and subjected to histological analysis to assess for stratification. Data obtained for cells cultured in i) KSMF at 2 x 10^4 (a and b) ii) in KSFM at 5 x 10^4 (c and d) and iii) with feeders at 5 x 10^4 (e and f). (Image taken at 40 x magnification).

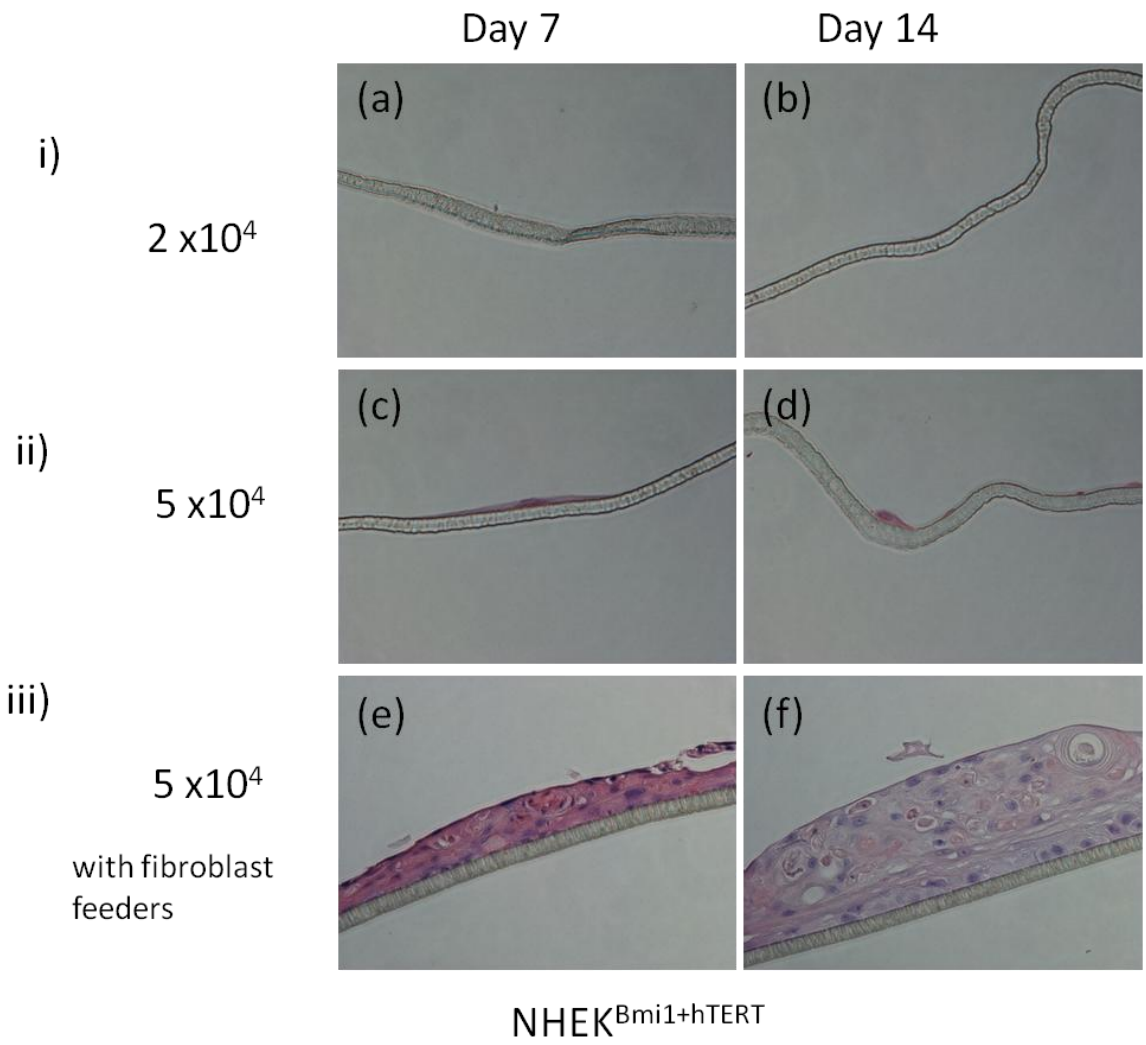

Figure 7. 4: Stratification of NHEKBmi1+hTERT on polycarbonate membranes after 7 and 14 days in culture i) KSFM at 2x104 ii) KSFM at 5 x 104 and iii) with feeders at 5 x 104.

$NHEK^{Bmi1+hTERT}$ cells were cultured on top of polycarbonate membranes under different conditions and seeding densities and subjected to histological analysis to assess for stratification. Data obtained for cells cultured in i) KSMF at 2 x 10^4 (a and b) ii) in KSFM at 5 x 10^4 (c and d) and iii) with feeders at 5 x 10^4 (e and f). (Image taken at 40 x magnification).

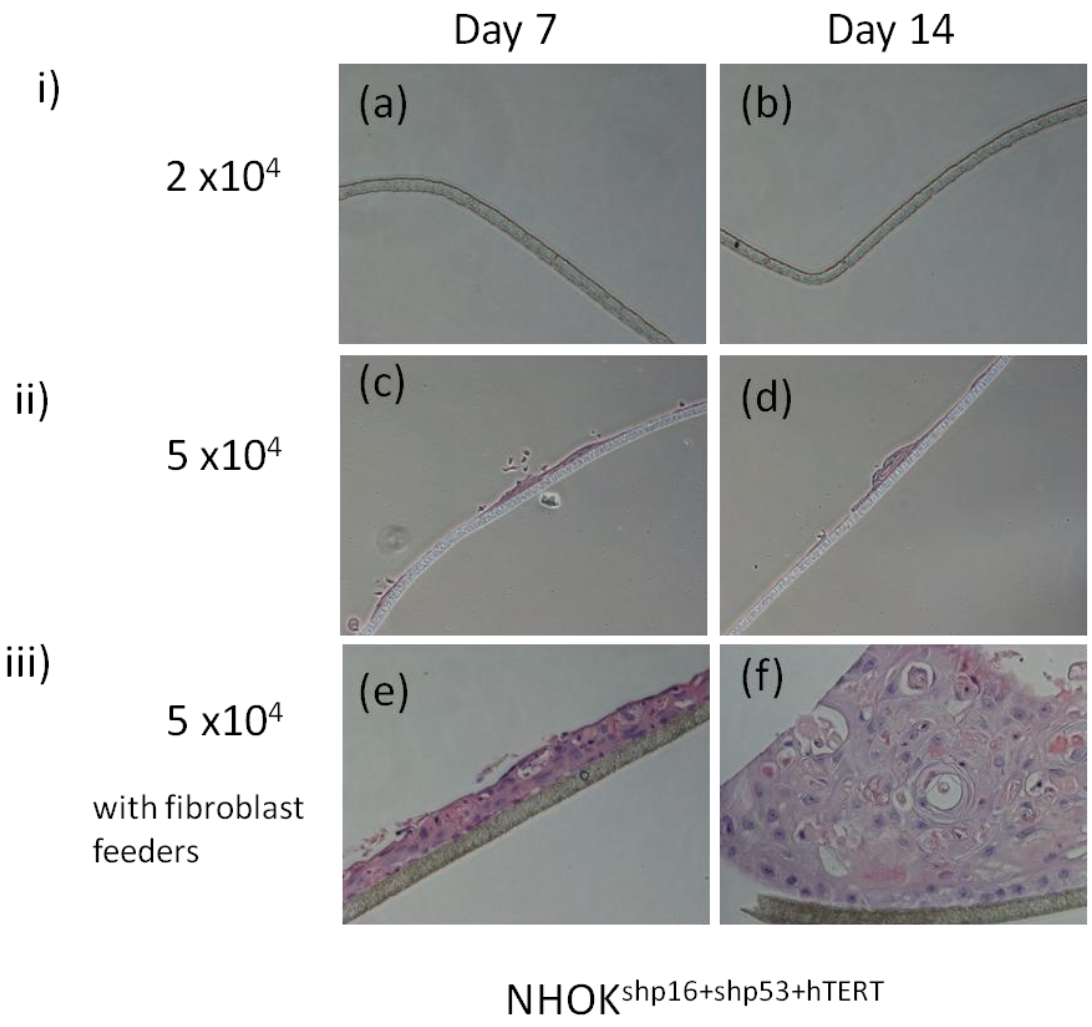

Figure 7. 5: Stratification of NHOKshp16+shp53+hTERT on polycarbonate membranes after 7 and 14 days in culture i) KSFM at 2x104 ii) KSFM at 5 x 104 and iii) with feeders at 5 x 104.

NHOK$^{shp16+shp53+hTERT}$ cells were cultured on top of polycarbonate membranes under different conditions and seeding densities and subjected to histological analysis to assess for stratification. Data obtained for cells cultured in i) KSMF at 2 x 10^4 (a and b) ii) in KSFM at 5 x 10^4 (c and d) and iii) with feeders at 5 x 10^4 (e and f). (Image taken at 40 x magnification).

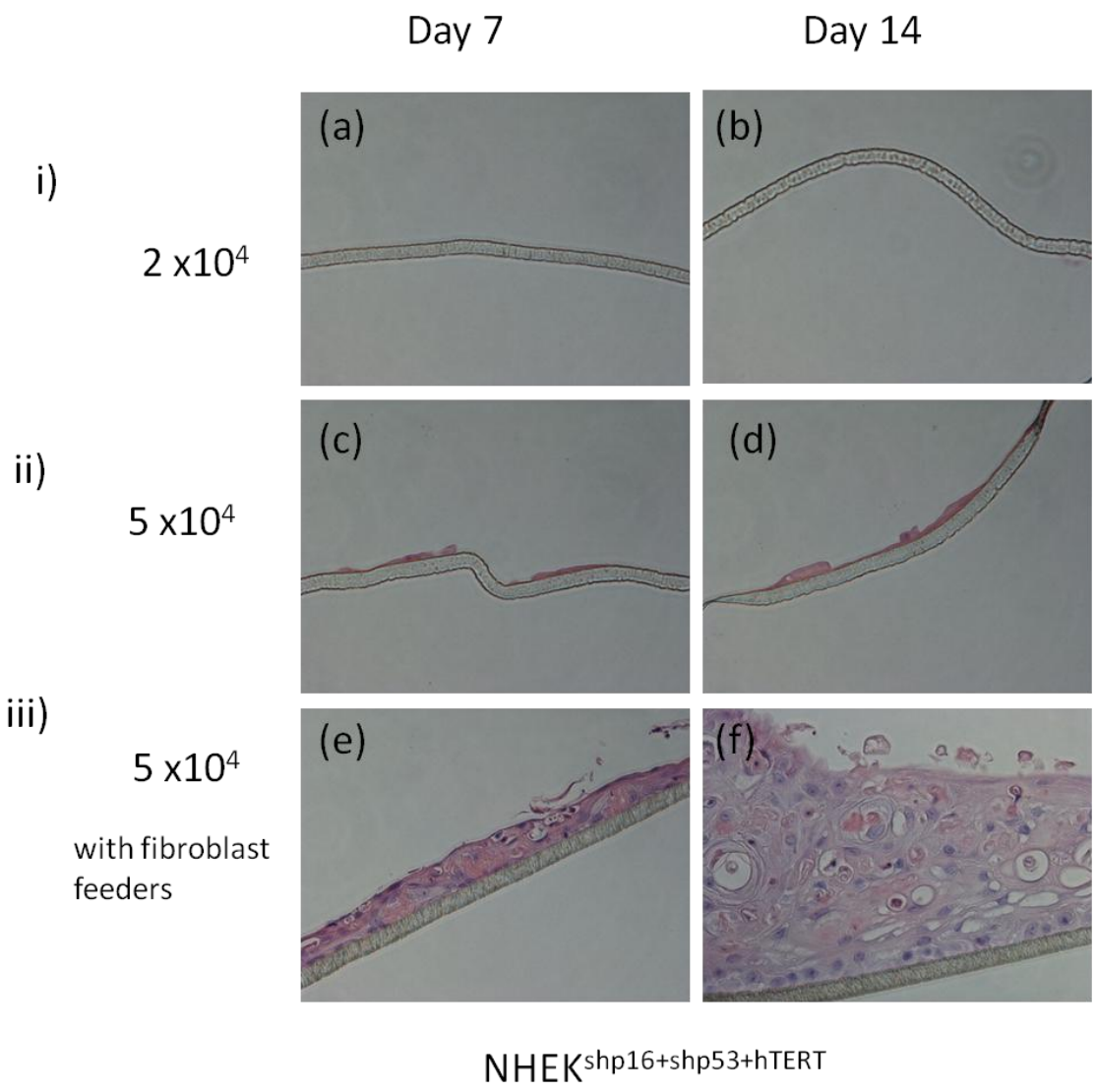

Figure 7. 6: Stratification of NHEKshp16+shp53+hTERT on polycarbonate membranes after 7 and 14 days in culture i) KSFM at 2x104 ii) KSFM at 5 x 104 and iii) with feeders at 5 x 104.

NHEK$^{shp16+shp53+hTERT}$ cells were cultured on top of polycarbonate membranes under different conditions and seeding densities and subjected to histological analysis to assess for stratification. Data obtained for cells cultured in i) KSMF at 2 x 10^4 (a and b) ii) in KSFM at 5 x 10^4 (c and d) and iii) with feeders at 5 x 10^4 (e and f). (Image taken at 40 x magnification).

7.3 Discussion

Stratification studies allow for a phenotypic assessment and characterization of cell lines and the different organotypic substrates used to assess stratification of cells include DED, collagen gel and polycarbonate membranes. Due to time restraints, it was not possible to use a variety of substrates and cells were cultured onto polycarbonate membranes and assessed for viability by MTT prior to membrane sectioning and histopathological analysis. MTT analysis demonstrated little growth when cultured in KSFM however this was significantly increased when cultured with feeders and in presence of serum, with cells stratifying into multiple layers. This is unsurprising as the cells were unable to adapt to KSFM beforehand and illustrates the need to fully adapt the cells to KSFM prior to culture on membrane inserts.

The methods by which cells are immortalized and their genetic constituents results in various patterns of cell stratification, for example; human cervical and foreskin epithelial cells immortalized by HPV proteins exhibit dysplastic differentiation *in vivo (Woodworth, Waggoner et al. 1990)* whereas similar studies in mice showed normal cells to form a well differentiated epithelium within 2-3 weeks. In contrast, a study immortalizing cell lines by 4 types of HPV found all 4 lines to exhibit dysplastic morphology and molecular alterations in gene expression, for example; delayed commitment to terminal differentiation, altered involucrin expression plus reduction in levels of involucrin plus keratin RNAs (Dürst, Bosch et al. 1991).

A comparison of the transduced cells with the normal pattern of NHOK and NHEK differentiation illustrates a different growth pattern and lack of appropriate terminal differentiation, instead displaying phenotype similar to that of pre-malignant or malignant cells. Studies on OKF6 cells have shown that despite exogenous hTERT expression and loss of $p16^{INK4a}$ function , the cells were still able to initiate program of terminal differentiation, express suprabasal differentiation-specific proteins and form differentiated epithelia in both *in vitro* (cultured on

collagen gel) and *in vivo* (grafted onto athymic mice) (Dickson *et al,* 2000). An initial attempt made at growing OKF6 and OKF4 cell lines on polycarbonate membranes did not demonstrate growth in serum free media and due to time constraints could not be optimized further under different conditions, thus highlighting the importance for optimizing the process prior to making final conclusions regarding $NHOK^{Bmi1+hTERT}$ and $NHEK^{Bmi1+hTERT}$ differentiation patterns. Additionally, it would have been useful to have included normal, non-transduced NHOK and NHEK cell lines as controls alongside $NHOK^{Bmi1+hTERT}$ and $NHEK^{Bmi1+hTERT}$ to allow comparison of growth rates and patterns of differentiations between cell lines in the same set of experiment.

7.4 Conclusions

$NHOK^{Bmi1+hTERT}$ and $NHEK^{Bmi1+hTERT}$ demonstrated little viability when cultured in serum free media, however, a slight increase was observed after increasing initial cell seeding density. There was a two- fold increase in viability when cultured with the support of feeders, thus pointing towards inadequate culture conditions for poor viability rather than an inability to stratify on cells behalf. When subjected to H&E, cells retained ability to stratify into multiple layers with feeders support although exhibited dysplastic differentiation patterns indicating need for further investigation.

Chapter 8:

Discussion

Chapter 8

Discussion

8.1 Discussion and Future Work

The hypothesis for this study had proposed that a cell line immortalized with intact p53 expression would result in genetically stable cells with similar characteristics to the parental lineage in comparison to currently available cell lines with silenced or spontaneously downregulated p53. As discussed below, this hypothesis has been proved correct from the acquired monolayer data demonstrating p53 expression alongside a p53-dependent apoptotic response and normal rates of cell proliferation however further analysis is required to determine genetic stability and make conclusions regarding 3D culture (discussed below). The first part of this study investigated optimum culture conditions for the growth of keratinocytes which were then maintained for the duration of the study. This was important in order to generate reliable, accurate and reproducible data as culture conditions have been shown to affect cell growth and proliferative potential with cell lines exhibiting an increase in population doublings with improved culture environments as well as minimizing the rate of stress-induced cellular transformations (Todaro and Green 1963) (Von Zglinicki 2002).

Keratinocytes were cultured in 10% serum (FAD) as well as two commercially available serum free culture mediums, KGM and KSFM, and assessed for DNA damage foci but did not show a significant difference between the percentage of positive cells across the three mediums. It had been expected that higher levels of stress-induced foci would be observed for cells cultured in 10% serum since serum has been reported to cause stress in cultured cells (Halliwell 2003). It is possible

that since the keratinocytes used in this study were being cultured in a feeder layer and directly immersed into a serum free culture environment as opposed to a gradual adaptation, this sudden change of culture environment may have subjected cells to high levels of internal stress thus explaining the higher percentage of damage induced foci levels found in serum-free cultured cells. As an additional comparative control, keratinocytes already established for growth in a serum free environment may have been a more accurate representation of serum free cells, although it is important to note that every cell line responds differently to serum free adaptation therefore this alone may not have sufficed as a control. Additionally, it would have been interesting to directly assess effects of serum reduction on cells by culturing cells in a range of serum concentrations to determine whether lowering the serum concentration had any effect on percentage of DNA damage positive cells.

An alternative approach to determine DNA damage-induced foci can be to co-stain with both 53BP1 and γH2AX markers as *in vivo* both of these seem to co-operate and work together in the DNA damage response by localising at sites of DNA damage and forming part of the protein group that initiates the DNA damage response (Fernandez-Capetillo, Lee et al. 2004). A comparison of p53 expression levels and its target genes such as $P21^{WAF}$ or $p16^{INK4a}$ by western blot analysis on lysates obtained from cells grown in the different culture mediums will be useful in determining extent of cellular stress. Alternative markers of DNA damage can also be used, for example; staining for the growth arrest- and DNA damage-inducible gene 153 (GADD153), shown to be induced by culturing cells in nutrient-depleted media, a condition that causes growth arrest (Kim, You et al. 2002).

Cells in culture behave differently from cells *in vivo* and one of the main reasons for this is that cell culture imposes a state of oxidative stress on cells, effectively resulting in a 'culture shock' that hinders growth potential (Halliwell 2003). Most

cells *in vivo* are exposed to low O_2 concentrations in the range of 1-10 mm Hg with some exceptions (including the epidermis and the cornea) and in contrast cell culture is normally performed under 95% air and 5% - 10% CO_2 which is approximately 150 mmHg O_2 tension. It has been shown that the higher the levels of oxygen tension, the higher the rate of ROS production (Collins 1999). Such oxidative stress results in cell death, cellular senescence, aberrant cell growth and inaccurate population doublings, for example; total lifespan of fibroblasts in culture was originally thought to be approximately between 40-50 PD but a recent study has shown that if cells are cultured at low O_2 tension, many more population doublings are possible and that this culture related oxidative stress has been linked to accelerated telomere shortening (Shay and Wright 2005).

Cells grown closer to physiological O_2 levels have been shown to have increased rates of cell proliferation and although a pilot study demonstrated a decrease in the percentage of DNA damage induced foci formed with culture in low O_2 (data not shown), due to large volumes of culture plates it was not possible to conduct an entire experiment within the available low O_2 culture facilities. It will be interesting to culture the successfully transduced cells alongside controls such as parent cells as well as OKF6 and OKF4 and compare growth rates to each other in low O_2 as well as in normal culture conditions.

Keratinocytes are deemed immortal if they continue to proliferate for an additional 50 PD beyond the parent cell line (Dickson, 2000). As discussed in Chapters 4 and 5, the transduction of cells with bmi1 plus hTERT resulted in successful lifespan expansion of both oral and epidermal keratinocytes whereas those transduced with shp16+hTERT required additional downregulation of p53. To further analyse the benefits of both immortalization protocols, a set of infections using both methods immediately prior to the onset of senescence will be beneficial in determining whether the proposed method rescues the cell from entering senescence, thereby

indirectly assessing its effectiveness at over-riding cell cycle regulatory mechanisms. Since tumourigenic lines are often unstable, with minimal dependence on growth factors and a tendency to proliferate rapidly, it will be interesting to culture transformed cell lines such as OKF6 and OKF4 as well as DNA tumour virus transformed cells alongside parental controls, thereby allowing for a direct comparison of the rate of proliferation with the transduced cells. Senescence associated β gal expression was noted in all of the cells that ceased proliferation although in hindsight the results of the β gal assay would have benefited from having an additional comparative control of non-transduced oral and epidermal keratinocytes at early and late passage.

Analysis of cell lysates via a PCR based TRAP assay demonstrated telomerase activity in the transduced cell lines, confirming successful introduction of hTERT into the cells. Weak telomerase expression was detected in normal, non-transduced cells and although somatic cells do not express telomerase per se, weak telomerase expression has sometimes been detected in normal epithelial and endothelial cells, for example after wound healing or for telomere maintenance. As an additional control, parent control cells from early and late passage could have been incorporated to show telomerase expression at different replicative time points since weak telomerase expression would be expected in culture unless there is reactivation of telomerase within the cells. Similarly, lysates from a variety of different population doublings from the transduced cells could have been tested to assess the differences in telomerase levels with time in culture to correlate with the transduction data.

As discussed in chapter 6, transduced cells were assessed for $p16^{INK4a}$ expression over time but it would have been helpful to add an additional comparative control of non-transduced cells when assessing $p16^{INK4a}$ expression over time, allowing for a direct comparison. Transduced and non-transduced cell lines can also be assessed

for expression of $p14^{ARF}$ and as it is expressed from the same locus as $p16^{INK4a}$ it will be interesting to see whether it is completely silenced or partially down-regulated in regards to its connection with $p16^{INK4a}$ as well as its role as a regulator of p53.

UVB is known to result in the generation of reactive oxygen species and induction of potentially mutagenic DNA damage and has been shown to induce p53 expression in cells (Hall et al., 1993). Interestingly, FACS analysis of cells treated with UVB damage displayed higher numbers of viable cells not only in the transduced cells expressing p53 but also, albeit to a lesser extent, in cells with silenced p53 which, although surprising, can be explained by many reasons. Firstly, DNA damage can induce $p16^{INK4a}$ methylation which can potentially induce the p53-dependent DNA damage response, often observed in immortal cells which have arisen spontaneously out of crisis (Al-Mohanna, Al-Khalaf et al. 2007). Additionally, it is important to remember that the apoptotic response is not completely p53 dependent but cells can also undergo apoptosis via death receptor pathways. This mode of p53-independent apoptosis occurs via regulatory proteins known as caspases which, once activated, bring about a number of changes within the cell leading to programmed cell death. A study on human diploid fibroblasts with silenced p53 found that treatment with UVB still resulted in G_1 cell cycle arrest, indicating that p53-independent mechanisms also control UVB-induced growth arrest (Borlon, Vankoningsloo et al. 2008)

Analysis for p53 target proteins involved in the DNA damage response for example gadd45, whose expression is linked to G_1 cell cycle arrest following DNA damage, and $p21^{WAF1}$ will provide additional data to support analysis of apoptosis in these cells since higher levels of expression in these proteins would be expected if apoptosis is indeed occurring via the p53-dependent apoptotic pathway. Furthermore, FACS analysis of cell samples can be performed to analyse cell cycle content revealing which phase of the cell cycle the cells are in. As before, if the apoptotic response is via p53 then a high G_1 cell content would be expected since

p53 regulates the cell cycle at the G_1 cell cycle checkpoint. As a cell responds to DNA damage by inducing either senescence or apoptosis depending upon cell type and extent of damage, the UVB treated cells can also be assessed for senescence associated β gal activity to determine level of senescence in these cells. Additionally, analysis of initiator and effector caspases by western blotting can be performed to allow a comparison of expression levels in cells treated to UVB and compared to untreated as well as non-transduced cells. If the cells were undergoing p53-independent apoptosis, the expression levels of initiator and effector caspases are expected to be much stronger than untreated controls. Such a combination of experiments would give an extensive overview of apoptosis analysis in these cells.

As mentioned in previous chapters, the use of serum in cell culture media is controversial for both ethical and scientific reasons and often results in phenotypical differences in cells leading to variation of the results. Since *in vitro* methods are among the most favoured methods to replace animal methods, there is a demand for reliable and scientifically better defined cell and tissue culture methods including quality assurance (Coecke, Goldberg et al. 2007).

Unfortunately the transduced cells did not adapt to serum free medium and there was not sufficient time remaining in the study to allow for an extensive adaptation study. It is important to remember that every cell type differs in cellular requirements and two approaches can be taken to adapt cells to serum free for future experiments. The first is the development of a novel serum free media specifically optimized for the growth of the specific cell type however this is a long and arduous process requiring meticulous consideration of use and concentration of many ingredients, for example basal medium, growth factors, supplements and fatty acids as well as ensuring that adapted cells retain native tissue biomarkers. For this reason it is recommended that, where possible, to adapt the cells to already established culture mediums and many transformed or newly transfected cell lines

can successfully be maintained in these enriched serum-free environments without adaptation.

A review of the literature has shown that the gradual reduction of the serum concentration increases the chances for successful adaptation of cells to a serum-free environment (Schröder, Matischak et al. 2004). Previous studies have successfully adapted cells to serum free media by stepwise decreasing the serum concentration in every other passage by 50% to wean cells off serum and in this way the serum concentration could be easily reduced from 10% (v/v) to 1.25% (v/v) (Schröder, Matischak et al. 2004). To further decrease the serum concentration, the study discovered that it was necessary to switch to a basal medium formulation richer in nutrients as well as coating the dishes with fibronectin and replacing HEPES buffer with a sodium carbonate buffer that gave higher cell densities (Schröder, Matischak et al. 2004). The literature favours a slow adaptation process for cells to adapt to the medium over an extended time frame and since the transduced cells showed promise when grown in 5% serum as opposed to the direct immersion method it is possible that they will be able to adapt in a similar manner.

As demonstrated in chapter 7, transduced cells failed to proliferate on polycarbonate membrane inserts in a serum free environment, but demonstrated potential when cultured with fibroblast feeders. Furthermore, despite proliferating in the presence of feeders, cells did not retain the differentiation patterns of native tissue but instead resembled phenotypes of differentiated transformed cells and this can be further confirmed by keratin profiling to assess patterns of keratinization through the stratified cell layers and compare with normal epithelia (Boukamp, Petrussevska et al. 1988).

It is possible that the transduced cells were subjected to cellular stress induced by the changeover to serum free media (Sinacore, Drapeau et al. 2000) or it may be that, unfortunately, retaining some cell cycle regulation does not necessarily translate

into a normal cellular phenotype. It is important to note that a pilot study using OKF6 and OKF4 cells on polycarbonate membrane inserts (data not shown) demonstrated poor proliferation, confirming the need to optimize serum free adaptation of cells and their culture onto polycarbonate membranes alongside other substrates such as matrigel or collagen gel.

8.2 Conclusions

To conclude, growth rates and cellular morphology of NHOK$^{bmi1+hTERT}$ was similar to parental cell lines in a monolayer and furthermore, as shown by UVB data, when compared to cells with downregulated p53 expression, these cells had higher levels of apoptotic cells. To further elucidate genetic stability of these cells, chromosomal karyotyping will be required to determine cell ploidy and potential chromosomal aberrations since immortalized cell lines often result in chromosome instability, as discussed in chapter 1. Finally, it is important to emphasize again that many of the experiments would have benefitted from parental, non-transduced controls to allow proper comparison with the transduced cells. Experiments would also have benefitted from aliquots of NHOK and NHEK cells frozen down regularly and used for additional controls. Furthermore, different NHOK strains could have been analyzed to assess reproducibility of immortalization methods however it must be noted that this was done on NHOK strain 882 but cells failed to evade senescence (Appendix 2).

This study confirmed the findings of Rheinwald and group on oral keratinocytes using a more established, developed and optimized retroviral infection protocol for the transduction of keratinocytes. This line will be useful for *in vitro* studies wishing to use a genetically stable alternative to current oral cell lines displaying alterations in p53, and possibly other spontaneous changes, as well as optimized further for organotypic studies. The optimized methodology can be utilized to reproduce the cell line for studies from different age groups and racial backgrounds that is not

possible to do for cell lines which have arisen spontaneously after culture crisis or are tumour-derived.

References

Abbott, A. (2003). "Cell culture: biology's new dimension." Nature **424**(6951): 870-872.

Abraham, R. (2002). "Checkpoint signalling: focusing on 53BP1." Nature Cell Biology **4**: E277-E279.

Allam, J. P., G. Stojanovski, N. Friedrichs, W. Peng, T. Bieber, J. Wenzel and N. Novak (2008). "Distribution of Langerhans cells and mast cells within the human oral mucosa: new application sites of allergens in sublingual immunotherapy?" Allergy **63**(6): 720-727.

Alonso, L. and E. Fuchs (2003). "Stem cells of the skin epithelium." Proceedings of the National Academy of Sciences of the United States of America **100**(Suppl 1): 11830-11835.

Athar, M., A. L. Kim, N. Ahmad, H. Mukhtar, J. Gautier and D. R. Bickers (2000). "Mechanism of ultraviolet B-induced cell cycle arrest in G2/M phase in immortalized skin keratinocytes with defective p53." Biochemal and Biophysical Research Communications **277**(1): 107-111.

Azechi, H., N. Nishida, Y. Fukuda, T. Nishimura, M. Minata, H. Katsuma, M. Kuno, T. Ito, T. Komeda and R. Kita (2000). "Disruption of the p16/cyclin D1/retinoblastoma protein pathway in the majority of human hepatocellular carcinomas." Oncology **60**(4): 346-354.

Bailey, S., J. Meyne, D. Chen, A. Kurimasa, G. Li, B. Lehnert and E. Goodwin (1999). "DNA double-strand break repair proteins are required to cap the ends of mammalian chromosomes." Proceedings of the National Academy of Sciences of the United States of America **96**(26): 14899-14904.

Banin, S. (1998). "Enhanced Phosphorylation of p53 by ATM in Response to DNA Damage." Science **281**(5383): 1674-1677.

Barrandon, Y. and H. Green (1987). "Three clonal types of keratinocyte with different capacities for multiplication." Proceedings of the National Academy of Sciences **84**(8): 2302-2306.

Ben-Porath, I. and R. A. Weinberg (2005). "The signals and pathways activating cellular senescence." The international journal of biochemistry & cell biology **37**(5): 961-976.

Blackburn, E. H. (2001). "Switching and signaling at the telomere." Cell **106**(6): 661-673.

Blackburn, E. H. and C. W. Greider (1985). "Identification of a specific telomere terminal transferase activity in Tetrahymena extracts." Cell **43**: 405-413.

Bohr, V., R. M. Anson, S. Mazur and G. Dianov (1998). "Oxidative DNA damage processing and changes with aging." Toxicology letters **102**: 47-52.

Bolzán, A. and M. Bianchi (2006). "Telomeres, interstitial telomeric repeat sequences, and chromosomal aberrations." Mutation Research/Reviews in Mutation Research **612**(3): 189-214.

Borlon, C., S. Vankoningsloo, P. Godard, F. Debacq-Chainiaux and O. Toussaint (2008). "Identification of p53-dependent genes potentially involved in UVB-mediated premature senescence of human skin fibroblasts using siRNA technology." Mechanisms of Ageing and Development **129**(3): 109-119.

Boukamp, P., R. T. Petrussevska, D. Breitkreutz, J. Hornung, A. Markham and N. E. Fusenig (1988). "Normal keratinization in a spontaneously immortalized aneuploid human keratinocyte cell line." The Journal of cell biology **106**(3): 761-771.

Bryan, T., A. Englezou, J. Gupta, S. Bacchetti and R. Reddel (1995). "Telomere elongation in immortal human cells without detectable telomerase activity." The EMBO journal **14**(17): 4240.

Bryan, T. M., A. Englezou, L. Dalla-Pozza, M. A. Dunham and R. R. Reddel (1997). "Evidence for an alternative mechanism for maintaining telomere length in human tumors and tumor-derived cell lines." Nature medicine **3**(11): 1271-1274.

Bush, J. A., K. Cheung, J. John and G. Li (2001). "Curcumin induces apoptosis in human melanoma cells through a Fas receptor/caspase-8 pathway independent of p53." Experimental cell research **271**(2): 305-314.

Campisi, J. (2003). "Cellular senescence and apoptosis: how cellular responses might influence aging phenotypes." Experimental gerontology **38**(1): 5-11.

Campisi, J. and F. d'Adda di Fagagna (2007). "Cellular senescence: when bad things happen to good cells." Nature reviews Molecular cell biology **8**(9): 729-740.

Campisi, J., S. Kim, C. Lim and M. Rubio (2001). "Cellular senescence, cancer and aging: the telomere connection." Experimental Gerontology **36**(10): 1619-1637.

Cepko, C. and W. Pear (2001). "Retrovirus infection of cells in vitro and in vivo." Current Protocols in Molecular Biology **1**: 9.14.1-9.14.6.

Cesare, A. J. and R. R. Reddel (2008). "Telomere uncapping and alternative lengthening of telomeres." Mechanisms of ageing and development **129**(1): 99-108.

Cesare, A. J. and R. R. Reddel (2010). "Alternative lengthening of telomeres: models, mechanisms and implications." Nature Reviews Genetics **11**(5): 319-330.

Cha, M. C. and P. P. Purslow (2010). "The activities of MMP-9 and total gelatinase respond differently to substrate coating and cyclic mechanical stretching in fibroblasts and myoblasts." Cell biology international **34**: 587-591.

Chen, C. and H. Okayama (1987). "High-efficiency transformation of mammalian cells by plasmid DNA." Molecular and cellular biology **7**(8): 2745-2752.

Chen, J., Y. Chen, C. Chen and Y. Wang (2001). "Loss of p16 and/or pRb protein expression in NSCLC:: An immunohistochemical and prognostic study." Lung Cancer **31**(2-3): 163-170.

Cheng, K., D. S. Cahill, H. Kasai, S. Nishimura and L. A. Loeb (1992). "8-Hydroxyguanine, an abundant form of oxidative DNA damage, causes G----T and A----C substitutions." Journal of Biological Chemistry **267**(1): 166-172.

Collins, A. R. (1999). "Oxidative DNA damage, antioxidants, and cancer." Bioessays **21**(3): 238-246.

Collins, K. (2000). "Mammalian telomeres and telomerase." Current opinion in cell biology **12**(3): 378-383.

Collins, K. and J. R. Mitchell (2002). "Telomerase in the human organism." Oncogene **21**(4): 564.

Collins, L. and C. Dawes (1987). "The surface area of the adult human mouth and thickness of the salivary film covering the teeth and oral mucosa." Journal of dental research **66**(8): 1300-1302.

Cook, J. A., D. Gius, D. A. Wink, M. C. Krishna, A. Russo and J. B. Mitchell (2004). "Oxidative stress, redox, and the tumor microenvironment." Seminars in radiation oncology **14**(3): 259-266.

Cooke, M. S., M. D. Evans, M. Dizdaroglu and J. Lunec (2003). "Oxidative DNA damage: mechanisms, mutation, and disease." The FASEB Journal **17**(10): 1195-1214.

Cristofalo, V. J., A. Lorenzini, R. Allen, C. Torres and M. Tresini (2004). "Replicative senescence: a critical review." Mechanisms of ageing and development **125**(10): 827-848.

Cristofalo, V. J. and R. J. Pignolo (1993). "Replicative senescence of human fibroblast-like cells in culture." Physiological reviews **73**(3): 617-638.

Darmon, M., J. Bottenstein and G. Sato (1981). "Neural differentiation following culture of embryonal carcinoma cells in a serum-free defined medium." Developmental biology **85**(2): 463-473.

de Lange, T. (2005). "Shelterin: the protein complex that shapes and safeguards human telomeres." Genes and Development **19**(18): 2100-2110.

Denicourt, C. and S. F. Dowdy (2004). "Cip/Kip proteins: more than just CDKs inhibitors." Genes and Development **18**(8): 851-855.

Dickson, M. A., W. C. Hahn, Y. Ino, V. Ronfard, J. Y. Wu, R. A. Weinberg, D. N. Louis, F. P. Li and J. G. Rheinwald (2000). "Human keratinocytes that express hTERT and also bypass a p16INK4a-enforced mechanism that limits life span become immortal yet retain normal growth and differentiation characteristics." Molecular and cellular biology **20**(4): 1436-1447.

Dimitrova, N., Y. C. M. Chen, D. L. Spector and T. de Lange (2008). "53BP1 promotes non-homologous end joining of telomeres by increasing chromatin mobility." Nature **456**(7221): 524-528.

Dimri, G., J. Martinez, J. Jacobs, P. Keblusek, K. Itahana, M. van Lohuizen, J. Campisi, D. Wazer and V. Band (2002). "The Bmi-1 oncogene induces telomerase activity and immortalizes human mammary epithelial cells." Cancer Research **62**(16): 4736-4745.

Dimri, G. P., X. Lee, G. Basile, M. Acosta, G. Scott, C. Roskelley, E. E. Medrano, M. Linskens, I. Rubelj and O. Pereira-Smith (1995). "A biomarker that identifies senescent human cells in culture and in aging skin in vivo." Proceedings of the National Academy of Sciences **92**(20): 9363-9367.

Do, L. (2003). "Serum-free cell culture–the ethical, scientific and economic choice." Biomedical scientist: 941-942.

Dürst, M., F. Bosch, D. Glitz, A. Schneider and H. Zur Hausen (1991). "Inverse relationship between human papillomavirus (HPV) type 16 early gene expression and cell differentiation in nude mouse epithelial cysts and tumors induced by HPV-positive human cell lines." Journal of virology **65**(2): 796-804.

Eckert, R. L., J. F. Crish and N. A. Robinson (1997). "The epidermal keratinocyte as a model for the study of gene regulation and cell differentiation." Physiological reviews **77**(2): 397-424.

Eckert, R. L., T. Efimova, S. R. Dashti, S. Balasubramanian, A. Deucher, J. F. Crish, M. Sturniolo and F. Bone (2002). "Keratinocyte survival, differentiation, and death: many roads lead to mitogen-activated protein kinase". Journal of Investigative Dermatology **7**: 36-40.

El-Deiry, W. S. (1998). "Regulation of p53 downstream genes". Seminars in Cancer Biology **8**(3): 345-357.

Elsayed, E. A., M. E. L. Demellawy and A. A. E. L. Shereef (2009). "Serum concentration effects on the kinetics and metabolism of Hela-s3 cell growth and cell adaptability for successful proliferation in serum free medium." World Applied Sciences Journal **6**(5): 608-615.

Erusalimsky, J. D. and D. J. Kurz (2005). "Cellular senescence in vivo: its relevance in ageing and cardiovascular disease." Experimental gerontology **40**(8): 634-642.

Evans, M. D., M. Dizdaroglu and M. S. Cooke (2004). "Oxidative DNA damage and disease: induction, repair and significance." Mutation Research/Reviews in Mutation Research **567**(1): 1-61.

Fernandez-Capetillo, O., A. Lee, M. Nussenzweig and A. Nussenzweig (2004). "H2AX: the histone guardian of the genome." DNA Repair (Amst) **3**(8-9): 959-967.

Fitzgerald, J. E., M. Grenon and N. F. Lowndes (2009). "53BP1: function and mechanisms of focal recruitment." Biochemical Society Transactions **37**(4): 897.

Fujimoto, R., N. Kamata, K. Yokoyama, N. Ueda, K. Satomura, E. Hayashi and M. Nagayama (2001). "Expression of telomerase components in oral keratinocytes and squamous cell carcinomas." Oral oncology **37**(2): 132-140.

Funayama, R. and F. Ishikawa (2007). "Cellular senescence and chromatin structure." Chromosoma **116**(5): 431-440.

Geradts, J. and P. Wilson (1996). "High frequency of aberrant p16 (INK4A) expression in human breast cancer." The American journal of pathology **149**(1): 15-20.

Gerlier, D. and N. Thomasset (1986). "Use of MTT colorimetric assay to measure cell activation." Journal of immunological methods **94**(1): 57-63.

Greco, D., K. S. Vellonen, H. C. Turner, M. Häkli, T. Tervo, P. Auvinen, J. M. Wolosin and A. Urtti (2010). "Gene expression analysis in SV-40 immortalized human corneal epithelial cells cultured with an air-liquid interface." Molecular vision **16**: 2109-2120.

Green, H., J. G. Rheinwald and T. T. Sun (1977). "Properties of an epithelial cell type in culture: the epidermal keratinocyte and its dependence on products of the fibroblast." Progress in Clinical and Biological Research **17**: 493-500.

Griffith, J. D., L. Comeau, S. Rosenfield, R. M. Stansel, A. Bianchi, H. Moss and T. De Lange (1999). "Mammalian telomeres end in a large duplex loop." Cell **97**: 503-514.

Gstraunthaler, G. (2003). "Alternatives to the use of fetal bovine serum: serum-free cell culture." Alternatives to Animal Experiments **20**(4): 275-281.

Guney, I., S. Wu and J. Sedivy (2006). "Reduced c-Myc signaling triggers telomere-independent senescence by regulating Bmi-1 and p16INK4a." Proceedings of the National Academy of Sciences **103**(10): 3645-3650.

Haga, K., S. Ohno, T. Yugawa, M. Narisawa-Saito, M. Fujita, M. Sakamoto, D. A. Galloway and T. Kiyono (2007). "Efficient immortalization of primary human cells by p16INK4a-specific short hairpin RNA or Bmi-1, combined with introduction of hTERT." Cancer Science **98**(2): 147-154.

Hahn, W. C. and M. Meyerson (2001). "Telomerase activation, cellular immortalization and cancer." Annals of Medicine **33**(2): 123-129.

Halliwell, B. (2003). "Oxidative stress in cell culture: an under-appreciated problem?" FEBS letters **540**(1-3): 3-6.

Hanahan, D. and R. A. Weinberg (2000). "The hallmarks of cancer." cell **100**(1): 57-70.

Harley, C. B., N. Kim, K. Prowse, S. Weinrich, K. Hirsch, M. West, S. Bacchetti, H. Hirte, C. Counter and C. Greider (1994). "Telomerase, cell immortality, and cancer". Cold Spring Harbor Laboratory Press **59**: 307-315.

Harley, C. B. and S. W. Sherwood (1997). "Telomerase, checkpoints and cancer." Cancer surveys **29**: 263-284.

Harvey, D. and A. Levine (1991). "p53 alteration is a common event in the spontaneous immortalization of primary BALB/c murine embryo fibroblasts." Genes & development **5**(12b): 2375-2385.

Hennings, H., D. Michael, C. Cheng, P. Steinert, K. Holbrook and S. H. Yuspa (1980). "Calcium regulation of growth and differentiation of mouse epidermal cells in culture." Cell **19**(1): 245-254.

Herbert, B. S., A. E. Hochreiter, W. E. Wright and J. W. Shay (2006). "Nonradioactive detection of telomerase activity using the telomeric repeat amplification protocol." Nature Protocols **1**(3): 1583-1590.

Higami, Y. and I. Shimokawa (2000). "Apoptosis in the aging process." Cell and Tissue Research **301**(1): 125-132.

Hofseth, L. J., S. P. Hussain and C. C. Harris (2004). "p53: 25 years after its discovery." Trends in pharmacological sciences **25**(4): 177-181.

Honegger, P., D. Lenoir and P. Favrod (1979). "Growth and differentiation of aggregating fetal brain cells in a serum-free defined medium". Nature **282**: 305-308.

Hu, W. and J. Aunins (1997). "Large-scale mammalian cell culture." Current opinion in biotechnology **8**(2): 148-153.

Itahana, K., G. Dimri and J. Campisi (2001). "Regulation of cellular senescence by p53." European Journal of Biochemistry **268**(10): 2784-2791.

Johnson, D. and C. Walker (1999). "Cyclins and cell cycle checkpoints." Annual review of pharmacology and toxicology **39**(1): 295-312.

Jones, P. H., S. Harper and F. M. Watt (1995). "Stem cell patterning and fate in human epidermis." Cell **80**(1): 83-93.

Kahl, C. and A. Means (2003). "Regulation of cell cycle progression by calcium/calmodulin-dependent pathways." Endocrine reviews **24**(6): 719-736.

Kamijo, T., J. Weber, G. Zambetti, F. Zindy, M. Roussel and C. Sherr (1998). "Functional and physical interactions of the ARF tumor suppressor with p53 and Mdm2." Proceedings of the National Academy of Sciences of the United States of America **95**(14): 8292-8297.

Kang, M. K., R. H. Kim, S. J. Kim, F. K. Yip, K. H. Shin, G. P. Dimri, R. Christensen, T. Han and N. H. Park (2007). "Elevated Bmi-1 expression is associated with dysplastic cell transformation during oral carcinogenesis and is required for cancer cell replication and survival." British Journal of Cancer **96**(1): 126-133.

Kanitakis, J. (2002). "Anatomy, histology and immunohistochemistry of normal human skin." European Journal of Dermatology **12**(4): 390-399.

Kastan, M. B., O. Onyekwere, D. Sidransky, B. Vogelstein and R. W. Craig (1991). "Participation of p53 protein in the cellular response to DNA damage." Cancer research **51**(23 Part 1): 6304-6311.

Kaul, S. C., R. R. Reddel, T. Sugihara, Y. Mitsui and R. Wadhwa (2000). "Inactivation of p53 and life span extension of human diploid fibroblasts by mot-2." FEBS letters **474**(2): 159-164.

Kessels, H., M. C. Wolkers and T. Schumacher (2005). "Gene transfer of MHC-restricted receptors." Methods in Molecular Medicine **109**: 201-214.

Kevles, D. J. and G. L. Geison (1995). "The experimental life sciences in the twentieth century." Osiris **10**: 97-121.

Khanna, K., M. Lavin, S. Jackson and T. Mulhern (2001). "ATM, a central controller of cellular responses to DNA damage." Cell death and differentiation **8**(11): 1052-1065.

Kim, N. W., M. A. Piatyszek, K. R. Prowse, C. B. Harley, M. D. West, P. L. Ho, G. M. Coviello, W. E. Wright, S. L. Weinrich and J. W. Shay (1994). "Specific association of human telomerase activity with immortal cells and cancer." Science **266**(5193): 2011-2015.

Kim, S., P. Kaminker and J. Campisi (2002). "Telomeres, aging and cancer: in search of a happy ending." Oncogene **21**(4): 503-511.

Kiyono, T., S. A. Foster, J. I. Koop, J. K. McDougall, D. A. Galloway and A. J. Klingelhutz (1998). "Both Rb/p16INK4a inactivation and telomerase activity are required to immortalize human epithelial cells." Nature **396**(6706): 84-88.

Koster, M. I. (2009). "Making an epidermis." Annals of the New York Academy of Sciences **1170**(1): 7-10.

Kotani, H., P. B. Newton III, S. Zhang, Y. L. Chiang, E. Otto, L. Weaver, R. M. Blaese, W. F. Anderson and G. J. McGarrity (1994). "Improved methods of retroviral vector transduction and production for gene therapy." Human gene therapy **5**(1): 19-28.

Krunic, D., S. Moshir, K. M. Greulich-Bode, R. Figueroa, A. Cerezo, H. Stammer, H. J. Stark, S. G. Gray, K. V. Nielsen and W. Hartschuh (2009). "Tissue context-activated telomerase in human epidermis correlates with little age-dependent telomere loss." Biochimica et Biophysica Acta (BBA)-Molecular Basis of Disease **1792**(4): 297-308.

Kulms, D., B. Pöppelmann, D. Yarosh, T. A. Luger, J. Krutmann and T. Schwarz (1999). "Nuclear and cell membrane effects contribute independently to the induction of apoptosis in human cells exposed to UVB radiation." Proceedings of the National Academy of Sciences **96**(14): 7974-7979.

Kyo, S. and M. Inoue (2002). "How to inhibit telomerase activity for cancer therapy." Current Medicinal Chemistry-Anti-Cancer Agents **2**(5): 613-626.

Latonen, L. and M. Laiho (2005). "Cellular UV damage responses—functions of tumor suppressor p53." Biochimica et Biophysica Acta (BBA)-Reviews on Cancer **1755**(2): 71-89.

Lee, K., G. Adhikary, S. Balasubramanian, R. Gopalakrishnan, T. McCormick, G. Dimri, R. Eckert and E. Rorke (2007). "Expression of Bmi-1 in epidermis enhances cell survival by altering cell cycle regulatory protein expression and inhibiting apoptosis." Journal of Investigative Dermatology **128**(1): 9-17.

Lee, K. M., K. H. Choi and M. M. Ouellette (2004). "Use of exogenous hTERT to immortalize primary human cells." Cytotechnology **45**(1): 33-38.

Levine, A. (1997). "p53, the cellular gatekeeper for growth and division." Cell **88**(3): 323-331.

Levy, L., S. Broad, A. Zhu, J. Carroll, I. Khazaal, B. Peault and F. Watt (1998). "Optimised retroviral infection of human epidermal keratinocytes: long-term expression of transduced integrin gene following grafting on to SCID mice." Gene therapy **5**(7): 913.

Lewis, D. A., Q. Yi, J. B. Travers and D. F. Spandau (2008). "UVB-induced senescence in human keratinocytes requires a functional insulin-like growth factor-1 receptor and p53." Molecular Biology of the Cell **19**(4): 1346-1353.

Lin, A. W., M. Barradas, J. C. Stone, L. Van Aelst, M. Serrano and S. W. Lowe (1998). "Premature senescence involving p53 and p16 is activated in response to constitutive MEK/MAPK mitogenic signaling." Genes & development **12**(19): 3008-3019.

Linder, S. and H. Marshall (1990). "Immortalization of primary cells by DNA tumor viruses." Experimental cell research **191**(1): 1-7.

Lisby, M. and R. Rothstein (2004). "DNA repair: keeping it together." Current biology **14**(23): 994-996.

Liu, J., Z. Bian, A. Kuijpers-Jagtman and J. Von den Hoff (2010). "Skin and oral mucosa equivalents: construction and performance." Orthodontics & craniofacial research **13**(1): 11-20.

Lloyd, A. (2002). "Limits to lifespan." Nature cell biology **4**(2): E25-E27.

Lloyd, C., Q. C. Yu, J. Cheng, K. Turksen, L. Degenstein, E. Hutton and E. Fuchs (1995). "The basal keratin network of stratified squamous epithelia: defining K15 function in the absence of K14." Journal of Cell Biology **129**: 1329-1329.

Lustig, A. J. (1999). "Crisis intervention: the role of telomerase." Proceedings of the National Academy of Sciences **96**(7): 3339-3341.

Marionnet, C., C. Pierrard, C. Vioux-Chagnoleau, J. Sok, D. Asselineau and F. Bernerd (2006). "Interactions between fibroblasts and keratinocytes in morphogenesis of dermal epidermal junction in a model of reconstructed skin." Journal of Investigative Dermatology **126**(5): 971-979.

Masutomi, K., E. Y. Yu, S. Khurts, I. Ben-Porath, J. L. Currier, G. B. Metz, M. W. Brooks, S. Kaneko, S. Murakami and J. A. DeCaprio (2003). "Telomerase maintains telomere structure in normal human cells." Cell **114**(2): 241-253.

Maurel, B. and A. Pareilleux (1985). "Effect of carbon dioxide on the growth of cell suspensions ofCathakanthus roseus." Biotechnology Letters **7**(5): 313-318.

Meek, D. W. (2004). "The p53 response to DNA damage." DNA Repair (Amst) **3**(8-9): 1049-1056.

Michael, D. and M. Oren (2002). "The p53 and Mdm2 families in cancer." Current opinion in genetics & development **12**(1): 53-59.

Milyavsky, M., I. Shats, N. Erez, X. Tang, S. Senderovich, A. Meerson, Y. Tabach, N. Goldfinger, D. Ginsberg and C. C. Harris (2003). "Prolonged culture of telomerase-immortalized human fibroblasts leads to a premalignant phenotype." Cancer research **63**(21): 7147-7157.

Minty, F., J. K. Thurlow, P. R. Harrison and E. K. Parkinson (2008). "Telomere dysfunction in human keratinocytes elicits senescence and a novel transcription profile." Experimental Cell Research **314**(13): 2434-2447.

Moll, R., I. Moll and W. W. Franke (1984). "Identification of Merkel cells in human skin by specific cytokeratin antibodies:: Changes of cell density and distribution in fetal and adult plantar epidermis." Differentiation **28**(2): 136-154.

Montagna, W. and R. A. Ellis (1960). "The skin of primates. II. The skin of the slender loris (Loris tardigradus)." American journal of physical anthropology **18**(1): 19-43.

Morin, G. B. (1989). "The human telomere terminal transferase enzyme is a ribonucleoprotein that synthesizes TTAGGG repeats." Cell **59**(3): 521-529.

Morita, S., T. Kojima and T. Kitamura (2000). "Plat-E: an efficient and stable system for transient packaging of retroviruses." Gene therapy **7**(12): 1063-1066.

Mosmann, T. (1983). "Rapid colorimetric assay for cellular growth and survival: application to proliferation and cytotoxicity assays." Journal of Immunological methods **65**(1-2): 55-63.

Mujaj, S., K. Manton, Z. Upton and S. Richards (2010). "Serum-free primary human fibroblast and keratinocyte coculture." Tissue Engineering Part A **16**(4): 1407-1420.

Nyberg, K. A., R. J. Michelson, C. W. Putnam and T. A. Weinert (2002). "Toward maintaining the genome: DNA damage and replication checkpoints." Annual review of genetics **36**(1): 617-656.

Ohtani, N., D. J. Mann and E. Hara (2009). "Cellular senescence: its role in tumor suppression and aging." Cancer science **100**(5): 792-797.

Olovnikov, A. M. (1996). "Telomeres, telomerase, and aging: origin of the theory." Experimental gerontology **31**(4): 443-448.

Ozturk, S. S. and B. O. Palsson (1991). "Growth, metabolic, and antibody production kinetics of hybridoma cell culture: 2. Effects of serum concentration, dissolved oxygen concentration, and medium pH in a batch reactor." Biotechnology progress **7**(6): 481-494.

Ramirez, R. D., B. S. Herbert, M. B. Vaughan, Y. Zou, K. Gandia, C. P. Morales, W. E. Wright and J. W. Shay (2003). "Bypass of telomere-dependent replicative senescence (M1) upon overexpression of Cdk4 in normal human epithelial cells." Oncogene **22**(3): 433-444.

Reddel, R. R. (2003). "Alternative lengthening of telomeres, telomerase, and cancer." Cancer Letters **194**(2): 155-162.

Reddel, R. R., S. E. Salghetti, J. C. Willey, Y. Ohnuki, Y. Ke, B. I. Gerwin, J. F. Lechner and C. C. Harris (1993). "Development of tumorigenicity in simian virus 40-immortalized human bronchial epithelial cell lines." Cancer research **53**(5): 985-991.

Reznikoff, C. A., L. J. Loretz, B. J. Christian, S. Q. Wu and L. F. Meisner (1988). "Neoplastic transformation of SV40-immortalized human urinary tract epithelial cells by in vitro exposure to 3-methylcholanthrene." Carcinogenesis **9**(8): 1427-1436.

Reznikoff, C. A., T. R. Yeager, C. D. Belair, E. Savelieva, J. A. Puthenveettil and W. M. Stadler (1996). "Elevated p16 at senescence and loss of p16 at immortalization in human papillomavirus 16 E6, but not E7, transformed human uroepithelial cells." Cancer research **56**(13): 2886-2890.

Rheinwald, J., W. Hahn, M. Ramsey, J. Wu, Z. Guo, H. Tsao, M. De Luca, C. Catricala and K. O'Toole (2002). "A two-stage, p16INK4A-and p53-dependent keratinocyte senescence mechanism that limits replicative potential independent of telomere status." Molecular and cellular biology **22**(14): 5157.

Rheinwald, J. G. and H. Green (1975). "Formation of a keratinizing epithelium in culture by a cloned cell line derived from a teratoma." Cell **6**(3): 317-330.

Rheinwald, J. G. and H. Green (1977). "Epidermal growth factor and the multiplication of cultured human epidermal keratinocytes." Nature **265**(5593): 421.

Rheinwatd, J. G. and H. Green (1975). "Seria cultivation of strains of human epidemal keratinocytes: the formation keratinizin colonies from single cell is." Cell **6**(3): 331-343.
Rhodes, D. and R. Giraldo (1995). "Telomere structure and function." Current Opinion in Structural Biology **5**(3): 311-322.

Ross, K., G. Parker and M. Whitaker (2008). "15. Cutaneous Biology." Medical and Surgical Dermatology **9**(3): 190-196.

Sedivy, J. M. (1998). "Can ends justify the means?: telomeres and the mechanisms of replicative senescence and immortalization in mammalian cells." Proceedings of the National Academy of Sciences **95**(16): 9078-9081.

Serrano, M., H. Lee, L. Chin, C. Cordon-Cardo, D. Beach and R. DePinho (1996). "Role of the INK4a locus in tumor suppression and cell mortality." Cell **85**(1): 27-38.

Sharpless, N. E. (2004). "Telomeres, stem cells, senescence, and cancer." Journal of Clinical Investigation **113**(2): 160-168.

Shay, J. W. and W. E. Wright (2005). "Senescence and immortalization: role of telomeres and telomerase." Carcinogenesis **26**(5): 867-874.

Shay, J. W., W. E. Wright and H. Werbin (1991). "Defining the molecular mechanisms of human cell immortalization." Biochimica et Biophysica Acta (BBA)/Reviews on Cancer **1072**(1): 1-7.

Shellis, R. and B. Berkovitz (2009). "Observations on the dental anatomy of piranhas (Characidae) with special reference to tooth structure." Journal of Zoology **180**(1): 69-84.

Sherr, C. (2001). "The INK4a/ARF network in tumour suppression." Nature reviews Molecular cell biology **2**(10): 731-737.

Sherr, C. J. (2000). "The Pezcoller lecture: cancer cell cycles revisited." Cancer research **60**(14): 3689-3695.

Sherr, C. J. (2006). "Divorcing ARF and p53: an unsettled case." Nature Reviews Cancer **6**(9): 663-673.

Shnitman Magal, S., A. Jackman, X. F. Pei, R. Schlegel and L. Sherman (1998). "Induction of apoptosis in human keratinocytes containing mutated p53 alleles and its inhibition by both the E6 and E7 oncoproteins." International journal of cancer **75**(1): 96-104.

Sinacore, M. S., D. Drapeau and S. Adamson (2000). "Adaptation of mammalian cells to growth in serum-free media." Molecular biotechnology **15**(3): 249-257.

Song, J., K. Izumi, T. Lanigan and S. E. Feinberg (2004). "Development and characterization of a canine oral mucosa equivalent in a serum-free environment." Journal of Biomedical Materials Research Part A **71**(1): 143-153.

Sorrell, J. M. and A. I. Caplan (2004). "Fibroblast heterogeneity: more than skin deep." Journal of cell science **117**(5): 667-675.

Squier, C.A and K. Brogden. Human oral mucosa: development, structure and function, Oxford (UK): Blackwell Scientific; 1976.

Squier, C. A. and M. J. Kremer (2001). "Biology of oral mucosa and esophagus." JNCI Monographs **2001**(29): 7-15.

Stansel, R. M., T. De Lange and J. D. Griffith (2001). "T-loop assembly in vitro involves binding of TRF2 near the 3′ telomeric overhang." The EMBO journal **20**(19): 5532-5540.

Stewart, S. A. and R. A. Weinberg (2000)." Telomerase and human tumorigenesis". Seminars in Cancer Biology **10**(6): 399-406.

Strasser, A., A. W. Harris, T. Jacks and S. Cory (1994). "DNA damage can induce apoptosis in proliferating lymphoid cells via p53-independent mechanisms inhibitable by Bcl-2." Cell **79**(2): 329-339.

Takai, H., A. Smogorzewska and T. de Lange (2003). "DNA Damage Foci at Dysfunctional Telomeres." Current Biology **13**(17): 1549-1556.

Tanaka, H., Y. Fujii, H. Hirabayashi, S. Miyoshi, M. Sakaguchi, H. Yoon and H. Matsuda (1998). "Disruption of the RB pathway and cell-proliferative activity in non-small-cell lung cancers." International Journal of Cancer **79**(2): 111-115.

Toouli, C. D., L. I. Huschtscha, A. A. Neumann, J. R. Noble, L. M. Colgin, B. Hukku and R. R. Reddel (2002). "Comparison of human mammary epithelial cells immortalized by simian virus 40 T-Antigen or by the telomerase catalytic subunit." Oncogene **21**(1): 128-139.

Vaughan, M. B., R. D. Ramirez, W. E. Wright, J. D. Minna and J. W. Shay (2006). "A three-dimensional model of differentiation of immortalized human bronchial epithelial cells." Differentiation **74**(4): 141-148.

Vermes, I., C. Haanen, H. Steffens-Nakken and C. Reutelingsperger (1995). "A novel assay for apoptosis: Flow cytometric detection of phosphatidylserine expression on early apoptotic cells using fluorescein labelled Annexine V." Journal of immunological methods **184**(1): 39-51.

Vermeulen, K., D. Van Bockstaele and Z. Berneman (2003). "The cell cycle: a review of regulation, deregulation and therapeutic targets in cancer." Cell Proliferation **36**(3): 131-149.

Wang, D., D. Liebowitz, F. Wang, C. Gregory, A. Rickinson, R. Larson, T. Springer and E. Kieff (1988). "Epstein-Barr virus latent infection membrane protein alters the human B-lymphocyte phenotype: deletion of the amino terminus abolishes activity." Journal of Virology **62**(11): 4173-4184.

Ward, I. M., K. Minn, K. G. Jorda and J. Chen (2003). "Accumulation of checkpoint protein 53BP1 at DNA breaks involves its binding to phosphorylated histone H2AX." Journal of Biological Chemistry **278**(22): 19579-19582.

Watt, F. (1988). "Effect of seeding density on stability of the differentiated phenotype of pig articular chondrocytes in culture." Journal of Cell Science **89**(3): 373-378.

Watt, F. M., S. Broad and D. M. Prowse (2004). "Cultivation and retroviral infection of human epidermal keratinocytes." Cell Biology: A Laboratory Handbook **1**: 133-138.

Wieser, M., G. Stadler, P. Jennings, B. Streubel, W. Pfaller, P. Ambros, C. Riedl, H. Katinger, J. Grillari and R. Grillari-Voglauer (2008). "hTERT alone immortalizes epithelial cells of renal proximal tubules without changing their functional characteristics." American Journal of Physiology-Renal Physiology **295**(5): F1365-F1375.

Wille Jr, J., M. Pittelkow, G. Shipley and R. Scott (2005). "Integrated control of growth and differentiation of normal human prokeratinocytes cultured in serum-free medium: clonal analyses, growth kinetics, and cell cycle studies." Journal of cellular physiology **121**(1): 31-44.

Woodworth, C., S. Waggoner, W. Barnes, M. Stoler and J. A. DiPaolo (1990). "Human cervical and foreskin epithelial cells immortalized by human papillomavirus DNAs exhibit dysplastic differentiation in vivo." Cancer research **50**(12): 3709-3715.

Xin, H., D. Liu and Z. Songyang (2008). "The telosome/shelterin complex and its functions." Genome Biology **9**(9): 232-238.

Yamakoshi, K., A. Takahashi, F. Hirota, R. Nakayama, N. Ishimaru, Y. Kubo, D. J. Mann, M. Ohmura, A. Hirao and H. Saya (2009). "Real-time in vivo imaging of p16Ink4a reveals cross talk with p53." The Journal of cell biology **186**(3): 393-407.

Yasumoto, S., C. Kunimura, K. Kikuchi, H. Tahara, H. Ohji, H. Yamamoto, T. Ide and T. Utakoji (1996). "Telomerase activity in normal human epithelial cells." Oncogene **13**(2): 433-439.

Yazdi, P., Y. Wang, S. Zhao, N. Patel, E. Lee and J. Qin (2002). "SMC1 is a downstream effector in the ATM/NBS1 branch of the human S-phase checkpoint." Genes & Development **16**(5): 571-582.

Zhu, C. H., V. Mouly, R. N. Cooper, K. Mamchaoui, A. Bigot, J. W. Shay, J. P. Di Santo, G. S. Butler-Browne and W. E. Wright (2007). "Cellular senescence in human myoblasts is overcome by human telomerase reverse transcriptase and cyclin-dependent kinase 4: consequences in aging muscle and therapeutic strategies for muscular dystrophies." Aging cell **6**(4): 515-523.

Zuckerman, V., K. Wolyniec, R. V. Sionov, S. Haupt and Y. Haupt (2009). "Tumour suppression by p53: the importance of apoptosis and cellular senescence." The Journal of pathology **219**(1): 3-15.

Zhu, A., I. Haase, et al. (1999). "Signaling via 1 integrins and mitogen-activated protein kinase determines human epidermal stem cell fate in vitro." Proceedings of the National Academy of Sciences **96**(12): 6728-6733.

http://www.rci.rutgers.edu/~uzwiak/AnatPhys/APFallLect7.html

http://www.stanford.edu/group/nolan/protocols/pro_helper_free.html

Appendix 1

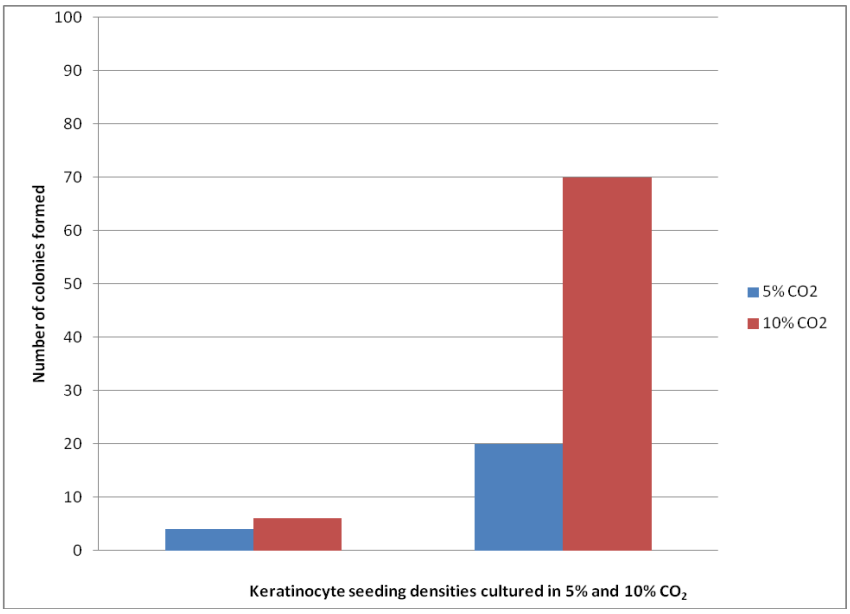

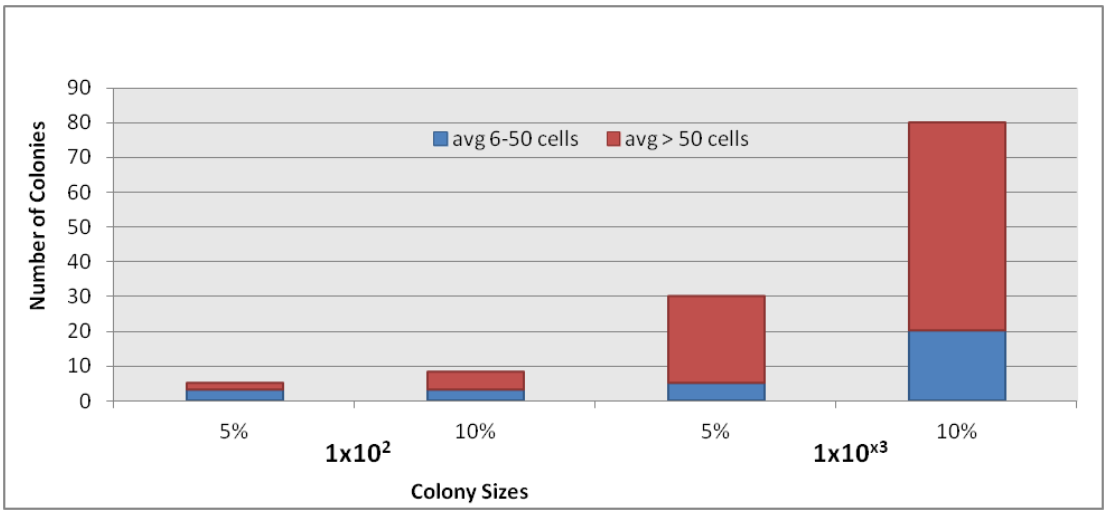

Appendix 1.2 Quantification of colony number and sizes. Cells cultured at 1 x 10^2 and 1 x 10^3 were cultured for 14 days and then colony counts performed. 2 plates were assessed per variable.

Appendix 2

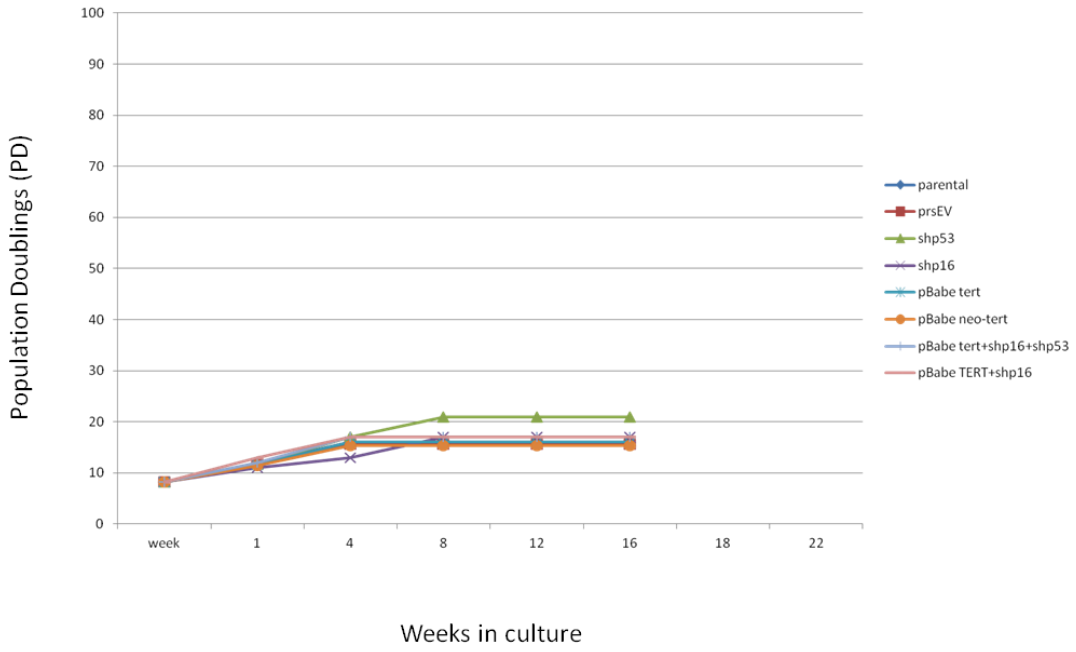

Appendix 2.1 Transduction of NHOK 882 (selected).

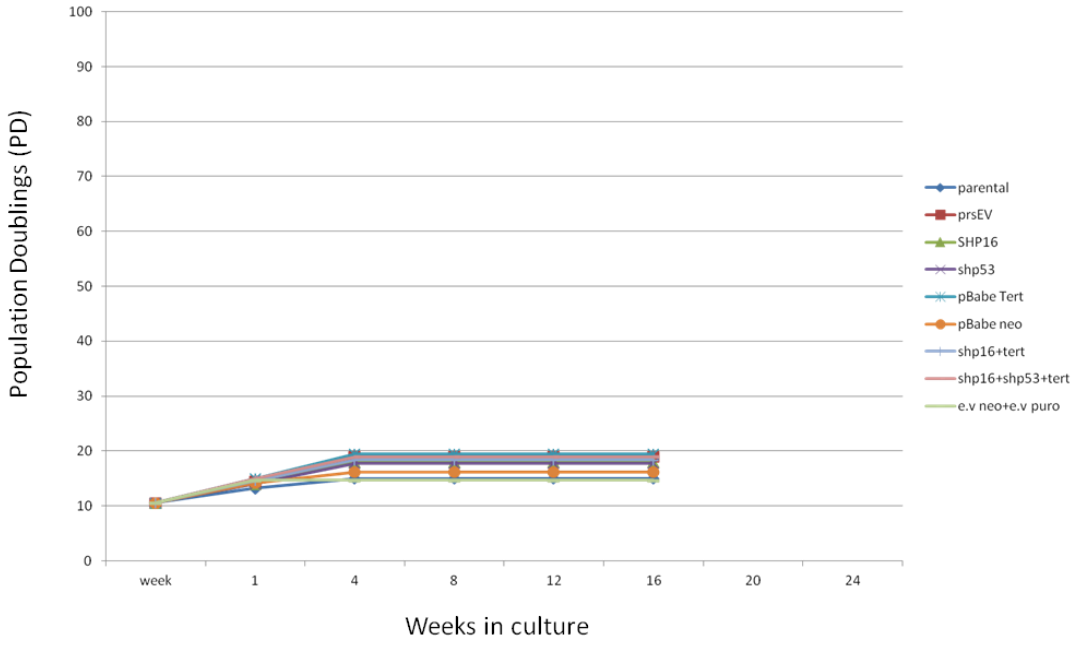

Appendix 2.2 Transductions of NHOK 882 (non-selected).